Cardiac Allograft Vasculopathy; Molecular pathology of the transplanted heart

Manon Huibers, University Utrecht, Faculty of Medicine, University Medical Center Utrecht, the Netherlands

Thesis Utrecht University, with a summary in Dutch

Layout design: Kimberley Teunissen
Cover design: Engbert Huibers "Accepting someone's heart"
Inspired by an artwork of Alfred Gockel "Hearts III"
Printed by: Proefschriftmaken.nl || Uitgeverij BOXPress
Published by: Uitgeverij BOXPress, 's-Hertogenbosch
ISBN: 978-94-6295-129-7

CARDIAC ALLOGRAFT VASCULOPATHY
MOLECULAR PATHOLOGY OF THE TRANSPLANTED HEART

CORONAIR LIJDEN NA HARTTRANSPLANTATIE
Moleculaire pathologie van het getransplanteerde hart

(met een samenvatting in het Nederlands)

PROEFSCHRIFT

ter verkrijging van de graad van doctor aan de Universiteit Utrecht op gezag van de rector magnificus, prof. dr. G.J. van der Zwaan, ingevolge het besluit van het college voor promoties in het openbaar te verdedigen op

maandag 13 april 2014 des middags te 4.15 uur

door

Manon Maria Hendrica Huibers
geboren op 24 december 1986 te Vught

Promotor:	Prof.dr. P. J. van Diest
Copromotoren:	Dr. R. A. de Weger Dr. N. de Jonge

Publication of this thesis was financially supported by:

Nederlandse Transplantatie Vereniging (NTV)

Financial support by the Dutch Heart Foundation for the publication of this thesis is gratefully acknowledged.

Financial support by the Heart & Lung Foundation Utrecht for the publication of this thesis is gratefully acknowledged.

Contents

Abbreviations

αSMA	Alpha smooth muscle actin
ACE	Angiotensin converting enzyme
AID	Activation-induced cytidine deaminase
AMR	Antibody-mediated rejection
APC	Antigen presenting cell
AT1R	Angiotensin-II type-1 receptor
AV	Allograft Vasculopathy
BIT	Benign Intima Thinkening
BMP	Bone morphogenic protein
CAV	Cardiac Allograft Vasculopathy
cDNA	complementary DNA
CMV	Cytomegalovirus
CTGF	Connective tissue growth factor
DC	Dendritic cell
DSA	Donor specific antibodies
ECM	Extracellular matrix
ECPC	Extra Cardiac Progenitor Cells
ELISA	Enzyme-Linked Immuno Sorbent Assay
ELS	Ectopic lymphoid structures
EMT	Epithelial-to-mesenchymal transition
Endo-MT	Endothelial-to-mesenchymal transition
EPC	Endothelial progenitor cells
EvG	Elastic van Giesson
FACS	Fluorescence Activated Cell Sorting
FFPE	Formalin Fixed Parafin Embedded
H-CAV	Histological-Cardiac Allograft Vasculopathy
HE	Hematoxilin and Eosin
HEV	High endothelial venules
HLA	Human leukocyte antigen
HLA-DR	Human leukocyte antigen DR
HRP	Horseradish peroxidase
HTx	Heart transplantation
HUVECs	Human umbilical vein endothelial cells
ID-1	Inhibitor of DNA binding 1
IFNγ	Interferon gamma
IHC	Immunohistochemistry
IL	Interleukin
iNOS	Inducible Isoform of Nitric Oxide Synthase
ISH	In situ hybridization
LMD	Laser Micro dissection
LVAD	Left Ventricular assist device
MICA	Major-histocompatibilitycomplex (MHC) class I-related chain A
miR	microRNA
MHC	Major Histocompatibility Complex
MMP	Matrix-metalloproteinases
MNC	Mononuclear cell
MR	Mannose Receptor
mRNA	messenger RNA
NI	Neo-intima
NI-LL	Neo-intima, luminal layer
NI-SMC	Neo-intima, smooth muscle cell/myofibroblast layer
PAI1	Plasminogen activator inhibitor 1
pAMR	pathological AMR
PBMC	Peripheral blood mononuclear cell
PDCD4	Programmed cell death protein 4
PD-L1	Programmed death–ligand1
Q-PCR	Quantitative-Polymerase Chain Reaction
RQ	Relative quantity
ScR	Scavenger Receptor
SMC	Smooth Muscle Cell
snRNA	small nucleolar RNA
STAT3	Signal transducer and activator of transcription 3
TGFβ	Transforming growth factor beta
Th	T helper cell
TIMP3	Tissue inhibitor of metalloproteinase 3
TLDA	Taqman low density array
TLO	Tertiary lymphoid organ
TLR	Toll like receptor
TNFα	Tumor Necrosis Factor alpha

Chapter 1.

GENERAL INTRODUCTION

Heart failure

Heart failure affects approximately 23 million people worldwide [1] which is an odd number to understand if applied on the world wide population. If we focus on numbers in the Netherlands it is estimated that between 20-30% of the general population will develop some kind of heart failure after the age of 70 [2]. For the population below the age of 60, the incidence of heart failure is 1 per 1,000 individuals [3]. Although deaths due to acute myocardial infarction are declining (n=6195 in 2012), death rates due to heart failure (acute or chronic) are still rising (n=6761 in 2012 [3]).

Heart failure is a complex syndrome characterized by a structural or functional impairment of ventricular filling or ejection of blood. Most heart failure patients have symptoms due to impaired left ventricular function [4]. Heart failure can be classified based on functional status (New York Heart Association = NYHA, class I-IV; [5]) or based on development and progression of the disease (American College of Cardiology / American Heart Association = ACC/AHA, stage A-D; [6]). The estimated number of patients in ACC/AHA stage D or NYHA class IV is between 15,600 and 156,000 [7]. Patients within these stages of heart failure have limited therapeutic options including extensive medication and especially heart transplantation (HTx) or permanent mechanical circulatory support [4].

In case of acute deterioration of heart failure status and in the absence of a donor heart, mechanical circulatory support, by a left ventricular assist device (LVAD), can be considered. In these cases, LVAD implantation is a lifesaving treatment for patients awaiting heart transplantation [8]. Worldwide, the use of mechanical circulatory support prior to heart transplantation increased to 37% in 2011 due to an increasing disbalance between patients on the waiting list and the availability or donor hearts. This percentage will certainly increase in the coming years. In many cases LVAD implantation is used as 'bridge to transplantation', however it can also be applied as 'bridge to recovery', 'bridge to decision/candidacy', or even 'destination therapy'. With increased experience and success rates of long term LVAD implantation [8], this therapy could be considered an alternative for transplantation (destination therapy; [9]).

Despite improvements in general therapy for heart failure, heart transplantation is still the gold standard for patients with end stage heart failure [10]. It is hampered though, by very limited "resources" and therefore, requires well considered choices for patient selection and inclusion. The current indication for heart transplantation is "end-stage heart disease not remediable by more conservative measures" [11]. The amount of suitable donor organs is often the limiting factor for transplantation [12] resulting in the Netherlands in approximately 40 heart transplantations per year in three academic centers [3] and worldwide more than 4,000 adult heart transplants each year [13]. Data show that the amount of available donor hearts in specifically Europe are decreasing over the years [13].

Heart transplantation and rejection

Short-term survival after heart transplantation has improved significantly by better immunosuppressive therapy and improved surgical with one year survival rates of 90%. Although the survival rates after heart transplantation have increased enormously in the last decade, cardiac allografts still fail in 30% of the cases within 10 years after transplantation[14]. Long-term survival after cardiac transplantation had no such improvements in the last decade [15].

The long-term survival after cardiac transplantation is compromised by several factors [15]. Allograft rejection can be caused by: hyper-acute rejection, acute cellular rejection (ACR), antibody-mediated rejection (AMR) or chronic rejection. In hyper-acute rejection, the allograft is rejected within minutes after transplantation. This is caused by antibodies, directed against allogeneic human leucocyte antigen (HLA) molecules, which are already present in the recipients circulation before transplantation and bind to the donor organ [16]. Donor-specific HLA antibodies can also be produced longer after transplantation which may lead to antibody-mediated rejection (AMR). Acute cellular rejection is mostly seen within the first month(s) after transplantation, when the immune system recognizes the transplanted organ as foreign and initiates rejection [17,18]. This is a T cell mediated immune reaction. Chronic rejection in the heart results in cardiac allograft vasculopathy (CAV) and occurs a few months or even years after transplantation. Multiple factors play a role in this process; not only the immune system (both T and B cell mediated) but also processes like vascular remodeling and fibrosis [14].

Cardiac Allograft Vasculopathy

After heart transplantation, chronic rejection in the form of cardiac allograft vasculopathy (CAV) is often observed. Thirty percent of the patients have CAV at five years after transplantation [17]. CAV is a pathological process that affects the vasculature of the transplanted heart. It is characterized by concentric thickening of the intima of the coronary vessels and the intra-myocardial microvasculature. This leads to a generalized diffuse narrowing of the vessel lumen and subsequently to ischemia in the graft [19]. CAV is difficult to diagnose; in the early stages patients are often asymptomatic, whereas in later stages patients can develop silent myocardial ischemia, recurrent heart failure or even sudden death. Diagnosis of CAV is predominantly performed by coronary angiography which focuses on luminal narrowing of the main coronary vessels. Recently, the ISHLT described guidelines for CAV diagnosis and classification, based on angiographic data [20]. Histo-pathologically, the severity of CAV can be identified at autopsy by the composition of the arterial wall [21].

CAV is often compared to atherosclerosis and although there are similarities, there are several aspects that are CAV specific [19]. In atherosclerosis research, an increasing amount of knowledge is gained about the extensive role of the immune system in the pathogenesis. But what causes the vascular wall changes in CAV? The pathology of CAV has various triggers and is two sided; with first a mainly immunological response resulting in a later fibrotic process.

Triggers for CAV

Various theories about the causes of CAV exist with immunological and non-immunological triggers. Risk factors can be divided into general cardiovascular risk factors and transplant related (immunological and non-immunological) risk factors (**Table 1**). Several reviews described these important risk factors for developing CAV [22–27]. In this introduction the most relevant causes for understanding the development of CAV will therefore be discussed from an immunological and "fibrotic" perspective.

Table 1. Risk factors for cardiac allograft vasculopathy.

Risk factors for CAV are divided into general cardiovascular risk factors and transplant related risk factors.

BMI = Body mass index, CMV = cytomegalovirus, HLA = Human leucocyte antigen

General Cardiovascular	Transplant associated
Smoking	CMV infection
Body weight (BMI>30)	Ischemia-reperfusion injury
Hypertension	Brain death
Hyperlipidemia	HLA mismatch
Diabetes mellitus	Donor specific antibodies
Age	Cold ischemic time
Gender	

Cytomegalovirus

Viral infections have been correlated with accelerated CAV where cytomegalovirus (CMV) is the best known [28]. Opportunistic infections often occur in patients that receive immunosuppressive drugs from which CMV is a major one in HTx-patients. CMV is a virus that invades several cell types that are involved in CAV; SMCs, fibroblasts, macrophages and endothelial cells [29]. By invading coronary artery endothelial cells, a pro-CAV state is created by activation of the recipient's immune system and upregulation of adhesion molecules. This promotes the adhesion, activation and trans-endothelial migration of leukocytes [25]. Furthermore, CMV inhibits the protective NO synthase pathway in endothelial cells, reduces apoptosis of SMCs, stimulates SMC proliferation and increases cytokine production of several cell types, especially the production of IFN-γ [30]. This stimulation of growth factors and the reduction in apoptosis contribute to intimal thickening.

Ischemia reperfusion injury

Transplantation of solid organs is often accompanied by ischemia-reperfusion injury (I-R injury)[31]. During ischemia, the blood supply is interrupted which leads to anaerobic metabolism. Ischemia activates the complement system, which in turn induces immune responses in the donor heart. It has been shown that in this cascade depositions of the complement component mannose-binding lectin (MBL) and C4d can be found at the site of ischemia-reperfusion induced apoptosis [32,33], suggesting that MBL can amplify reperfusion induced inflammation. Animal studies showed reduction of post ischemic myocardial reperfusion injury by depletion of MBL [34]. However, the role of MBL after heart transplantation has not been extensively investigated. Low levels of MBL in the circulation are correlated to an increased incidence of early CAV development and acute rejection episodes. Recipients with MBL deficiency had fewer acute graft rejection episodes compared to patients with normal levels of MBL [35,36].

During reperfusion, reactive oxygen species are released that cause injury to the allograft but also result in upregulation of adhesion molecules on endothelial cells [23]. This is followed by release of stress proteins like heat shock proteins and uric acid [26,31]. These stress proteins can trigger the innate immune system via toll like receptors (TLRs). The activation of TLRs in turn can lead to both innate and adaptive immune responses, described later in this chapter.

Donor related factors

Several donor related factors can influence the development of CAV. Especially brain death of the donor can have a huge impact on the allograft and with that the recipient's prognosis[37]. One of the theories is that brain death results in acute activation of IL-6 receptors [38]. This causes an inflammatory response which may lead to allograft damage and in time to CAV. Another mechanism in brain death includes a calcium overflow injury that affects cardiomyocytes and coronary SMCs, resulting in less efficient contraction of the heart. Furthermore, brain death results in an elevation of matrix metalloproteinases (MMPs) and pro-apoptotic factors which can contribute to the development of CAV [37,39]. Donor age is an important factor in solid organ transplantations, it is correlated with concomitant atherosclerosis of coronary vessels in the graft which might be hard to differentiate from CAV. In HTx patients however, no relation was found between the age of the donor and the severity of CAV [40].

The risk of CAV increases with the number of HLA mismatches between patient and donor, but also the number and duration of cellular rejection episodes increases because mismatched HLA molecules trigger the alloimmune response [24,39,41]. This indicates that, besides other risk factors, also the amount of HLA mismatches between donor and recipient plays an important role in CAV development.

Immunological mechanisms underlying CAV

The general theory is that CAV is mediated by an allo-immune process. An indication for this theory is that CAV only affect donor arteries and not recipient arteries. New evidence to support this shows that patients that receive heart-lung transplantation (HLTx) develop significantly less severe CAV compared to HTx patients. The suggested hypothesis states that this is due to immune tolerance known as 'the combi-effect' [42]. This effect may be related to the relatively high and persistent levels of chimerism induced by the transplanted lung[43]. Meaning that the immune reaction concentrates in the lungs or the immune response distributes across a larger reaction area, which leads to less immune activation in the heart and therefore less CAV. This combi-effect is also seen in heart-kidney transplantation [42]. These data indicate a link between activity of an allo-immune response and the development of CAV.

The human immune system consists of a variety of cells which all play their role in the process of rejection. The main reason why a graft is rejected is because there are major antigenic differences between a donor and a host, expressed as differences in human leukocyte antigen (HLA) on the cell surface [12]. By recognition of the foreign HLA, cellular and humoral immunity is initiated. The cellular immunity can be activated via three pathways: the direct [1], the indirect [2] and the semi-direct [3] pathway. In the direct pathway [1], the major histocompatibility complex (MHC) molecules on the donor cell surface are directly recognized by T cells of the host. When the host T cells encounter the donor APCs, they recognize the foreign MHC complex, with or without antigen-peptide, and become activated[12]. The activation of the T cells takes place in the transplanted heart or after the APCs migrated to the draining lymph nodes [19]. In the indirect pathway [2], the host APCs process donor MHC and present them as antigens to host T cells. The semi-direct pathway [3] involves host APCs that acquire donor MHC via cell-cell contact, which activates the host T cells [12]. Mismatched donor HLA class-I epitopes have to be presented in MHC class-II molecules of recipient APC in order to induce T cell activation, followed by subsequent B cell help resulting in donor specific antibodies. However, not all mismatched HLA class-I epitopes can be presented by patient class-II molecules, as this depends on the binding ability of class-II for the respective allogeneic class-I peptides. This means that specific class-I mismatches may cause allo-immune responses in patients with appropriate MHC class-II molecules, whereas the same class-I mismatches may not lead to allo-responses as they cannot be presented by that patients' class-II molecules [44]. In addition, the sum of HLA class-I epitopes (HLA-A, B and C) expressed by patients may result in the inability of specific (e.g. HLA-A) allogeneic HLA molecules to be recognized as foreign as they are made up of the same patchwork of patient class-I epitopes 45. However, next to these mechanisms other components of the immune system such as the complement system also contribute to rejection of an allograft (**Figure 1. Immunological mechanisms in CAV**).

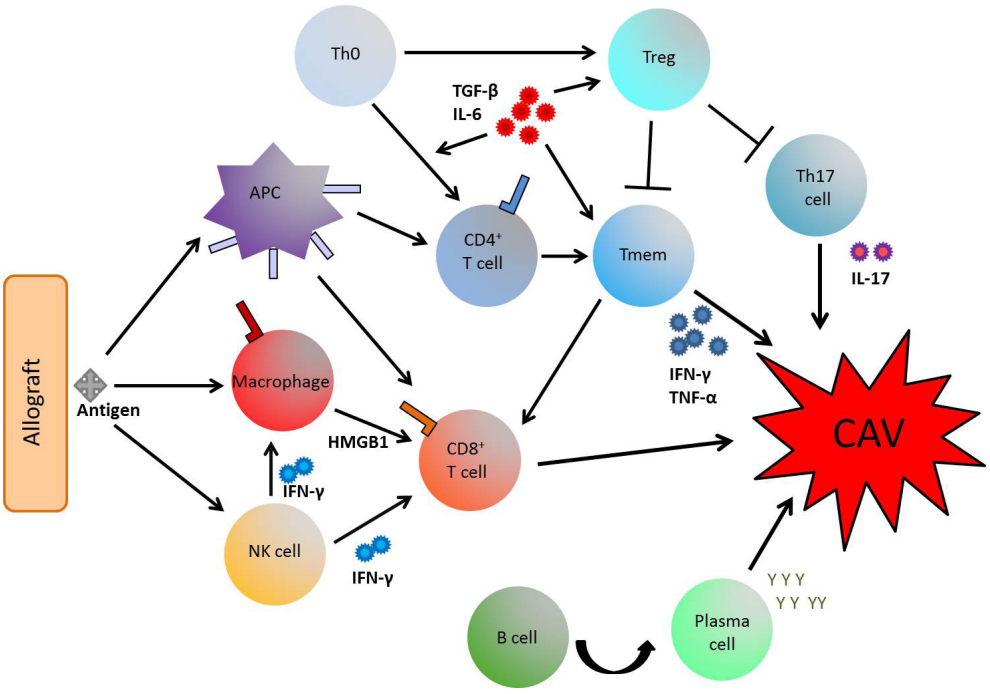

Figure 1. Immunological mechanisms in CAV. Overview of the most important immune cells involved in the development of CAV. The transplanted heart (allograft) is recognized by antigen presenting cells (APC), macrophages and natural killer cells (NK cell). The foreign antigen is taken up by APCs and presented to $CD8^+$ and $CD4^+$ T cells. Macrophages and NK cells take up antigen en attack the allograft directly and/or stimulate $CD8^+$ T cells. Produced cytokines induce regulatory T cells (Treg) and memory T cells (Tmem). The Treg inhibits the activation of Th17 and Tmem cells. B cells do not only differentiate into plasma cells to make antibodies but also support $CD8^+$ T cells. Th17, Tmem, $CD8^+$ T cells together with antibodies can lead to rejection of the transplanted heart.

Adaptive immunity

$CD4^+$ and $CD8^+$ T cells

CAV lesions in HTx patients mainly contain (activated) T cells. These T cells are mostly present in the adventitia and neointima where $CD4^+$ T cells are the majority [46]. Most of the $CD4^+$ T cells were Th1, which correlates with the cytokines and chemokines that were found, mainly TGF-β, IFN-γ and CCR4 [46,47].

As described above, the $CD4^+$ and $CD8^+$ T cells are generally activated by recognition of foreign (allo-)antigens. This recognition is either directly or indirectly via APCs. Besides $CD4^+$/$CD8^+$ cells, also APCs secrete cytokines that can modulate the host T cell response to graft vascular cells and influence the differentiation of naïve T cells [48]. IFN-γ for example, can lead to Th1 and cytotoxic T cell (CTL) differentiation. Also transforming growth factor β (TGF-β) is abundantly present in all vascular layers [47]. TGF-β is a pro-inflammatory and

regulatory cytokine which stimulates the SMCs to migrate into the intima which leads to a profibrotic state. Besides IFN-γ and TGF-β, IL-12 is a key cytokine which promotes CTL differentiation from resting $CD8^+$ T cells, but also supports Th1 initiation and NK cell activation [48].

After HTx the amount of direct alloreactive T cells decreases, but because the processing of foreign donor-antigens by APCs is still continuing, the amount of indirect alloreactive T cells increases [12]. In CAV, many infiltrating lymphocytes express the markers of memory T cells [46,47] suggesting that from the direct alloreactive T cells, the memory T cells are most stable.

Memory T cells

Memory T cells are believed to be important in the process of chronic allograft rejection. If recipients are primed, the memory T cells are alloreactive and may cause rejection episodes [49]. Though it was found that memory T cells are present in CAV lesions, the exact mechanism of how memory T cells contribute to the pathogenesis of CAV is not elucidated yet. The OX40-OX40L interaction has been suggested as one of the activating pathways [50]. OX40-OX40L binding is the result of an interaction between OX40, which is present on T cells, NK cells and neutrophils, and its ligand OX40L which is present on DCs, B cells and endothelial cells. The OX40-OX40L interaction is important for the activation of T cells in general, but also for the survival and homeostasis of memory T cells. After blockage of OX40-OX40L interaction in a mouse model, the memory T cell population in the arteries of HTx mice declined as was the infiltration of $CD4^+$ and $CD8^+$ T cells. As a consequence, these mice developed less severe CAV. This suggests that the memory T cells recruit the effector T cells [50]. Furthermore, memory T cells contribute to the development of CAV by secretion of cytokines, like IFN-γ and TNF-α [50] which are pro-inflammatory, that stimulate the development of CAV.

T helper 17 cells

Next to T helper cells, cytotoxic T cells, and memory T cells, the role of T helper-17 cells in allograft rejection is becoming clear. TGF-β is abundantly present in CAV lesions and can, together with IL-6 or IL-21, differentiate naïve T cells to Th17 cells. Furthermore, IL-6 and IL-21 lead to proliferation of Th17 cells [51]. Th17 cells are differentiated T cells which mainly produce IL-17. Even before the discovery of the Th17 cells a correlation was found between IL-17 and CAV [52]. IL-17 is a pro-inflammatory cytokine and has several other functions; it stimulates production of IL-6, upregulates chemoattractants, and recruits neutrophils to the site of inflammation [52,53]. Human endothelial cells cultured with IL-17 showed an increased expression of several adhesion molecules and inflammatory gene expression in SMCs [54]. This suggests a role for IL-17 in CAV.

To confirm this, IL-17 was tested in a humanized-mouse model for human artery allograft rejection. When IL-17 was neutralized in this model, the graft had a prolonged survival and inhibition of IL-17 showed decreased pro-inflammatory gene expression within the graft [54]. These results indicate that IL-17 contributes to CAV, but does not provide evidence for the involvement of Th17 cells. Recently, it was shown that the severity of CAV was abrogated

in T-bet$^{-/-}$ mice with suppressed Th17 differentiation and functionality[55]. T-bet$^{-/-}$ mice without suppression of Th17 cells displayed a destructive inflammatory response leading to severe CAV and huge neutrophil infiltration [52]. It remains unclear why this severe response is not inhibited by regulatory T cells (Tregs). In a healthy individual, TGF-β expression which induces Th17 cells also initiates the development and differentiation of Tregs in an inverse relation [53].

Regulatory T cells

Tregs are a population of T cells that prevent immune reactions against self-antigens [49]. The best described Treg is a CD4$^+$ T cell that expresses CD25 and FoxP3 induced by TGF-β. One of the theories why Tregs do not inhibit the inflammatory response that initiates CAV, is that differentiated T cells can be modified into another lineage. This means that these T cells can change in case they encounter other signals from the microenvironment, for example they can convert towards Th17 cells by IL-6 [52]. By conversion, the regulatory activity of the Tregs is decreased, which influences the Th17 response and possibly the subsequent CAV development [51,52].

Tregs are shown to be important in inducing tolerance. Recipient mice which were tolerant for their heart allograft showed high levels of Tregs, but when Tregs were depleted, the tolerance was abrogated [49]. This abrogated tolerance might be due to OX40-costimulation between DCs and T cells, that inhibit Treg induction [49]. Furthermore, they discovered that memory T cells inhibit the induction of Tregs *in vitro* and in an *in vivo* mouse model [43].

The role of Tregs in the development of CAV was studied in humans by *ex vivo* expansion of Tregs that were relocated into human arteries and transplanted in a chimeric humanized mouse. By addition of these Tregs, the *in vivo* development of CAV was prevented impairing infiltration and effector function of leukocytes [56]. This inhibitory effect is confirmed in HTx patients resulting in a decrease of Th1 cells that is related to an increase of Tregs, indicating a role for Tregs in the human system, although more research is required for confirmation [57].

γδ T cells are T cells which contain a T cell receptor with a γ- and a δ- chain. γδ T cells make up 5% of the human T cell population [58]. They have the ability to become active without antigen recognition presented on MHC molecules, which makes them contributors to the first line of defense in tissue. Recent reports showed that host γδ T cells might accelerate both acute and chronic allograft rejection [58]. To investigate the role of γδ T cells in CAV, Zhu *et al.* used γδ T cell deficient mice which received heterotopic HTx. The γδ T cell deficiency led to a reduced infiltration of leukocytes and a decreased expression of inflammation initiators IFN-γ and HMGB1, which in turn resulted in an increased allograft survival. Furthermore, they found that the amount of CD25$^+$FoxP3$^+$ Tregs was enlarged compared to the control mice. This also led to less severe CAV and prolonged allograft survival [58]. These results provide further evidence that Tregs play a significant role in maintaining tolerance, and when the Tregs are depleted or suppressed this leads to accelerated CAV.

B cells

Next to the several types of T cells, B cells are also a major contributor to adaptive immunity. B cells are mostly known for their ability to differentiate into plasma cells and produce antibodies, which also contribute to the pathogenesis of CAV. Donor specific antibodies (DSA) are an important risk factor for antibody mediated rejection (AMR) and CAV. They are reactive with human leukocyte antigen (HLA) molecules of the donor or other (donor-related) molecules. Graft endothelial cells express HLA in a high amount, which causes the DSAs to target these cells. By accumulating on the graft endothelial cells, the complement system is activated [37]. Endothelial cells are highly resistant to cell lysis due to expression of CD59 which protects them from complement mediated cell lysis [59,60]. Nevertheless, several studies have indicated that non-complement fixing HLA antibodies can also exert a direct pathogenic effect on the graft [61,62]. Direct effects have been observed by HLA antibodies due to their ability to crosslink HLA molecules on cells. In vitro studies showed that HLA class-I antibodies can activate endothelial cells and induce their proliferation, stimulate exocytosis of granules that contain prothrombotic mediators and increase the production of vascular endothelial growth factor [63–65]. Crosslinking of HLA class-II by antibodies induced apoptosis directly in monocytes and B cells [66,67], and class-II expressing fibroblasts were induced to produce several cytokines, chemokines and prostaglandin E2 [68]. Thus the detrimental effects of HLA antibodies on allografts are both complement dependent and independent, and cross linking of HLA class-I versus -II induces different intracellular effects on targeted cells. However, in 30-50% of all HTx patients with CAV, no detectable circulating antibodies were detected [69]. This does not mean that B cells do not play a role in these patients. B cells also affect T cell responses by, for example, co-stimulation and cytokine production [69]. To find out if B cells might play a role in human HTx, Wehner et al. studied 16 cardiac transplants with advanced chronic rejection. They described infiltrates of B cells and plasma cells mainly in the fibrotic areas of the adventitia and the neo-intima. These infiltrates were significantly more pronounced in arteries affected by CAV than in control arteries [27].

Zeng and colleagues studied the role of antibodies and B cells in CAV with a mouse model. The mice that were depleted of antibodies had the same severity of CAV than control mice. But mice which lacked next to antibodies also B cells showed minimal CAV. Furthermore, CAV was restored in these mice upon an adoptive transfer of B cells that were unable to differentiate into plasma cells [69]. These results suggest that B cells can also contribute to CAV independent of antibodies.

The findings by Zeng *et al*. are contradictory to the results of Gareau et al. They found that antibodies produced by plasma cells are responsible for damaging SMCs in the media of coronary arteries [70]. A further investigation about the possible supporting role of B cells to T cells was performed by Zeng et al. The alloreactive T cell responses were declined in the absence of B cells: both the T cell activity and their cytokine production were reduced.

Taken together it is obvious that the exact role of B cells and antibody production in CAV is not elucidated yet, however clinical studies support a potential role of antibodies [16,71]. How HLA or non-HLA antibodies [72,73] are formed and what their role is in CAV remains to be elucidated.

Innate immunity

Next to cells from the adaptive immune system, also the innate immune system contributes to the immunologic responses that may lead to CAV.

Toll like receptors

CAV is correlated with persistent inflammation where innate toll like receptors (TLR) contribute to the inflammatory state [26]. TLRs are activated by both endogenous and exogenous ligands and are expressed on various cell types such as dendritic cells and epithelial cells. TLRs on epithelial cells are responsible for upregulation of chemoattractants, while TLRs on dendritic cells are important in naïve T cell priming [31].

When tissue damage occurs after HTx, endogenous ligands are released. Also damage-associated molecular pattern molecules (DAMPs) such as heat shock protein [70] (HSP70) and high-mobility group box 1 (HMGB1) are produced [74]. These endogenous ligands signal via TLRs, mostly TLR4. I-R injury can promote a TLR4-dependent response or stimulate pro-inflammatory molecules such as TNF and IL-6 which excites the general alloimmune response. Via these mechanisms, TLRs can be activated after HTx and stimulate both the innate and the adaptive immune response, which can lead to rejection.

Macrophages

Macrophages are professional APCs that act both in the innate and in the adaptive immune response. The exact role of macrophages in CAV is not known, but it is plausible that macrophages play a role in the initiation of the adaptive immune response in CAV, as they are abundantly present in the neo-intima of CAV arteries, and secrete HMGB1 in response to cytokines (IFN-γ and TNF) and TLR ligands [48]. HMGB1 can act on T cells and influences cytokine production or differentiation. Macrophages also contain Fc receptors, which are capable to respond to antibodies that recognize foreign DSA or complement factors. Besides, they also produce growth factors and chemokines, which possibly stimulates the proliferation of the neointima [75].

Depletion of macrophages in mice reduced the development of CAV, whereas inhibition of the phagocytotic capabilities of macrophages did not abrogate the process. Also delayed depletion of macrophages did not diminish CAV. This indicates that macrophages are significant in initiating CAV, although they seemed not to be required in the maintenance of CAV lesions [75].

Natural killer cells

An important player in innate immunity is the natural killer (NK) cell. Until a few years ago, the general concept was that NK cells do not contribute to rejection of solid organs [47]. Recently, there is accumulating evidence that NK cells are involved in the development of CAV after HTx

[76]. When mature NK cells or total NK cells were depleted in mice, CAV decreased significantly or did not develop at all. Furthermore, CAV lesions that did develop were infiltrated by NK cells and macrophages [76]. Also parental-to-F1 HTx demonstrated that NK cells are involved in the development of CAV [77]. Even though the F1 mice are tolerant for the donor antigens, CAV was prospering. As a control, in none of the heart isotransplants CAV developed [77]. After establishing the presence of NK cells in the lesions, their cytotoxicity showed to be significantly higher in the F1 hybrid mice compared to control, causing inflammation and with that CAV [77]. Recipients which were IFN-γ deficient did not develop CAV which supports that NK cells contribute to the pathogenesis of CAV, and the presence of IFN-γ is mandatory. NK cells support maturation of dendritic cells and secrete cytokines such as IFN-γ, which promote an antigen specific $CD8^+$ T cell response [74]. This discovery represents a link between the innate and the adaptive immune system.

NK cells also have been implicated in the pathogenesis of virus-induced CAV. After inoculation of a virus, NK cell activity is increased and graft tolerance reduced [28]. By using the parent-to-F1 strategy in combination with virus inoculation in $Rag^{-/-}$mice, the role of NK cells and CAV in the arteries was measured. Twenty-eight days after HTx, both NK cells and macrophages were found in the CAV lesions of the mice. In contrast, in only 1 out of 7 mice depleted of NK cells CAV developed [28].

Overall, these studies suggest that NK cells do play a significant role in the pathogenesis of CAV. However, the functional studies on NK cells are only performed in mice. No human studies on the functional mechanism of NK cells in CAV have been described.

Complement system

The complement system is a mechanism that is composed by three pathways: the classical, the alternative and the lectin pathway [78]. It can amplify the reaction of both the innate as the adaptive immune system. The complement system is in the pathogenesis of CAV mainly activated by the deposition of DSA to the graft endothelial cells [79]. Human vascular endothelial cells and SMC are sensitive to various components of the complement system. This influences cellular differentiation and proliferation of the intima, which can finally lead to fibrosis [78]. The complement system can modulate a variety of cells among which macrophages, T- and B cells, thereby contributing to the process of CAV [78].

Immune induced Fibrosis

Activation of all these immunological mechanisms has great impact on the heart allograft. Cytokines, chemokines, and pro- and anti-fibrotic factors are secreted by immune cells and influence the various layers of the arterial wall and might lead to coronary artery fibrosis (**Figure 2. Fibrotic mechanisms in CAV**). In especially later stages, vessels which are affected by CAV show outward compensation. Remodeling of the vessel in early stages of CAV preserves the lumen, but is also correlated with reduced endothelial function and SMC contractility [48]. Some research shows that the neo-intima is composed out of two layers: a luminal layer (NI-LL), which is composed out of loose connective tissue with infiltrated mononuclear cells, and a SMC layer (NI-SMC) which contains SMCs or myofibroblasts [46,80]. Although others state that the neo-intima exists of just one layer [81]. Despite these differences, the general concept is that the intima is thickened.

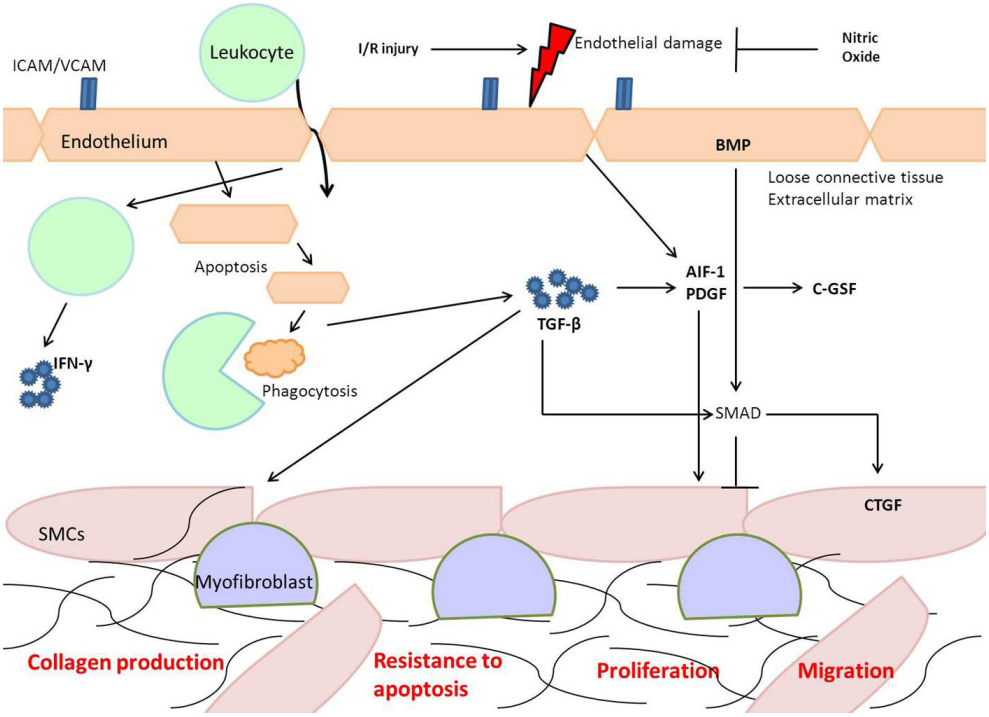

Figure 2. Fibrotic mechanisms in CAV. After heart transplantation, endothelial damage is likely to occur. This results in upregulation of adhesion molecules and leukocytes transmigrating through the endothelial layer. There they produce several cytokines like IFN-γ causing phagocytosis of apoptotic endothelial cells. After phagocytosis, TGF-β is produced. TGF-β stimulates several processes: production of AIF-1 and PDGF, activation of SMAD proteins, resistance to apoptosis and upregulation of collagen production by SMCs. The SMAD proteins that are activated by TGF-β stimulate CTGF production by SMCs, which causes increased proliferation and migration of SMCs. SMAD proteins that are activated by BMP inhibit these SMC processes. The increased collagen production, resistance to apoptosis and increased proliferation and migration of SMCs lead to fibrosis.

Endothelial cells and fibrosis

The endothelial layer in the coronary vessel wall plays an essential role in the perception of signaling and changes in blood pressure [82]. In patients that underwent HTx, the endothelium of the donor heart is the first biological border that the host immune system will recognize. There are a few theories about the role of the endothelium in this process, among which the response to injury theory [83]. The local availability of nitric oxide (NO) is reduced in patients with endothelial dysfunction. Reduction of NO initiated and progressed local oxidative stress and stimulation of inflammatory genes which respond to oxidants [83]. By increased adherence of leukocytes, SMCs are activated by the inflammatory cytokines and migrate from the media to the intima (donor derived) or from the circulation to the intima (host derived) [80,82].

Probably, there are also interactions between the endothelial layer of the donor and the endothelium of the host, but the precise mechanism is not fully elucidated yet. Endothelial cells from the host might integrate in the endothelium of the graft and replace the graft endothelial layer [83,84]. In situ hybridization studies showed that the endothelial cell replacement was mostly present in the small epicardial and intramyocardial vessels, the site where CAV develops first [84,85]. If the graft endothelial layer is damaged, the endothelial cells are discarded, undergo apoptosis and circulate in the blood. The progenitor cells then migrate to the site of injury, will take their place and promote the repair process [84,85].

The role of smooth muscle cells in fibrosis

The majority of cells in the CAV intima are SMCs of which many different sources are described: (1) the intima, the SMCs simply proliferate; (2) the media, the SMCs are migrated which is mostly shown in animal studies [80,86]; (3) progenitor cells present in the medial/adventitial border or (4) circulating host cells, recruited to vessel injury [14]. Some indicate that the neo-intimal SMCs showed a different phenotype than medial SMCs [87]. Others demonstrated that the neo-intimal cells in human coronary arteries were derived from pre-existing donor SMCs or myofibroblasts [88]. Circulating progenitor cells were not involved in the formation of neo-intimal SMCs in this patient group. This contradicts animal studies where host progenitor cells do play a role in neo-intimal SMC formation [87,89].

Also SMCs from an already existing neo-intima can be a source for intimal thickening. Research demonstrated a role for the so called process of 'benign intimal thickening' (BIT). The normal human coronary arteries contain a thickened intima composed of SMCs longitudinal positioned within the artery. This layer developed during life and is lacking in animals. The donor BIT layer is preserved throughout the transplantation procedure [80]. By I-R injury after transplantation, this layer is damaged which causes activation of the immune system finally resulting in an extra CAV intimal layer on top of the BIT [80].

All these studies pin-point sources for the neo-intimal SMCs, but the exact triggers that cause the neo-intima thickening and why the SMCs proliferate, remains to be elucidated.

Allograft inflammatory factor-1

Data from several studies indicate a role for allograft inflammatory factor-1 (AIF-1). AIF-1 is a cytoplasmic calcium-binding protein which is expressed in medial and neo-intimal SMCs in allograft-injured arteries [90]. AIF-1 is solely produced in response to inflammatory cytokines such as IFN-γ and TGF-β. The expression of AIF-1 measured in biopsies from heart transplant recipients was correlated with the development of CAV [91]. AIF-1 stimulates intimal thickening by triggering SMCs to migrate. Next to migration, it also stimulates SMC proliferation by inducing cytokine granulocyte-colony stimulating factor (G-CSF) [90].

Next to AIF-1, growth factors such as platelet-derived growth factor (PDGF) and transforming growth factor (TGF) stimulate SMC proliferation and vascular remodeling. PDGF can be produced by all cells in the arterial wall and infiltrating immune cells [92]. It does not only have a strong chemotactic and mitogenic effect on SMCs but also on fibroblasts [93,94]. The expression of PDGF was significantly increased in arteries that were affected by CAV [93,95]. Although PDGF is expressed in low levels in the wall of healthy arteries, its production is increased after endothelial injury as a result of HTx [92,95].

Other studies demonstrated that all PDGF ligands and receptors are upregulated in the intima during chronic rejection, which resulted in increased TGF-β production in fibroblasts and cardiac fibrosis.

Immune cells causing fibrosis

Next to endothelial cells and SMCs, immune cells contribute to fibrosis by secretion of cytokines and chemokines.

TGF-β and related cytokines

In CAV fibrosis mainly takes place in the Luminal layer of the intima (NI-LL) where large amounts of TGF-β are present [47]. Other research demonstrates that TGF-β promotes fibrosis via T cell signaling [53] and upregulates the collagen synthesis in SMCs. Collagen is one of the most abundant molecules present in the thickened intima [96]. Also MMPs are locally increased by TGF-β and create a positive feedback loop for intimal thickening by boosting the availability of TGF-β [96].

Next to the direct effects of TGF-β, it also induces modulator proteins, like connective tissue growth factor (CTGF), that enhance its effects [96]. CTGF is secreted by SMCs in the ECM after activation of SMAD by TGF-β and is found to be an important mediator in the development of interstitial fibrosis. CTGF increases ECM production, fibroblast proliferation, and enhancement of adhesion by other cells such as leukocytes resulting in increased fibrosis [97].

Part of the TGF-β superfamily is bone morphogenic protein (BMP) which can also activate transcription factors of the SMAD group. Since BMP binds with different affinity to SMAD proteins, the activation gives a different outcome then when TGF-β activates SMAD proteins [98]. Also cell type and environmental triggers affect the actions of SMAD proteins. As

binding of TGF-β to SMAD promotes fibrosis in the heart, binding of BMP to SMAD provides beneficial effects for the heart [98].

Additional research indicated that BMP-7 preserves the endothelial phenotype and reverses the actions of TGF-β. According to several researchers, endothelial cells undergo an endothelial-to-mesenchymal transition (EndoMT) which means that endothelial cells differentiate into cardiac SMC-like and fibroblast-like cells [99,100]. This transition is initiated under influence of TGF-β. The severity of fibrosis is determined by the balance between TGF-β and BMP-7 and the preservation of endothelial function [99].

Next to BMP-7, suppressor of cytokine signaling 1 (SOCS1) is also a preserver of endothelial function [101]. SOCS1 is expressed by endothelial cells as a response to pro-inflammatory cytokines that are released by infiltrating immune cells. The activation of SOCS1 results in a decrease in cytokine production which showed to be essential for the preservation of endothelial function in graft arteriosclerosis [101].

IFN-γ

IFN-γ is one of the most important pro-inflammatory cytokines and produced by several cell types such as $CD8^+$ T cells, Th1 cells and NK cells. In CAV arteries, not only IFN-γ but also IFN-γ inducible chemokines, such as RANTES (regulated on activation, normal T cell expressed and secreted) and ITAC (Interferon-inducible T-cell alpha chemoattractant), were present [46]. Furthermore, IFN-γ and its chemokines were found in the intima and the adventitia but not in the media. Because the SMCs are present in great numbers in the media and are able to inhibit T cells that respond to endothelial cells, this might be the reason why the media layer of the vessel wall is the least infiltrated by T cells in CAV [48].

Next to cells of the immune system, IFN-γ inducible chemokines can also modulate various vascular cells. They stimulate angiogenesis and growth factor-generated SMC proliferation [102]. The effects that IFN-γ inducible chemokines add to the development of CAV, but will not be further discussed. Furthermore, it was found in a human artery graft mouse model that IFN-γ is also able to induce cell proliferation and cell death of SMCs [48]. IFN-γ primes SMCs to Fas-induced apoptosis by relocation of Fas to the cell surface suggesting a role for apoptosis in CAV.

Aim of this thesis

CAV is a disease which has a high prevalence in HTx patients. It is characterized by concentric thickening of the coronary artery wall of the transplanted heart. The pathogenesis of CAV is complex; various cell types from both the host and the donor play a role. Activation of immunological components affects the vasculature of the heart allograft. Although a lot of knowledge is gained about the processes that underlie the pathogenesis of CAV in the past few decades, there are still gaps in our knowledge. By clarifying the exact roles of all these different components, a solution for CAV may come in reach.

We have the unique opportunity to study allograft vasculopathy in hearts after transplantation, collected at autopsy in our Pathology department. Technicians, pathologists, residents, PhD-students, nurse practitioners, cardiologists, cardiothoracic surgeons, and many others were involved to establish this collection. Only this collection made it possible to set up this research.

The aim of this thesis was (1) to study the pathogenesis of Cardiac Allograft Vasculopathy on a morphological, cellular, and even molecular level. Furthermore (2) the purpose of this thesis was to study the role of ectopic lymphoid structures surrounding CAV arteries. Understanding the role of these structures in for example AMR could indicate what therapeutic possibilities there are for future treatment options. Ultimately, we aimed (3) to identify a molecular target against the inducing allograft response and/or the fibrosis, and test the ability of this therapy in a well-established humanized mouse model for CAV.

In **chapter 2** histological phenotypes of CAV are determined and linked to clinical characteristics. Subsequently, the process of fibrosis within the vessel wall is studied in more detail in **chapter 3**. Next to CAV arteries lymphoid clusters are often seen, **chapter 4** reports on the composition of these ectopic lymphoid structures and determines whether these structures resemble tertiary lymphoid organs. Since strong evidence was found for a humoral immune response in these lymphoid structures, the B cell response and antigenic targets of local antibodies are studied in **chapter 5**. Since donor and recipient are involved in CAV, **chapter 6** gives an overview describing both sides of the story. For functional studies on transplant rejection, humanized mouse models can be used which are presented in **chapter 7**. New possible therapeutics for CAV might be found in microRNA regulation. In **chapter 8**, the changes in microRNA expression between CAV and normal arteries is reported. MicroRNAs validated in the human situation were further analyzed in **chapter 9** using a well-established humanized mouse model for CAV. **Chapter 10** contains a general discussion with future perspectives in this field of research.

Part of this chapter is submitted for publication

Manon A.A. Jansen MSc[1], Henny G. Otten PhD[2], Roel A. de Weger PhD[1], Manon M.H. Huibers MSc[1]
Department of Pathology[1] and Laboratory of Translational Immunology[2], University Medical Center Utrecht

References

1. Alraies, M. & Eckman, P. Adult heart transplant: indications and outcomes. *J. Thorac. Dis.* **6**, 1120–8 (2014).
2. Bleumink, G. S. et al. Quantifying the heart failure epidemic: Prevalence, incidence rate, lifetime risk and prognosis of heart failure - The Rotterdam Study. *Eur. Heart J.* **25**, 1614–1619 (2004).
3. Leening, M. J. G. et al. Heart disease in the Netherlands: A quantitative update. *Netherlands Hear. J.* **22**, 3–10 (2014).
4. Yancy, C. W. et al. 2013 ACCF/AHA guideline for the management of heart failure: A report of the American college of cardiology foundation/american heart association task force on practice guidelines. *J. Am. Coll. Cardiol.* **62**, (2013).
5. Hunt, S. A. et al. ACC/AHA 2005 guideline update for the diagnosis and management of chronic heart failure in the adult. *J Am Coll Cardiol* **46**, e1–82 (2005).
6. Hunt, S. A. et al. ACC / AHA Practice Guidelines ACC / AHA Guidelines for the Evaluation and Management of Chronic Heart Failure in the Adult. *J Am Coll Cardiol* **38**, 2101–2113 (2001).
7. Stehlik, J. et al. The Registry of the International Society for Heart and Lung Transplantation: Twenty-eighth Adult Heart Transplant Report--2011. J. *Hear. lung Transplant.* **30**, 1078–94 (2011).
8. Lok, S. I. et al. Corrigendum to "Single-centre experience of 85 patients with a continuous-flow left ventricular assist device: Clinical practice and outcome after extended support" [Eur J Cardiothorac Surg 2013;44: E233-8]. *Eur. J. Cardio-thoracic Surg.* **45**, 400 (2014).
9. Lahpor, J. et al. European results with a continuous-flow ventricular assist device for advanced heart-failure patients. *Eur. J. Cardio-thoracic Surg.* **37**, 357–361 (2010).
10. Carrier, M. & Perrault, L. P. Surgical Treatments for Patients With Terminal Heart Failure: Mechanical Support Compared With Transplantation. *Can. J. Cardiol.* **1**–4 (2014).
11. De Jonge, N. et al. Guidelines for heart transplantation. *Netherlands Hear. J.* **16**, 79–87 (2008).
12. Angaswamy, N. et al. Interplay between immune responses to HLA and non-HLA self-antigens in allograft rejection. *Hum Immunol* **74**, 1478–1485 (2013).
13. Lund, L. H. et al. The registry of the International Society for Heart and Lung Transplantation: thirty-first official adult heart transplant report--2014; focus theme: retransplantation. *J. Hear. lung Transplant.* **33**, 996–1008 (2014).
14. Pober, J. S., Jane-wit, D., Qin, L. & Tellides, G. Interacting mechanisms in the pathogenesis of cardiac allograft vasculopathy. *Arter. Thromb Vasc Biol* **34**, 1609–1614 (2014).
15. Lund, L. H. et al. The Registry of the International Society for Heart and Lung Transplantation: Thirtieth Official Adult Heart Transplant Report--2013; focus theme: age. *J Hear. Lung Transpl.* **32**, 951–964 (2013).
16. Kittleson, M. M. & Kobashigawa, J. A. Antibody-mediated rejection. *Curr Opin Organ Transpl.* **17**, 551–557 (2012).
17. Costello, J. P., Mohanakumar, T. & Nath, D. S. Mechanisms of chronic cardiac allograft rejection. *Tex Hear. Inst J* **40**, 395–399 (2013).
18. Berry, G. J. et al. The 2013 International Society for Heart and Lung Transplantation Working Formulation for the standardization of nomenclature in the pathologic diagnosis of antibody-mediated rejection in heart transplantation. *J. Hear. Lung Transplant.* **32**, 1147–1162 (2013).
19. Angelini, A. et al. Coronary cardiac allograft vasculopathy versus native atherosclerosis: difficulties in classification. *Virchows Arch* **464**, 627–635 (2014).
20. Mehra, M. R. et al. International Society for Heart and Lung Transplantation working formulation of a standardized nomenclature for cardiac allograft vasculopathy-2010. *J. Hear. lung Transplant.* **29**, 717–27 (2010).
21. Lu, W. H. et al. Diverse morphologic manifestations of cardiac allograft vasculopathy: A pathologic study of 64 allograft hearts. *J. Hear. Lung Transplant.* **30**, 1044–1050 (2011).
22. Sanchez Lazaro, I. J. et al. Influence of traditional cardiovascular risk factors in the recipient on the development of cardiac allograft vasculopathy after heart transplantation. *Transpl. Proc* **40**, 3056–3057 (2008).
23. Vassalli, G. et al. Alloimmunity and nonimmunologic risk factors in cardiac allograft vasculopathy. *Eur Hear. J* **24**, 1180–1188 (2003).
24. Valantine, H. Cardiac allograft vasculopathy after heart transplantation: risk factors and management. *J Hear. Lung Transpl.* **23**, S187–93 (2004).
25. Weis, M. & Cooke, J. P. Cardiac allograft vasculopathy and dysregulation of the NO synthase pathway. *Arter. Thromb Vasc Biol* **23**, 567–575 (2003).
26. Schmauss, D. & Weis, M. Cardiac allograft vasculopathy: recent developments. *Circulation* **117**, 2131–2141 (2008).
27. Wehner, J. R. & Baldwin 3rd, W. M. Cardiac allograft vasculopathy: do adipocytes bridge alloimmune and metabolic risk factors? *Curr Opin Organ Transpl.* **15**, 639–644 (2010).
28. Graham, J. A. et al. Viral infection induces de novo lesions of coronary allograft vasculopathy through a natural killer cell-dependent pathway. *Am J Transpl.* **9**, 2479–2484 (2009).
29. Streblow, D. N., Orloff, S. L. & Nelson, J. A. Acceleration of allograft failure by cytomegalovirus. *Curr Opin Immunol* **19**, 577–582 (2007).
30. Potena, L. et al. Acute rejection and cardiac allograft vascular disease is reduced by suppression of subclinical cytomegalovirus infection. *Transplantation* **82**, 398–405 (2006).

31. Obhrai, J. & Goldstein, D. R. The role of toll-like receptors in solid organ transplantation. *Transplantation* **81**, 497–502 (2006).
32. Collard, C. D. et al. Complement activation after oxidative stress: role of the lectin complement pathway. *Am. J. Pathol.* **156**, 1549–1556 (2000).
33. Castellano, G. et al. Therapeutic targeting of classical and lectin pathways of complement protects from ischemia-reperfusion-induced renal damage. *Am. J. Pathol.* **176**, 1648–1659 (2010).
34. Jordan, J. E., Montalto, M. C. & Stahl, G. L. Inhibition of mannose-binding lectin reduces postischemic myocardial reperfusion injury. *Circulation* **104**, 1413–1418 (2001).
35. Fiane, A. E. et al. Low mannose-binding lectin and increased complement activation correlate to allograft vasculopathy, ischaemia, and rejection after human heart transplantation. *Eur Hear. J* **26**, 1660–1665 (2005).
36. Fildes, J. E. et al. Mannose-binding Lectin Deficiency Offers Protection From Acute Graft Rejection After Heart Transplantation. J. Hear. Lung Transplant. **27**, 1353–1356 (2008).
37. Cohen, O., De La Zerda, D. J., Beygui, R., Hekmat, D. & Laks, H. Donor brain death mechanisms and outcomes after heart transplantation. Transpl. Proc **39**, 2964–2969 (2007).
38. Plenz, G. et al. The interleukin-6/interleukin-6-receptor system is activated in donor hearts. *J. Am. Coll. Cardiol.* **39**, 1508–1512 (2002).
39. Colvin-Adams, M. & Agnihotri, A. Cardiac allograft vasculopathy: current knowledge and future direction. *Clin. Transplant.* **25**, 175–184 (2011).
40. Eskandary, F. A. et al. Lack of donor and recipient age interaction in cardiac transplantation. *J Hear. Lung Transpl.* **33**, 629–635 (2014).
41. Crudele, V. et al. Human leukocyte antigen-DR mismatch is associated with increased in-hospital mortality after a heart transplant. *Exp Clin Transpl.* **11**, 346–351 (2013).
42. Guihaire, J. et al. Comparison of cardiac allograft vasculopathy in heart and heart-lung transplantations: a 15-year retrospective study. *J Hear. Lung Transpl.* **33**, 636–643 (2014).
43. Paantjens, A. W. M. et al. Chimerism of dendritic cell subsets in peripheral blood after lung transplantation. *J. Heart Lung Transplant.* **30**, 691–697 (2011).
44. Otten, H. G., Verhaar, M. C., Borst, H. P. E., Hené, R. J. & Zuilen, A. D. Van. Pretransplant donor-specific HLA class-I and -II antibodies are associated with an increased risk for kidney graft failure. *Am. J. Transplant.* **12**, 1618–1623 (2012).
45. Duquesnoy, R. J. The antibody response to an HLA mismatch: A model for nonself-self discrimination in relation to HLA epitope immunogenicity. *Int. J. Immunogenet.* **39**, 1–9 (2012).
46. Van Loosdregt, J. et al. The chemokine and chemokine receptor profile of infiltrating cells in the wall of arteries with cardiac allograft vasculopathy is indicative of a memory T-helper 1 response. *Circulation* **114**, 1599–1607 (2006).
47. Hagemeijer, M. C. et al. T cells in cardiac allograft vasculopathy are skewed to memory Th-1 cells in the presence of a distinct Th-2 population. *Am J Transpl.* **8**, 1040–1050 (2008).
48. Tellides, G. & Pober, J. S. Interferon-gamma axis in graft arteriosclerosis. *Circ Res* **100**, 622–632 (2007).
49. Ge, W. et al. Regulatory T cells are critical to tolerance induction in presensitized mouse transplant recipients through targeting memory T cells. *Am J Transpl.* **10**, 1760–1773 (2010).
50. Wang, H. et al. Memory T Cells Mediate Cardiac Allograft Vasculopathy and are Inactivated by Anti-OX40L Monoclonal Antibody. *Cardiovasc Drugs Ther* **28**, 115–122 (2014).
51. Heidt, S., Segundo, D. S., Chadha, R. & Wood, K. J. The impact of Th17 cells on transplant rejection and the induction of tolerance. *Curr Opin Organ Transpl.* **15**, 456–461 (2010).
52. Chadha, R., Heidt, S., Jones, N. D. & Wood, K. J. Th17: contributors to allograft rejection and a barrier to the induction of transplantation tolerance? *Transplantation* **91**, 939–945 (2011).
53. Faust, S. M. et al. Role of T cell TGFbeta signaling and IL-17 in allograft acceptance and fibrosis associated with chronic rejection. *J Immunol* **183**, 7297–7306 (2009).
54. Rao, D. A. et al. Interleukin (IL)-1 promotes allogeneic T cell intimal infiltration and IL-17 production in a model of human artery rejection. *J Exp Med* **205**, 3145–3158 (2008).
55. Shi, X. et al. Tim-1-Fc suppresses chronic cardiac allograft rejection and vasculopathy by reducing IL-17 production. *Int J Clin Exp Pathol* **7**, 509–520 (2014).
56. Nadig, S. N. et al. In vivo prevention of transplant arteriosclerosis by ex vivo-expanded human regulatory T cells. *Nat Med* **16**, 809–813 (2010).
57. Roldan, C. et al. Correlation of immunological markers with graft vasculopathy development in heart transplantation. *Transpl. Proc* **44**, 2653–2656 (2012).
58. Zhu, H. et al. gammadelta T cell receptor deficiency attenuated cardiac allograft vasculopathy and promoted regulatory T cell expansion. *Scand J Immunol* **78**, 44–49 (2013).
59. Brooimans, R. A., Van der Ark, A. A., Tomita, M., Van Es, L. A. & Daha, M. R. CD59 expressed by human endothelial cells functions as a protective molecule against complement-mediated lysis. *Eur. J. Immunol.* **22**, 791–797 (1992).
60. Budding, K., van de Graaf, E. A. & Otten, H. G. Humoral immunity and complement effector mechanisms after lung transplantation. *Transpl. Immunol.* 8–13 (2014).
61. Tait, B. D. et al. Consensus guidelines on the testing and clinical management issues associated with HLA and non-HLA antibodies in transplantation. *Transplantation* **95**, 19–47 (2013).

62. Otten, H. G. et al. The significance of pretransplant donor-specific antibodies reactive with intact or denatured human leucocyte antigen in kidney transplantation. *Clin. Exp. Immunol.* **173**, 536–543 (2013).
63. Yamakuchi, M. et al. Antibody to human leukocyte antigen triggers endothelial exocytosis. *Proc. Natl. Acad. Sci. U. S. A.* **104**, 1301–1306 (2007).
64. Jindra, P. T. et al. Anti-MHC Class I Antibody Activation of Proliferation and Survival Signaling in Murine Cardiac Allografts. *J. Immunol.* **180**, 2214–2224 (2008).
65. Jindra, P. T., Jin, Y.-P., Rozengurt, E. & Reed, E. F. HLA class I antibody-mediated endothelial cell proliferation via the mTOR pathway. *J. Immunol.* **180**, 2357–2366 (2008).
66. Zand, M. S. et al. Polyclonal rabbit antithymocyte globulin triggers B-cell and plasma cell apoptosis by multiple pathways. *Transplantation* **79**, 1507–1515 (2005).
67. Gross, U., Schroder, A. K., Haylett, R. S., Arlt, S. & Rink, L. The superantigen staphylococcal enterotoxin A (SEA) and monoclonal antibody L243 share a common epitope but differ in their ability to induce apoptosis via MHC-II. *Immunobiology* **211**, 807–814 (2006).
68. Kato-Kogoe, N. et al. Fibroblasts stimulated via HLA-II molecules produce prostaglandin E and regulate cytokine production from helper T cells. *Lab. Invest.* **90**, 1747–1756 (2010).
69. Zeng, Q. et al. B cells mediate chronic allograft rejection independently of antibody production. *J Clin Invest* **124**, 1052–1056 (2014).
70. Gareau, A., Hirsch, G., Lee, T. & Nashan, B. Contribution of B cells and antibody to cardiac allograft vasculopathy. *Transplantation* **88**, 470–477 (2009).
71. Kobashigawa, J. et al. Report from a consensus conference on antibody-mediated rejection in heart transplantation. *J Hear. Lung Transpl.* **30**, 252–269 (2011).
72. Rose, M. L. Role of anti-vimentin antibodies in allograft rejection. *Hum Immunol* **74**, 1459–1462 (2013).
73. Tonsho, M., Michel, S., Ahmed, Z., Alessandrini, A. & Madsen, J. C. Heart transplantation: challenges facing the field. *Cold Spring Harb Perspect Med* **4**, (2014).
74. Millington, T. M. & Madsen, J. C. Innate immunity and cardiac allograft rejection. *Kidney Int Suppl* S18–21 (2010). doi:10.1038/ki.2010.417
75. Kitchens, W. H. et al. Macrophage depletion suppresses cardiac allograft vasculopathy in mice. Am J *Transpl.* 7, 2675–2682 (2007).
76. Hirohashi, T. et al. A novel pathway of chronic allograft rejection mediated by NK cells and alloantibody. *Am J Transpl.* **12**, 313–321 (2012).
77. Uehara, S., Chase, C. M., Colvin, R. B., Russell, P. S. & Madsen, J. C. Further evidence that NK cells may contribute to the development of cardiac allograft vasculopathy. *Transpl. Proc* **37**, 70–71 (2005).
78. Wehner, J., Morrell, C. N., Reynolds, T., Rodriguez, E. R. & Baldwin 3rd, W. M. Antibody and complement in transplant vasculopathy. *Circ Res* **100**, 191–203 (2007).
79. Jane-Wit, D. et al. Alloantibody and complement promote T cell-mediated cardiac allograft vasculopathy through noncanonical nuclear factor-kappaB signaling in endothelial cells. *Circulation* **128**, 2504–2516 (2013).
80. Devitt, J. J. et al. Impact of donor benign intimal thickening on cardiac allograft vasculopathy. J. *Hear. lung Transplant.* **32**, 454–60 (2013).
81. Mitchell, R. N. Graft vascular disease: immune response meets the vessel wall. *Annu Rev Pathol* **4**, 19–47 (2009).
82. Colvin-Adams, M., Harcourt, N. & Duprez, D. Endothelial dysfunction and cardiac allograft vasculopathy. *J Cardiovasc Transl Res* **6**, 263–277 (2013).
83. Hollenberg, S. M. et al. Coronary endothelial dysfunction after heart transplantation predicts allograft vasculopathy and cardiac death. *Circulation* **104**, 3091–3096 (2001).
84. Minami, E., Laflamme, M. A., Saffitz, J. E. & Murry, C. E. Extracardiac progenitor cells repopulate most major cell types in the transplanted human heart. *Circulation* **112**, 2951–2958 (2005).
85. De Weger, R. A. et al. Stem cell-derived cardiomyocytes after bone marrow and heart transplantation. *Bone Marrow Transpl.* **41**, 563–569 (2008).
86. Devitt, J. J., King, C. L., Lee, T. D. & Hancock Friesen, C. L. Early innate immune events induced by prolonged cold ischemia exacerbate allograft vasculopathy. *J Cardiothorac Surg* **6**, 2 (2011).
87. Zheng, Q., Liu, S. & Song, Z. Mechanism of arterial remodeling in chronic allograft vasculopathy. *Front Med* **5**, 248–253 (2011).
88. Atkinson, C. et al. Neointimal smooth muscle cells in human cardiac allograft coronary artery vasculopathy are of donor origin. *J. Hear. Lung Transplant.* **23**, 427–435 (2004).
89. Hillebrands, J. L., Klatter, F. A. & Rozing, J. Origin of vascular smooth muscle cells and the role of circulating stem cells in transplant arteriosclerosis. *Arterioscler. Thromb. Vasc. Biol.* **23**, 380–387 (2003).
90. Chen, X., Kelemen, S. E. & Autieri, M. V. AIF-1 expression modulates proliferation of human vascular smooth muscle cells by autocrine expression of G-CSF. Arter. *Thromb Vasc Biol* **24**, 1217–1222 (2004).
91. Autieri, M. V et al. Allograft inflammatory factor-1 expression correlates with cardiac rejection and development of cardiac allograft vasculopathy. *Circulation* **106**, 2218–2223 (2002).
92. Raines, E. W. PDGF and cardiovascular disease. *Cytokine Growth Factor Rev* **15**, 237–254 (2004).
93. Song, G., Fang, Y., Wang, X., Wu, S. & Song, H. The effects of platelet-derived growth factor in rat cardiac allograft vasculopathy and fibrosis. *Transpl. Proc* **40**, 2716–2719 (2008).

94. Tuuminen, R. et al. PDGF-A, -C, and -D but not PDGF-B increase TGF-beta1 and chronic rejection in rat cardiac allografts. *Arter. Thromb Vasc Biol* **29**, 691–698 (2009).
95. Iida, M., Tanabe, K., Matsushima-Nishiwaki, R., Kozawa, O. & Iida, H. Adenosine monophosphate-activated protein kinase regulates platelet-derived growth factor-BB-induced vascular smooth muscle cell migration. *Arch Biochem Biophys* **530**, 83–92 (2013).
96. Khan, R., Agrotis, A. & Bobik, A. Understanding the role of transforming growth factor-beta1 in intimal thickening after vascular injury. *Cardiovasc Res* **74**, 223–234 (2007).
97. Booth, A. J. et al. Connective tissue growth factor promotes fibrosis downstream of TGFbeta and IL-6 in chronic cardiac allograft rejection. *Am J Transpl.* **10**, 220–230 (2010).
98. Euler-Taimor, G. & Heger, J. The complex pattern of SMAD signaling in the cardiovascular system. *Cardiovasc Res* **69**, 15–25 (2006).
99. Zeisberg, E. M. et al. Endothelial-to-mesenchymal transition contributes to cardiac fibrosis. *Nat Med* **13**, 952–961 (2007).
100. Chen, P. Y. et al. FGF regulates TGF-beta signaling and endothelial-to-mesenchymal transition via control of let-7 miRNA expression. *Cell Rep* **2**, 1684–1696 (2012).
101. Qin, L. et al. SOCS1 prevents graft arteriosclerosis by preserving endothelial cell function. *J Am Coll Cardiol* **63**, 21–29 (2014).
102. Zhao, D. X. et al. Differential expression of the IFN-gamma-inducible CXCR3-binding chemokines, IFN-inducible protein 10, monokine induced by IFN, and IFN-inducible T cell alpha chemoattractant in human cardiac allografts: association with cardiac allograft vasculopathy and. *J Immunol* **169**, 1556–1560 (2002).

Chapter 2.

DISTINCT PHENOTYPES OF CARDIAC ALLOGRAFT VASCULOPATHY AFTER HEART TRANSPLANTATION:

A HISTPATHOLOGICAL STUDY

Manon M.H. Huibers MSc [1], Aryan Vink MD PhD [1], Johannes Kaldeway MD MSc [1], André Huisman PhD [1], Kim Timmermans MSc [1], Max Leenders MSc [2], Marguèrite E.I. Schipper MD [1], Jaap R. Lahpor MD PhD [3], Hans J.H. Kirkels MD PhD [4], Corinne Klöpping MD [4], Nicolaas de Jonge MD PhD [4], Roel A. de Weger PhD [1]

Departments of Pathology [1], Gastroenterology & Hepatology [2], Cardio Thoracic Surgery [3], and Cardiology [4], University Medical Center Utrecht, the Netherlands

Published
Atherosclerosis. 236(2):353-359 (2014)

Abstract

Introduction:
Long-term survival after heart transplantation (HTx) is hampered by cardiac allograft vasculopathy (CAV). Better understanding of the pathophysiological mechanisms of CAV might have considerable consequences for therapeutic approaches in the future. The aim of the present study was to investigate the histological phenotypes of CAV in relation with clinical patient characteristics.

Methods and results:
Coronary cross-sections from 51 HTx patients were obtained at autopsy. Four histological CAV phenotypes were identified (H-CAV 0-3). H-CAV 0 is as seen in normal coronary arteries; only a single layer of longitudinal oriented smooth muscle cells. In H-CAV 1 to 3 a second intimal layer is formed on top of the longitudinal oriented smooth muscle cell layer with predominantly (H-CAV 1) mononuclear inflammatory infiltrate in loose connective tissue, (H-CAV 2) a second layer of smooth muscle cells in different orientation, or (H-CAV 3) a fibrotic intimal lesion. H-CAV stage was significantly related with time after transplantation, age at transplantation, the amount of atherosclerotic disease and the occurrence of infection. In addition, morphometric analysis revealed that higher H-CAV types have a relatively larger intimal area, accompanied by a thinner media and unaltered luminal area.

Conclusions:
CAV in an ongoing process that can be classified into four different phenotypes. These phenotypes are related to time after transplantation, age at transplantation, the amount of atherosclerotic disease and the occurrence of infection. Our results suggest that early CAV consists of high inflammatory lesions, whereas longer after transplantation a more fibrotic phenotype of CAV can be observed.

Introduction

Currently, heart transplantation (HTx) is the last treatment option for patients with end-stage heart failure. The incidence of acute rejection after HTx has decreased remarkably over the last 20 years [1]. However, Cardiac Allograft Vasculopathy (CAV), which has great impact on long-term survival, remains difficult to treat. CAV [2,3] is characterized by wall thickening of the coronary arteries dissimilar to classic atherosclerosis [4]. Thickening of the intimal layer in CAV causes progressive luminal narrowing [5,6] which in some patients can already be detected within the first year after HTx [7].

Intimal thickening is present in normal coronary arteries and starts to develop during childhood 8. Intimal thickening exists of a longitudinal layer of smooth muscle cells (SMCs) [6,9] covered by endothelial cells. In CAV the neo-intima consists of two layers: the original intimal thickening that has been developed in the donor consisting of SMCs lying adjacent to the internal elastic layer (IEL) and an extra (new) inner layer at the luminal side consisting of loose connective tissue, smooth muscle cells and infiltrated mononuclear cells (MNCs) [6,10,11] covered by endothelial cells. This inflammatory infiltrate is driven by an immune reaction underlying this process of CAV [12,13]. The MNCs are captured in diffusely organized fibrous tissue [14]. The intimal fibrotic process is likely caused by T-cells producing interferon gamma (IFNγ) and transforming growth factor beta (TGFβ) which induces the growth of the connective tissue [15-18].

For clinical purposes the ISHLT proposed a standardized way to define CAV using angiography [19]. In addition, intra vascular ultrasound (IVUS) can be used to characterize this process [20,21]. However, both these techniques do not display the exact composition of the arterial wall. For now this composition can only be visualized by histopathology of explanted hearts after re-transplantation or autopsy hearts from HTx-patients. In this way the histology of CAV has been described [22], but no studies have associated histological findings with measurements for quantitative analysis and clinical patient characteristics.

In atherosclerotic plaque development, luminal narrowing can be compensated for by expansive remodeling of the arterial wall thereby preventing luminal stenosis of the artery [23]. Recently it has been demonstrated in IVUS studies that also in CAV the lumen can be preserved by outward remodeling of the arterial wall [24,25].

The aim of the present study was to examine the composition and amount of CAV in relation to time after transplantation and clinical patient characteristics. In addition we studied arterial remodeling of the CAV arteries.

Materials and Methods

Patient population

The study was performed in the University Medical Center Utrecht, The Netherlands. Coronary arteries from HTx patients were collected at autopsy. From 1985 until 2011 465 patients underwent HTx of which 185 patients died. In 93 patients autopsy was performed; in the other 92 patients this was not performed because of logistical reasons. In 51 of the 93 patients, enough coronary arteries were collected, allowing analysis.

All patients were initially treated with triple immunosuppressive therapy: cyclosporine / azathioprine / prednisone or tacrolimus / mycophenolate mofetil / prednisone. In both regimens prednisone was discontinued within the first year. No sirolimus or everolimus was used in these patients, except in one.

Normal coronary arteries from autopsies of non-transplanted adult (n=4) and pediatric patients (n=3) with a non-cardiac death were used as controls. All research was performed on material originally obtained for diagnostic purposes. The study met the criteria of the code of proper use for human tissue that is used in The Netherlands [26].

Clinical patient characteristics

Clinical patients characteristics, described as risk factors for CAV were collected from the patients charts of all 51 HTx patients [27-29]. These parameters were: patient age at HTx, donor age, age difference between patient and donor, type of immunosuppressive therapy (cyclosporine / tacrolimus), gender and gender mismatch of patient and donor, HLA mismatch (0-6), primary cardiac diagnosis of the patient (dilated cardiomyopathy / ischemic heart disease / congenital heart disease / hypertrophic cardiomyopathy / restrictive cardiomyopathy), ischemic time of the donor heart, occurrence of acute cellular rejection according to the ISHLT consensus criteria (yes/no and amount of episodes; [30]), and occurrence of infection (no infection / CMV infection / any other infection). In addition the time after transplantation and the cause of death were recorded.

(Immuno)histochemistry

Consecutive tissue sections of Formalin Fixed and Paraffin Embedded (FFPE) coronary arteries were stained with haematoxylin and eosin (H&E) and Elastic von Gieson (EvG). A selection of sections was also stained immunohistochemically for α-smooth muscle actin (αSMA) to study vessel wall composition.

Analysis of CAV vessels

We defined four phenotypes to classify CAV in histological sections (H-CAV) based on the amount of MNCs and the amount and density of connective tissue: histological-CAV (H-CAV) 0, 1, 2, and 3 (**Figure 1**). H-CAV 0, no or only a few scattered MNCs in the intimal layer with normal pre-existing intimal thickening with longitudinal arranged smooth muscle cells. H-CAV 1, loose connective tissue containing MNC infiltrate on top of the pre-existing neo-intima SMC layer (NI-SMC), forming a Neo-Intima luminal layer (NI-LL). H-CAV 2, NI-LL with more solid connective tissue with abundant presence of αSMA positive cells. H-CAV 3, NI-LL consisting of dense connective tissue with only few αSMA positive cells or MNC.

Atherosclerosis was recognized by predominantly eccentric plaque formation in the vessel wall as previously described [8] and scored according to the extent in the slides (no = no signs of atherosclerosis, minor = less than 50% of the circumference of the coronary wall is affected, and abundant = more than 50% of the circumference is affected).

Each arterial section was scored for the H-CAV stage in a blinded way. All patients were assigned one H-CAV stage by analyzing the H&E and αSMA stains of all coronary arteries available of the patient. When more sections per patient were scored, the mean H-CAV score was taken and rounded to a whole number (namely 0, 1, 2, or 3). When atherosclerosis was seen, the sections without plaque formation were scored for H-CAV stage. The phenotypes of H-CAV were initially determined by two independent observers, in case of disagreement the case was revised at a multi-head microscope until consensus was reached. Weighted quadratic kappa between both observers was moderate (k=0.6).

Coronary artery morphometric measurements

The EvG stains were used for morphometric measurements. Slides were converted to digital format at 200x enlargement by an AperioScanScope XT scanner (Vista, CA, USA) equipped with Olympus 20x objectives (NA 0.75 plan apo) and a resolution of 0.50 µm/pixel. Measurements were performed using ImageScope software (Aperio version 10.0.36.1805). Lines were manually drawn along the external elastic layer (EEL), the IEL, the NI-SMC/NI-LL border and the endothelial layer (**Supplemental Figure S1**). The surface area within these lines was calculated by the ImageScope software and expressed in μm^2. Cross-sectional areas of the media, NI-SMC, NI-LL and whole NI layer were calculated as follows: area within EEL - area within IEL = area media; area within IEL - area within SMC-LL border = area NI-SMC; area within SMC-LL border - area lumen = area NI-LL. When comparing vessels between patients, areas were expressed as fractions of total vessel cross-sectional area (area within EEL). When more sections per patient were measured, the mean fraction per patient was calculated and expressed as "relative surface area".

Statistics

The normality assumption of variables was tested using a Kolmogorov-Smirnov test. Mann-Whitney U tests (with Bonferroni correction) and Kruskal-Wallis tests were used to compare non-normally distributed continuous parameters. A Jonckheere-Terpstra test was done to verify the assumption that an increasing H-CAV stage is related to longer time post-HTx. Fisher's exact tests were performed to analyze the relation between two categorical parameters. Normally distributed factors were compared using a one-way analysis of variance (ANOVA) with Bonferoni correction. For the measured coronary arteries, the relative surface areas of total vessel cross-sectional area of every layer were averaged per patient and their values plotted against the H-CAV type. Data were analyzed using SPSS version 15.0. P-values <0.05 were considered statistically significant for all analyses.

Results

Baseline clinical patient characteristics

Baseline patient characteristics are presented in **table 1**. Due to the fact that the study population also included patients from the eighties and nineties (inclusion 1985-2011), the number of deaths caused by acute cellular rejection is high (25.5%) and the median survival low (1.17 years). This survival time is shorter than the average survival time in our center, but is biased by the fact that relatively more patients within the first years after the transplantation were presented for autopsy, because patients that survive longer after HTx are often not presented at the hospital for autopsy. During transplantation the amount of atherosclerotic disease in the donor hearts was investigated by palpation or coronary angiography. Of the 51 donor hearts, palpation was recorded as normal in 42 out of 44 cases (96%) and when angiography was done this was diagnosed as normal in 7 out of 8 cases (88%). The only angiography that was diagnosed as abnormal showed a 50-70% stenosis distally in the LAD and RCX. The two patients with abnormal palpation recordings showed only mild plaque formation in the distal end of the RCA.

Table 1. Patient characteristics. [a] values (percentage), [b] mean (standard deviation), [c] median (interquartile range). HTx = Heart Transplantation, LVAD = Left Ventricular Assist Device, CAV = Cardiac Allograft Vasculopathy

	Characteristics	**n**		
RECIPIENT	Gender male [a]	51	39	77%
	Primary cardiac diagnosis [a]	50		
	- Dilated cardiomyopathy		19	37%
	- Ischemic cardiomyopathy		27	53%
	- Congenital heart disease		1	2%
	- Hypertrophic cardiomyopathy		1	2%
	- Restrictive cardiomyopathy		2	4%
	Cardiovascular risk factors			
	- High cholesterol [a]	33	9	27%
	- Hypertension [a]	33	5	15%
	- Diabetes mellitus [a]	33	3	9%
	- Current smoker [a]	33	1	1%
	- Past smoker [a]	33	21	64%
	- BMI [b]	48	24.3	(3.5)
TRANSPLANT				
	Age at HTx (years) [b]	51	47	(11.1)
	Donor age (years) [b]	50	42	(10.6)
	Donor angigraphy normal [a]	8	7	88%
	Donor palpation heart normal [a]	44	42	96%
	LVAD pre-HTx [a]	50	9	18%
AUTOPSY				
	Time post HTX (years) [c]	51	1.17	(0.04-7.05)
	Cause of death [a]	51		
	- Cardiac			
	b) CAV		10	17%
	a) Acute cellular rejection		13	26%
	c) Other		10	20%
	- Vascular (aneurysm/stroke)		2	4%
	- Sepsis (infection)		4	8%
	- Malignancy		2	4%
	- Pulmonary cause		9	18%
	- Unknown		1	2%

Histological phenotypes of CAV

H-CAV 0 was observed in all control coronary arteries. Coronary arteries of HTx patients (505 arterial segments from 51 patients; median [IQR] = 8 [4-14] per patient) were categorized in CAV types (**Figure 1**). No CAV (H-CAV 0) was observed in 9 (18%) patients, 4 of these patients died immediately after HTx (0 days). CAV was observed in 42 patients (82%). From the total study population (n=51), 12 (24%) showed H-CAV 1, 16 (31%) H-CAV 2, and 14 (28%) H-CAV 3. Classical atherosclerosis was found in 35 of the patients (69%); 15 (29%) of these patients showed mild and 20 (39%) more abundant atherosclerosis. In many CAV-cases (15/42) all vessels in each patient showed the same H-CAV stage. In the other patients (27/42) there was maximal a difference of one CAV- stage.

A pinpoint lumen or total occlusion of the lumen was observed in 11/51 (22%) patients. In 4 of these patients a thrombus was superimposed on CAV (all scored as H-CAV 2; **Supplemental Figure S2**). Endothelial damage was observed in all these 4 cases of thrombus formation.

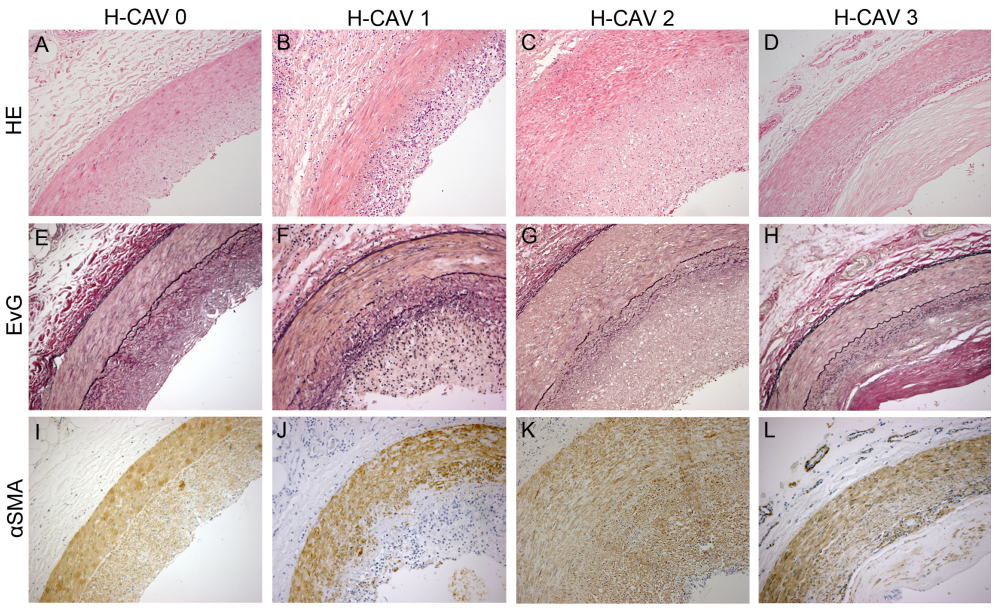

Figure 1. Histological CAV types. Coronary arteries from HTx patients; the four different CAV stages characterized by their histological appearance (H-CAV). Hematoxylin&eosin (HE; A, B, C, D), Elastica von Gieson (EvG; E, F, G, H) and alpha smooth muscle actin (αSMA; I, J, K, L) stains are shown side by side. H-CAV 0 showing media and NI-SMC layer (A, E, I). H-CAV 1 showing lymphocytic infiltrate in NI (B, F, J). αSMA expression in media and NI-SMC layer, but not in NI-LL. H-CAV 2 showing further solidifying NI-LL (C, G, K). αSMA expression in media, NI-SMC and NI-LL. H-CAV 3 showing media, NI-SMC and NI-LL consisting of solid fibrous connective tissue (D, H, L). αSMA expression in media and SMC layer, but hardly in fibrotic connective tissue. Original magnification 100x.

H-CAV phenotypes in relation to clinical patient characteristics

A significant association was found between H-CAV stage and time after HTx (p<0.001; **Supplemental Table S1; Figure 2**). The Jonkheere-Terpstra test revealed a significant trend in the data indicating ascending medians as the H-CAV stage inclines (J=789, z=5.207, r=0.729).

In addition, age at HTx, the number of broad HLA mismatches, bypass time, the occurrence of infection during follow-up, cause of death, and the degree of atherosclerosis were all related to H-CAV stage during autopsy (**Supplemental Table S1; Figure 2**). Results on the number of broad HLA mismatches and bypass time will be further described in the supplemental information.

Patients with H-CAV 3 during autopsy were older at the moment of transplantation than patients that showed H-CAV 1 or 2 (p=0.019 and 0.007 for H-CAV 1 and 2 versus H-CAV-3, respectively). However, no significant association was found between donor age and H-CAV type (p=0.106). Although the presence of infection was associated with H-CAV stage (p=0.011), the type of CMV infection (primary or reactivation) was not associated with H-CAV stage (data not shown). Cause of death was significantly related to H-CAV type at autopsy (n=51, p<0.001). Subgroup analysis of only the cardiac causes of death (n=33: CAV, Acute rejection, or other cardiac cause) revealed that the cause of death is still significantly related to H-CAV type (p<0.001). The degree of atherosclerosis was higher as the H-CAV stage was higher (p=0.007).

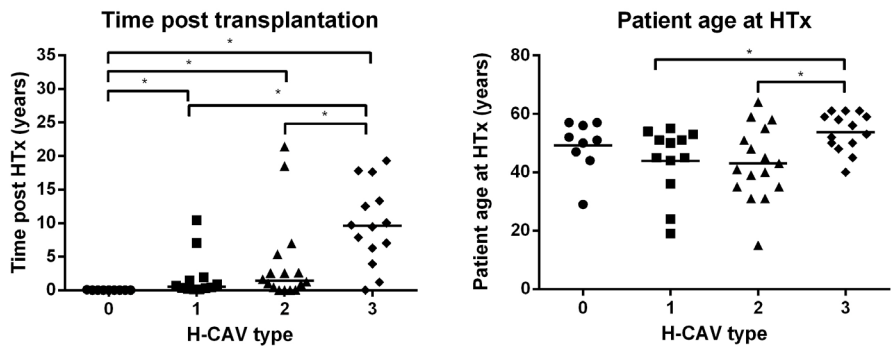

Figure 2. Histological CAV types versus clinical patient characteristics. Time post transplantation (years; Kruskal-Wallis p<0.001) and Patients age at HTx (years; ANOVA p=0.031) are significantly related to H-CAV phenotype. * $p < 0.05$ with Bonferoni correction. HTx = heart transplantation

CAV and arterial remodeling

Morphometric analysis was performed on 323 cross-sections of coronary arteries of 38 patients (median [IQR] 8 [3-12] per patient). The relative cross-sectional area of the different vessel layers was determined per patient and analyzed in relation to their H-CAV stage (**Figure 3**). Higher H-CAV groups revealed a larger relative cross sectional area of the intima (p=0.001). When the intima was divided into a pre-existing intimal thickening (NI-SMC) layer and the newly formed CAV layer (NI-LL), the larger intimal areas in the higher H-CAV types could be totally explained by the NI-LL layer (p=0.002). Strikingly, the increased relative intimal areas in the higher H-CAV types did not lead to a smaller relative luminal area (p=0.277). The relative medial area was smaller in the higher H-CAV types (p=0.001). The relative decrease in media area suggests outward remodeling leading to an increase in diameter of the vessel with stretching of the media.

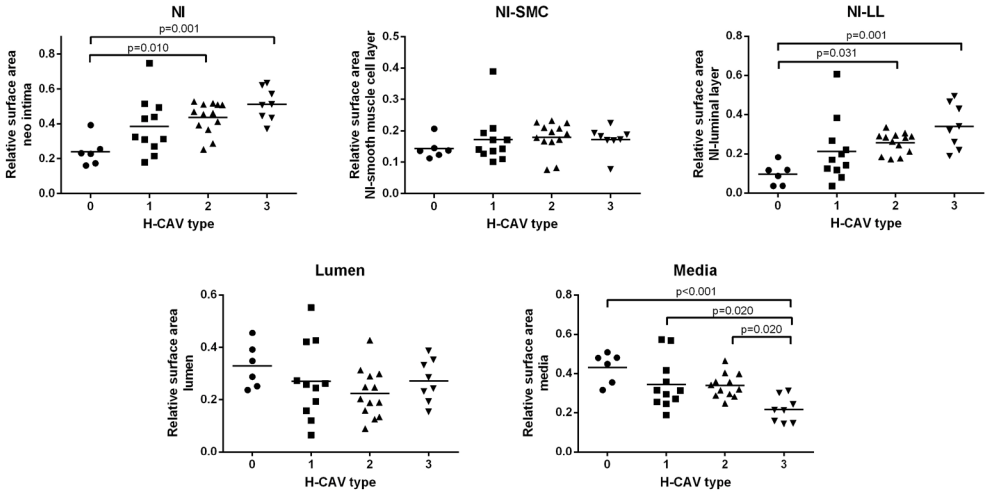

Figure 3. Histological CAV types versus arterial measurements. Relative cross-sectional area of the different vessel layers was determined per patient and analyzed against their H-CAV stage. NI, NI-LL, and medial area showed significant changes between the Histological CAV stages (ANOVA p=0.001, p=0.002, and p=0.001 respectively). NI-SMC (pre-existing intimal thickening) and luminal area did not change over the different H-CAV stages (p>0.05).

Discussion

CAV is widely regarded as a proliferative process induced by an allo-immune response resulting in luminal narrowing [12]. In this post-mortem study we observed three histopathological patterns of CAV: 1. infiltration of mononuclear inflammatory cells in the intima, 2. infiltration of mononuclear cells in combination with smooth muscle cells and loose connective tissue and 3. dense connective tissue without significant inflammatory infiltrate. To the best of our knowledge this is the first study in which different histopathological phenotypes of CAV are related to clinical patient characteristics. H-CAV stage was correlated with time after transplantation, age at transplantation, the amount of atherosclerotic disease and the occurrence infection.

The observation of different H-CAV types is in accordance with the results of Lu *et al* [22] who noted a variety of lesion types in CAV. Their fibromuscular intimal thickening with infiltration of lymphocytes and macrophages might relate to our H-CAV stage 2. In our study H-CAV type was fairly constant in cross-sections of coronary arteries within patients, which is consistent with earlier research [5]. This suggests that CAV is a generalized process affecting all coronary arteries of the patient.

Different H-CAV types were associated with time after the transplantation. This observation is in accordance with results from IVUS studies showing a significant correlation between time post-HTx and the composition of the intimal lesions [20,24]. From our cross-sectional study it is unclear whether these different H-CAV types represent different stages of the same process over time, or represent different patient groups. If these different H-CAV types are sequential stages of the same process, all patients that develop CAV after HTx will run through all H-CAV types. Initially lymphocytes will infiltrate the intima and then a proliferative fibrotic response is induced by this inflammatory reaction.

Another possibility is that different types represent different patient populations: one with very serious CAV that shows a fierce inflammatory reaction (H-CAV 1 and 2 with eventually stenosis) and one with a more gradual CAV with only minimal inflammatory infiltrate. We observed more luminal thrombi in H-CAV 2 with accompanying endothelial damage, suggesting that the inflammatory reaction is more frequently accompanied by damage of endothelial cells and subsequent thrombus formation.

A second interesting finding of this study is the association between different H-CAV types and age at transplantation. Patients with higher H-CAV type (more fibrotic reaction) were older than patients with low H-CAV types (more inflammatory infiltrate). A possible

explanation for this observation could be the fact that aging is frequently associated with a decline in immune function [31,32]. Possibly this chronic inflammatory reaction is less intense in elderly individuals resulting in more chronic fibrotic reaction, whereas in younger individuals a more fierce inflammatory reaction can be observed. We did not find an association between donor age and H-CAV types. Previous studies have found an association between donor age and the onset of CAV, where older donors conferred a higher risk of developing CAV [33,34]. Our end-stage cross-sectional study cannot determine the influence of risk factors on the 'onset' of CAV, but can only state if the risk factor is related to the CAV phenotype after death. Therefore, our data cannot directly be translated to previous studies where CAV-onset is recorded in time with the use of angiography.

A third observation in this study was the correlation between H-CAV stage and the presence of atherosclerotic lesions. In most cases a distinction between atherosclerotic lesions and CAV was possible. Most atherosclerotic lesions are eccentric and contain an atheroma consisting of extracellular lipids, whereas CAV is concentric and mostly consisting of smooth muscle cells and connective tissue with or without an infiltrate of lymphocytes. We observed that in some arteries the CAV related NI-LL proliferation covers the atherosclerotic plaque, suggesting that already existing atherosclerotic plaques in the donor heart might influence the histological outcome of CAV in the recipient. This is in line with an IVUS study that demonstrated that the presence of a necrotic core early after HTx is linked to older donor age, suggesting that part of the lesions had already developed in the donor [20]. A possible explanation for the observed correlation between H-CAV stage and presence of atherosclerotic lesions might therefore be that the atherosclerotic lesions had already been developed in the donor, thereby making the intimal layer and the endothelium of the coronary arteries more vulnerable for the development of intimal lesions induced by the chronic immune reaction of the CAV. Recently it was demonstrated that also in children atherosclerotic lesions containing atheromas can be observed after transplantation suggesting that not all atherosclerotic lesions develop before the transplantation [22]. This was confirmed in an IVUS study where atherosclerotic lesions became more prevalent with time post-HTx, especially in patients with cardiovascular risk factors like male gender and diabetes [20]. If these atherosclerotic lesions develop after the transplantation, it might be inferred from our study that patients or donor hearts that are prone to develop atherosclerotic lesions also develop more fibrotic CAV lesions as compared to patients without development of atherosclerotic lesions in the transplanted heart. Atherosclerosis and CAV are both slowly developing lesions in an older recipient group in which multiple factors such as cardiovascular risk factors might play a role. Therefore the development of H-CAV 3 lesions might be influenced by multiple factors.

The final observation of our study was the correlation between infection and H-CAV stage at autopsy. This finding confirms the results of a previous study where CMV-positive recipients had more plaque burden and greater plaque area in coronary arteries after heart transplantation [20,35].

Due to the fact that the study population also includes patients from the eighties and nineties of the last century, the percentage of acute cellular rejection is relatively high. In addition, median survival of the study population was lower than average survival in our center. This can be explained by the fact that autopsies are more often performed in patients that die in the first years after the transplantation. Due to the high number of missing values in the analysis of acute cellular rejection in relation to H-CAV type, the number of patients studied may be too small to find a statistically significant correlation. Also in the analysis of

recipient cardiovascular risk factors and infection in relation to H-CAV stage the relatively low number of patients might have influenced the results. Within the first period post-transplant patients receive higher immune suppression than later after transplant. This change in overall immunosuppression might have influenced our finding of different phenotypes of CAV that are related to the time after transplantation.

In the clinical setting, most institutions study CAV using coronary-angiography. Also, the ISHLT standardized nomenclature for clinical CAV grading is mainly based on angiography [19,36]. However this technique only displays the lumen of the vessel and does not give information about the composition of the arterial wall and remodeling of the vessel wall will not be detected [19,37]. IVUS has brought improvement due to its possibility to visualize different components of the arterial wall [25,38]. With Virtual Histology IVUS (VH-IVUS) information can be obtained about vessel wall composition [20, 24, 37]. For diagnostic and therapeutic purposes it would be valuable to correlate histological findings with IVUS characteristics.

Early stages of CAV, in a proliferating phase will be more susceptible to therapy than the end-stage, fibrotic types. This has become more urgent since indeed two recent studies showed that treatment with mTOR inhibitors (everolimus or sirolimus) is more effective in early CAV than in later CAV stages [39, 40]. This indicates that information about the composition of the arterial wall is crucial for future therapeutics in CAV.

The higher H-CAV types revealed a bigger relative area of the NI confirming that the higher H-CAV lesions are in general larger. When the intimal layer was divided in a pre-existing intimal hyperplasia / atherosclerosis layer and a CAV layer, the increased size of the intimal layers could be totally explained by the luminal CAV layer. This, however, did not result in progressive luminal narrowing, as no significant difference between the different H-CAV types was seen. The fact that the relative area of the media was smaller in the higher H-CAV types suggests stretching of smooth muscle cells and that outward remodeling of the vessel compensated for the increased intimal area, thereby preventing the lumen from narrowing. This is in accordance with previous IVUS observations [24, 25].

Although remodeling takes place, CAV is noted as a major cause of death later after transplant. The current study examined epicardial coronary which we demonstrated to have the ability to outward-remodel. However, the smaller (micro)vaculature within the heart might not be able to remodel and that is the place where occlusion of the arteries can be detected first. The occlusion of these small vessels causes tiny myocardial infarctions that eventually result in a patchy fibrotic structure within the myocardium potentially leading to recurrence of heart failure and death.

In summary, CAV lesions can be divided in different phenotypes that are associated with time after HTx, age, accompanying atherosclerotic lesions and infections. The higher stages of CAV consist of larger intimal lesions which do not lead to more luminal stenosis due to outward remodeling of the vessel wall. The characterization of these H-CAV types may be important for the choice of future therapeutics. A schematic overview of these results is presented in **figure 4**.

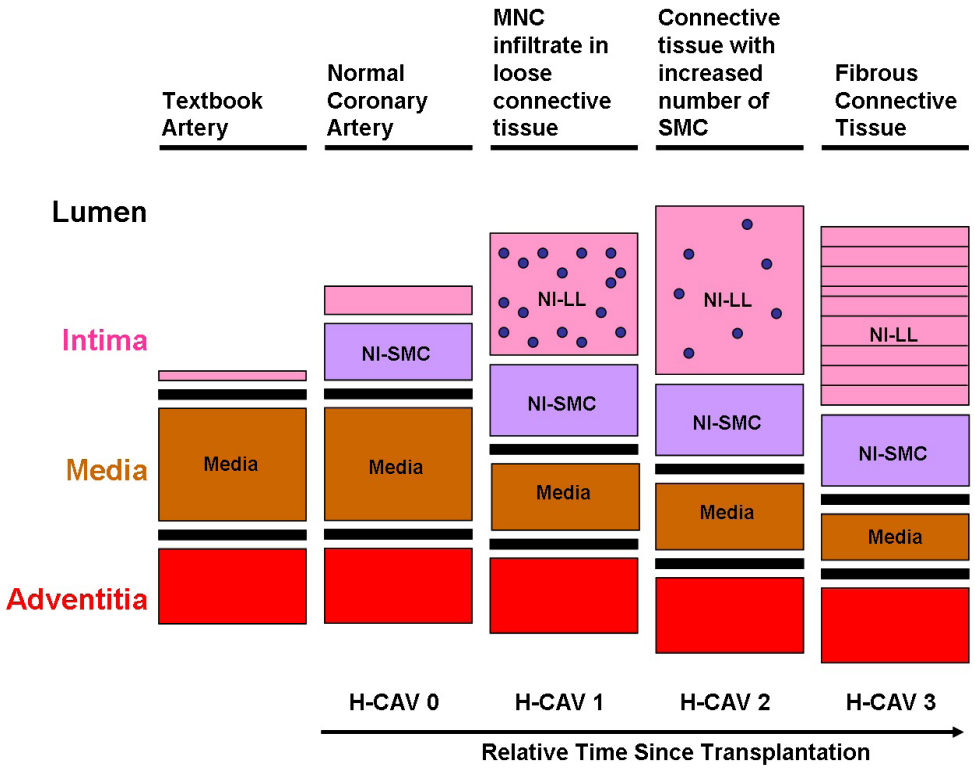

Figure 4. Schematic presentation of CAV. The left panel demonstrates the coronary artery of a newborn. Changes in vessel wall architecture are displayed as relative in time since transplant and H-CAV type. Early after transplantation the NI-LL is infiltrated by T-lymphocytes as a consequence of rejection. In reaction to this infiltration loose connective tissue becomes more solid and eventually results in a fibrous layer. After a peak in NI thickness and luminal narrowing, this process is reversed. As the media progressively gets thinner over time, the SMC layer seems relatively spared. The speed and intensity of this process varies between individuals, so no definite values can be set along the axes. H-CAV=Histological Cardiac Allograft Vaculopathy, NI-LL=neo intima luminal layer, NI-SMC=neo intima smooth muscle cell layer, MNC=mononuclear cell.

Acknowledgements

We would like to acknowledge H.G. Otten, PhD for his help on HLA mismatch analysis.

References

1. Stehlik,J. et al. The registry of the International Society for Heart and Lung Transplantation: 29th official adult heart transplant report-2012. *J. Heart Lung Transplant.* **31**, 1052-1064 (2012).
2. Billingham,M.E. Cardiac transplant atherosclerosis. *Transplant. Proc.* **19**, 19-25 (1987).
3. Crespo-Leiro,M.G., Marzoa-Rivas,R., Barge-Caballero,E., & Paniagua-Martin,M.J. Prevention and treatment of coronary artery vasculopathy. *Curr. Opin. Organ Transplant.* **17**, 546-550 (2012).
4. Rahmani,M., Cruz,R.P., Granville,D.J., & McManus,B.M. Allograft vasculopathy versus atherosclerosis. *Circ. Res.* **99**, 801-815 (2006).
5. Billingham,M.E. Histopathology of graft coronary disease. *J. Heart Lung Transplant.* **11**, S38-S44 (1992).
6. van Loosdregt,J. et al. The chemokine and chemokine receptor profile of infiltrating cells in the wall of arteries with cardiac allograft vasculopathy is indicative of a memory T-helper 1 response. *Circulation* **114**, 1599-1607 (2006).
7. Yeung,A.C. et al. Incidence and progression of transplant coronary artery disease over 1 year: results of a multicenter trial with use of intravascular ultrasound. Multicenter Intravascular Ultrasound Transplant Study Group. *J. Heart Lung Transplant.* **14**, S215-S220 (1995).
8. Virmani,R., Kolodgie,F.D., Burke,A.P., Farb,A., & Schwartz,S.M. Lessons from sudden coronary death: a comprehensive morphological classification scheme for atherosclerotic lesions. *Arterioscler. Thromb. Vasc. Biol.* **20**, 1262-1275 (2000).
9. Devitt,J.J. et al. Impact of donor benign intimal thickening on cardiac allograft vasculopathy. *J. Heart Lung Transplant.* **32**, 454-460 (2013).
10. Atkinson,C. et al. Neointimal smooth muscle cells in human cardiac allograft coronary artery vasculopathy are of donor origin. *J. Heart Lung Transplant.* **23**, 427-435 (2004).
11. Hagemeijer,M.C. et al. T cells in cardiac allograft vasculopathy are skewed to memory Th-1 cells in the presence of a distinct Th-2 population. *Am. J. Transplant.* **8**, 1040-1050 (2008).
12. Mitchell,R.N. Graft vascular disease: immune response meets the vessel wall. *Annu. Rev. Pathol.* **4**, 19-47 (2009).
13. Valantine,H.A. Cardiac allograft vasculopathy: central role of endothelial injury leading to transplant "atheroma". *Transplantation* **76**, 891-899 (2003).
14. Johnson,D.E., Gao,S.Z., Schroeder,J.S., DeCampli,W.M., & Billingham,M.E. The spectrum of coronary artery pathologic findings in human cardiac allografts. *J. Heart Transplant.* **8**, 349-359 (1989).
15. Huibers,M. et al. Intimal fibrosis in human cardiac allograft vasculopathy. *Transpl. Immunol.* **25**, 124-132 (2011).
16. Lebastchi,A.H. et al. Transforming growth factor beta expression by human vascular cells inhibits interferon gamma production and arterial media injury by alloreactive memory T cells. *Am. J. Transplant.* **11**, 2332-2341 (2011).
17. Tellides,G. et al. Interferon-gamma elicits arteriosclerosis in the absence of leukocytes. *Nature* **403**, 207-211 (2000).
18. Tellides,G. & Pober,J.S. Interferon-gamma axis in graft arteriosclerosis. *Circ. Res.* **100**, 622-632 (2007).
19. Mehra,M.R. et al. International Society for Heart and Lung Transplantation working formulation of a standardized nomenclature for cardiac allograft vasculopathy-2010. *J. Heart Lung Transplant.* **29**, 717-727 (2010).
20. Hernandez,J.M. et al. Virtual histology intravascular ultrasound assessment of cardiac allograft vasculopathy from 1 to 20 years after heart transplantation. *J. Heart Lung Transplant.* **28**, 156-162 (2009).
21. Tsutsui,H. et al. Lumen loss in transplant coronary artery disease is a biphasic process involving early intimal thickening and late constrictive remodeling: results from a 5-year serial intravascular ultrasound study. *Circulation* **104**, 653-657 (2001).
22. Lu,W.H. et al. Diverse morphologic manifestations of cardiac allograft vasculopathy: a pathologic study of 64 allograft hearts. *J. Heart Lung Transplant.* **30**, 1044-1050 (2011).
23. Glagov,S., Weisenberg,E., Zarins,C.K., Stankunavicius,R., & Kolettis,G.J. Compensatory enlargement of human atherosclerotic coronary arteries. *N. Engl. J. Med.* **316**, 1371-1375 (1987).
24. Konig,A. et al. Assessment and characterization of time-related differences in plaque composition by intravascular ultrasound-derived radiofrequency analysis in heart transplant recipients. *J. Heart Lung Transplant.* **27**, 302-309 (2008).
25. Torres,H.J. et al. Prevalence of cardiac allograft vasculopathy assessed with coronary angiography versus coronary vascular ultrasound and virtual histology. *Transplant. Proc.* **43**, 2318-2321 (2011).
26. van Diest,P.J. No consent should be needed for using leftover body material for scientific purposes. *For. BMJ* **325**, 648-651 (2002).
27. Kobashigawa,J. What is the optimal prophylaxis for treatment of cardiac allograft vasculopathy? *Curr. Control Trials Cardiovasc. Med.* **1**, 166-171 (2000).
28. Rhodes,L.R. Cardiac allograft vasculopathy. *Crit Care Nurs. Q.* **27**, 10-16 (2004).
29. Stehlik,J. et al. The Registry of the International Society for Heart and Lung Transplantation: Twenty-eighth Adult Heart Transplant Report--2011. *J. Heart Lung Transplant.* **30**, 1078-1094 (2011).
30. Stewart,S. et al. Revision of the 1990 working formulation for the standardization of nomenclature in the diagnosis of heart rejection. *J. Heart Lung Transplant.* **24**, 1710-1720 (2005).
31. Goronzy,J.J. & Weyand,C.M. Understanding immunosenescence to improve responses to vaccines. *Nat. Immunol.* **14**, 428-436 (2013).
32. Martins,P.N. et al. Age and immune response in organ transplantation. *Transplantation* **79**, 127-132 (2005).
33. Nagji,A.S. et al. Donor age is associated with chronic allograft vasculopathy after adult heart transplantation: implications for donor allocation. *Ann. Thorac. Surg.* **90**, 168-175 (2010).

34. Stoica,S.C. et al. The cumulative effect of acute rejection on development of cardiac allograft vasculopathy. *J. Heart Lung Transplant.* **25**, 420-425 (2006).
35. Fearon,W.F. et al. Changes in coronary arterial dimensions early after cardiac transplantation. *Transplantation* **83**, 700-705 (2007).
36. Prada-Delgado,O., Estevez-Loureiro,R., Paniagua-Martin,M.J., Lopez-Sainz,A., & Crespo-Leiro,M.G. Prevalence and prognostic value of cardiac allograft vasculopathy 1 year after heart transplantation according to the ISHLT recommended nomenclature. *J. Heart Lung Transplant.* **31**, 332-333 (2012).
37. Cai,Q., Rangasetty,U.C., Barbagelata,A., Fujise,K., & Koerner,M.M. Cardiac allograft vasculopathy: advances in diagnosis. *Cardiol. Rev.* **19**, 30-35 (2011).
38. Logani,S., Saltzman,H.E., Kurnik,P., Eisen,H.J., & Ledley,G.S. Clinical utility of intravascular ultrasound in the assessment of coronary allograft vasculopathy: a review. *J. Interv. Cardiol.* **24**, 9-14 (2011).
39. Masetti,M. et al. Differential effect of everolimus on progression of early and late cardiac allograft vasculopathy in current clinical practice. *Am. J. Transplant.* **13**, 1217-1226 (2013).
40. Matsuo,Y. et al. Attenuation of cardiac allograft vasculopathy by sirolimus: Relationship to time interval after heart transplantation. *J. Heart Lung Transplant.* **32**, 784-791 (2013).

Supplemental information

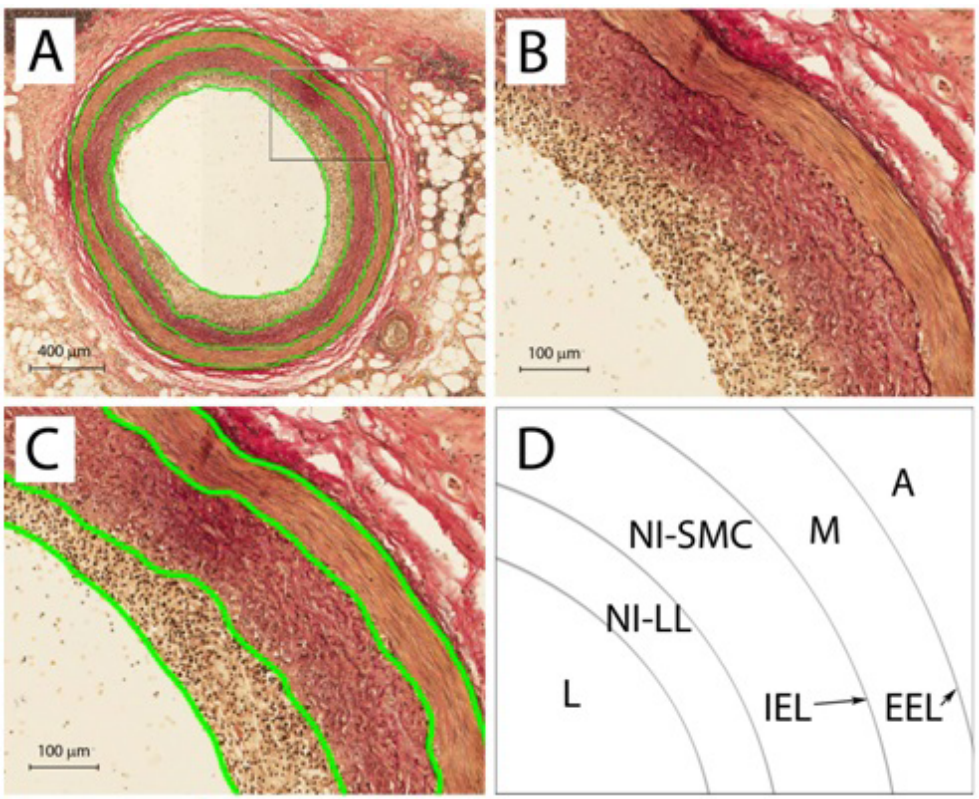

Figure S1. Measurement method. A: Coronary artery with cardiac allograft vasculopathy. Lines are drawn along the EEL, IEL, SMC-LL boundary and lumen. **B**: Enlargement of inset in 'A' showing different layers in detail without lines drawn. **C**: Enlargement of inset in 'A' showing different layers in detail with lines drawn. **D**: Schematic representation of the enlargement in 'C'. All pictures are excerpts from scans, taken from software program Aperio, original magnification 200x. A = Adventitia, EEL = External Elastic Lamina, IEL = Internal Elastic Lamina, L = lumen, NI-LL = Neo Intima Luminal Layer, M = Media, NI-SMC = Neo Intima Smooth Muscle Cell Layer

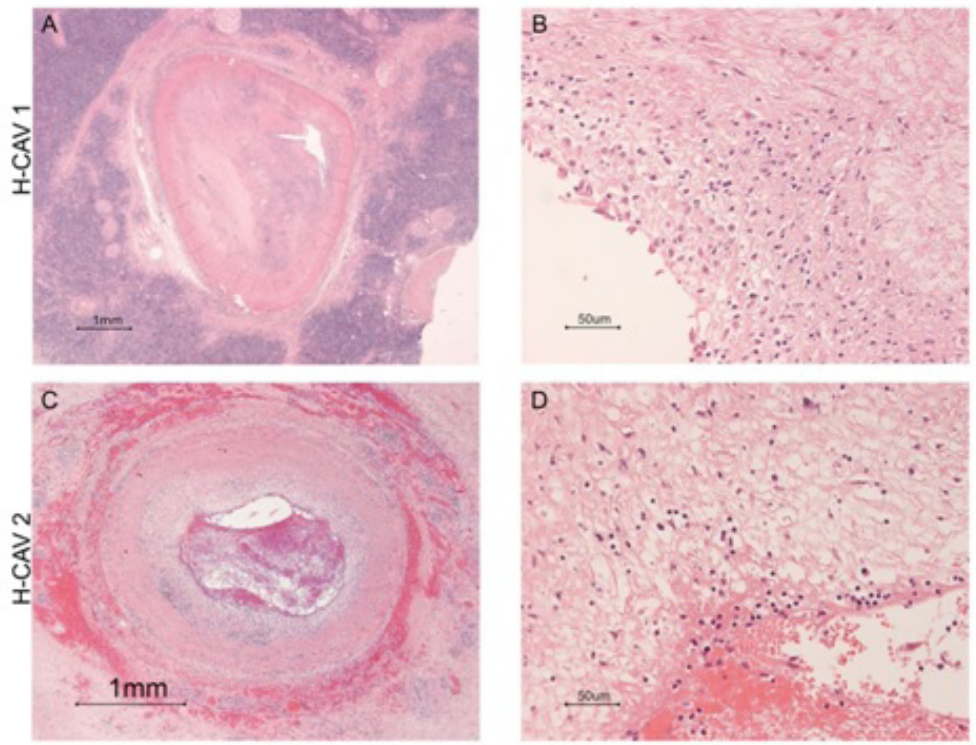

Figure S2. Stenosis of CAV vessels. A (magnification 10x) and **B** (100x), CAV superimposed on an atherosclerotic plaque with a pinpoint lumen of <1 mm. **C** (magnification 20x) and **D** (100x), occluding thrombus superimposed on a CAV lesion. H-CAV = histological CAV

Broad HLA mismatches and bypass time

The number of broad HLA mismatches (0.047) and bypass time (p=0.037) were borderline significant related to H-CAV stage during autopsy (**Supplemental table S1**).

The number of broad HLA mismatches was high in all groups (median of 6 for the H-CAV 0 group and 4 for the H-CAV 1, 2 and 3 groups). Post-hoc analysis revealed that the observed difference between groups was only explained by a significant difference between H-CAV 0 and H-CAV 3. All patients in the H-CAV 0 group died within one month. From the results of our study it cannot be inferred whether this high number of broad HLA-mismatches played a role in the short survival in this group. Probably studies in very large patient cohorts are needed to exactly study the role of the number of broad HLA-mismatches, donor specific antibody development and CAV lesion formation.

Bypass time is significantly related to H-CAV stage (p=0.037) showing longer bypass time for patients with H-CAV 0. This could be explained by the fact that patients with H-CAV 0 died early after transplant which could indicate initial poor graft function, difficult surgical procedure and therefore longer bypass time.

Table S1. Clinical characteristics and H-CAV type at autopsy

	N	H-CAV 0 n=9	1 n=12	2 n=16	3 n=14	P-value
Patient age (years)	51	49 (9)	44 (12)	43 (13)	54 (7)	**0.031**[b]
Donor age (years	50	42 (13)	37 (12)	42 (11)	47 (5)	0.106[b]
Age difference patient-donor (years)	50	6.9 (18.7)	5.9 (18.1)	0.8 (13.7)	5.9 (5.9)	0.670[b]
Age difference patient-donor (≤ 0)	19	-9.1 (10.0)	-8.9 (14.0)	-10.2 (7.0)	-2.8 (0.6)	0.732[b]
Age difference patient-donor (> 0)	31	19.6 (13.0)	18.3 (9.7)	9.3 (11.3)	8.2 (4.1)	0.055[b]
Immunosuppressive therapy	46					0.284[a]
- cyclosporin		3 (60%)	10 (90.9%)	12 (75%)	13 (92.9%)	
- tacrolimus		2 (40%	1 (9.1%)	4 (25%)	1 (7.1%)	
Gender patient	51					0.647[a]
- male		8 (88.9%)	8 (66.7%)	13 (81.3%)	10 (71.4%)	
- female		1 (11.1%)	4 (33.3%)	3 (18.8%)	4 (28.6%)	
Gender donor	50					0.798[a]
- male		4 (44.4%)	7 (63.6%)	8 (50%)	6 (42.9%)	
- female		5 (55.6%)	4 (36.4%)	8 (50%)	8 (57.1%)	
Gender mismatch patient / donor	50					0.715[a]
- male / male		4 (44.4%)	6 (54.5%)	7 (43.8%)	6 (42.9%)	
- male / female		0 (0%)	1 (9.1%)	1 (6.3%)	0 (0%)	
- female / female		1 (11.1%)	3 (27.3%)	2 (12.5%)	4 (28.6%)	
HLA mismatch broad (0-6)	47	6.0 (4.5-6.0)	4.0 (3.0-6.0)	4.0 (3.0-5.3)	4.0 (3.5-4.5)	**0.047**[c]
Primary cardiac diagnosis	50					0.704[a]
- dilated cardiomyopathy		4 (44.1%)	5 (45.5%)	7 (43.8%)	3 (21.4%)	
- ischemic cardiomyopathy		5 (55.6%)	5 (45.5%)	7 (43.8%)	10 (71.4%)	
- congenital cardiomyopathy		0 (0%)	0 (0%)	1 (6.3%)	0 (0%)	
- hypertrophic cardiomyopathy		0 (0%)	1 (9.1%)	0 (0%)	0 (0%)	
- restrictive cardiomyopathy		0 (0%)	0 (0%)	1 (6.3%)	1 (7.1%)	
High cholesterol recipient	33					0.338[a]
- yes		3 (50%)	1 (11%)	1 (14%)	4 (36%)	
- no		3 (50%)	8 (89%)	6 (86%)	7 (64%)	
Hypertension recipient	33					0.731[a]
- yes		1 (17%)	2 (22%)	0 (0%)	2 (18%)	
- no		5 (83%)	7 (78%)	7 (100%)	9 (82%)	
Diabetes mellitus recipient	33					0.316[a]
- yes		0 (0%)	2 (22%)	1 (14%)	0 (0%)	
- no		6 (100%)	7 (78%)	6 (86%)	11 (100%)	
Past smoker recipient	33					0.385[a]
- yes		2 (33%)	7 (78%)	5 (71%)	7 (64%)	
- no		4 (67%)	2 (22%)	2 (29%)	4 (36%)	
BMI recipient	48	25.7 (4.9)	23.7 (3.4)	23.5 (3.1)	24.5 (2.9	0.477[b]
Ischemic time donor heart (min)	49	160 (35)	152 (44)	152 (29)	176 (39)	0.270[b]

	N	H-CAV 0 n=9	1 n=12	2 n=16	3 n=14	P-value
Bypass time (min)	47	166 (118-254)	107 (99-121)	116 (104-150)	139 (120-153)	**0.037[c]**
X-clamp time (min)	48	73.1 (10.9)	69.8 (13.7)	75.4 (13.5)	75.9 (14.3)	0.675[b]
Occurrence of acute rejection	36					0.106[a]
- yes		-	9 (90%)	7 (50%)	7 (59%)	
- no		-	1 (10%)	7 (50%)	5 (42%)	
Number of treated acute rections episodes	36	-	2.5 (1.0-3.0)	0.5 (0.0-1.0)	1.5 (0.0-3.0)	0.053[c]
Number of acute rejection episodes (> grade 0R)	37	-	2.0 (1.0-3.0)	0.0 (0.0-3.5)	2.0 (0.0-4.5)	0.388[c]
Number of acute rejection episodes (> grade)	37	-	1.0 (0.0-1.0)	0.0 (0.0-1.0)	0.0 (0.0-1.5)	0.417[c]
Infection	38					**0.011[a]**
- no infection		-	4 (36.6%)	7 (68.6%)	0 (0%)	
- CMV infection		-	5 (30.8%)	5 (38.5%)	4 (30.8%)	
- other infection		-	3 (21.4%)	2 (14.3%)	9 (64.3%)	
Time post HTx (years)	51	0.005 (0.00-0.02)	0.541 (0.22-1.80)	1.440 (0.13-4.65)	9.582 (5.68-14.40)	**< 0.001[c]**
Cause of death donor	50					0.397[a]
- Trauma capitis		3 (33.3%)	3 (27.3%)	3 (18.8%)	1 (7.1%)	
- CVA / SAB		5 (55.6%)	5 (45.5%)	11 (68.8%)	10 (71.4%)	
- Brain tumor		0 (0%)	0 (0%)	0 (0%)	2 (14.3%)	
- Suicide		0 (0%)	1 (9.1%)	1 (6.3%)	1 (7.1%)	
- Gunshot wound		0 (0%)	0 (0%)	1 (6.3%)	0 (0%)	
- other		1 (11.1%)	2 (18.2%)	0 (0%)	0 (0%)	
Cause of death patient	51					**< 0.001[a]**
- Cardiac						
a) CAV	10	0 (0%)	1 (8.3%)	4 (25%)	5 (35.7%)	
b) Acute rejection	13	0 (0%)	9 (75%)	4 (25%)	0 (0%)	
c) Others	10	5 (55.6%)	1 (8.3%)	3 (18.8%)	1 (7.1%)	
- Vascular (aneurysm / stroke)	2	0 (0%)	0 (0%)	0 (0%)	2 (14.3%)	
- Sepsis (infection)	4	2 (22.2%)	0 (0%)	1 (6.3%)	1 (7.1%)	
- Malignancy	2	0 (0%)	0 (0%)	1 (6.3%)	1 (7.1%)	
- Pulmonary cause	9	2 (22.2%)	0 (0%)	3 (18.8%)	4 28.6%)	
- Unknown	1	0 (0%)	1 (8.3%)	0 (0%)	0 (0%)	
Atherosclerosis	51					**0.007[a]**
- no		4 (25%)	8 (50%)	4 (25%)	0 (0%)	
- yes, minor		2 (13.3%)	3 (20%)	5 (33.3%)	5 (33.3%)	
- yes abundant		3 (15%)	1 (5%)	7 (35%)	9 (45%)	

[a] values (percentage within H-CAV stage): Fisher's exact test, [b] mean (standard deviation): ANOVA, [c] median (interquartile range): Kruskal-Wallis test. HTx = Heart Transplantation, n = patients included, p = p-value, X-clamp = cross clamp, CMV = Cytomegalovirus

Chapter 3.

INTIMAL FIBROSIS IN HUMAN CARDIAC ALLOGRAFT VASCULOPATHY

Manon Huibers, MSc; Nicolaas De Jonge, MD,PhD†; Joyce Van Kuik, BSc*; Erica Siera-De Koning, BSc*; Dick Van Wichen, BSc*; Hub Dullens, PhD*; Marguérite Schipper, MD*, and Roel De Weger, PhD**

*Departments of *Pathology, and †Heart and Lung, University Medical Center Utrecht, The Netherlands.*

Published
Transplant Immunology. 25(2-3):124-132 (2011)

Abstract

Human Cardiac Allograft Vasculopathy (CAV) is one of the major complications for patients after heart transplantation. It is characterized by a concentric luminal narrowing due to (neo) intimal expansion in the coronary arteries of donor hearts after heart transplantation. In this process fibrosis plays an important role. Aim of this study is to analyze the factors and cells involved in this fibrotic process.

Coronary arteries from five heart transplantation patients and three controls were obtained at autopsy. Quantitative real-time PCR was performed on mRNA obtained from various arterial layers isolated by laser micro dissection. Positive gene expression was confirmed by immunohistochemistry and/or *in situ* hybridisation.

The strongest mRNA expression of fibrotic factors (predominantly pro-fibrotic) was found in the neo-intima. Especially, connective tissue growth factor expression was higher in the CAV vessels than in the controls. The lymphocyte activity of interferon gamma was only detected in CAV vessels. Furthermore as shown by in situ hybridisation, the lymphocytes producing interferon gamma also expressed transforming growth factor beta. Anti-fibrotic factors, such as bone morphogenic protein 4, were only expressed in $CD3^-/CD68^-$ stromal cells. Macrophages present in the CAV and control vessels showed to be of the M2 type and did not produce any fibrotic factor(s).

In conclusion, T-cells producing both interferon gamma and transforming growth factor beta, may play an important role in the fibrotic process in CAV vessels by upregulation of connective tissue growth factor production.

Introduction

Cardiac Allograft Vasculopathy (CAV) is one of the major complications in long-term survival of heart transplant (HTx) recipients [1, 2]. CAV is characterized by a concentric intra-luminal obstructive thickening of the intima of the coronary arteries [3, 4]. A major difference between atherosclerosis and CAV is that the internal and external elastic laminae, normally destroyed in atherosclerosis, remain intact in CAV [5]. CAV clinically often presents as silent myocardial infarction, heart failure or sudden death [6, 7]. At present, there is no suitable preventive treatment or therapy for CAV available [6, 7].

The neo-intima (NI) seen in CAV vessels is composed of two distinct layers: 1) a luminal layer (NI-LL) consisting of loose connective tissue infiltrated by mononuclear cells, and 2) a layer (NI-SMC) composed of smooth muscle cells or myofibroblasts directly adjacent to the lamina elastica interna [8-11].

Several factors are involved in the pathogenesis of CAV. The cellular immune response against the allograft is suggested to be one of major importance. Especially T-helper 1 cells seem to play a major role [11-14]. Macrophages are obviously also involved, but their role has been studied in less detail [15]. Although the production of most cytokines is hampered in HTx patients (due to immunosuppressive treatment), interferon-γ (IFN-γ) can be detected and has been implicated as an important mediator of CAV [12, 13, 16-18].

As reported earlier the NI in CAV vessels sometimes consists almost completely of fibrotic tissue [3]. Our study focuses on the analysis of the fibrotic process in CAV and the role of T-cells and macrophages herein. Therefore we analyzed the expression of pro- and anti-fibrotic factors, extra-cellular matrix (ECM) components as well as the presence of macrophages in various layers of the arterial wall. Messenger ribonucleic acid (mRNA) expression was established by quantitative real-time PCR (Q-PCR) performed on distinct micro-dissected layers of the coronary arteries. Location of the expressed mRNAs was determined by *in situ* hybridization (ISH) and cells producing these factors were identified by double ISH and immunohistochemistry (IHC).

Materials and Methods

Patient population

Coronary arteries of five non-transplanted and five HTx patients were obtained at autopsy. Informed consent of all patients was obtained prior to HTx. Anonymous use of redundant tissue for research purposes is part of the standard treatment agreement with patients in our hospital [19]. All HTx patients were treated with a triple immunosuppressive therapy of cyclosporine A, azathioprine and steroids. Characteristics of the patients and of the arteries used in the different experimental approaches are summarized in **Table 1.**

Control coronary arteries without CAV were taken from 3 patients who died due to non-cardiac problems (i.e. prostate carcinoma, hepatic cirrhosis, and lung embolism, respectively). These autopsy hearts were obtained within 4-6 hours after death. All biopsies were snap frozen in liquid nitrogen and stored at -80°C, or were fixed in formalin and embedded in paraffin. No differences in histomorphology and Q-PCR data were found in the coronary arteries of all three control hearts.

Tissue laser micro-dissection, RNA isolation and cDNA synthesis

Arteries with CAV were divided into various layers by tissue laser micro-dissection; two intimal layers (NI-LL and NI-SMC), a tunica media, and a tunica adventitia (**Supplemental Figure 1**). The layers were micro-dissected, RNA was isolated and cDNA was made as described in the supplemental data. The method used to isolate mRNA from laser micro-dissected layers of frozen CAV vessels was performed as recently described [9, 20].

Quantitative real-time PCR (Q-PCR)

Q-PCR was performed on mRNAs isolated from the various arterial layers obtained by laser micro dissection. Total mRNA quality was checked before PCR was performed. Positive gene expression was confirmed by either IHC or ISH. The primer-probe combinations used for Q-PCR were obtained from Applied Biosystems (Foster City, CA) and applied either in a low density array or as single assays (Taqman® Gene Expression Assays). The low density arrays were used according manufacturer's instructions. For the single assays per well 12.5 µl Taqman universal master mix (Applied Biosystems) was used and 1.25 µl primer-probe, 6.25 µl milliQ, and 5 µl cDNA sample was added. The Q-PCR reactions were carried out by the 7900HT sequence detection system of Applied Biosystems. Thermal cycling comprised a denaturation step at 95 ^{0}C for 10 min followed by 45 cycles of 95 ^{0}C for 15 sec and 600 C for 60 sec. All assays were performed in triplicate. In the presented data the difference between the triplicates did not exceed a cycle threshold (Ct) value of 0.8 (2x Standard Deviation of all triplicates). To quantify the data the comparative quantification cycle (Cq) method was used (**Supplemental data**).

Immunohistochemistry (IHC) and Double-immunofluorescent IHC

Coronary arteries were evaluated after application of conventional immunoperoxidase staining or by immunofluorescence (IHC), as previously described [11]. IHC procedures varied for each antibody used. Details of the antibodies used and the (double) IHC method are previously described [9, 11]. Negative control sections were included, in which the primary antibody was omitted, or replaced by an isotype-matched control antibody. To determine the percentage of positively stained cells at least 100 mononuclear cells were counted at two positions in the vascular layer.

In situ hybridization (ISH) in combination with IHC or ISH

ISH-IHC double staining experiments were performed using labelled PCR products to identify cells expressing cytokine or growth factor related mRNA [21, 22]. Anti-CD3 and anti-CD68 monoclonal antibodies were used to characterize the cells expressing the mRNA. This procedure up to the hybridisation step was performed under RNAse free conditions. PCR products were made using specific primers (see **supplemental data**), sequenced and blasted against the human genome to verify their specificity. The PCR products were labelled with either digoxigenin or biotin by re-PCR pending on use for single hybridisation or immuno/hybrido double staining. The specificity of ISH was confirmed by positive and negative control [23] (**Supplemental data**).

Statistical analysis

Data was analyzed using Graphpad Prism 4.0. All data are expressed as mean ± Standard Error of the Mean. Statistical analysis was performed using the Mann-Whitney test (CAV versus controls) or Wilcoxon signed rank test (comparing various CAV layers). P-values < 0.05 were considered statistically significant.

Results

mRNA Expression of fibrotic factors, cytokines and ECM components

The Q-PCR data of mRNA expression in the various layers of the coronary arteries are presented in **Figure 1 and 2**. In control arteries expression of the tested genes was higher in the tunica intima compared to the media. Bone morphogenic protein (BMP) 7, Interferon gamma (IFN-γ) and Matrix-metalloproteinases (MMP) 9 were not expressed in control arteries. In general, the mRNA expression measured in CAV NI-SMC and media was low.

Q-PCR data of the anti- and pro-fibrotic factors and cytokines are presented in **Figure 1**. The differences between the expression of the anti-fibrotic factors Inhibitor of DNA binding 1 (ID-1) and BMP-4 between CAV and control arteries were small. ID-1 was significantly more expressed in the adventitia compared to the media. BMP-7 was only expressed in the tunica adventitia of CAV in one patient. The three pro-fibrotic factors tested in this study were plasminogen activator inhibitor 1 (PAI-1)/Serpine, Connective tissue growth factor (CTGF) and Transforming growth factor beta (TGF-β). PAI-1/Serpine was expressed lower in CAV NI-SMC than in the intima of control arteries (not significant). However, within the different CAV layers the adventitia showed stronger mRNA expression compared to the NI-SMC and media ($p<0.05$). CTGF, on the other hand, showed a stronger expression in CAV NI-LL than in the controls, however this was not significant ($p>0.05$). Within the CAV layers, CTGF showed higher expression in the adventitia compared to the media ($p<0.05$). TGF-β mRNA expression did not differ considerably between CAV and control, but again within the CAV vessel the higher mRNA expression was seen in the NI-LL and adventitia. The higher expression of Interleukin (IL) 6 in control intima and CAV adventitia compared to CAV intima was remarkable, but due to variable expression the differences were not significant ($p>0.05$).

IFN-γ was the only cytokine strongly expressed in CAV and lacking in controls. Other cytokines were only marginally expressed in both CAV and control (**supplemental Figure 2**).

Q-PCR data of extra cellular matrix components and MMPs are depicted in **Figure 2**. Smooth muscle actin (ACTA-2/α-SMA) showed hardly any differences between control layers and CAV NI-LL, NI-SMC and media. However, the adventitia of the CAV vessels showed a significant decrease compared to NI-SMC and media ($p<0.05$). MMP-2 expression was especially high in the CAV adventitia in comparison to the control tunica media ($p<0.05$) and CAV media ($p<0.05$). The expression of MMP-9 was absent in control arteries and high in NI-LL of CAV. Collagen mRNA was detected in all layers of the CAV arteries (**Figure 2**). In comparison to the control arteries the expression did not differ substantially. Collagen mRNA within the CAV vessel was expressed strongest in the NI-LL and adventitia, lower in the NI-SMC, and lowest (but still detectable) in the media.

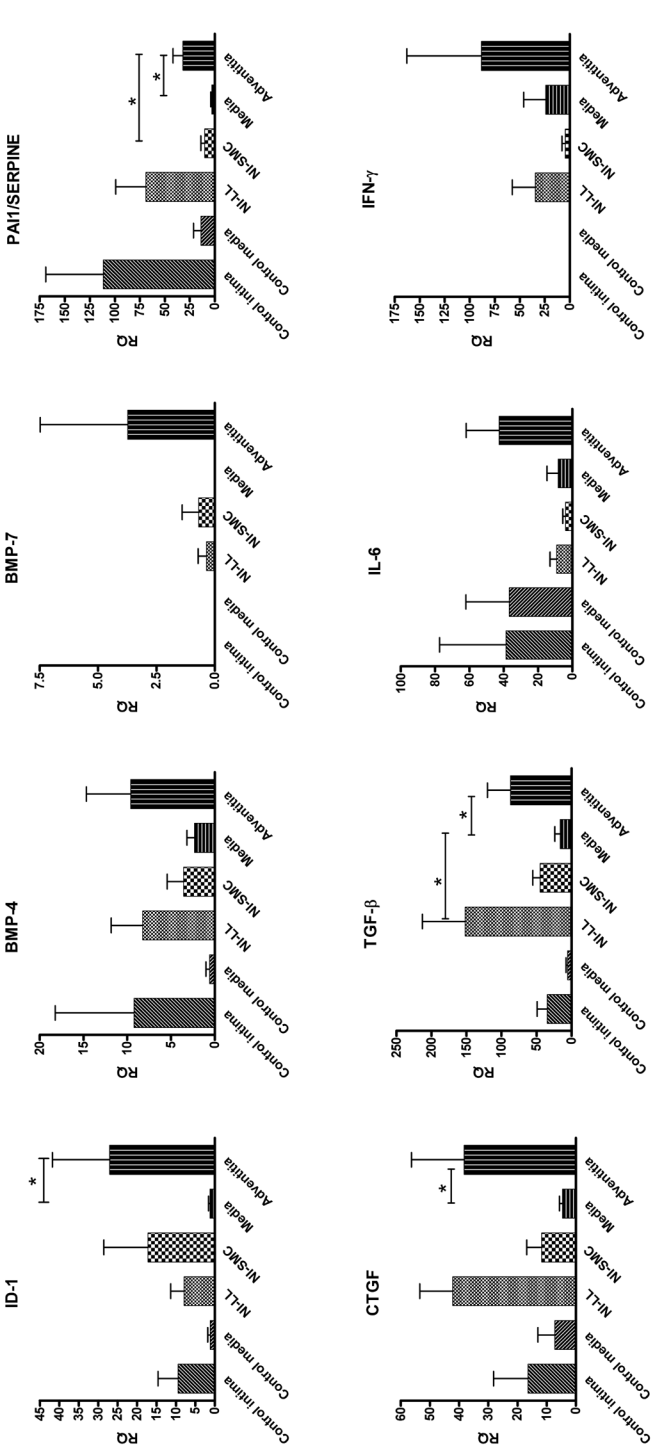

Figure 1. mRNA expression of fibrotic factors. Relative quantities (RQ) of mRNA expression determined by Q-PCR of anti-fibrotic factors (ID-1, BMP-4 and BMP-7), pro-fibrotic factors (PAI-1, CTGF and TGF-β) and cytokines (IL-6 and IFN-γ) in different layers of CAV and control arteries. *p<0.05.

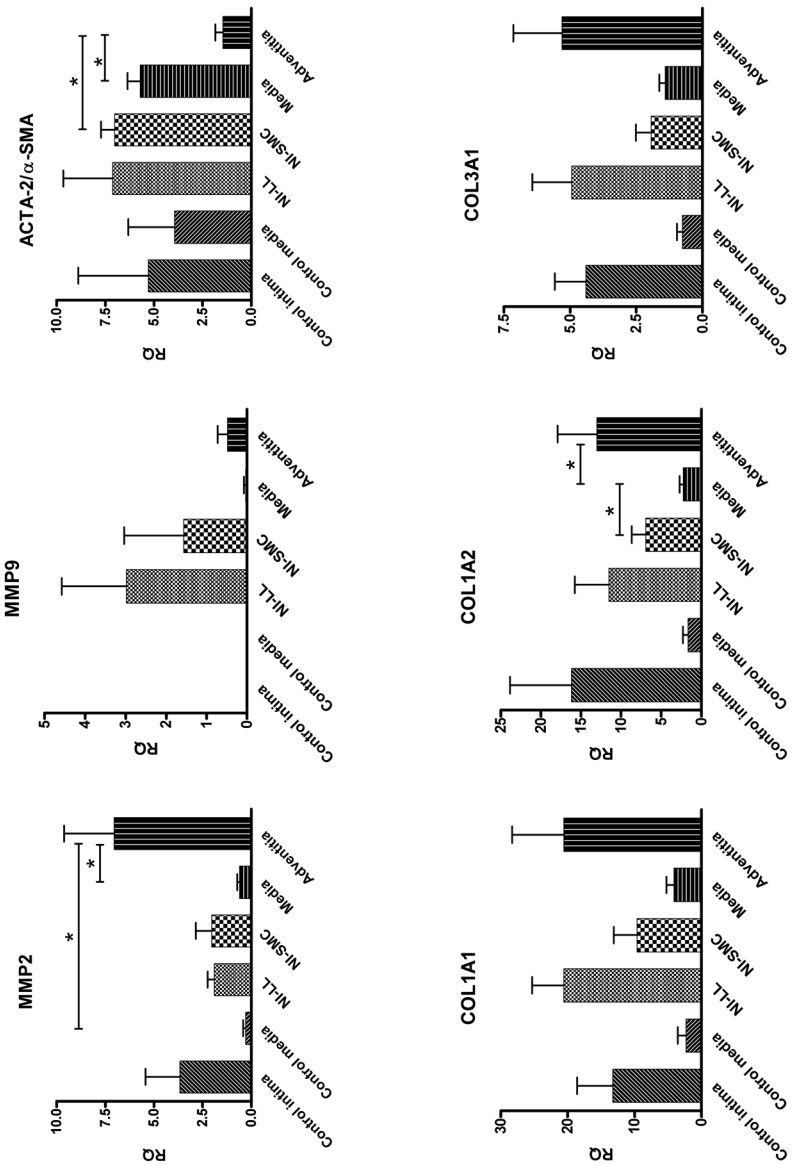

Figure 2. mRNA expression ECM components and MMPs. Relative quantities (RQ) of mRNA expression determined by Q-PCR of matrix metalloproteinases (MMP2 and MMP9) and extra cellular matrix components (ACTA-2/α-SMA, Collagen 1A1, 1A2, and 3A1) in different layers of CAV and control arteries. *p<0.05.

mRNA Expression of macrophage markers

Q-PCR data of macrophage markers (CD14, CD40, CD80, CD68, HLA-DR, mannose receptor (MR), scavenger receptor (ScR), toll like receptor (TLR) 4, and TLR8) are presented in **Figure 3**. In control arteries all macrophage markers that were detected showed a raised expression in the intima compared to the media (not significant). CD80, HLA-DR, and TLR8 mRNA was not detected in the control arteries. In CAV, most macrophage markers (except ScR and TLR8) showed the strongest expression in the NI-LL and adventitia compared to the NI-SMC and media. Compared to CAV NI-LL, macrophage markers CD40, CD80, CD68 ($p<0.05$), HLA-DR, MR, and TLR4 showed a lower expression in control intima. CD14, MR, and ScR (typical M2 macrophage markers) showed comparable expression in CAV and controls. No expression of Inducible isoform of Nitric Oxide Synthase (iNOS), typical for M1-macrophages, was detected (data not shown).

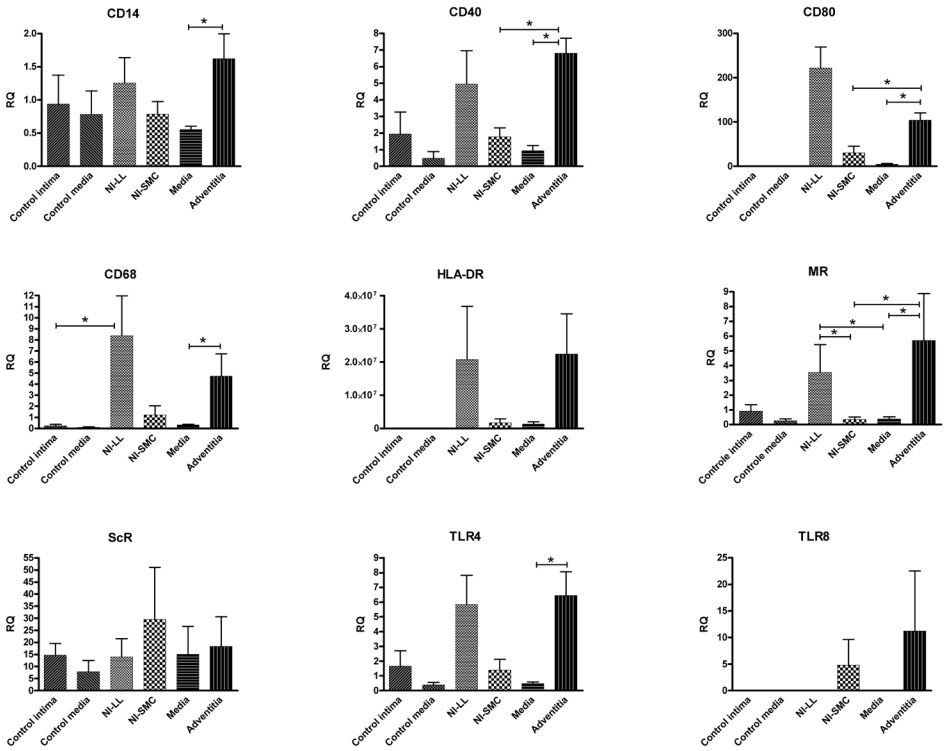

Figure 3. mRNA expression Macrophage markers. Relative quantities (RQ) of mRNA expression determined by Q-PCR of macrophage markers (CD14, CD40, CD80, CD68, HLA-DR, MR, ScR, TLR4, TLR8) in different layers of CAV and control arteries. *$p<0.05$.

Location of macrophages

The IHC of the macrophage markers CD68, MR, ScR and TLR4 confirmed the Q-PCR data, both on distribution and M2-typing. The distribution of MR, ScR and TLR4 as judged by IHC was similar to CD68 in CAV and controls, as indicated in **Figure 4**. In CAV the number of macrophages, especially in the mono nuclear cell infiltrate in the intima, was higher than in the control intima.

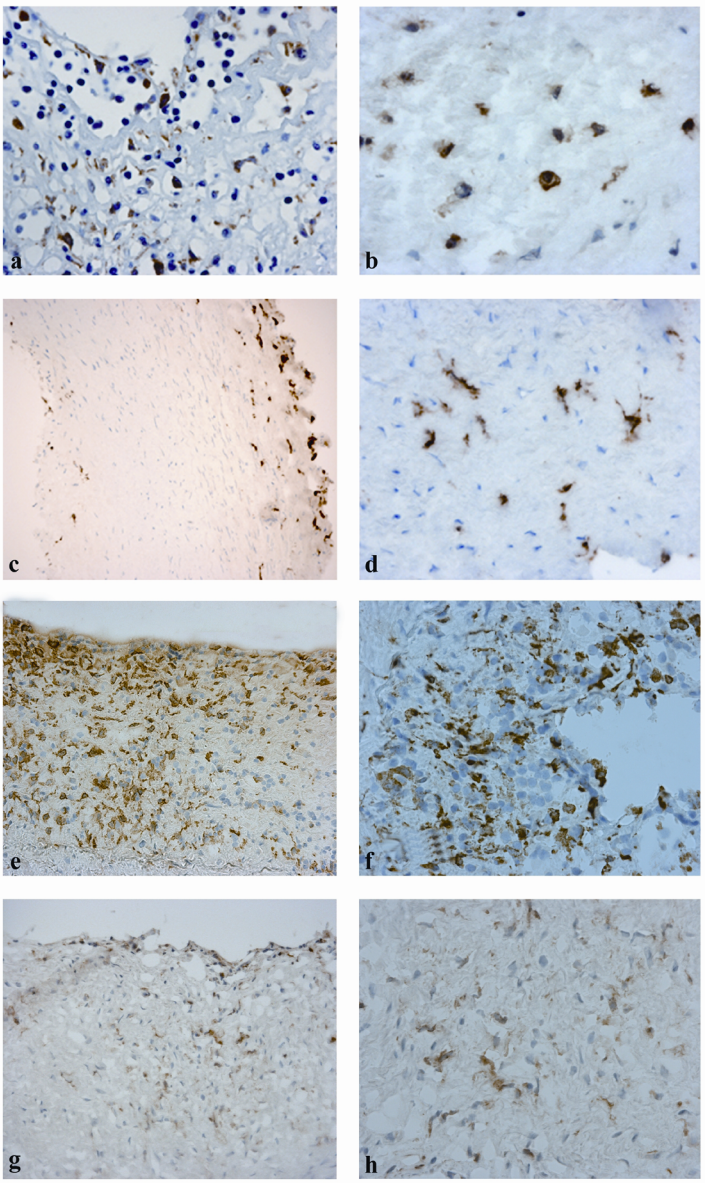

Figure 4. Immunohistochemistry of macrophage markers. IHC of macrophages in CAV and controls. CD68+ macrophages were detected in all vascular layers in CAV and although in smaller numbers, also in control. **(a)** IHC of CD68 showing numerous positive macrophages in the NI-LL (x200); **(b)** IHC of Scavenger receptor (ScR; CD204) showing positive macrophages in NI-LL (x200); **(c)** IHC of Mannose receptor (MR; CD206) showing few positive macrophages in control, mainly localized in the adventitia and few in the intima (left) (x100); **(d)** IHC of MR showing slender positive macrophages in control intima (x200); **(e)** IHC of MR showing positive macrophages in CAV NI-LL and NI-SMC layers (x100); **(f)**: IHC of MR showing large positive macrophages in NI-LL (x200); **(g)** IHC of TLR4 showing positive macrophages in CAV, mainly localized in the NI-LL (x100); **(h)** IHC of TLR4 showing positive macrophages in NI-LL (x200).

IHC and ISH of fibrotic factors

The results of the Q-PCR demonstrated highest mRNA expression of fibrotic factors in the NI-LL and adventitia of CAV. IHC of ID-1 in a CAV artery confirmed this location (**Figure 5a and 5b**). According to the Q-PCR data, MMP-2 and MMP-9 were expressed in CAV. This was confirmed by both IHC and ISH for MMP-2 and IHC for MMP-9 in the NI-LL of CAV (**Figure 5c-e**). IHC demonstrates that MMP-2 is present in stromal cells in the NI-LL and in most other layers of CAV arteries. In control, the IHC reaction for MMP-2 was also positive in stromal cells (data not shown). IHC of CAV arteries for MMP-9 showed location in the endothelial lining, in myofibroblasts in the intima and smooth muscle cells in the media (**Figure 5e**). In control arteries MMP-9 was lacking, except for some incidental staining of endothelial cells (data not shown). TGF-β was expressed by stromal cells in the intimal layers of CAV and control arteries (**Figure 5f**), and in mono nuclear cells in CAV (**Figure 6**).

Double ISH of TGF-β or IFN-γ combined with CD3 (**Figure 6c**) or CD68 (**Figure 6d**) demonstrated that in initimal mono nuclear cell infiltrate TGF-β and IFN-γ were co-expressed in about 50% of CD3 positive cells, but not in CD68 positive cells. Moreover, double ISH of TGF-β and IFN-γ demonstrated that the cells that expressed TGF-β also expressed IFN-γ both in intima and adventitia of CAV (**Figure 6e and 6f**). Double ISH/IHC showed BMP-4 mRNA expression to be localized in CD3 negative and CD68 negative (stromal) cells (**Figure 6a and 6b**). In the adventitia, some CD68 positive cells expressed BMP-4.

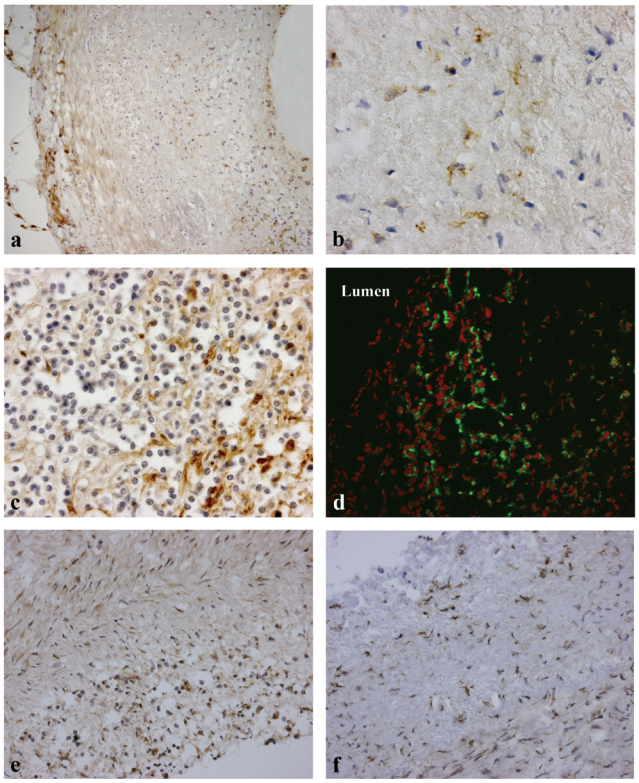

Figure 5. ISH and IHC of ID-1 and MMPs. (a) IHC of ID-1 in CAV showing the most positive cells in the NI-LL and adventitia (x20) and **(b)** ID-1 positive cells in NI-LL of CAV (x200); **(c)** IHC of MMP-2 in NI-LL of CAV showing positive stromal cells (x200); **(d)** ISH of MMP-2 (green, with red nuclear staining) in the intima of CAV (x100); **(e)** IHC of MMP-9 in NI-LL of CAV showing numerous positive cells (x40); **(f)** IHC of TGF-β in control artery, showing positive stromal cells (x40)

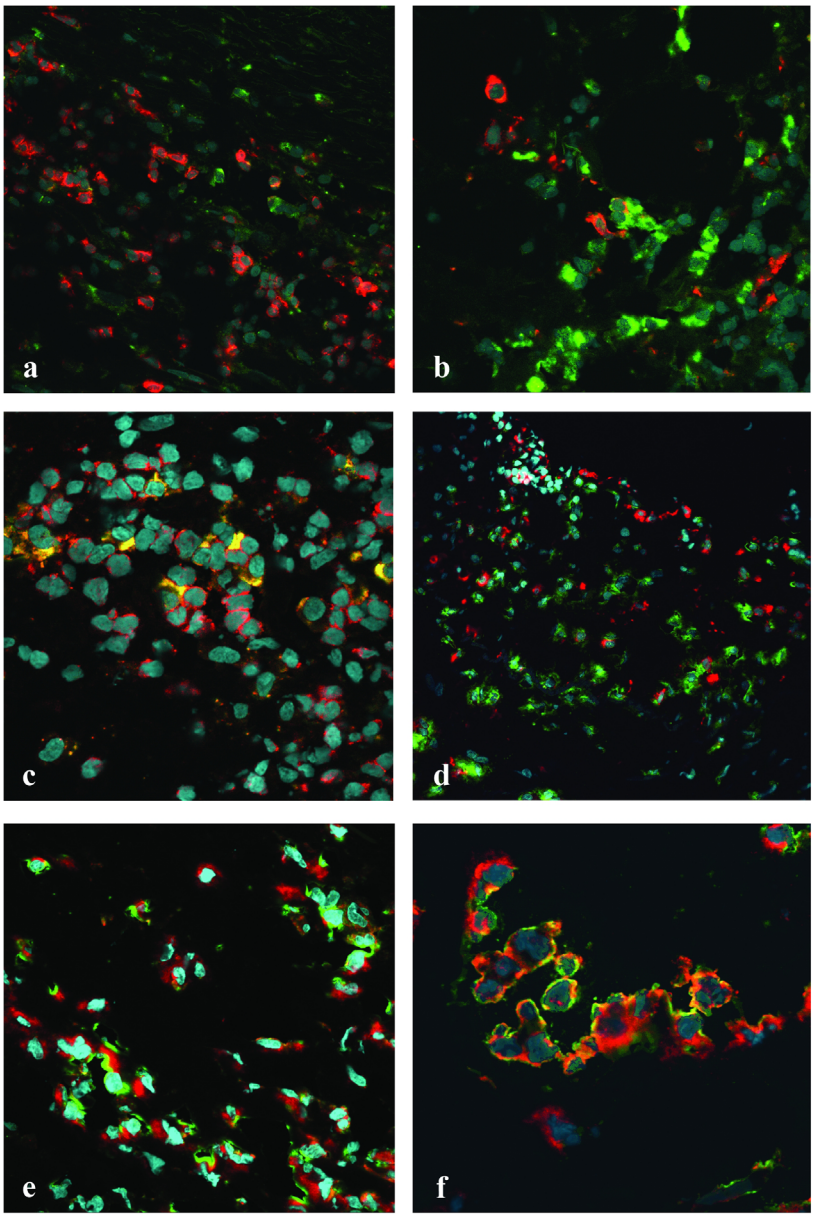

Figure 6. Localization of BMP-4, TGF-β and IFN-γ in T-cells and macrophages in NI-LL. (a) ISH of BMP-4 (green) combined with IHC for CD3 (red), showing no double positive cells (x 300); **(b)** ISH of BMP-4 (green) combined with IHC for CD68 (red), without overlap in staining (x 300); **(c)** ISH of TGF-β (green) combined with IHC for CD3 (red), showing double staining (yellow) of many T-cells (x 300); **(d)** ISH of TGF-β (green) combined with IHC (red) for CD68, showing almost no double stained cells (x 200); **(e)** ISH of TGF-β (green) combined with ISH for IFN-γ (red) in the NI-LL, showing a large number of cells with both a green and red staining surrounding a nucleus (x 200); **(f)** ISH of TGF-β (green) combined with ISH for IFN-γ (red) in the adventitia, showing yellow double staining in many cells (x 250)

Discussion

CAV has long been considered as a result of solely SMC migration from the tunica media to the tunica intima [1, 3]. However, a SMC layer is also present in the intima of coronary arteries from healthy individuals and CAV is actually characterized by a fibrotic response in the NI-LL [11]. This study focussed on the characterization of the fibrotic process in human CAV vessels.

Our results showed that the mRNA expression of the fibrotic factors TGF-β, CTGF and PAI1/serpine was high in the NI-LL and tunica adventitia, compared to the NI-SMC and tunica media in CAV arteries. Apparently, the main pro-fibrotic activity in CAV originates in the NI-LL and tunica adventitia, whereas the NI-SMC and tunica media do hardly show fibrotic activity. However, the differences in expression of the fibrotic factors between control and CAV arteries were remarkably small. Although the tunica intima of the control coronary arteries is morphologically the counter part of the NI-SMC layer of CAV, in general the healthy intima shows an mRNA expression pattern similar to the NI-LL, whereas the healthy media shares more characteristics with the NI-SMC.

The anti-fibrotic factors (BMP-4, BMP-7 and ID1) did not show large differences between the CAV and control arteries. However, in CAV the anti-fibrotic response tended to be strongest in the adventitia. BMP-7 was absent in control arteries, and weekly expressed in the CAV intima. BMP-7 might be produced as a reaction to the fibrotic response in an attempt to inhibit fibrosis, although a stronger production seemed to be needed to achieve that goal.

In view of the observed fibrosis in the NI-LL, a larger difference in expression of fibrotic factors between CAV and control was to be expected. The pro-fibrotic factors CTGF and TGF-β only showed a marginal (non-significant) increase in mRNA expression in the NI-LL compared to control arteries. The most remarkable difference between control and CAV was the localization of TGF-β. Results of ISH analysis showed expression of TGF-β in stromal cells in the intima both in control and CAV vessels. In CAV arteries, TGF-β is also produced by infiltrating active T-cells present in the intima. This 'extra' TGF-β production may favour a pro-fibrotic response in the intima [11].

Recently, Tellides et al showed that IFN-γ induces tunica intima proliferation in human arteries [13, 16]. We showed that in CAV there is indeed a strong expression of IFN-γ that is lacking in control arteries. This IFN-γ is produced by the same T-cells that also produce TGF-β (**Figure 6**), as shown by ISH/IHC and double ISH analysis. Together, these data may suggest that the pro-fibrotic response is induced by the infiltrating T-cells that produce both TGF-β and IFN-γ. The role of other cytokines (Il-1A, IL-2, IL-4, IL-10, IL-12B, IL-17, IL-23 and TNF-α) is limited as the production of these cytokines in CAV was lacking; most likely due to the applied immunosuppression in HTx patients [16, 18]. Only the pro-inflammatory cytokine IL-6 may add to the fibrotic response, since even low expression of this particular cytokine is relevant for fibrotic responses [24].

Macrophages are also important in the development of CAV as shown in an experimental animal model [15]. Macrophages can be divided in a) M1-macrophages (positive for CD68, iNOS, and TLR4, and negative for MR, ScR and CD14) and b) M2-macrophages (positive for CD68, CD14, MR, ScR and TLR4, and negative for iNOS) [25]. The CD68 positive macrophages that are abundantly present in the areas of mono nuclear cell infiltrates in the neo-intima in CAV arteries appeared to be of the M2-type. In fact, these macrophages are of the M2c type (low ScR, high MR), which induce tissue remodelling and matrix deposition [25]. M2

macrophages were also detected (in lower numbers) in the tunica intima of control arteries. So the number of macrophages increases during CAV development, but the type of tissue macrophages was the same. In the adventitia of the CAV arteries only few BMP-4 and IFN-γ positive macrophages were observed, the role of these macrophages in the fibrotic response seems therefore limited. So, the M2 macrophages are probably important in the homeostasis and/or remodelling of the vessel wall by producing MMP [26].The expression of TGF-β by small stromal cells, most likely myofibroblasts, seems to be important in normal homeostasis of the coronary artery, as this was also observed in all control arteries.

Considering the role of T-cells and macrophages in more detail, it is interesting to note that Th1 cells do stimulate the production of MMP in macrophages [26]. MMP-2 and MMP-9 them selves do play an important role in remodelling processes and in the activation of latent TGF-β leading to stimulation of the fibrotic process [23, 27]. In our hands MMP-2 was expressed similarly in both control and CAV arteries, whereas MMP-9 was only expressed in CAV arteries, in where fibrosis was clearly seen. In other words, T-helper cells might play a role in the pathogenesis of CAV by stimulating MMP production of macrophages.

In conclusion, our data suggest that T-cells play an important role in the fibrosis of CAV (**Figure 7**). This role might be twofold; 1) producing cytokines like TGF-β and IFN-γ, that stimulate fibroblasts to induce fibrosis, and 2) stimulating macrophages to produce MMP. The latter can in turn stimulate remodelling and keep the fibrotic response going, by TGF-β and possibly CTGF activation. So, influencing the fibrotic response in CAV might become possible through interference of IFN-γ and TGF-β producing T-helper cells.

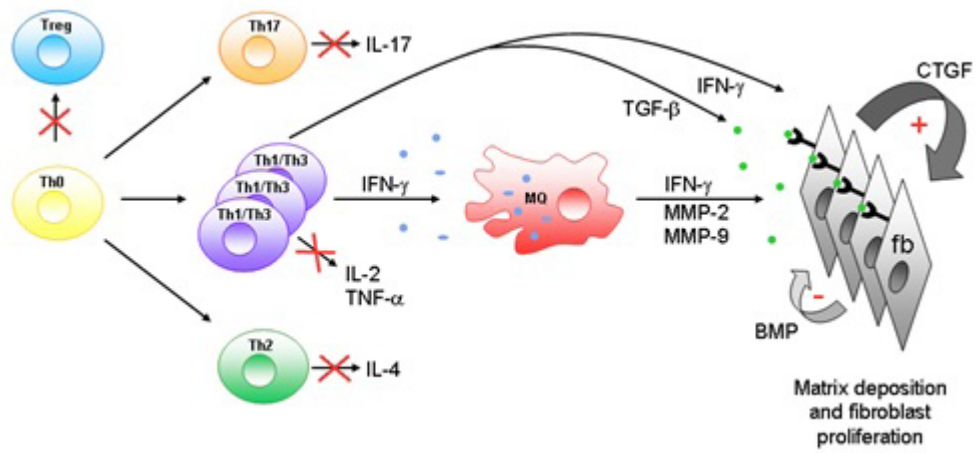

Figure 7. Schematic representation of pro-fibrotic response in CAV intima. Infiltrating lymphocytes in the NI-LL are mainly T-helper cells. Macrophages are the second largest population in the neo-intima. Tregs were not detected and although some markers for Th-2 and Th-17 cells were observed no substantial cytokine production of IL-4 or IL-17 was detected. Also cytokines characteristic for Th-1, like IL-2 and TNF-α, were not or only marginally detected. The infiltrated Th-cells produced however, both TGF-β (Th-3) and IFN-γ (Th-1). Both cytokines could stimulate fibrosis directly by activating the pro-fibrotic response (up-regulating CTGF and PAI-1) in stromal cells and myo-fibroblasts. Activation could also be induced indirectly via macrophages that after stimulation produce MMPs and/or IFN-γ. Treg = regulatory T cell, Th = helper T cell, MQ = Macrophage, fb = fibroblast

Study limitations

The small number of patients and the small numbers of controls are a main limitation of this study. Coronary arteries were only included if they contained a clear NI layer with loose connective tissue and an infiltrate of mononuclear cells and when sufficient vessel tissue could be obtained. Besides, they (both CAV and controls) should not have any form of atherosclerosis which could bias our results. These criteria meant that of our population only five CAV patients remained. However, this was enough to obtain sufficient amounts of mRNA for Q-PCR analysis. Due to the small number of samples the mRNA expression did only rarely reach statistical significance but mainly indicated a trend, which was confirmed with IHC and/or ISH.

References

1. George,J.F., Pinderski,L.J., Litovsky,S., & Kirklin,J.K. Of mice and men: mouse models and the molecular mechanisms of post-transplant coronary artery disease. *J. Heart Lung Transplant.* **24**, 2003-2014 (2005).
2. Weis,M. & Von Scheidt,W. Cardiac allograft vasculopathy: a review. *Circulation* **96**, 2069-2077 (1997).
3. Billingham,M.E. Histopathology of graft coronary disease. *J. Heart Lung Transplant.* **11**, S38-S44 (1992).
4. Mitchell,R.N. & Libby,P. Vascular remodeling in transplant vasculopathy. *Circ. Res.* **100**, 967-978 (2007).
5. Rahmani,M., Cruz,R.P., Granville,D.J., & McManus,B.M. Allograft vasculopathy versus atherosclerosis. *Circ. Res.* **99**, 801-815 (2006).
6. Gao,S.Z. et al. Acute myocardial infarction in cardiac transplant recipients. *Am. J. Cardiol.* **64**, 1093-1097 (1989).
7. Suzuki,J., Isobe,M., Morishita,R., & Nagai,R. Characteristics of chronic rejection in heart transplantation: important elements of pathogenesis and future treatments. *Circ. J.* **74**, 233-239 (2010).
8. Atkinson,C. et al. Neointimal smooth muscle cells in human cardiac allograft coronary artery vasculopathy are of donor origin. *J. Heart Lung Transplant.* **23**, 427-435 (2004).
9. Hagemeijer,M.C. et al. T cells in cardiac allograft vasculopathy are skewed to memory Th-1 cells in the presence of a distinct Th-2 population. *Am. J. Transplant.* **8**, 1040-1050 (2008).
10. Houser,S., Muniappan,A., Allan,J., Sachs,D., & Madsen,J. Cardiac allograft vasculopathy: real or a normal morphologic variant? *J. Heart Lung Transplant.* **26**, 167-173 (2007).
11. Van Loosdregt J. et al. The chemokine and chemokine receptor profile of infiltrating cells in the wall of arteries with cardiac allograft vasculopathy is indicative of a memory T-helper 1 response. *Circulation* **114**, 1599-1607 (2006).
12. Miura,M. et al. Monokine induced by IFN-gamma is a dominant factor directing T cells into murine cardiac allografts during acute rejection. *J. Immunol.* **167**, 3494-3504 (2001).
13. Tellides,G. & Pober,J.S. Interferon-gamma axis in graft arteriosclerosis. *Circ. Res.* **100**, 622-632 (2007).
14. Zhao,D.X. et al. Differential expression of the IFN-gamma-inducible CXCR3-binding chemokines, IFN-inducible protein 10, monokine induced by IFN, and IFN-inducible T cell alpha chemoattractant in human cardiac allografts: association with cardiac allograft vasculopathy and acute rejection. *J. Immunol.* **169**, 1556-1560 (2002).
15. Kitchens, W.H. et al. Macrophage depletion suppresses cardiac allograft vasculopathy in mice. *Am. J. Transplant.* **7**, 2675-2682 (2007).
16. Tellides,G. et al. Interferon-gamma elicits arteriosclerosis in the absence of leukocytes. *Nature* **403**, 207-211 (2000).
17. Wang,Y. et al. Interferon-gamma induces human vascular smooth muscle cell proliferation and intimal expansion by phosphatidylinositol 3-kinase dependent mammalian target of rapamycin raptor complex 1 activation. *Circ. Res.* **101**, 560-569 (2007).
18. Yi,T. et al. Human allograft arterial injury is ameliorated by sirolimus and cyclosporine and correlates with suppression of interferon-gamma. *Transplantation* **81**, 559-566 (2006).
19. van Diest,P.J. No consent should be needed for using leftover body material for scientific purposes. *For. BMJ* **325**, 648-651 (2002).
20. Roepman,P. et al. Dissection of a metastatic gene expression signature into distinct components. *Genome Biol.* **7**, R117 (2006).
21. Van Hoffen,E. et al. T cell apoptosis in human heart allografts: association with lack of co-stimulation? *Am. J. Pathol.* **153**, 1813-1824 (1998).
22. Klein,S.C. et al. An improved, sensitive, non-radioactive in situ hybridization method for the detection of cytokine mRNAs. *APMIS* **103**, 345-353 (1995).
23. Bruggink,A.H. et al. Type IV collagen degradation in the myocardial basement membrane after unloading of the failing heart by a left ventricular assist device. *Lab Invest* **87**, 1125-1137 (2007).
24. Wehner,J.R. & Baldwin,W.M., III Cardiac allograft vasculopathy: do adipocytes bridge alloimmune and metabolic risk factors? *Curr. Opin. Organ Transplant.* **15**, 639-644 (2010).
25. Mantovani,A. et al. The chemokine system in diverse forms of macrophage activation and polarization. *Trends Immunol.* **25**, 677-686 (2004).
26. Oviedo-Orta,E., Bermudez-Fajardo,A., Karanam,S., Benbow,U., & Newby,A.C. Comparison of MMP-2 and MMP-9 secretion from T helper 0, 1 and 2 lymphocytes alone and in coculture with macrophages. *Immunology* **124**, 42-50 (2008).
27. Haas,T.L. et al. Involvement of MMPs in the outward remodeling of collateral mesenteric arteries. *Am. J. Physiol Heart Circ. Physiol* **293**, H2429-H2437 (2007).

Supplemental Material

Laser tissue microdissection, RNA isolation and cDNA synthesis

Frozen tissue sections of 10 µm were mounted on 1 mm RNAse free PEN membrane slides (P.A.L.M. Microlaser technologies AG, Bernried, Germany), air-dried and fixed in 96% ethanol for 30 sec. Subsequently, slides were rinsed with 70% ethanol, washed with RNAse-free water and stained for 30 sec with RNAse-free haematoxylin. The slides were rinsed two times with RNAse-free water, followed by dehydration in ethanol. Different arterial layers (Supplemental Fig. 1) were dissected using the P.A.L.M MicroBeam System and collected in LPC microfugetubes (P.A.L.M.). Total RNA was isolated using the PicoPure RNA isolation kit according to the manufacturer's instructions (Arcturus Bioscience, Sunnyvale, CA). Synthesis of cDNA was performed by adding 2 µl oligo dT(15) primers (0.50 µg; Promega Corporation, Phoenix, AZ), 2 µl of random primers (0.50 µg; Promega) and 4 µl dNTP's (25 mM; Invitrogen Corporation, Carlsbad, CA) to 44 µl RNA derived from the RNA isolation procedure. This solution was heated in a closed Eppendorf tube for 5 min at 65^{0}C and subsequently, the tube was cooled to room temperature. Sixteen µl 5x RT-buffer (Invitrogen), 8 µl 0.1M DTT (Invitrogen) and 2 µl RNasin (Promega) was added and vigorously mixed and heated for 2 min at 37^{0}C. Finally, 2 µl SuperScript RNaseH-Reverse Transcriptase (Promega) was added and heated in a closed Eppendorf tube for 50 min at 37^{0}C, followed by 15 min at 70^{0}C.

Real time quantitative-PCR data analysis (Q-PCR)

To quantify the data the comparative Cq method was used. Relative quantity was defined as $2^{-\Delta\Delta Cq}$, in which ΔCq = Cq (target) – Cq (reference), ΔΔCq = ΔCq (sample) - ΔCq (calibrator). As reference the housekeeping gene GAPDH was used, which was shown to be the most stable of various housekeeping genes in heart tissue. The calibrator (vascular cDNA) is a sample used for normalization and allows the comparison of the expression level of a specific gene between the different layers. This method is semi-quantitative because the absolute amount of RNA was not determined.

Double-immunofluorescent immunohistochemistry

Antibodies and pre-treatments used in double-staining experiments are summarized in supplementary **Table S1**. The following procedure as described previously was applied to all incubations [9, 11]. Sections were pre-absorbed using 10% normal serum (corresponding to the species of the secondary antibody) in phosphate buffered saline (PBS; blocking buffer) for 30 min, and incubated with the primary antibody for 1 hr in blocking buffer, followed by incubation with HRP-labelled secondary antibody for 30 min. Subsequently, the staining was amplified by incubation with TRITC-conjugated tyramide diluted 1:50 in amplification diluents (NEL 702, Perkin Elmer Life Sciences, Boston, MA) for 30 min. The residual endogenous peroxidase activity was blocked by incubating the slides for 20 min in block buffer (1% H_2O_2 in PBS). The

previous steps were repeated for the second cascade, that was amplified with FITC-conjugated tyramide diluted 1:50 in amplification diluents (NEL 701, Perkin Elmer Life Sciences) for 5 min. In between the different incubations, the slides were washed in PBS/0.05% Tween-20. Finally, slides were counterstained by either incubation with DAPI or TOPRO-3 Iodide (Invitrogen Europe BV, Leiden, NL), respectively for 3 or 10 min.

Double ISH/Immunohistochemical (IHC) staining

To identify cell types expressing a certain mRNA, RNA ISH and RNA ISH/ IHC double staining was performed as described previously [21, 22]. In this procedure up to the hybridisation step, experiments were performed under RNAse free conditions with RNAse free reagents. PCR products were made using specific primers:

MMP-2 forward: ATT-CCG-CTT-CCA-GGG-CAC-ATC
MMP-2 reverse: GTT-AAA-GGC-GGC-ACC-ACT-CG
γ-IFN forward: AAC-TAC-TGA-TTT-CAA-CTT-CTT,
γ-IFN reverse: ATT-ACT-GGG-ATG-CTC-TTC,
TGF-β forward: TGT-CCA-GGC-TCC-AAA-TGT-AG,
TGF-β reverse: AAC-CAC-AAC-GAA-ATC-TAT-GA,
BMP-4 forward: ATT-AGC-CGA-TCG-TTA-CCT-CA,
BMP-4 reverse: TAC-CAC-CTT-ATC-ATA-CTC-ATC.

All PCR products were sequenced and blasted against the human genome to verify their specificity. The PCR products were labelled with either digoxigenin or biotin by re-PCR in the presence of labelled nucleotides, pending on further use for single hybridisation or immuno/ hybrido doubles staining. The specificity of ISH was confirmed by positive and negative controls. Tonsil sections were used as positive control, and negative controls were obtained by omission of the probe from the hybridization mixture. ISH was performed as previously described [4,5]. Frozen slides were fixed in buffered formalin for one hr, rinsed in PBS, blocked for endogenous peroxidase for 30 min, rinsed in PBS, incubated with proteinase K (prot.K) solution for 7 min (10 µl prot.K (10 mg/ml) in 100 ml PBS at 37 °C, rinsed in PBS again, fixed in buffered formalin to block prot.K for 5 min, rinsed in PBS, incubated in Triton X-100 in PBS (50 µl Triton X-100 (10%) in 100 ml PBS) for 10 min, rinsed in PBS, dehydrated in ethanol 50%, 70%, 96% and 100% and dried at room temperature. The following hybridisation mixture was prepared: 30 µl formamid 100 %, 20 µl TE buffer 0.1x 10 µl SSC 20x, 1 µl t-RNA (100 mg\ml), 10 µl Herring Sperm DNA, 5 µl digoxigenin labelled probe, 24 µl RNAse free water. Total volume is 100 µl. The hybridization mixture was boiled in water for 7 min to denature both DNA probes, cooled on ice for 10 min, and 25-30 µl of hybmix was applied to the tissue slide and covered with a cover slip. Slides were put on a hot plate at 47 °C for 10 min and afterwards incubated in a humidified chamber overnight in an oven at 37°C. The cover slip was removed and slides were rinsed in 30% formamid/ SSC 2x solution for 30 min at room temperature. The same solution was preheated in a water bath at 42°C and slides were incubated in this solution at 42°C for 10 min, rinsed in PBS, and incubated with HRP labelled sheep anti-digoxigenin 1:2,500 in PBS supplemented with 10% Normal Human Serum (NHS) for 30 min, rinsed in PBS and HRP was visualized with Tyramide Signal Amplification FITC (TSA- FITC) kit for 30 min, rinsed and

residual peroxidase was blocked with blocking reagent for 30 min. Slides were incubated with rabbit anti-CD3 or mouse anti-CD68 respectively for 1 hr, rinsed in PBS and incubated with swine anti-rabbit HRP or rabbit anti-mouse HRP respectively, supplemented with 10% normal sheep serum and 10% NHS for 30 min. These second antibodies were visualized with TSA-TRITC kit for 30 min. Slides were counterstained with TOPRO 3 iodide diluted 1:500 in PBS for 20 min, embedded with Vectashield and covered with a cover slip. The slides were examined with a fluorescent microscope or a Leica TCS-SP2 confocal laser scan microscope (CLSM).

Dual mRNA in situ-hybridisation with biotin and digoxigenin labeled DNA PCR probes

The first steps of this reaction were the same as the in the immuno-hybrido double staining procedure. The hybridization mixture was prepared as follows: 30 µl formamid 100 %, 20 µl TE buffer 0,1x,10 µl SSC 20x, 1 µl t-RNA (100 mg\ ml), 10 µl Hearing Sperm DNA, 5 µl digoxigenin labelled probe 1, 1.25 µl biotin labelled probe 2 and 22.75 µl RNAse free water, Total volume is 100 µl. The right balance between both probes was determined by testing. This hybridization mixture was boiled in water for 7 min to denature both DNA probes, and cooled on ice for 10 min. Then 25-30 µl of hybmix was applied to the tissue per slide, and covered with a cover slip. The slides were incubated on a hot plate at 47 °C for 10 min and subsequently, incubated in a humidified chamber overnight in an oven at 37°C. The cover slip was removed and the slides were rinsed in 30% formamid/ SSC 2x solution for 30 min at room temperature. The same solution was preheated in a water bath at 42°C and slides were incubated in this solution at 42°C for 10 min, rinsed in PBS, and incubated in a solution of rabbit anti digoxigenin-HRP labelled and mouse anti-biotin in a dilution of 1:1,000 and 1:50 respectively in PBS/BSA 1% for 1 hr. Subsequently, the slides were rinsed in PBS and the HRP labelled antibody was visualized with TSA FITC amplification kit diluted 1:50 in amplification diluents for 20 min. Slides were rinsed again in PBS and the mouse anti- biotin antibody was cross-linked before blocking the HRP labelled antibody with formalin fixation for 5 min. Again rinsed in PBS and the HRP of the Rabbit anti-digoxigenin was blocked with blocking reagent for 30 min. After rinsing in PBS, the slides were incubated with a HRP labelled rabbit anti-mouse IgG antibody diluted 1:250 in PBS supplemented with 10% NHS for 30 min, rinsed in PBS, and this second HRP labelled antibody was visualized with TSA TRITC amplification kit in the same dilution as the FITC step. After rinsing in PBS, nuclei were counterstained with TOPRO-3 iodide diluted 1:500 in PBS for 20 min. The slides were covered with a cover slip and embedded in Vectashield as anti fading reagent. The slides were evaluated with a CLSM.

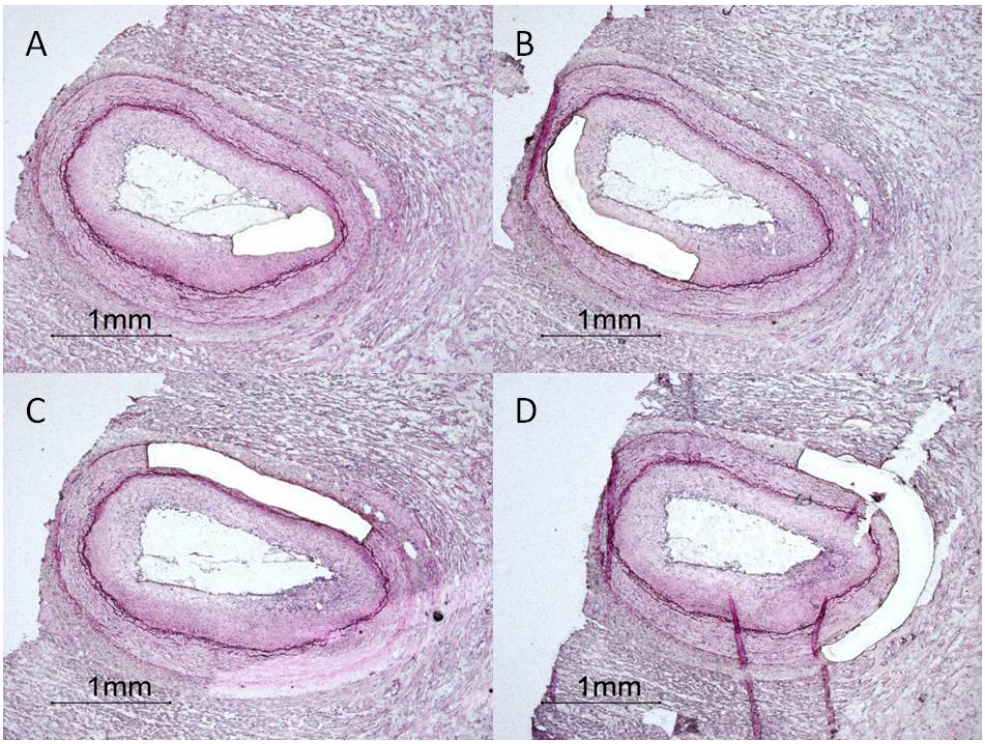

Figure S1: Laser Microdissection Different layers from coronary arteries were isolated by laser microdissection. **A**: NI-LL, **B**: NI-SMC, **C**: media and **D**: adventitia.

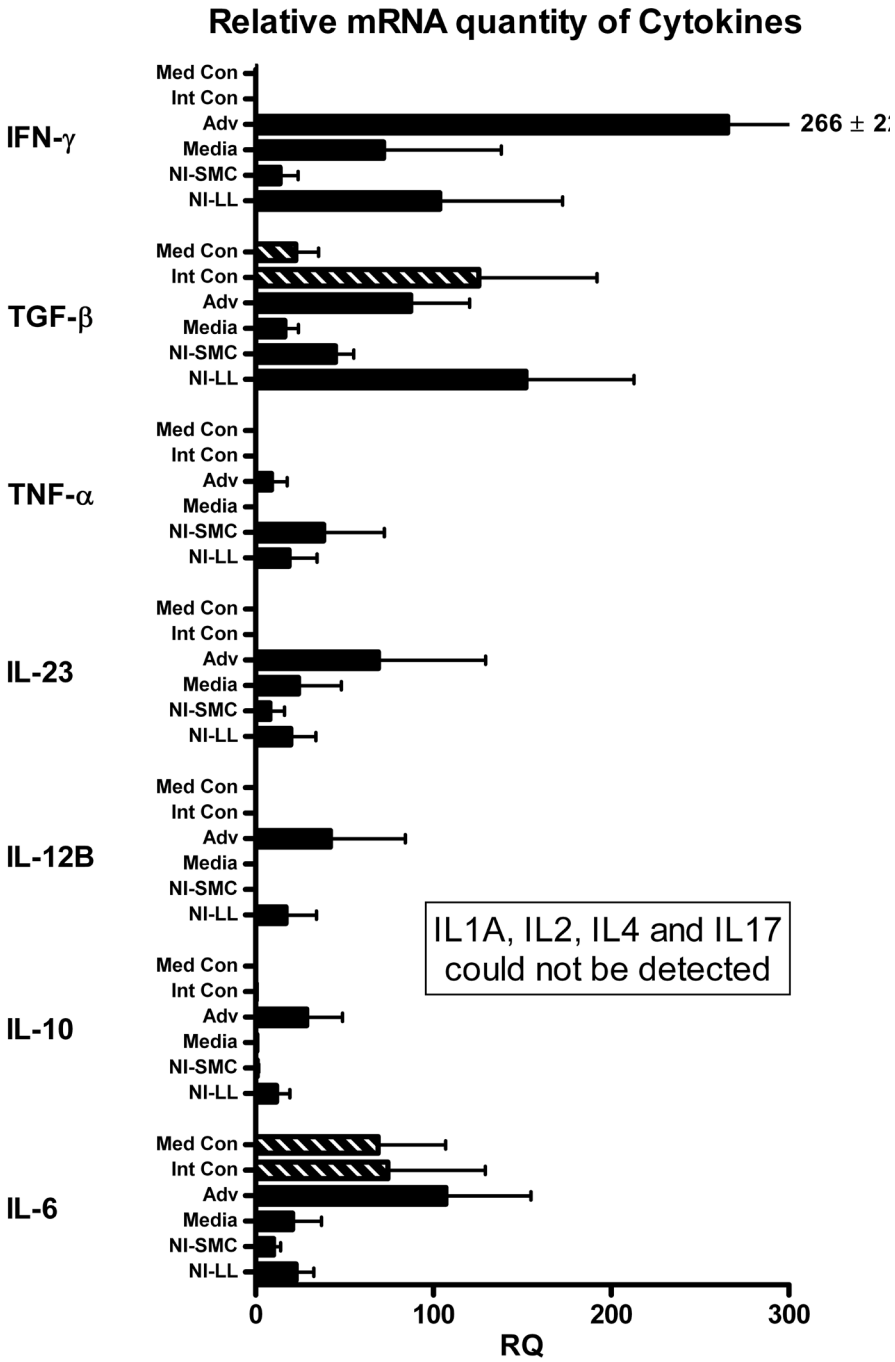

Figure S2. Q-PCR data of cytokine mRNA. Mean Relative Quantity ± SEM of mRNA of the various layers of CAV and control

Table S1. Characteristics of antibodies used for immunohistochemistry. P: paraffin, F: frozen, Rb: rabbit, Go: goat, Mo:mouse, PO:peroxidase, PV:powervision

Factor	P/F	Antigen Retrieval	Characteristic	Dilution	Isotype	Company	Secondary antibody
ID-1	F	-	Inhibitor of DNA binding 1	1-100	Rb	Santa Cruz Biotechnology Inc.; Santa Cruz, CA USA SC-488	Rb PV
PAI-1	F	-	Plasminogen Activator Inhibitor 1	1-100	Go	Abcam Ltd; Cambridge, UK ab-14197	RbαGoPO Rb PV
CTGF	F	-	Connective Tissue Growth Factor	1-50	Rb	Abcam Ltd; Cambridge, UK ab-6992	Rb PV
TGF-β1	P	EDTA		1-50	Rb	Santa Cruz Biotechnology Inc.; Santa Cruz, CA USA SC-146	Rb PV
MMP-2	F	-	Matrix Metalloproteinase 2	1-50	Mo	Neomarker Lab Vision Incorp. Fremont USA Ab4-vc2	Mo PV
MMP-9	F	-	Matrix Metalloproteinase 9	1-50	Mo	Neomarker Lab Vision Incorp. Fremont USA Ab-1 (Clone GE-213)	RbαGoPO Rb PV
CD1a	F	-	Human Thymocyte Antigen 1	1-10	Mo	Immunotech, Marseille, France, 1590	RbαGoPO Rb PV
CD3	F	-		1-50	Mo	Roche Diagnostics Nederland B.V., Almere 347340	RbαGoPO Rb PV
CD20	P	citrate		1-600	Mo	Dakopatts Glostrup, DK M755	Mo PV
CD68	P	citrate	Macrosialin	1-500	Mo	Novacastra Labs Ltd, Newcastle, UK, NCL CD68-KP1	Mo PV
CD284	F	-	Toll-like receptor 4 (TLR4)	1-20	Mo	Hycult Bio Technologies Uden, The Netherlands, HBT HTA 125	RbαGoPO Rb PV
CD206	F	-	Mannose Receptor (MR)	1-80	Mo	Serotec LtD, Kidlington Oxford, UK, mca 2155	RbαGoPO Rb PV
CD204	F	-	Scavenger Receptor (ScR)	1-40	Mo	Transgenic inc: Kumamoto, Japan, msra clone sra-e5	RbαGoPO Rb PV
RbαMoPO				1-250	Rb	Dakocytomation, Glostrup, DK P0161	
RbαMoPO				1-250	Rb	Dakocytomation, Glostrup, DK P0160	
Rb PV					Go	Immunologic DPVR-110 HRP, Duiven, The Netherlands	
Mo PV					Go	Immunologic DPVM-110 HRP, Duiven, The Netherlands	

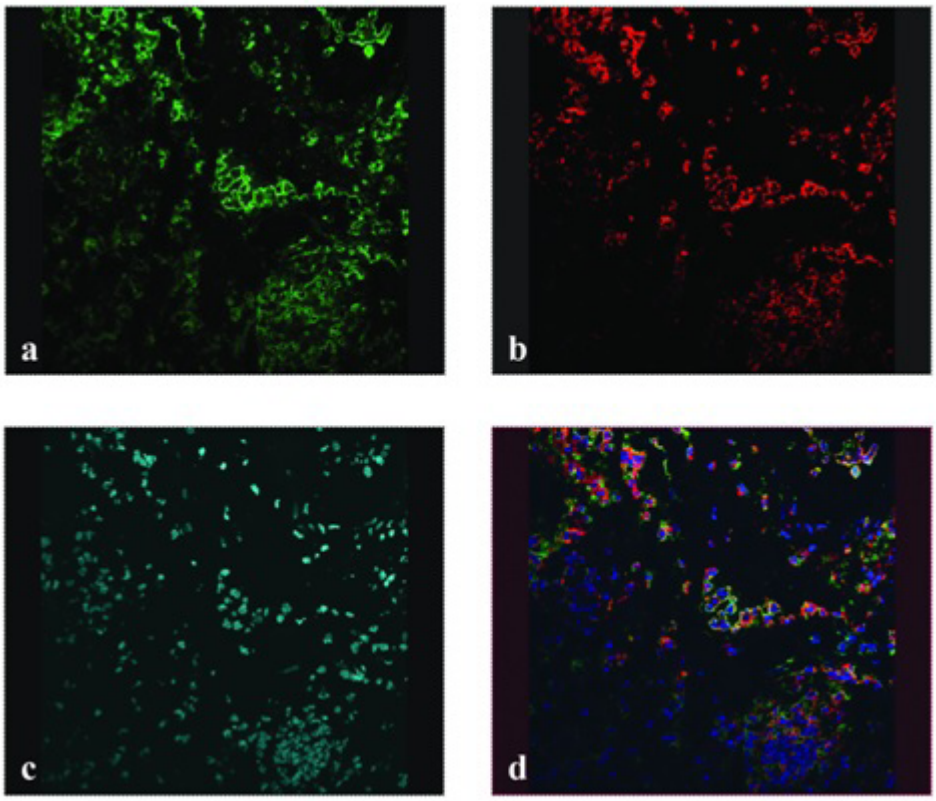

Figure S3. CLSM evaluation of a double in situ hybridisation experiment. A. ISH for γ-IFN (green) of infiltrating cells in the adventitia, **B**. same area stained by ISH for TGF-β (red), and **C**. stained for nuclei by TOPRO-3 iodide (blue), and **D**. the channel merged of a-c. Note at the right bottom an ExVascMNC area with a relatively weak staining for γ-IFN and TGF-β compared to the MNC in the adventitia.

Chapter 4.

THE COMPOSITION OF ECTOPIC LYMPHOID STRUCTURE SUGGESTS INVOLVEMENT OF A LOCAL IMMUNE RESPONSE IN CARDIAC ALLOGRAFT VASCULOPATHY

M.M.H. Huibers MSc [1], A. J. Gareau PhD [2], A. Vink MD PhD [1], R. Kruit MSc [1], H. Feringa BSc [1], J.M.T. Beerthuijzen BSc [1], E. Siera-de Koning BSc [1], T. Peeters BSc [1], N. de Jonge MD PhD [3], R.A. de Weger PhD1, T.D.G. Lee PhD [2,4,5]

Departments of Pathology [1] and Cardiology [3], University Medical Center Utrecht the Netherlands and Departments of Pathology [2], Surgery [4], and Microbiology & Immunology [5], Dalhousie University, Canada

Published
Journal of Heart and Lung Transplantation. doi: 10.1016/j.healun.2014.11.022 (2014). (Epub ahead of print)

Abstract

Background:
Cardiac allograft vasculopathy (CAV) is a multifactorial pathology limiting the survival of cardiac transplants. The etiology of CAV is unclear, but antibody and cellular-mediated responses have been implicated. We, and others, have observed ectopic lymphoid structures (ELS) surrounding epicardial coronary arteries with CAV. The potential contribution of these ELS to CAV has not been elucidated.

Methods:
Epicardial coronary arteries were collected from 59 transplant patients at two centers and studied for ELS presence and composition using immunohistochemistry. The intima and ELS were isolated and expression of genes involved in tertiary lymphoid organ (TLO) formation was measured by Q-PCR.

Results:
ELS presence was related to survival after transplantation ($p=0.013$) and histological composition of CAV ($p<0.001$). ELS contain B and T lymphocytes, macrophages and antibody-producing (IgM and/or IgG) plasma cells. A subpopulation of B lymphocytes appeared to be $CD20^{+}CD27^{+}$ memory B lymphocytes. The mRNA expression of TLO markers (lymphotoxin-β, CCL19 and CCL21) was significantly higher in ELS than in the neointimal lesions. Although the ELS observed in this study exhibited some TLO markers, they did not exhibit distinct B and T lymphocyte-rich areas normally found in classical TLOs.

Conclusions:
The cellular composition of the ELS differs from the cellular infiltrate in CAV intimal lesions. The presence of memory B lymphocytes and IgM- and IgG-producing plasma cells suggests that ELS are related to local antibody production potentially contributing to antibody-mediated CAV. ELS associated with coronary vessels containing CAV show features of underdeveloped TLOs; classical TLOs may not develop due to patient immunosuppression.

Introduction

Cardiac allograft vasculopathy (CAV) develops in the majority of heart transplant (HTx) recipients[1] due to a chronic immune response directed against the donor heart[2]. In the epicardial coronary vessels, CAV is characterized by arterial intimal thickening[3], the etiology of which has been linked to antibody-mediated rejection (AMR; [4,5]). In this study, we examine potential sites of local production of anti-donor antibodies involved in CAV.

In histological studies, clusters of inflammatory cells in the adventitia of the vascular wall and in the adipose tissue surrounding the epicardial coronary arteries have been observed[6]. We use the term ectopic lymphoid structures (ELS) to describe these structures, which have not been previously characterized in the coronary vessels with CAV. The presence of ELS may reflect an ongoing process of lymphoid neogenesis, leading to tertiary lymphoid organ (TLO) formation in response to the persistent allostimulation provided by the graft. TLOs have been associated with sites of chronic inflammation7 and described in transplant settings[8,9].

The aim of this study was to define the components of these ELS. We hypothesize that ELS are linked in a causative manner to CAV by providing a source of activated effector lymphocytes in close proximity to affected vessels. Confirming such a link could provide a potential therapeutic target that can be controlled to prolong the lifespan of patients following heart transplantation.

Materials and Methods

Patient population and tissue procurement

Autopsy databases from the Capital District Health Authority (Canada) and University Medical Center Utrecht (the Netherlands) were searched for patients who died following heart transplantation (with or without CAV) and from which archival coronary artery tissue was available. For study eligibility, a sample of the proximal region of at least one of the major coronary arteries (left anterior descending, left circumflex, right coronary artery) was required; fifty-nine patients met this criteria. Tissue was obtained under approval of the respective institutional ethical organizations (Capital Health Research Ethics Board REB #CDHA-RS2011-339 and Medical Ethics Committee #12/387).

Histological measurements and categorization

Formalin-fixed, paraffin-embedded coronary artery sections (5μm) were stained with Haematoxylin and eosin (H&E) to visualize CAV and ELS. All patients were categorized using a quantitative method according to the median size and number of ELS, as described in detail in the Supplemental Methods. Patients with a mean ELS area of <300μm^2 were categorized as ELS-1, and patients with a mean ELS area of >300μm^2 were characterized as ELS-2.

Immunohistochemistry

Endogenous peroxidase activity was blocked with 3% hydrogen peroxide. Antigen retrieval was performed using EDTA solution (pH=9.0) or citrate solution (pH=6.0) depending on the marker (**Supplemental Table 1**). Sections were incubated with the primary antibody diluted in serum when necessary, followed by incubation with HRP or biotinylated species-specific secondary antibody (**Supplemental Table 1**). Staining for all markers (except pNAD) was completed using a two-step process; for pNAD detection, a rabbit anti-rat polyclonal antibody was used as secondary antibody followed by incubation with a tertiary antibody with HRP label (BrightVision anti-rabbit HRP, Immunologic, Duiven, the Netherlands). Biotinylated secondary antibodies were incubated with a peroxidase avidin/biotin complex. Enzymatic activity was detected using a diaminobenzidine (DAB) solution. For double staining of pNAD and D2-40, slides were incubated with primary antibody against D2-40, antigen retrieval was performed using citrate solution, and the three-step process for pNAD detection, described above, was completed. All sections were counterstained with Haematoxylin (diluted 1:1 with Aqua Dest for T-Bet and FoxP3 counterstaining). For each stain, tonsil or lung tissue was used as a positive control. Species-specific isotype-matched irrelevant antibodies (IgG1 isotype and IgG2a isotype), or omission of the primary antibody, were used as negative controls. Sections were analyzed using digital images (200x, for markers FoxP3 and T-Bet) or light microscopy (400x, all other markers). Quantification of immunohistochemistry was performed by calculating the percentage of positively stained cells for the specific marker divided by the total number of infiltrated mononuclear cells in the field of view.

Immunofluorescence

Memory B lymphocytes were identified using mouse anti-CD20 and rabbit anti-CD27 antibody diluted in 5% normal goat serum (**Supplemental Table 1**). Secondary antibodies included a goat anti-mouse conjugated to Alexa 488 (Invitrogen Corporation, Carlsbad, CA) and a goat anti-rabbit conjugated to Alexa 555 (Invitrogen). Hoescht 33342 at a dilution of 1:5,000 (Invitrogen) was used as a nuclear counterstain. Digital images of immunofluorescence were captured using a Zeiss Axiovert 200M microscope (Carl Zeiss, Thornwood, NY) and a Hamamatsu Orca R2 camera (Hamamatsu, Boston, MA).

Laser Tissue Microdissection, RNA isolation, cDNA synthesis and Q-PCR

Ten patients with ELS that had high quality samples stored at -80ºC were used for mRNA expression analysis. To interpret the patient samples correctly, a 'calibrator' reference sample containing lymph node and placental tissue was included. 10 µm frozen tissue sections were cut and placed on PEN-foil-mounted glass slides (PALM Microlaser Technologies, Carl Zeiss, Bernried, Germany) and stained with Haematoxylin. From every patient, an area of approximately $12*10^6$ μm^2 was microdissected from the coronary artery intima and ELS using

the Robot-Microbeam (PALM Microlaser Technologies). Tissue pieces were collected in LPC microfuge tubes for RNA isolation.

Total RNA isolation was performed using the Picopure RNA isolation kit according to manufacturer's instructions (Arcturus, Applied Biosystems, and Foster City, CA). RNA was eluted in 33µl, concentration was measured using the Nanodrop, and RNA was stored at -80°C.

cDNA synthesis was performed by adding 1.5 µl oligo DT primers (0.50 lg; Promega Corporation, Phoenix, AZ), 1.5 µl of random primers (0.50 lg; Promega) and 3 µl dNTP's (25 mM; Invitrogen) to 33 µl RNA. This mix was heated in a closed Eppendorf tube for 5 min at 65°C and cooled to room temperature. 12 µl FS-buffer (Invitrogen), 6 µl DTT (Invitrogen) and 3 µl RNasin (Promega) were added, vigorously mixed and heated for 2 min at 37°C. 3 µl Superscript RNAse H-Reverse Transcriptase (Promega) was added and heated in a closed Eppendorf tube for 50 min at 37°C, followed by 15 min at 70°C, resulting in a total of 63 µl cDNA which was diluted to a total volume of 180 µl by adding MilliQ water.

The primer/probe FAM labelled combinations used for Q-PCR were ordered from Applied Biosystems (Foster City, CA). The mRNA expression levels of the following markers were studied: CD3, GATA3, RORC, T-Bet, FoxP3, IFN-γ, TGF-β, CCR3, CCR7, CX3CR1, CCL11, CCL19, CCL21, CCL22, CXCL13, LTβ and LTβR. Per sample, 6.25 µl master mix (Applied Biosystems), 0.625 µl Assay on Demand and 3.13 µl MiliQ was used and 2.5 µl cDNA was added. Q-PCR was performed by using the Viia 7 detection system (Applied Biosystems). Thermal cycling included a denaturation step at 95°C for 10 min, followed by 40 cycles of 95°C for 15 sec and 60°C for 60 sec. Data quantification was performed using the comparative Ct method with GAPDH as a housekeeping gene and calibrator samples for normalization. All assays were performed in duplicate; in the presented data the difference in cycle threshold (Cq) between the replicates did not exceed 0.5 Cq. Relative Quantification (RQ) values were calculated using the comparative Cq method
($RQ = 2^{-\Delta\Delta Cq}$, where $\Delta Cq = Cq_{target} - Cq_{reference}$, $\Delta\Delta Cq = \Delta Cq_{sample} - \Delta Cq_{calibrator}$).

Statistical analysis

Normality of parameters was checked using a Kolmogorov-Smirnov test. When two categorical parameters were tested for their relation, a Fisher's exact test was performed. Continuous parameters comparing groups of two were analyzed using a student's two-tailed t-test or Mann-Whitney U test. Results comparing groups of three or more were analyzed by one-way ANOVA or Kruskal-Wallis test with Bonferroni correction in post-hoc analysis. Parametric parameters are displayed as mean with standard deviation (SD) and non-parametric parameters were displayed as median with interquartile range (IQR). All statistics were performed using SPSS (version 20) and visualized with GraphPad Prism® (version 6; San Diego, CA). Values of $p<0.05$ are considered significant.

Results

Classification of the ELS

Patients in our cohort were classified into three categories based on mean size of the ELS surrounding the coronary vessels and assigned a value of ELS-0, ELS-1 or ELS-2 (**Figure 1A-C**). These ELS are focal structures, but when present in the transplanted heart they are seen along all arteries of the coronary tree. Of the 59 patients, 25 showed ELS (**Figure 1D**); 4 of these were excluded from ELS analysis due to tissue damage or scanning issues that resulted in an inability to effectively quantify ELS parameters. The median area (p=0.004, **Figure 1E**) and the median number of ELS (p=0.001, **Figure 1F**) per artery was significantly higher in the ELS-2 patients compared to ELS-1 patients.

ELS in relation to patient characteristics

Of the 59 patients examined, 34 patients were ELS-0. Patients in this ELS-0 group less than 6months post-transplant (n=21) were excluded from patient characteristic analysis since they could not have developed CAV in this short period. This left 13 patients in the ELS-0 group. The ELS-1 and ELS-2 groups were as above (n=20 and n=5 respectively) for most patient characteristic, however group size varies due to incomplete medical records. Pre- and post-transplant characteristics of patient and donor were analyzed (**Table 1**). LVAD implantation pre-transplant was found to be significantly related to ELS-category (p=0.034). Although this was based on only small numbers (n=4, **Table 1**) it is worth noting that all patients with previous LVAD implantation had ELS surrounding their coronaries (ELS-1 n=2, ELS-2 n=2). Primary cardiac diagnosis, donor age, ischemic time, gender mismatch patient/donor, CMV status patient/donor, immune suppression post-transplant, rejection episodes, Quilty lesions, neo-intimal lesion size, and cause of death were not significantly related to ELS category (**Table 1**).

We found a significant relationship between ELS category and time post-transplant (p=0.002); patients with ELS-2 had consistently shorter post-transplant survival times than the patients in ELS-0 (selected for >6months post-transplant) and ELS-1 (p=0.003 and 0.015 respectively; **Table 1** and **Figure 1G**).

We also found a significant association between the type of neointimal lesion in the coronaries and ELS category (**Table 1**, p=0.002). All patients with only carryover benign intimal thickening (BIT)[10] were in the ELS-0 category and early after transplant (<6 months, data not shown). 20 of 25 patients with ELS had fibrotic lesions consisting of well-organized connective tissue with very little lymphocytic infiltration. Only 5 of the 25 patients with ELS had lymphocytic lesions, characterized by a thin layer of BIT covered by a loose connective tissue layer with lymphocytic infiltration (primarily T cells and macrophages). 4 out of these 5 patients were in the ELS-2 category. Additionally, histological CAV type[11] was significantly related to ELS category (p=0.011, **Table 1**), where patients with H-CAV2 and 3 were mainly in the ELS-1 category (57% and 69%, respectively). Also, patients with large clusters (ELS-2) were mainly in the H-CAV1 category (4 out of 5). The surface area of the ELS was largest

in tissue derived from the shortest post-transplant survivors and decreased over time, remaining relatively constant in those patients who survived >5 yr (r=-0.538 p=0.012, **Figure 1H**). The median number of ELS was highest in tissue derived from the shortest survivors and remained relatively constant in those patients who survived >5 yr (r=-0.601 p=0.004, **Figure 1I**). The distance measured from the external elastic lamina of each coronary artery to the ELS was smaller in the patients that survived longer as compared to patients that died within the first years after transplantation (r=-0.601 p=0.004, **Supplemental Figure 2**).

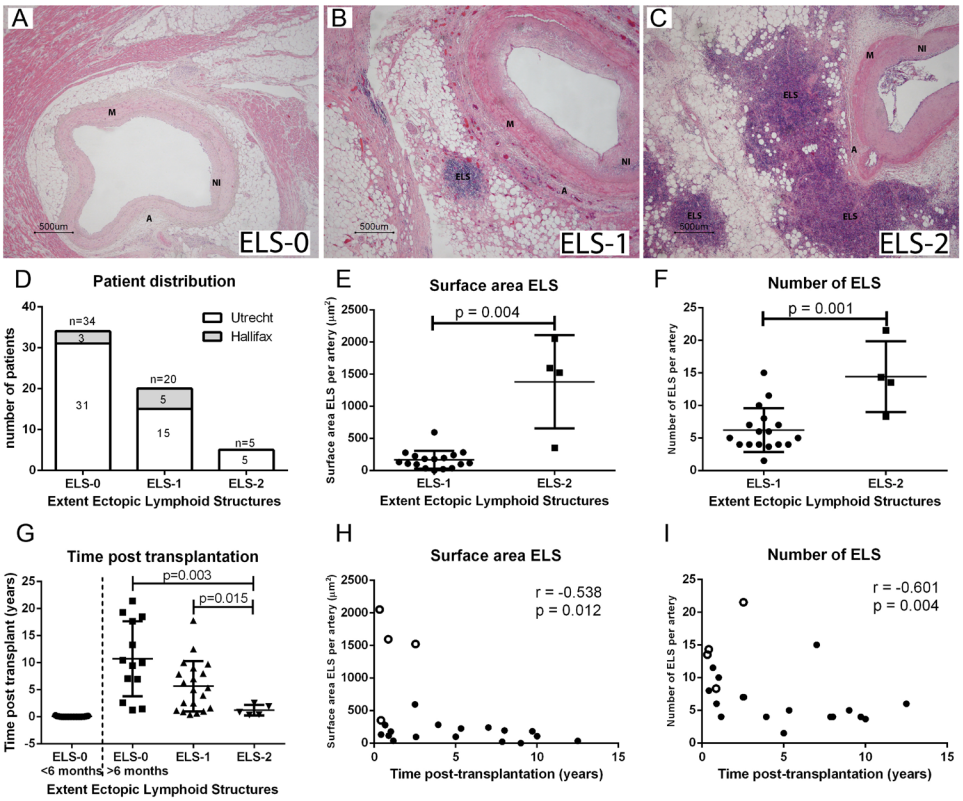

Figure 1. ELS in cardiac transplant patients. (A) ELS-0 patient with no ectopic lymphoid structures (ELS) surrounding the coronary arteries (A = adventitia, M = media, NI = neointima). **(B)** ELS-1 patient with ELS surrounding the coronaries (mean size <300µm2). **(C)** ELS-2 patient with large ELS surrounding the coronaries (mean size >300µm2). **(D)** Distribution of patients from Canada and the Netherlands according to ELS category. (E, F, H, I) 25 patients showed ELS; 4 of these were excluded from quantitative ELS analysis due to technical issues. **(E)** The mean surface area of ELS is significantly higher in ELS-2 patients (p=0.004). Bars display mean with standard deviation. **(F)** The mean number of ELS per artery is significantly higher in ELS-2 patients (p=0.001). **(G)** Time post-transplant for the different groups of ELS. ELS-0 patients <6months post-transplant are excluded from statistical analysis, defined by the dotted line. Patients with ELS-2 were always shorter after transplant than the remaining patients in ELS-0 (>6months post-transplant) and ELS-1 patients (p=0.003 and 0.015 respectively). **(H)** The surface area of the ELS decreases with time post-transplant (p=0.012, r=-0.538). Closed dots indicate ELS-1 patients, whereas open dots indicate ELS-2 patients. **(I)** The mean number of ELS decreases with time post-transplant (p=0.004, r=-0.601).

Table 1. Patient characteristics. Group size varies due to incomplete medical records. IQR = Interquartile range, SD = standard deviation, LVAD = left ventricular assist device, CMV = cytomegalovirus, EMB = endomyocardial biopsy, HTx = heart transplantation, NI = neointima, H-CAV = histological CAV, [a] Fisher's Exact Test, [b] Kruskal-Wallis Test, [c] ANOVA

		Extent Ectopic Lymphoid Structures			
	ELS Time posttransplants	**ELS-0 (none)** >6monts	**ELS-1 (<300um²)** all	**ELS-1 (<300um²)** all	**p-value**
Primary Cardiac diagnosis	Number (%) Dilated cardiomyopathy Ischemic heart disease Restrictive / hypertrophic	n=13 4 (36%) 8 (42%) 1 (50%)	n=15 5 (46%) 10 (53%) 0 (0%)	n=4 2 (18%) 1 (5%) 1 (50%)	0.266[a]
LVAD pre-transplant	Number (%) Yes No	n=13 0=(0%) 13 (46%)	n=15 2 (50%) 13 (46%)	n=4 2 (50%) 2 (7%)	**0.034[a]**
Donor age	(years) Median (IQR)	n=13 47 (38-51)	n=15 47 (43-52)	n=4 38 (24-48)	0.349[b]
Ischemic time	(minutes) Mean (SD)	n=13 151 (40)	n=15 163 (36)	n=4 160 (12)	0.681[c]
Gender Patient / donor	Number (%) m/m m/f f/f f/m	n=13 5 (33%) 3 (43%) 4 (44%) 1 (100%)	n=15 8 (53%) 4 (57%) 3 (33%) 0 (0%)	n=4 2 (13%) 0 (0%) 2 (22%) 0 (0%)	0.771[a]
CMV status Patient / donor	Number (%) -/- -/+ +/- +/+	n=12 2 (33%) 2 (25%) 4 (57%) 4 (44%)	n=15 4 (66%) 3 (38%) 3 (43%) 5 (56%)	n=3 0 (0%) 3 (38%) 0 (0%) 0 (0%)	0.314[a]
Immune suppression	Number (%) Cyclosporin Tacrolimus	n=13 12 (43%) 1 (25%)	n=15 14 (50%) 1 (25%)	n=4 2 (7%) 2 (50%)	0.118[a]
Rejection episodes recorded	Number (%) Yes	n=13 10 (48%)	n=15 8 (38%)	n=4 3 (14%)	0.449[a]
Quality in EMB recorded	Number (%) Quilty A or B or both	n=13 13 (43%)	n=15 14 (47%)	n=5 3 (10%)	0.053[a]
Time post HTx	(days) Median (IQR)	n=13 3659 (1746-6595)	n=20 1886 (468-3194)	n=5 315 (135-812)	**0.002[b]**
Relative NI lesion size	Mean (SD)	n=13 0.42 (0.15	n=20 0.51 (0.13)	n=5 0.46 (0.07)	0.133[c]
CAV lesion type	Number (%) Lymphocytic Fibrotic	n=13 3 (38%) 10 (33%)	n=20 1 (13%) 19 (63%)	n=5 4 (50%) 1 (3%)	**0.002[a]**
H-CAV type	Number (%) H-CAV1 H-CAV2 H-CAV3	n=13 3 (38%) 5 (36%) 5 (31%)	n=20 1 (13%) 8 (57%) 11 (69%)	n=5 4 (50%) 1 (7%) 0 (0%)	**0.011[a]**
Cause of death	Number (%) CAV Acute Rejection Other	n=13 3 (27%) 2 (22%) 8 (44%)	n=20 7 (64%) 4 (44%) 9 (50%)	n=5 1 (9%) 3 (33%) 1 (6%)	0.337[a]

ELS contain B lymphocytes, T lymphocytes, and macrophages

ELS display a large number of T lymphocytes ($CD3^+$, **Figure 2A**) and B lymphocytes ($CD20^+$, **Figure 2B**), and smaller number of macrophages ($CD68^+$; **Figure 2C**). We found that the cellular composition was different between the neointimal infiltrate and ELS (**Figure 2J**). The neointimal infiltrate consisted of 30% T lymphocytes and 20% macrophages, whereas almost no B lymphocytes could be detected in the lesions. We found no significant difference in cellular composition between ELS groups (**Figure 2J**).

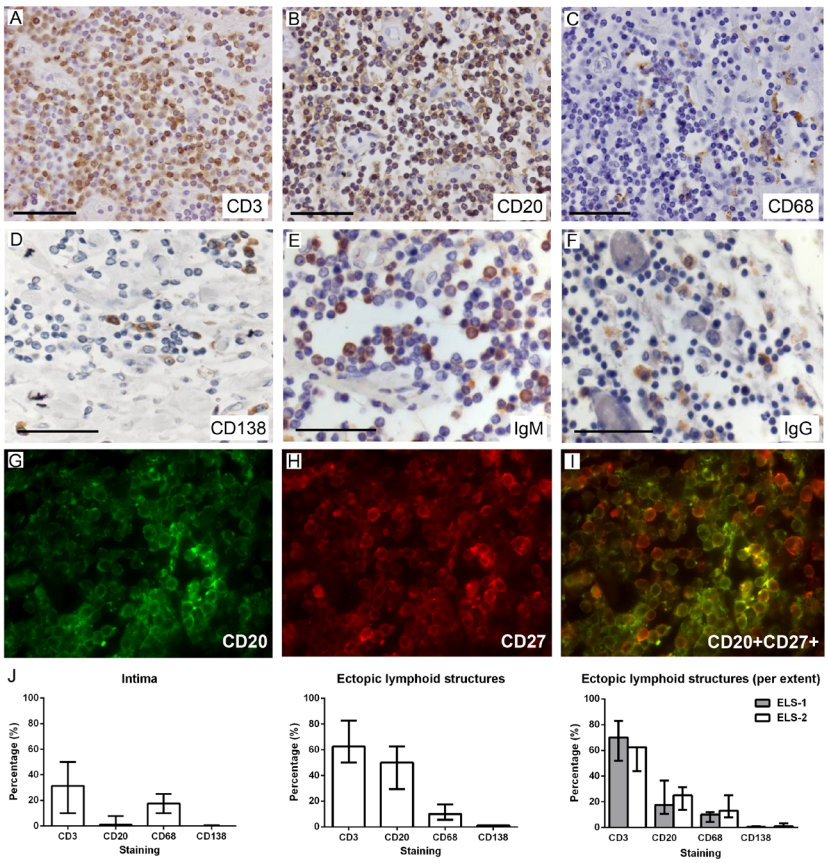

Figure 2. ELS contain B lymphocytes, T lymphocytes and macrophages and are sites of active antibody production. Cellular composition is quantified from immunohistochemical staining for: **(A)** CD3 (line indicates 50 μm), **(B)** CD20, and **(C)** CD68. ELS contain plasma cells (CD138; Figure **2D**) that produce: **(E)** IgM and **(F)** IgG. Memory B lymphocytes positive for CD20 and CD27 are present in ELS (Figure **2G-I**). The neointima is primarily composed of T lymphocytes and macrophages (Figure **2J**), whereas the ELS contain mainly T lymphocytes and B lymphocytes (Figure **2J**). The ELS contain about 50% B lymphocytes (CD20) and only a few plasma cells (CD138), whereas the intima barely contains any B lymphocytes. Categorizing this data on ELS type (Figure **2J**) does not change the cellular composition (bars display median with interquartile range).

ELS are areas of active antibody production

ELS contained plasma cells in small numbers and they were occasionally found isolated throughout the adventitia (**Figure 2D**). There were no plasma cells in the media and only a small number of patients had plasma cells in the neointimal lesions. Despite the low number of plasma cells, they were actively producing IgM and IgG (**Figure 2E and 2F**, respectively). In ELS-1 patients, IgM was present in 14 of 19 patients and IgG was present in 10 of the 19 patients (**Table 2**). IgM and IgG were present in all ELS-2 patients, where a significant number of ELS-1 and ELS2 patient had IgG (**Table 2**, p=0.047)

Some patients showed $CD20^{+}CD27^{+}$ memory B lymphocytes in ELS (**Figure 2G-I**); there was a significant relationship between ELS category and presence of memory B cells. Memory B lymphocytes were found in 13 of the 19 ELS-1 patients and all ELS-2 patients (**Table 2**, p=0.027). Only one ELS-0 patient had memory B-cells in the adventitial tissue (**Table 2**).

Table 2. Staining characteristics. a Fisher's Exact Test, ND = not determined, due to small numbers

	Extent of ectopic lymphoid structures			
+ (%)	**ELS-0** n=5	**ELS-1** n=19	**ELS-2** n=5	**p-value** [a]
IgG	1 (20%)	10 (53%)	5 (100%)	**0.047**
IgM	2 (40%)	15 (79%)	5 (100%)	0.086
Memory B	1 (20%)	13 (68%)	5 (100%)	**0.027**
pNAD	1 (50%)	12 (86%)	5 (100%)	0.384
D2-40	2 (100%)	13 (93%)	4 (100%)	ND
CD1a	0 (0%)	5 (36%)	4 (80.0%)	0.153
CD21	1 (50%)	5 (36%)	2 (40%)	ND

T lymphocytes are mainly T helper cells

T lymphocytes within ELS were mainly $CD4^{+}$ T helper (Th) cells (**Figure 3A**), with both a population of putative regulatory T lymphocytes (Treg, **Figure 3C**) and Th1 cells ($Tbet^{+}$, **Figure 3D**), although $CD8^{+}$ T lymphocytes were present as well (**Figure 3B**). T cell phenotype distribution was similar in the neointima and the ELS (**Figure 3E**). Q-PCR (**Figure 3F**) showed that the expression of CD3 was significantly higher in the ELS compared to the intima (p=0.020; **Figure 3**). FoxP3 (Treg) is significantly higher in the ELS (p=0.016). CCR7 (lymphoid attraction marker) and $IFN\gamma$ were abundantly expressed in the ELS compared to CAV lesions (p=0.042 and 0.049, respectively). Additionally, GATA3 (Th2 cells) and CCL11 (expressed by Th2 cells) showed higher expression levels in the ELS compared to the intima (p=0.040 and 0.012 respectively).

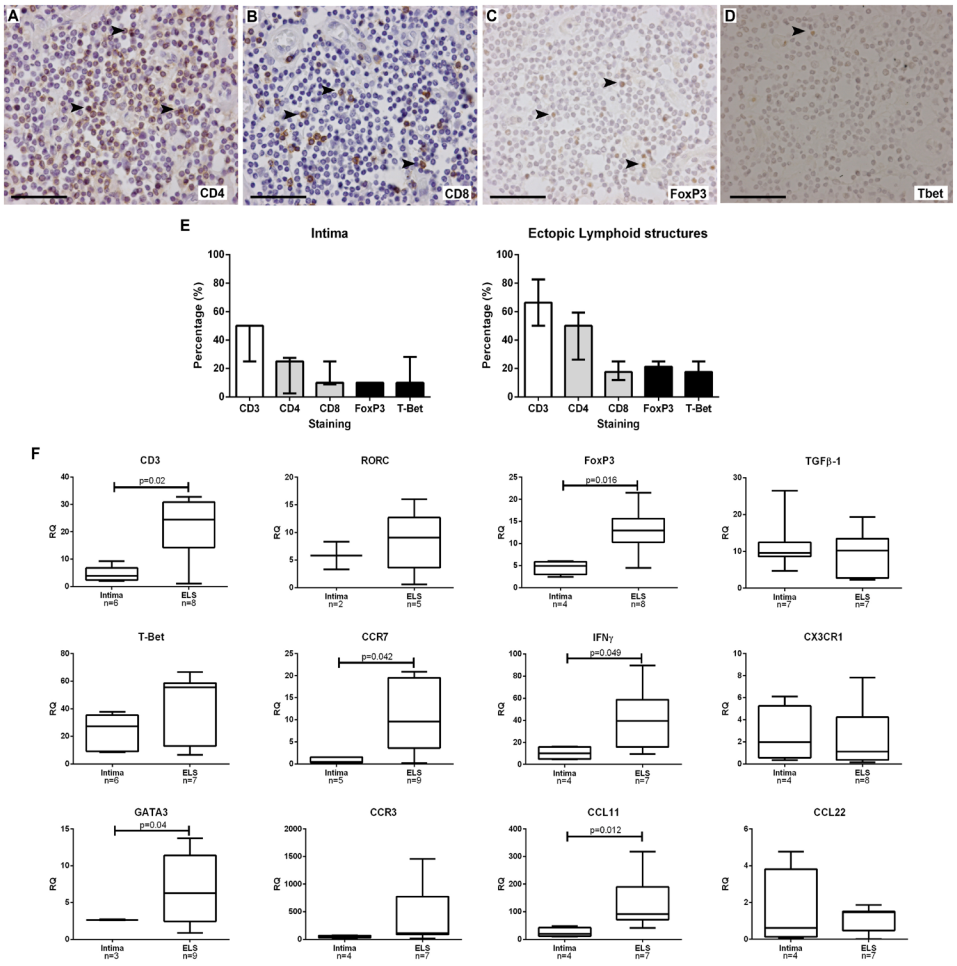

Figure 3. T lymphocytes: Mainly a T-helper cell phenotype. Most T lymphocytes within the ELS are T helper cells (CD4; Figure **3A**, line indicates 50 µm), however cytotoxic T lymphocytes are also present (CD8; Figure **3B**). This T helper cell population contains regulatory T lymphocytes (FoxP3; Figure **3C**) and T helper 2 cells (T-bet; Figure **3D**). The T cell distribution in the intima of CAV arteries is the same as the distribution in the ELS and consists of mainly T helper cells (Figure **3E**). **(F)** Q-PCR data shows a significantly higher amount of CD3, FoxP3, CCR7, IFNγ, GATA3, and CCL11 expression in the ELS compared to the intima (box plots represent median with interquartile ranges). RQ=relative quantity.

Macrophages polarize towards an M2-type within the ELS

The predominant type of macrophages (CD68$^+$, **Figure 4A**) found in the ELS are the type 2 (M2) (CD163$^+$, scavenger receptor/CD204$^+$, mannose receptor/CD206$^+$, **Figure 4D-F**) rather than (M1) macrophages (**Figure 4B**, iNOS$^+$ cells were rarely found)[12]. Macrophages comprised 15% of the infiltrate in the intima and 10% of the ELS (**Figure 4G**). M2-macrophage markers CD163, CD204, and CD206 were highly expressed in the intimal lesions and ELS. CCR7 (M1-macrophage marker) was highly expressed in the ELS but could also be found on T lymphocytes (**Figure 4C**).

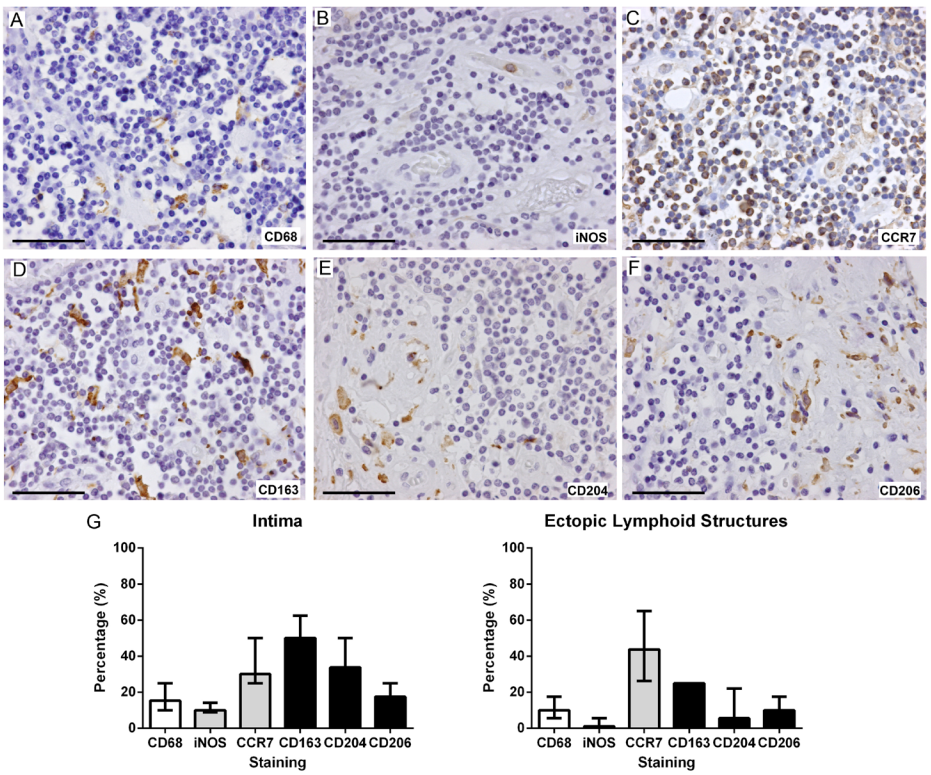

Figure 4. Macrophages: Polarization towards M2-type in chronic inflammation. (A) Macrophages (CD68) are present in the ELS (line indicates 50 µm). Of these macrophages, very few exhibit M1-type markers (iNOS; Figure **4B**), whereas many of them show positive markers for the M2-type (CD163, CD204, and CD206; Figure **4D-F**). Many cells are positive for CCR7 (Figure **4C**). (G) Quantification of the IHC data shows similar macrophage profiles in the intima and the ELS, with the exception of CCR7 which is more abundant in the ELS (bars display median with interquartile range).

ELS exhibit characteristics of tertiary lymphoid organs

The ELS studied here lacked some specific cell types required for classification as a classical TLO (**Table 2**). Two types of vessels are critical in TLOs for influx and outflow of immune cells; high endothelial venules (pNAD, **Figure 5A**) and lymphatic vessels (D2-40, **Figure 5B**). When $pNAD^+$ vessels were present these were mainly located within the ELS. When rare $D2\text{-}40^+$ vessels were found within the ELS; they were mainly located on the outer edges of the ELS and outer surface of the transplanted heart. Subtypes of dendritic cells, including interdigitating dendritic cells (CD1a, **Figure 5D**) and follicular dendritic cells (CD21, **Figure 5E**) need to be present to display antigens within this network. $CD1a^+$ cells were rarely found in the ELS, and when they were present, they were noticed primarily in ELS-2 patients. In addition, $CD21^+$ cells were rarely found, but when found they formed networks within the central area of the ELS without forming a clear follicular structure. Other TLO markers were measured by Q-PCR in ELS and compared to their expression level in the intima of CAV arteries within the same patient. LTβ ($p=0.019$), CCL19 ($p=0.005$), and CCL21 ($p=0.005$) showed significantly higher expression in ELS compared to intimal tissue (**Figure 5F**). A schematic overview of all markers involved in TLO formation measured here is shown in **Figure 5G**.

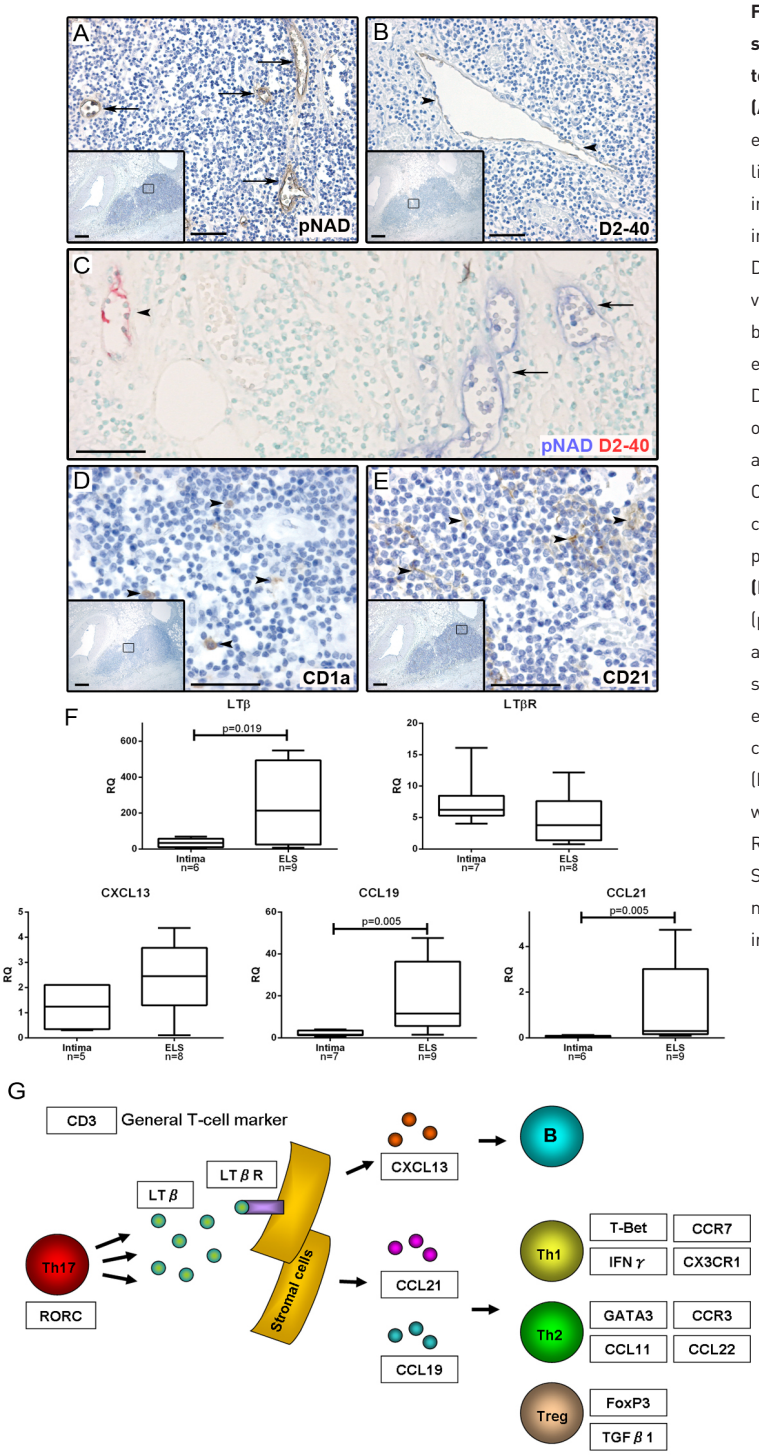

Figure 5. ELS contain some characteristics of tertiary lymphoid organs. **(A)** pNAD+ vessels (high endothelial venules) lie within the ELS (line indicates 50 μm; inset line indicates 500μm) and **(B)** D2-40+ vessels (lymphatic vessels) can sometimes be found on the outer edges of the clusters. **(C)** Double staining shows no overlap between pNAD and D2-40 markers. **(D)** CD1a+ or **(E)** CD21+ cells can be found but are not present in every patient. **(F)** TLO-markers like LTβ (p=0.019), CCL19 (p=0.005), and CCL21 (p=0.005) show significantly higher expression in ELS compared to intimal tissue (bars display median with interquartile range, RQ=Relative Quantity. **(G)** Schematic overview of markers and cell types involved in TLO formation.

Discussion

Until recently, little attention has been paid to the clusters of inflammatory cells surrounding epicardial coronary arteries in developing CAV. Their consistent presence suggests that these ELS warrant close examination based on their location and cellular composition. In our two-center study (Halifax, Canada and Utrecht, The Netherlands) 34 out of 59 patients did not have ELS (ELS-0). This group showed a large distribution in time post-transplant; therefore the group was split into early (<6months) and late (>6months) post-transplant subgroups. The early group was excluded from further analysis since one of the primary goals of this paper was to investigate the relationship between ELS and CAV and these patients could not have developed CAV in this short period.

By excluding the early ELS-0 subgroup, none of the remaining patients had carryover BIT only, meaning that all patients without CAV were also without ELS surrounding their coronary arteries. Time post-transplant in patients with ELS-0 or ELS-1 was longer compared to patients with ELS-2. The aggressive immunological reaction in the ELS-2 group (large ELS combined with or without acute rejection) may be a potential explanation for the early deaths. A significant relationship between CAV lesion type and ELS type was found. These data indicate a link between lesion formation and ELS[11].

The ELS observed may represent the initial stages of TLO development. TLOs have been found in animal models of long-term allograft rejection[9,13], but it is likely that the absence of immunosuppression in these models allowed for expression of the chemokines and cytokines necessary to support complete TLO formation. The types of immune cells are of a mixed T cell phenotype within ELS, containing Tregs, Th1 and Th2 cells. The high expression of CCR7, a chemokine receptor involved in lymph-node homing of naïve T lymphocytes and Tregs[14], within ELS suggests a local balancing of effector and regulatory mechanisms and lymphoid neogenesis. Others have shown that ELS can also generate effector and memory T lymphocytes which lead to allograft rejection[8]. The Tregs found within ELS may have migrated from the local inflammatory site in an attempt to suppress the alloimmune response[15]. Because of the close association of FoxP3 with Treg in most cases, we assume that the observed FoxP3 T cells are Treg[16]. Even if this is not the case in the ELS, it further suggests that active immune processes are occurring there. Additionally, mainly M2-macrophages were observed, which are associated with chronic inflammation, in the ELS[17].

The majority of our patients contained HEVs (pNAD) within the ELS, and lymph vessels (D2-40) surrounding the ELS. Chronically rejected grafts often have defects in lymphatic drainage to lymph nodes[18], causing accumulation of immune cells, local production of soluble factors (e.g. lymphotoxin), and formation of TLOs[18]. The high expression of LTβ, a cytokine that supports lymphoid neogenesis, within the ELS supports the idea that the ELS may represent the early stages of TLO formation. Additionally, the high expression of CCR7 indicates continuous homing of dendritic cells and subpopulations of T lymphocytes[14]. The ligands of CCR7, CCL19 and CCL20 are also highly expressed in ELS, corresponding with previous findings regarding naïve T cell (CCL19, CCL21), B cell (CXCL13) and DC (CCL21) recruitment[8,19].

Given that animal models of CAV have demonstrated a significant role for antibody in the induction of neointimal lesions[20,21] particular attention was paid to the presence of antibody in ELS. ELS contained many B lymphocytes, but not organized into germinal centers

as in classical TLOs[7]. These data are consistent with previous studies implicating intragraft B lymphocytes in promoting chronic rejection[22,23]. Furthermore, the presence of $CD20^{+}CD27^{+}$ memory B lymphocytes in the ELS is particularly concerning based on their ability to produce very specific antibody at a rapid rate and their resistance to traditional CD20-targeting therapies[24]. Little data currently exists on the role of memory B lymphocytes in cardiac transplant rejection, and their presence has not previously been reported in graft tissue. This is likely to be a very important area of study given the fact that memory T lymphocytes are also being strongly implicated in graft rejection[25].

IgM and/or IgG were found in the majority of patients with ELS, and it is likely that the locally-produced antibody can access the vessel and contribute to vascular remodelling in some manner, although antigenic targets of these locally-produced antibodies remain unknown. It has been demonstrated that local graft-derived DSAs were better prognostic markers for antibody-mediated kidney transplant damage than serum antibodies[26]. We hypothesize that the close proximity of the ELS to the coronaries allows the antibody produced there to be transported into the vessel and cause damage via a complement-dependent pathway. Additionally, complement-independent mechanisms of antibody-mediated damage can activate endothelial cells and medial smooth muscle cells[27]. The timing of appearance and the structure of ELS demonstrates that they are not Quilty lesions, which have no association with transplant vasculopathy in the epicardial coronaries[28,29].

Although the data presented here provide more insight into the function of the ELS closely associated with CAV in the epicardial coronary arteries, these findings still do not provide direct evidence of the beneficial or detrimental role of ELS in the transplant. While some groups state that the presence of ELS is damaging due to continuous antigen exposure and constant immune activation[30], others consider them as benign or beneficial[9,31]. The function of ELS in a transplant setting remains controversial and requires further study.

Limitations

This study is an end-stage autopsy study with only one time point for ELS classification per patient. Autopsy is mainly requested in patients that die early after transplant which could have the potential to skew our patient population. We also recognize that although this is a dual center study, our patient cohorts are small and within this small cohort we have some missing values because of privacy concerns or inability for follow-up. However, we do not believe that these limitations influenced our findings regarding ELS composition and function.

Acknowledgements

We would like to thank Joyce van Kuik for her Q-PCR support, and Dr. Michael Hart-Matyas, Tanya Myers and Brenda Ross for assistance with other technical aspects of this work. This work was supported by a travelling award from the International Society for Heart and Lung Transplantation to AJG.

References

1. Christie, J. & Edwards, L. The Registry of the International Society for Heart and Lung Transplantation: 29th adult lung and heart-lung transplant report—2012. ... *Lung Transplant.* **31**, 1073–1086 (2012).
2. Colvin-Adams, M. & Agnihotri, A. Cardiac allograft vasculopathy: current knowledge and future direction. *Clin. Transplant.* **25**, 175–184 (2011).
3. Billingham, M. E. Histopathology of graft coronary disease. *J. Hear. lung Transplant.* **11**, S38–44 (1992).
4. Nath, D. S. et al. Donor-specific antibodies to human leukocyte antigens are associated with and precede antibodies to major histocompatibility complex class I-related chain A in antibody-mediated rejection and cardiac allograft vasculopathy after human cardiac transplantat. *Hum. Immunol.* **71**, 1191–6 (2010).
5. Wu, G. W. et al. Asymptomatic antibody-mediated rejection after heart transplantation predicts poor outcomes. *J. Heart Lung Transplant.* **28**, 417–22 (2009).
6. Van Loosdregt, J. & Oosterhout, M. van. The chemokine and chemokine receptor profile of infiltrating cells in the wall of arteries with cardiac allograft vasculopathy is indicative of a memory T–helper 1. *Circulation* **114**, 1599–1607 (2006).
7. Neyt, K., Perros, F., GeurtsvanKessel, C. H., Hammad, H. & Lambrecht, B. N. Tertiary lymphoid organs in infection and autoimmunity. *Trends Immunol.* **33**, 297–305 (2012).
8. Nasr, I. W. et al. Tertiary lymphoid tissues generate effector and memory T cells that lead to allograft rejection. *Am. J. Transplant.* **7**, 1071–9 (2007).
9. Brown, K., Sacks, S. H. & Wong, W. Tertiary lymphoid organs in renal allografts can be associated with donor-specific tolerance rather than rejection. *Eur. J. Immunol.* **41**, 89–96 (2011).
10. Devitt, J. J. et al. Impact of donor benign intimal thickening on cardiac allograft vasculopathy. **J. Hear. lung Transplant. 32**, 454–60 (2013).
11. Huibers, M. M. H. et al. Distinct phenotypes of cardiac allograft vasculopathy after heart transplantation: A histopathological study. *Atherosclerosis* **236**, 353–359 (2014).
12. Geissmann, F., Gordon, S., Hume, D. A., Mowat, A. M. & Randolph, G. J. Unravelling mononuclear phagocyte heterogeneity. *Nat. Rev. Immunol.* **10**, 453–60 (2010).
13. Baddoura, F. K. et al. Lymphoid neogenesis in murine cardiac allografts undergoing chronic rejection. *Am. J. Transplant* **5**, 510–516 (2005).
14. Förster, R., Davalos-Misslitz, A. C. & Rot, A. CCR7 and its ligands: balancing immunity and tolerance. *Nat. Rev. Immunol.* **8**, 362–71 (2008).
15. Zhang, N. et al. Regulatory T cells sequentially migrate from inflamed tissues to draining lymph nodes to suppress the alloimmune response. *Immunity* **30**, 458–69 (2009).
16. Gavin, M. & Torgerson, T. Single-cell analysis of normal and FOXP3-mutant human T cells: FOXP3 expression without regulatory T cell development. *Proc Natl Acad Sci U S A.* **103**, 6659–64 (2006).
17. Torroella-Kouri, M., Rodríguez, D. & Caso, R. Alterations in macrophages and monocytes from tumor-bearing mice: evidence of local and systemic immune impairment. *Immunol. Res.* **57**, 86–98 (2013).
18. Thaunat, O. & Patey, N. Chronic rejection triggers the development of an aggressive intragraft immune response through recapitulation of lymphoid organogenesis. *J. Immunol.* **185**, 717–28 (2010).
19. Hjelmström, P. et al. Lymphoid tissue homing chemokines are expressed in chronic inflammation. *Am. J. Pathol.* **156**, 1133–8 (2000).
20. Russell, P. & Chase, C. Coronary atherosclerosis in transplanted mouse hearts. II. Importance of humoral immunity. *J. Immunol.* **152**, 5135–5141 (1994).
21. Gareau, A., Hirsch, G., Lee, T. & Nashan, B. Contribution of B cells and antibody to cardiac allograft vasculopathy. *Transplantation* **88**, 470–477 (2009).
22. Wehner, J., Fox-Talbot, K. & Halushka, M. B cells and plasma cells in coronaries of chronically rejected cardiac transplants. ... **89**, 1141–1148 (2010).
23. Colvin, R. B. et al. Emerging role of B cells in chronic allograft dysfunction. *Kidney Int.* **(119):S13**-, S13–7 (2010).
24. Kamburova, E. G. et al. A Single Dose of Rituximab Does Not Deplete B Cells in Secondary Lymphoid Organs but Alters Phenotype and Function. *Am. J. Transplant.* **13**, 1503–1511 (2013).
25. Poggio, E. D. & Augustine, J. J. Alloreactive T cells and ¨the persistence of memory¨. *Kidney Int.* **84**, 1074–6 (2013).
26. Bachelet, T. et al. Kidney intragraft donor-specific antibodies as determinant of antibody-mediated lesions and poor graft outcome. *Am. J. Transplant.* **13**, 2855–64 (2013).
27. Valenzuela, N. M., McNamara, J. T. & Reed, E. F. Antibody-mediated graft injury: complement-dependent and complement-independent mechanisms. *Curr. Opin. Organ Transplant.* **19**, 33–40 (2014).
28. Zakliczynski, M. et al. Quilty effect correlates with biopsy-proven acute cellular rejection but does not predict transplanted heart coronary artery vasculopathy. *J. Heart Lung Transplant.* **28**, 255–9 (2009).
29. Chu, K. E., Ho, E. K., de la Torre, L., Vasilescu, E. R. & Marboe, C. C. The relationship of nodular endocardial infiltrates (Quilty lesions) to survival, patient age, anti-HLA antibodies, and coronary artery disease following heart transplantation. *Cardiovasc. Pathol.* **14**, 219–24 (2005).

30. Thaunat, O. et al. Lymphoid neogenesis in chronic rejection: evidence for a local humoral alloimmune response. *Proc. Natl. Acad. Sci. U. S. A.* **102**, 14723–8 (2005).
31. Le Texier, L. et al. Long-term allograft tolerance is characterized by the accumulation of B cells exhibiting an inhibited profile. *Am. J. Transplant.* **11**, 429–438 (2011).

Supplemental Material

Measurements of ectopic lymphoid structures

Measurements were performed using ImageScope software (Aperio version 10.0.36.1805), or Adobe Photoshop CS5 (San Jose, CA). 34 of 59 patients showed no evidence of ELS and were classified as ELS-0. In patients with ELS, a 3 mm radius was drawn around each coronary artery; this radius was measured from the external elastic lamina (Supplemental Figure 1). The distance and surface area of each ELS from the external elastic lamina (EEL) of an affected coronary artery was measured. Additionally, the total number of ELS was enumerated per affected artery. From this data, the mean number of ELS per artery and mean ELS surface area was calculated. Patients were then categorized according to the mean surface area of the ELS around the coronary arteries; patients with a mean ELS area of <300μm2 were categorized as ELS-1 patients, and patients with a mean ELS area of >300μm2 were characterized as ELS-2 patients. Scoring was done by measuring ELS around at least two coronary arteries.

To calculate relative lesion area, lines were traced along the external elastic lamina (EEL), internal elastic lamina (IEL), and the endothelial layer. The cross-sectional areas of the entire vessel and neointimal lesions were calculated as follows: total vessel area = area within EEL and neointimal lesion = area within IEL – area lumen. Relative neointimal lesion size was calculated by dividing the area of the neointimal lesion by the total vessel area.

Immunohistochemistry

Paraffin embedded tissue samples were cut in 5 μm sections. Sections were deparaffinized and endogenous peroxidase activity was blocked with 3% hydrogen peroxide. Antigen retrieval was performed using EDTA solution (pH=9.0) or citrate solution (pH=6.0) depending on the desired marker (**Supplemental Table 1**). Sections were incubated with various primary antibodies diluted in serum when necessary (**Supplemental Table 1**). Species-specific secondary antibodies with HRP or biotin label were incubated on sections (**Supplemental Table 1**). Staining for all markers was completed with a two-step process, with the exception of the pNAD staining for HEVs that required a three-step process. A rabbit anti-rat polyclonal antibody was used as secondary antibody followed by incubation with a tertiary antibody with HRP label (BrightVision anti-rabbit HRP, Immunologic, Duiven, the Netherlands) for detection. Secondary antibodies with biotin label were incubated with a peroxidase avidin/biotin complex. Enzymatic activity was detected using a diaminobenzidine (DAB) solution. For double staining of pNAD and D2-40, slides were incubated with primary antibody against D2-40, antigen retrieval was performed using citrate solution, and the three-step process for pNAD detection was completed. All sections were counterstained with Haematoxylin (diluted 1:1 with Aqua Dest for T-Bet and FoxP3 counterstaining). For each immunohistochemical stain, tonsil or lung

tissue was used as positive controls. Species-specific isotype-matched irrelevant antibodies (IgG1 isotype and IgG2a isotype), or omission of the primary antibody in the staining process were used as negative controls. Immunohistochemical stained sections were analyzed with scanned images (200x, FoxP3 and T-Bet) or light microscopy (400x, all other stainings). The quantification of the immunohistochemistry was performed by calculating the percentage of positively stained cells for the marker in question as part of the amount of mononuclear cells.

Laser Tissue Microdissection, RNA isolation, cDNA synthesis and Q-PCR

Ten patients with clusters were used for further mRNA expression analysis. To interpret the patient samples correctly a 'calibrator' reference sample was included which contained lymph node and placental tissue. Frozen tissue sections of 10 µm were cut and placed on PEN-foil-mounted glass slides (PALM Microlaser Technologies, Bernried, Germany). Tissue sections were stained with Haematoxylin and air dried. From every patient, the intima of coronary arteries and the ELS were microdissected, with a surface area of approximately $12*10^6$ μm^2 each using the Robot-Microbeam (PALM Microlaser Technologies, Carl Zeiss, Bernried, Germany). Microdissected tissue pieces were collected in LPC microfuge tubes for RNA isolation.

Total RNA isolation was performed using the Picopure RNA isolation kit according to manufacturer's instructions (Arcturus, Applied Biosystems, Foster City, CA). RNA was eluted in 33 µl, RNA concentration was measured using the Nanodrop and RNA was stored at -80°C.

Synthesis of cDNA was performed by adding 1.5 µl oligo DT primers (0.50 lg; Promega Corporation, Phoenix, AZ), 1.5 µl of random primers (0.50 lg; Promega) and 3 µl dNTP's (25 mM; Invitrogen Corporation, Carlsbad, CA) to 33 µl RNA derived from the RNA isolation procedure. This mix was heated in a closed Eppendorf tube for 5 min at 65°C and thereafter cooled to room temperature. Next, 12 µl FS-buffer (Invitrogen), 6 µl DTT (Invitrogen) and 3 µl RNasin (Promega) were added and vigorously mixed and heated for 2 min at 37°C. Finally, 3 µl Superscript RNAse H-Reverse Transcriptase (Promega) was added and heated in a closed Eppendorf tube for 50 min at 37°C, followed by 15 min at 70°C. This resulted in a total of 63 µl cDNA, which was diluted to a total volume of 180 µl by adding Mili Q water.

The primer/probe FAM labelled combinations used for the Q-PCR were ordered from Applied Biosystems (Foster City, CA). The mRNA expression levels of the following markers were studied: CD3, GATA3, RORC, T-Bet, FoxP3, IFN-γ, TGF-β, CCR3, CCR7, CX3CR1, CCL11, CCL19, CCL21, CCL22, CXCL13, LTβ and LTβR. Per sample, 6.25 µl master mix (Applied Biosystems), 0.625 µl Assay on Demand and 3.13 µl MiliQ was used and 2.5 µl cDNA was added. Q-PCR was performed by using the Viia 7 detection system (Applied Biosystems). Thermal cycling included a denaturation step at 95°C for 10 min, followed by 40 cycles of 95°C for 15 sec and 60°C for 60 sec. To quantify the data, the comparative Ct method was used. As Q-PCR reference, the house keeping gene GAPDH was used. The calibrator was used for normalization. All assays were performed in duplicate; in the presented data the difference in cycle threshold (Cq) between the replicates did not exceed 0.5 Cq. Relative Quantification (RQ) values were calculated using the comparative Cq method ($RQ = 2^{-\Delta\Delta Cq}$, in which $\Delta Cq = Cq_{target} - Cq_{reference}$, $\Delta\Delta Cq = \Delta Cq_{sample} - \Delta Cq_{calibrator}$).

Table S1. Antibodies used for immunohistochemistry. Dil = Dilution, Rab = rabbit, Mo = mouse

	Primary step						Secondary step		
Antigen retrieval	**Antibody**		**Clone (firm)**	**Host**	**Dil.**	**Diluted in**	**Secondary Ab**	**Firm**	**Dil.**
EDTA	CD3	T-cells	F7.2.38 (Dako)	Rab	1:900	PBS/BS A 1%	Bright vision Anti-Rabbit HRP	Immunologic	-
Citrate	CD8 CAN	Cytotoxic T-cells	GR93390-2 (Abcam)	Rab	1:200	5% goat serum	polyclonal biotinylated anti-rabbit	Vector Labs	1:500
Citrate	CD8 NL	Cytotoxic T-cells	C8/144B (Dako)	Mo	1:50	PBS/BS A 1%	Bright vision Anti-mouse HRP	Immunologic	-
Citrate	CD4 CAN	T-helper cells	EPR6855 (Abcam)	Rab	1:100	5% goat serum	polyclonal biotinylated anti-rabbit	Vector Labs	1:500
EDTA	CD4 NL	T-helper cells	4B12 (Monosan)	Mo	1:200	PBS/BS A 1%	Bright vision Anti-mouse HRP	Immunologic	-
EDTA	FoxP3	Regulatory T-cells	236A/E7 (Abcam)	Mo	1:1200	10% human serum	Bright vision Anti-mouse HRP	Immunologic	-
EDTA	TBet	T-helper 1 cells	Lot H0210 (Santa Cruz Biotechnology)	Rab	1:2000	10% human serum	Bright vision Anti-mouse HRP	Immunologic	-
Citrate	CD68 CAN	Macrophages	514H12 (Abcam)	Mo	1:40	5% goat serum	polyclonal biotinylated anti-rabbit	Bethyl Laboratories	1:500
Citrate	CD68 NL	Macrophages	Kp1 (Novacastra Biologicals)	Mo	1:800	PBS/BS A 1%	Bright vision Anti-mouse HRP	Immunologic	-
EDTA	iNOS	M1-macrophages	Sp126 (Novus Biologicals)	Rab	1:30	PBS/BS A 1%	Bright vision Anti-mouse HRP	Immunologic	-
Citrate	CCR7	M1-macrophages, T-Cells, etc...	CD1678 (Cell Applications)	Rab	1:20000	10% human serum	Bright vision Anti-mouse HRP	Immunologic	-
Citrate	CD163	M2-macrophages	10D6 (Novacastra)	Mo	1:400	PBS/BS A 1%	Bright vision Anti-mouse HRP	Immunologic	-

EDTA	CD204	M2-macrophages	SRA-E5 (Transgenic)	Mo	1:1200	10% human serum	Bright vision Anti-mouse HRP	Immunologic	-
Citrate	CD206	M2-macrophages	5C11 (Abnova)	Mo	1:1200	PBS/BS A 1%	Bright vision Anti-mouse HRP	Immunologic	-
Citrate	CD20	B-cells	L26 (Abcam San Francisco, CA, USA)	Mo	1:50	5% goat serum	polyclonal biotinylated anti-rabbit	Bethyl Laboratories	1:500
Citrate	CD20 (IF)	B-cells	L26 (Abcam San Francisco, CA, USA)	Mo	1:50	5% goat serum	Alexa588 conjugated goat anti-mouse	Invitrogen	1:500
Citrate	CD20	B-cells	L26 (Dako)	Mo	1:1000	PBS/BS A 1%	Bright vision Anti-mouse HRP	Vector labs	-
Citrate	IgM	IgM producing cells	EPR5539 (Abcam)	Rab	1:100	5% goat serum	polyclonal biotinylated anti-rabbit	Vector labs	1:500
Citrate	IgG	IgG producing cells	EPR4421 (Abcam)	Rab	1:500	5% goat serum	polyclonal biotinylated anti-rabbit	Vector labs	1:500
Citrate	CD138 CAN	Plasma cells	GR52674-1 (Abcam)	Rab	1:50	5% goat serum	polyclonal biotinylated anti-rabbit	Vector labs	1:500
Citrate	CD138 NL	Plasma cells	B-B4 (Abdserotec)	Mo	1:1000	PBS/BS A 1%	Bright vision Anti-mouse HRP	Immunologic	
Citrate	CD27 (IF)	Memory B cells	EPR8569 (Abcam)	Rab	1:100	5% goat serum	Alexa 555 conjugated goat anti-mouse	Invitrogen	1:500
EDTA	CD21	Follicular dendritic cells	2G9 (Novacastra)	Mo	1:800	PBS/BS A 1%	Bright vision Anti-mouse HRP	Immunologic	-
EDTA	CD1a	Interdigitating dendritic cells	010 (Immunotech)	Mo	1:10	PBS/BS A 1%	Bright vision Anti-mouse HRP	Immunologic	-
Citrate	pNAD (3 step IHC)	High Endothelial Venules	MECA-79 (Biolegend)	Rat	1:50	PBS/BS A 1%	Rabbit-anti-Rat	Rockland (batch 112-4107)	1:5000
-	Podopianin (D2-40)	Lymphatic vessels	D2-40 (Covance	Mo	1:200	PBS/BS A 1%	Bright vision Anti-mouse HRP	Immunologic	-

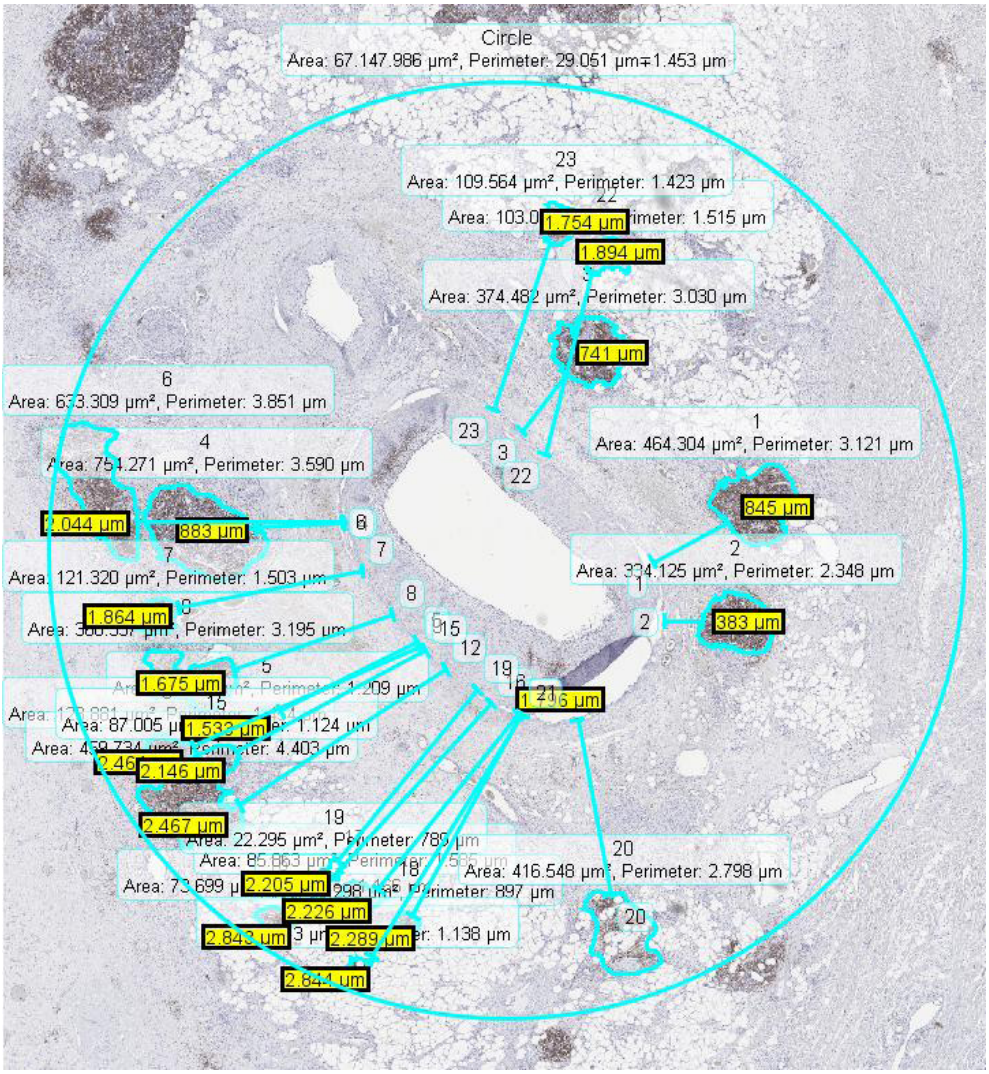

Figure S1. ELS measurements. ELS were only included in this study if they were in a 3.0 mm radius of the external elastic lamina of the affected artery, as seen in the figure below. Within this 3.0 mm area, the distance from the external elastic lamina and area of each individual ELS was determined. The number of individual ELS in the 3.0 mm was also enumerated.

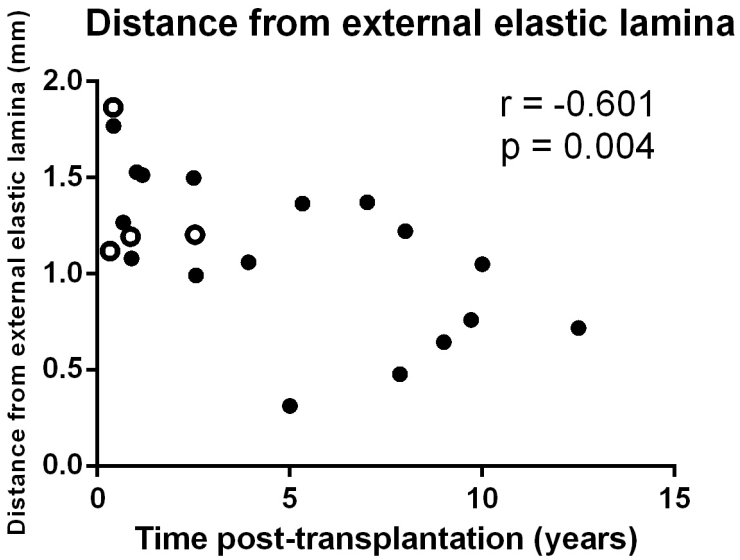

Figure S2. ELS distance from External Elastic Lamina. The mean distance from the ELS to the coronary artery decreases with time post-transplant (p=0.004, r=-0.601). Closed dots indicate ELS-1 patients, whereas open dots indicate ELS-2 patients.

Chapter 5.

ANTIGENIC TARGETS OF LOCAL ANTIBODIES PRODUCED IN ECTOPIS LYMPHOID STRUCTURES IN CARDIAC ALLOGRAFTS

M.M.H. Huibers MSc [1], J.M.T. Beerthuijzen BSc [1], A.J. Gareau PhD [2], E. Siera-de Koning BSc [1], J. van Kuik BSc [1], E.G. Kamburova PhD [3], N. de Jonge MD PhD [4], T.D.G. Lee PhD [5,6,7] H.G. Otten PhD [3], R.A. de Weger PhD [1]

Departments of Pathology [1], Cardiology [4] & Laboratory of Translational Immunology [3], University Medical Center Utrecht, the Netherlands. Department of Internal Medicine [2], University of Manitoba, Departments of Pathology [5], Surgery [6], Microbiology and Immunology [7], Dalhousie University, Canada.

Manuscript in preparation

Abstract

Background:
Cardiac allograft vasculopathy (CAV) is an immune-mediated vascular pathology that limits the survival of cardiac transplants involving humoral and cell-mediated events. Ectopic lymphoid structures (ELS) surrounding coronary arteries are observed in patients with evident CAV and contain high numbers of B cells. The aim of this study was to determine cellular interactions and investigate the antigenic targets of the antibodies produced in the ELS.

Methods:
Epicardial coronary arteries (n=56) were collected on autopsy from heart transplant patients and studied for the presence of ELS. Cellular interactions were studied by mRNA expression levels using Q-PCR from laser microdissected tissue sections (n=10) from selected cytokines. Double immunohistochemistry was done to test whether plasma cells were positive for IgG and IgM. Clonality of plasma cells was tested using PCR and in situ hybridisation for kappa and lambda. IgG and IgM levels in tissue lysates of ELS were measured by ELISA, typed for donor specific HLA and non-HLA antibodies (vimentin and angiotensin-II receptor type-1).

Results:
Cytokine and receptor expression is higher in ELS than in coronary vessel layers. This effect is in particular seen in large extensive ELS (predominantly CD20, CXCR3, IFNγ and TGFβ). Plasma cells within and around ELS produce IgG or IgM antibodies. The B cells are polyclonal. IgG and IgM were detected in epicardial tissue from the explanted hearts but levels were significantly higher in cardiac transplant patients with large ELS ($p<0.05$) than with small ELS. In 4/21 lysates from patients with ELS (19%) donor specific HLA type-II antibodies were detected. Also non-HLA antibodies were present; no anti-vimentin antibodies were detected, but in 11/21 ELS patients (52%) anti-angitensin-II receptor type-1 was detected.

Conclusion:
The detected cytokine profile suggests active recruitment and proliferation of T- and B-lymphocytes within ELS. The absence of certain interleukins could be explained by immune suppression of these transplanted patients. Patients with ELS exhibit actively antibody producing plasma cells with no monoclonal expansion. Interestingly, these locally produced antibodies are in some cases directed against the donor HLA-II type or non-HLA antigens. Local antibody production may mediate rejection that has major consequences for the graft and are hard to detect in the systemic circulation.

Introduction

Cardiac Allograft Vasculopathy (CAV) is a pathogenic vascular remodeling process often referred to as the 'Achilles heel' of long-term cardiac graft rejection[1]. CAV is characterized by the formation of a progressive neointimal lesion which can eventually occlude coronary arteries and lead to ischemic graft damage. Despite the development of excellent immunosuppressive therapies preventing acute rejection in the majority of patients, long-term outcomes have not improved over the past two decades[2].

It is well-accepted that CAV is mediated via the recipient's adaptive immune mechanisms, and in particular, it has been demonstrated that after cardiac transplantation, next to an active T-cell response, antibodies and B cells contribute to long-term cardiac graft rejection[3,4]. Serum antibodies directed against donor HLA molecules, as well as other self-antigens like vimentin, myosin, major-histocompatibility-complex class I-related chain A (MICA) and angiotensin-II type-1 receptor (AT1R) have been found post-transplant[5,6] and are associated with poor graft survival and worse patient outcomes. Several clinical studies have demonstrated that the presence of antibodies post-transplant is associated with increased risk of developing CAV and poor graft survival[7].

Previously, it has been shown that ectopic lymphoid structures (ELS) in the coronary arteries of cardiac transplant recipients are immunologically active areas of antibody production *(Chapter 4, Huibers et al 2014 JHLT accepted for publication)*. The formation of these ELS could be attempts of the recipient's immune system to form tertiary lymphoid organs (TLOs) to eliminate the persistent antigenic stimulus provided by the donor organ[8,9]. This is consistent with other reports of lymphoid aggregates surrounding coronary vessels with CAV[10].

To reveal the role of these ELS surrounding the coronary arteries of transplanted hearts the cytokine profile of these areas was studied. Based on previous observations of naïve and memory B cells, and IgM and IgG positive cells within ELS close to the CAV vessels, the antigenic target of these locally-produced antibodies was determined. We hypothesized that the locally-produced antibody is targeting the MHC classes I and II expressed on the donor tissue. In this way antibody mediated rejection processes may have major local consequences for the graft that might be hard to detect in the systemic circulation.

Methods

Patient population

The autopsy database from University Medical Center Utrecht (Netherlands) was searched for patients that died post-HTx between 1987 and 2013 and had coronary artery material available for this study. Fifty-six patients were included that met these criteria. All 56 patients were scored for the presence of ELS as previously described and classified as ELS-0, ELS-1, or ELS-2 *(Chapter 4, Huibers et al 2014 JHLT accepted for publication)*. Thirty-three of these patients did not have ELS (ELS-0, 33/56=59%), 18 patients had small clusters (ELS-1, 18/56=32%), and 5 had extensive clusters in their epicardial tissue (ELS-2, 5/56=9%).

The focus of this study was on the function of the ELS surrounding coronary arteries, therefore mainly material from patients with ELS was included for analysis (**Table 1**). Patients without ELS or explanted hearts served as control. For immunohistochemistry (IHC) 21 samples were tested (ELS-0 n=2) and pathological AMR (pAMR) status was determined in patients with ELS (ELS-1 and ELS-2, n=20) and one control (ELS-0, n=1). Gene expression could only be determined in fresh frozen tissue, where the coronary artery was located in the same sample as the ELS (n=10). Clonality analysis was done using the Biomed method (n=3) and *in situ* hybridization (ISH) and IHC for kappa/lambda light chain (n=9). Enzyme-Linked Immuno Sorbent Assay (ELISA) for IgG and IgM was performed on all samples where fresh frozen epicardial tissue was available (n=56). Luminex HLA screening was done on mainly patients with ELS (n=21, ELS-0 n=4).

Table 1. Patient population. ELS = Ectopic Lymphoid Structures, H-CAV = Histological Cardiac Allograft Vasculopathy, M = Male, F = Female, HTx = Heart transplantation, FF = Fresh Frozen, IHC = Immunohistochemistry, AMR = Antibody Mediated Rejection, ISHLT = International society of Heart and Lung Transplantation, ISH = In Situ Hybridization, x = data available, (.) = no data available.

Case number	Extent ELS	H-CAV stage	Gender	Time post-HTx (years)	Material available (- no FF. + FF heart ++ FF heart and coronary	HTC	AMR based on ISHLT criteria	Gene expression	Clonality assay	kappal / lambda ISH	kappa / lambda IHC	ELISA	Luminex - Quick Scan	Luminex - Single Antigen Assay	Non-HLA antibodies
1	1	1	M	0.67	-	x	.	.	.	.	.	.	.	.	.
2	1	2	M	0.42	+	x	x	.	.	.	.	x	x	x	x
3	1	2	M	1.02	+	x	x	.	.	.	.	x	x	x	x
4	1	3	F	7.86	+	x	x	.	.	x	.	x	x	.	x
5	1	3	M	7.01	+	x	x	.	.	x	.	x	x	x	x
6	1	3	M	12.50	+	x	x	.	.	.	.	x	x	.	x
7	1	3	M	17.80	+	x	x	.	.	.	.	x	x	.	x
8	1	3	M	15.74	+	.	x	.	.	.	.	x	x	.	x
9	1	3	M	3.50	+	.	x	.	.	.	.	x	x	.	x
10	1	2	M	2.56	++	x	x	x	.	x	.	x	x	.	x
11	1	2	M	0.89	++	x	x	x	.	.	.	x	x	.	x
12	1	3	F	1.17	++	x	.	x	.	.	.	x	x	.	x
13	1	3	F	9.71	++	x	x	.	.	.	.	x	x	.	x
14	1	3	M	3.93	++	x	x	.	.	.	.	x	x	.	x
15	1	2	M	1.61	++	x	x	x	.	x	.	x	x	.	x
16	1	2	M	5.33	++	x	x	x	.	x	x	x	x	.	x
17	1	3	M	6.26	++	x	x	x	.	.	.	x	x	.	x
18	1	3	M	11.55	++	.	x	x	.	.	.	x	x	.	x
19	2	1	M	0.41	-	x	.	.	.	.	.	.	.	.	.
20	2	1	F	1.91	++	x	x	x	x	x	.	x	x	.	x
21	2	1	F	0.33	++	x	x	.	.	x	.	x	x	.	x
22	2	1	M	0.86	++	x	x	x	x	.	.	x	x	.	x
23	2	2	M	2.54	++	x	x	x	x	x	x	x	x	x	x

Histology and Immunohistochemistry

Tissue was formalin-fixed, paraffin-embedded, serially sectioned on a microtome (4 µm), deparaffinized in xylene, hydrated through an ethanol series and cleared in running water. Tissue sections were stained with haematoxylin and eosin (H&E) to visualize the extent of ELS.

For immunohistochemistry sections were deparaffinized and endogenous peroxidase activity was blocked with 3% hydrogen peroxide. Antigen retrieval was performed using EDTA solution (pH=9.0) or citrate solution (pH=6.0). Sections were incubated with various primary antibodies (CD20, CD138, AID, C4d, CD3; **Supplemental Table 1**). Species-specific secondary antibodies with HRP or biotin label were incubated on sections. Staining for all markers was completed with a two-step process. Enzymatic activity was detected using a diaminobenzidine (DAB) solution. Sections were counterstained with Mayer's Haematoxylin.

Pathological AMR detection was done using previously described criteria[11] with IHC of C4d as main parameters. The percentage of positivity in the capillaries was scored, where C4d was considered positive if >50% was stained. Morphological changes of endothelial cells and C4d staining of cardiomyocytes were not taken into account due to ischemia (infarction) caused after death. T cell staining (CD3) was used in addition to determine cellular rejection or mixed rejection (cellular and antibody mediated) according to previously described guidelines[11–13].

For immunofluorescence antigen retrieval was performed using a heat-mediated method in sodium citrate buffer with a 2100-Retriever (Electron Microscopy Sciences, Hatfield PA). Endogenous peroxidase activity was blocked with 3% hydrogen peroxide in 1x PBS. Tissue sections were incubated with monoclonal anti-human IgG antibody (1:500 in 5% normal goat serum) or with monoclonal anti-human IgM antibody (1:100 in 5% normal goat serum). This was followed by incubation with a goat anti-rabbit conjugated to Alexa 555 (Invitrogen, Eugene, OR) at a 1:500 dilution. For detection of plasma cells, sections were then incubated with monoclonal anti-human CD138 antibody (1:50 in 5% normal goat serum) followed by incubation with a goat anti-rabbit conjugated to Alexa 488 (Invitrogen) at a dilution of 1:500. Hoescht 33342 at a dilution of 1:5,000 (Invitrogen) was used as a nuclear counterstain. Digital images of immunofluorescence were captured using a Zeiss Axiovert 200M microscope and a Hamamatsu Orca R2 camera (Hamamatsu, Boston, MA).

Gene expression analysis

Ten patients with ELS were used for further mRNA expression analysis (**Table 1**). Snap frozen tissue samples were cut in 10 µm sections and placed on PEN-foil-mounted glass slides (PALM Microlaser Technologies, Bernried, Germany). Tissue sections were stained with Haematoxylin and air dried. For every sample the coronary arterial layers (intima, media, and adventitia) and ELS were laser microdissected, with a surface area of $\pm 12^{*}10^{6}$ μm^{2} using the Robot-Microbeam (PALM). Microdissected tissue samples were collected in LPC microfuge tubes for total RNA isolation.

Total RNA isolation was performed using the miRNeasy Micro kit according to manufacturer's instructions (Qiagen, Hilden, Germany). RNA was eluted in 30ul, the concentration was measured using the Nanodrop (Thermo Scientific, Wilmington, DE USA) and stored at -80°C. Of the eluted RNA 14 µl was diluted to a volume of 33 µl for total cDNA

synthesis.

For cDNA synthesis 1.5 µl oligo dT primers (Promega Corporation, Fitchburg, Wisconsin, USA), 1.5 µl random primers (Promega) and 3µl dNTPs (Invitrogen Corporation, Carlsbad, CA, USA) were added to 33 µl RNA. The mix was heated for 5 min at 65°C and thereafter cooled to room temperature. Next, 12µl 5x First Strand buffer (Invitrogen), 6µl 0.1M DTT (Invitrogen) and 3µl RNasin (Invitrogen) were added, vigorously mixed and heated for 2 min at 37°C. Finally, 3µl Superscript III Reverse Transcriptase (Invitrogen) was added and heated for 5 min at 37°C and 15 min at 70°C. This resulted in 63 µl cDNA, which was diluted to a total volume of 126 µl.

Markers for the mRNA expression levels included IL-2, IL-4, IL-6, IL-7, IL-10, IL-12, IL-17, IL-23, CXCR3, CD20, IFNγ, TGFβ, and TNFα. These cytokines were selected because of their association with TLOs and leukocytes found in ELS. Per sample 6.25 µl Taqman Universal MasterMix (Life Technologies, Carlsbad, CA., USA), 0.625 µl Taqman gene expression assay (TGEA) (Life Technologies), 3.13 µl MilliQ and 2.5 µl cDNA were added. Quantitative PCR analysis was performed using ViiA 7 detection system (Life Technologies). Thermal cycling contained 10min denaturation at 95°C, followed by 40 cycles of 15sec at 95°C and 60sec at 60°C. For analysis GAPDH was used as reference housekeeping gene and a calibrator sample was used for normalization. All assays were performed in duplicate; in the presented data the difference in cycle threshold (Cq) between the replicates did not exceed 0.5 Cq. Relative Quantification (RQ) values were calculated using the comparative Cq method ($RQ = 2^{-\Delta\Delta Cq}$, in which $\Delta Cq = Cq_{target} - Cq_{reference}$, $\Delta\Delta Cq = \Delta Cq_{sample} - \Delta Cq_{calibrator}$).

Clonality analysis

To test for clonality of cells within the ELS two analyses were performed; plasma cell clonality using in situ hybridization for kappa-lambda mRNA (n=9), and B cell clonality using PCR (Biomed; n=3, [14]).

Plasma cell clonality was tested using *in situ* hybridization for kappa-lambda mRNA, where no clonality was assumed since ELS are active areas of antibody production. Paraffin-embedded tissue samples were cut in 4µm sections, deparaffinized and endogenous peroxidase was blocked with 3% hydrogen peroxide. Endogenous biotin was blocked with an avidin/biotin blocking kit (Vector Laboratories, Burlingame, CA). After incubation with proteinase K (Cenbima, Lugo, Spain) for 9min at room temperature, sections were incubated with Kappa-biotin/Lambda-Digoxigenin probe (Cenbimo) for 1hr at 62°C in a Thermobrite (Abbott Molecular Inc, Chicago, Illinois). This was followed by incubation of α-digoxigenin-AF for 30min and subsequently incubated with Permanent Liquid Red (DAKO, Glostrup, Denmark) for 10min. Thereafter, α-biotin-HRP was incubated for 1hr, detected with DAB solution for 30min. All sections were briefly counterstained with Mayer's Haematoxylin and air dried.

We tested three patients with extensive clusters (ELS-2) for clonality of B cells with PCR. IGH and IGK B cell clonality (IgH-A, -B, -C, -D, and IgK-A, -B) was tested according to manufacturer's instructions (Biomed, InVivoScribe, San Diego, CA).

Antibody quantification in tissue

All HTx patients with frozen epicardial tissue available were included for antibody analyses. Five explanted hearts were included as control (**Table 1**). Snap frozen tissue samples were cut in 10 µm sections. Only epicardial tissue was collected (myocard was torn off) in pre-chilled, microbeads-containing tubes. The collected tissue was weighted and 300 µl of complete extraction buffer was added. The extraction buffer consisted of 100 mM Tris (pH 7.4), 150 mM NaCl, 1 mM EGTA, 1 mM EDTA, 1% Triton-X-100, and 0.5% Sodium deoxycholate. Lysates were homogenized for 3 x 35 sec cycles using a beadshaker (MO BIO Laboratories, Carlsbad, CA, USA) and placed on an orbital shaker for 2 hrs at 4°C, centrifuged for 20 min, and the supernatant was harvested and stored at -80°C.

Enzyme-Linked Immuno Sorbent Assay (ELISA) for human IgG and IgM was performed according to manufacturer's instructions (Abcam, Cambridge, UK). For IgG detection tissue lysates of explanted hearts (no ELS) were 1,000x diluted and of autopsy hearts (ELS-1 and ELS-2) 10,000x diluted in PBS. For IgM detection the dilution was 100x and 1000x for explanted and autopsy hearts, respectively. All assays were performed in duplicate (accepted difference ≤10%) and read by a Microplate Reader Benchmark (Biorad, Hercules, CA) at 450nm. Readings were subtracted at 570nm from those at 450nm to correct optical imperfections. In the presented data the antibody concentration is displayed after correction for tissue weight as µg/ml/mg tissue.

HLA antibody assays

Patients with ELS (n=21; ELS1 n=17 and ELS2 n=4) were tested for HLA specificity using Luminex (Labscan 100, xMAP technology; Luminex, Austin, USA). Lysates of patients without ELS (ELS0 n=4) and explanted hearts (n=5) were used as control. The Luminex assay was performed using the Lifecodes Lifescreen deluxe kit (Immucor Gen-Probe) according to manufacturer's. Measurements were performed using a Luminex LX200 system in combination with the xPONENT software (Luminex, Austin, TX). Data were analysed with the LIFECODES MATCH IT! Antibody Software 1.1 (Immucor, Gen-Probe, Stamford, CT).

Non-HLA antibody detection

For non-HLA antibody detection vimentin [15,16] and angiotensin-II type 1 receptor (AT1R; [17,18]) antigens were chosen. Anti-vimentin IgG and IgM antibodies in lysates of patients with and without ELS were measured with a locally developed solid phase assay on a Luminex platform. In brief, carboxylated magnetic microspheres (Bio-rad, Veenendaal, The Netherlands) were covalently coupled with anti-His tag antibody (R&D Systems, Minneapolis, CA) by following the procedures recommended by Luminex. Next, His-tagged recombinant human vimentin (R&D systems) was incubated with the microspheres, resulting in a vimentin-bead complex. Lysates were incubated in a 1:5 dilution with the vimentin-bead complex in a phosphate-based buffer containing NaCl, Tween-20, sodium azide, and bovine serum albumin (assay buffer) for 30 min on a shaker. Patients with anti-vimentin antibodies were used as positive controls. Beads were

washed twice with assay buffer and subsequently incubated with goat anti-human IgG-PE or donkey anti-human IgM-PE to detect anti-vimentin IgG or IgM antibodies respectively. After 30 min beads were washed twice with assay buffer and the fluorescence intensity was measured on an Luminex LX200 system in combination with the xPONENT software. Anti-AT1R IgG antibodies were tested using ELISA according to manufacturer's instructions (One Lambda inc, Canoga Park, CA). Since IgG levels in our lysates are lower than in normal plasma, our lysates were initially tested in a 1:1 dilution.

Statistical analysis

Normality of parameters was checked using the Kolmogorov-Smirnov test. Continuous parameters comparing three groups or more were analyzed by one-way ANOVA or Kruskal-Wallis test with Bonferroni correction in post-hoc analysis. Parametric parameters are displayed as mean with standard deviation (SD) and non-parametric parameters were displayed as median with interquartile range (IQR). All statistics were performed using SPSS (IBM SPSS Statistics 20, New York, USA) and visualized with GraphPad Prism® (version 6; San Diego, CA). Values of $p<0.05$ were considered significant.

Results

ELS are immunologically active areas of antibody production

Immunohistochemical staining of ELS for antibody demonstrated the presence of IgG in 13 of 21 patients (**Figure 1A**), and IgM in 18 of 21 patients (**Figure 1B**). Additionally, immunohistochemical staining demonstrates the presence of activation-induced cytidine deaminase (AID) (**Figure 1C**), suggestive of germinal center activity. Out of the 21 patients examined for AID presence, the ELS in 5 patients were positive; 4 of these were ELS-1 patients.

Immunofluorescent staining for IgG (**Figure 1D**) and CD138 (**Figure 1E**) demonstrates IgG-producing plasma cells (**Figure 1F**, merge) in ELS. We have previously reported the presence of this antibody isotype in ELS *(Chapter 4 Huibers et al 2014 JHLT accepted for publication)*.

For histological antibody mediated rejection (AMR) analysis C4d staining of septal biopsies was performed (**Supplemental table 2**). A few hearts after autopsy showed ischemic changes and the start of infarction areas, probably caused by death. Cardiomyocytes stained positive in these cases for C4d because of complement activation. This staining was not taken into account when C4d slides were scored. Furthermore, only 3 patients showed signs of AMR based on C4d positive capillaries.

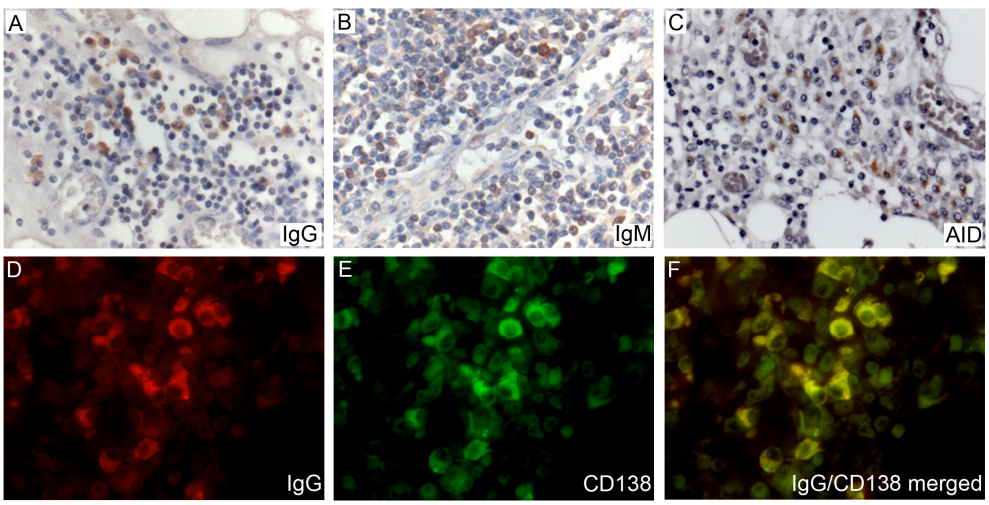

Figure 1. Antibody-producing plasma cells in ELS post-transplant. IgG and IgM are present in ectopic lymphoid structures. Immunohistochemical staining of typical ELS demonstrates positivity for the IgG subclass (**A**; image taken at 40x magnification) and positivity for the IgM subclass (**B**; 40x magnification). Germinal centre activity can be seen in ELS in some patients. Immunohistochemical staining shows the presence of activation-induced cytidine deaminase (AID) in ELS (**C**; 40x magnification). Antibody-producing plasma cells are present in ELS post-transplant. Immunoflourescent staining of ELS at 100x magnification demonstrates cells expressing IgG (**D**), CD138 (**E**), and the merged image showing CD138+ plasma cells staining positive for IgG (**F**).

B cells in ELS contain an oligoclonal pattern

In normal tissues the distribution of kappa and lambda is approximately 60% and 40%, respectively. When only one clone proliferates, being kappa of lambda, this implicates a monoclonal expansion. *In situ* hybridization of kappa and lambda light chain mRNA in ELS showed a mixed population of plasma cells with a normal distribution of kappa (brown) and lambda (red; **Figure 2A-D**). Also double IHC of kappa and lambda protein displayed the same distribution (**Figure 2E**).

In PCR analysis the polyclonal population of B cells was confirmed (**Figure 2F**). All patient material tested showed a normal 'oligoclonal' peak distribution as seen in tissue lymphocyte infiltrates.

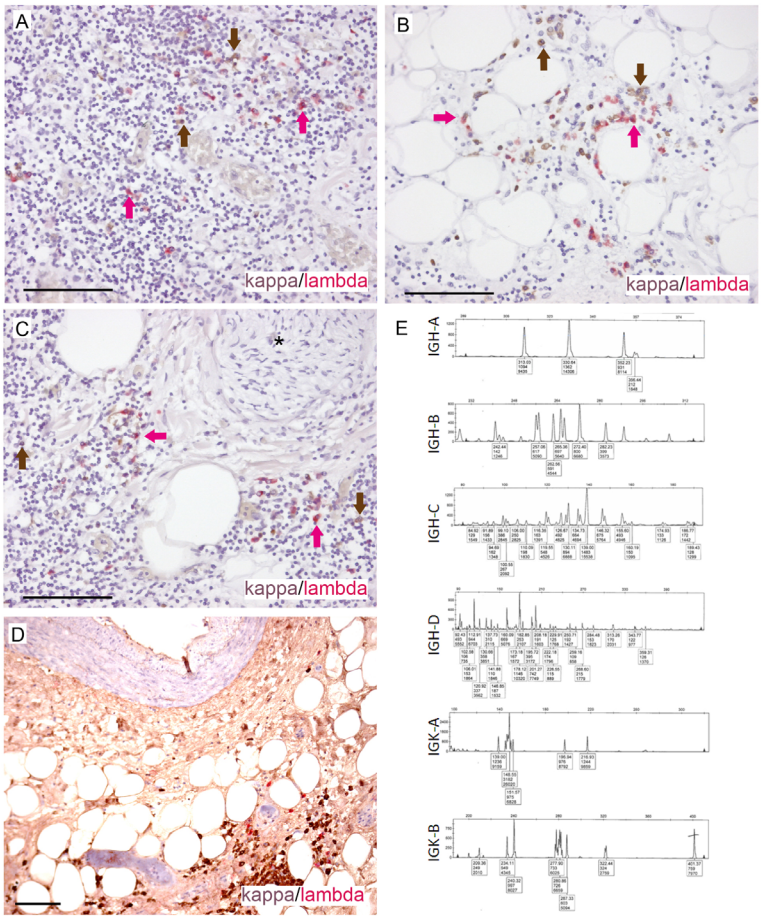

Figure 2. B cells in ELS contain an oligoclonal pattern. Double mRNA in situ hybridization of kappa (brown) and lambda (red) probes show a mixed pattern of plasma cells within the center of ELS (**A**; image taken at 20x magnification), within the epicardial adipose tissue (**B**), or surrounding a nerve (**C**). Also double IHC shows a mixed population of kappa and lambda positive plasma cells (**D**, 10x). In addition, PCR analysis of B cells by the Biomed method did show oligoclonal patterns (**E**). Bars represent 100μm.

IgG and IgM levels in epicardial tissue with ELS

IgG and IgM levels in ELS (n=21) was determined with ELISA and corrected for input tissue weight. Explanted hearts (n=5) and patients without ELS (ELS-0, n=27) were taken along as controls.As shown in IHC staining (**Figure 1A-B**) IgG and IgM antibodies were also detected in epicardial tissue by ELISA (**Figure 3A and 3C**). Also explanted hearts (no transplantation) have detectable levels of antibodies, especially IgG, but predominantly lower than in transplanted hearts. Absolute levels of IgG were overall higher in all groups than the levels of IgM, ranging to a maximum of 35 µg/ml/mg or 5 µg/ml/mg, respectively. IgG and IgM levels in the epicardium after HTx are higher than in the epicardium from explanted hearts, suggesting detectable antibody levels induced by transplantation.

IgG levels did not show statistical differences between the four groups (p=0.0977) probably due to large variation. However a trend is visible with larger clusters having more IgG present (**Figure 3A**). IgM was significantly different between the four groups (p=0.0003), with again larger clusters containing more IgM (**Figure 3C**). Especially in the ELS-2 patients the amounts of IgM were very high; ~4 x higher than in the other groups.

Next we hypothesized that antibodies formed in time, resulting in higher levels of IgG and IgM in patients later after transplant. Patients longer after transplant (>6 months) have higher levels of antibodies (IgG and IgM) than patients short after transplant (<6 months; **Figure 3B and 3D**). In the group without clusters (ELS-0) this effect was significant (IgG p=0.0155, IgM p=0.0005). No statistics could be performed on the other comparisons due to small sample size in the short-term group (ELS-1 and ELS-2 <6 months, n=1).

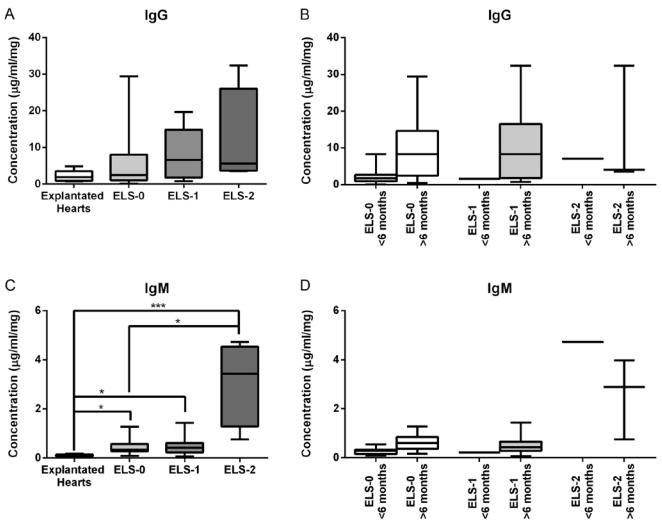

Figure 3. IgG and IgM levels are highest in tissue with ELS. IgG and IgM levels were measured in tissue lysates with ELISA where the concentration (µg/ml) were corrected for input of tissue weight (mg), resulting in µg/ml/mg. IgG levels in explanted hearts, transplanted hearts without ELS (ELS-0) and with ELS (ELS-1 and ELS-2) show a trend in higher levels present with more ELS without statistical significance (p=0.0977; **A**). IgM levels in explanted hearts, transplanted hearts without ELS (ELS-0) and with ELS (ELS-1 and ELS-2) show statistical significance (p=0.0003), with higher antibody levels in patients with larger ELS (**C**). Patients longer after transplant (>6months) show higher levels of IgG and IgM (**B** and **D**, respectively). ELS = ectopic lymphoid structures, * p<0.050

Four patients contain high amounts of Donor Specific antibodies in epicardial tissue

Luminex experiments were performed to determine against what antigens the detected antibodies in epicardial tissue were directed. Epicardial tissue from 25 HTx patients (ELS-0 n=4, ELS-1 n=17, ELS-2 n=4) and as controls 5 explanted hearts were tested. From these 30 lysates only 4 lysates were positive in the screening experiment for HLA antibodies (**Table 2**).

None of the control (explanted hearts) samples showed detectable antibodies against HLA. The four positive samples were all from HTx patient with ELS. All four samples contained HLA-antibodies specific for the donor HLA-type (4/21 ELS patients = 19%), all against class II HLA antigens. Three samples were from ELS-1 patients (3/17 = 18% DSA) and one sample was from an ELS-2 patient (1/4 = 25%).

All four tissue lysates showed high levels of Donor Specific Antibodies against HLA-II. Overall, the concentration of IgG in tissue lysate is 1,000x lower than in serum (**Figure 3**). The fact that we pick up levels of DSAs suggests large amounts of the IgG molecules that are specifically directed against donor HLA antigens.

The last plasma sample prior to death was also tested for HLA antibodies with different time intervals between blood withdrawal and death. The two plasma samples 3 days before death showed the same DSAs as we detected in tissue, whereas the two other samples (longer before death) did not show any HLA-antibody.

Table 2. donor specific HLA antibodies. Single antigens were determined with the Luminex (Materials and methods). Italics depicts mismatched HLA types. Italics + underlined depicts mismatched HLA types and donor specific antibodies. ELS = ectopic lymphoid structures, H-CAV = histological Cardiac Allograft Vasculopathy, HTx = heart transplantation, M = Male, P = patient, D = donor, DSA = donor specific antibodies, neg = negative.

Time post-HTx (days)		HLA type	DSA (tissue)	non-DSA (tissue)	plasma time point before death	DSA plasma	non-DSA (plasma)
153	P	Class-I: A24(9), A31 (19), B51(5), B55(22), CW9(3)					
		Class-II: DR13(6), DQ1, DR52			3 days		
	D	Class-I: *A2, B7, B60(40),* CW3, *CW7*	neg	neg		A2, B40	B13, B27, B17
		Class-II: *DR4, DR8, DQ3, DQ4, DR53*	DQ3, DQ4	DQ2		DQ3, DQ4, DR53, DR4, DR8	DQ2, DR9
372	P	Class-I: A2, A29(19), B44(12), B60(4), CW3					
		Class-II: DR13(6), DR7, DQ2, DR52, DR53			3 days		
	D	Class-I: *A3,* A29(19), B44(12), *B7, CW7*	neg	neg		B7	B42, B54, B81, B82, A34, B55, B56, B57, CW4, CW6, CW17, CW18
		Class-II: *DR4, DR9, DQ3, DR53*	DQ7(3)	neg		DQ3, DR4	DQ4, DQ2, DR12
2562	P	Class-I: A1, A2, B8, B38(16)					
		Class-II: DR17(3), DR13(6), CW7 DQ1, DQ2			4 years		
	D	Class-I: A2, *A23(9), B44(12), B60(40*	neg	neg		neg	neg
		Class-II: *DR4,* DR13(6), DQ1, *DQ3,* DR52, *DR53*	DQ3, DR53	neg		neg	neg
926	P	Class-I: A1, A2, B7					
		Class-II: DR15(2), DQ6(1)			1,5 years		
	D	Class-I: A2, *A68(28), B51(5), B60(40)*	neg	neg		neg	neg
		Class-II: *DR4, DR11(5), DQ7(3), DR52, DR53*	DQ7(3)	DQ2, DQ4		neg	neg

Non-HLA antibodies are present in patients with ELS

To determine if antibodies directed to non-HLA antigens were present we performed analysis of anti-vimentin and anti-AT1R antibodies. None of the controls (explanted hearts or HTx patients without ELS) had antibodies towards vimentin or AT1R. In patient with ELS anti-vimentin IgG and IgM antibodies were not detected by luminex analysis (**Figure 4**), whereas our positive control sample (plasma with anti-vimentin antibodies) showed clear positive values.

Anti-AT1R IgG testing showed six patients to be positive (>17 U/ml) for AT1R-antibodies and five at risk (>10-17 U/ml). It is interesting to note that from the four patients with DSAs, two cases show donor specific HLA antibody production in combination with AT1R (non-HLA) antibody production (one at risk 11 U/ml and one positive 26 U/ml). From all cases post-HTx, eleven (11/25 HTx patients = 44%) contained AT1R antibodies. All these 11 cases had ELS formation (11/21 ELS patients = 52%). Nine samples with AT1R antibodies were from ELS-1 patients (9/17 ELS-1 = 53%) and two from ELS-2 patients (2/4 = 50%).

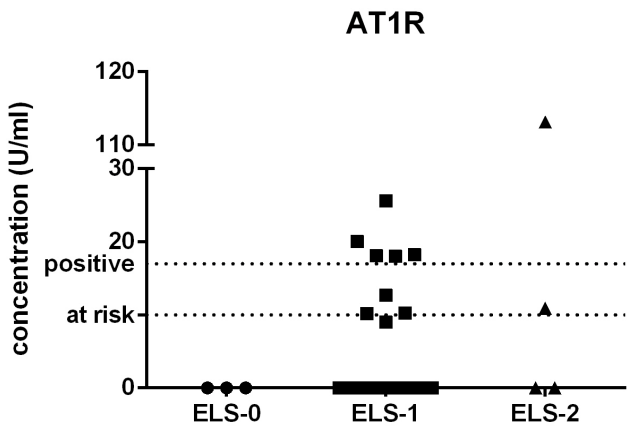

Figure 4. non-HLA antibody levels; AT1R. AT1R-antibodies were measured with ELISA where 6 samples showed to be positive (>17 U/ml) and 5 at risk (>10 U/ml). AT1R = Angiotensin-II receptor type-1

Cytokine profile in ELS

In order to determine the function of ELS cytokine profiles, associated with immune cells in ELS and ELS maintenance, were analyzed **(Figure 5)**. Levels of IL-2, IL-4, IL-12, and IL-17 were not or barely detected in intima, media, and adventitia. Comparison of the four areas for the other cytokines and receptors showed that gene expression was high in ELS compared to intima, and media. For some targets, mRNA expression is very similar in ELS and adventitia (IL-6 and IL-10), which can be explained by their close proximity. Statistical analysis showed significant differences between the four tissue areas for IL6 ($p=0.0034$), IL7 ($p=0.0006$), IL10 ($p=0.0009$), IL23 ($p=0.0004$), CXCR3 ($p=0.0018$), CD20 ($p=0.0002$), TNFα ($p=0.0054$), TGFβ ($p=0.0006$), and IFNγ, ($p=0.0101$).

We hypothesized that patients with extensive ELS have higher cytokine expression

due to a more fierce immune response. When split on extent, patients in the ELS-2 category do have higher cytokine gene expression compared to the ELS-1 category, although the cellular composition in in these groups is the same *(Chapter 4 Huibers et al 2014 JHLT accepted for publication;* **Supplemental figure 1**).

Association between expression of different genes within the ELS was tested using correlation analysis (presented in **Supplemental table 3**). A significant positive correlation of CD20 with TGFβ (r=0.717, p=0.030) and IL-7 (r=0.881, p=0.004) was found, suggesting association between B cells and expression of these cytokines. TGFβ was also positively correlated with IL-6 (r=0.667, p=0.050) and IL-10 (r=0.750, p=0.020). Another positive correlation was found between IL-7 and TNFα (r=0.893, p=0.007). Our data also shows activity in the adventitia where CXCR3 seems to play an important role. Gene expression of this receptor is significantly correlated with TNFα, TGFβ, IFNγ, and CD20, where also expression of these genes are related to each other.

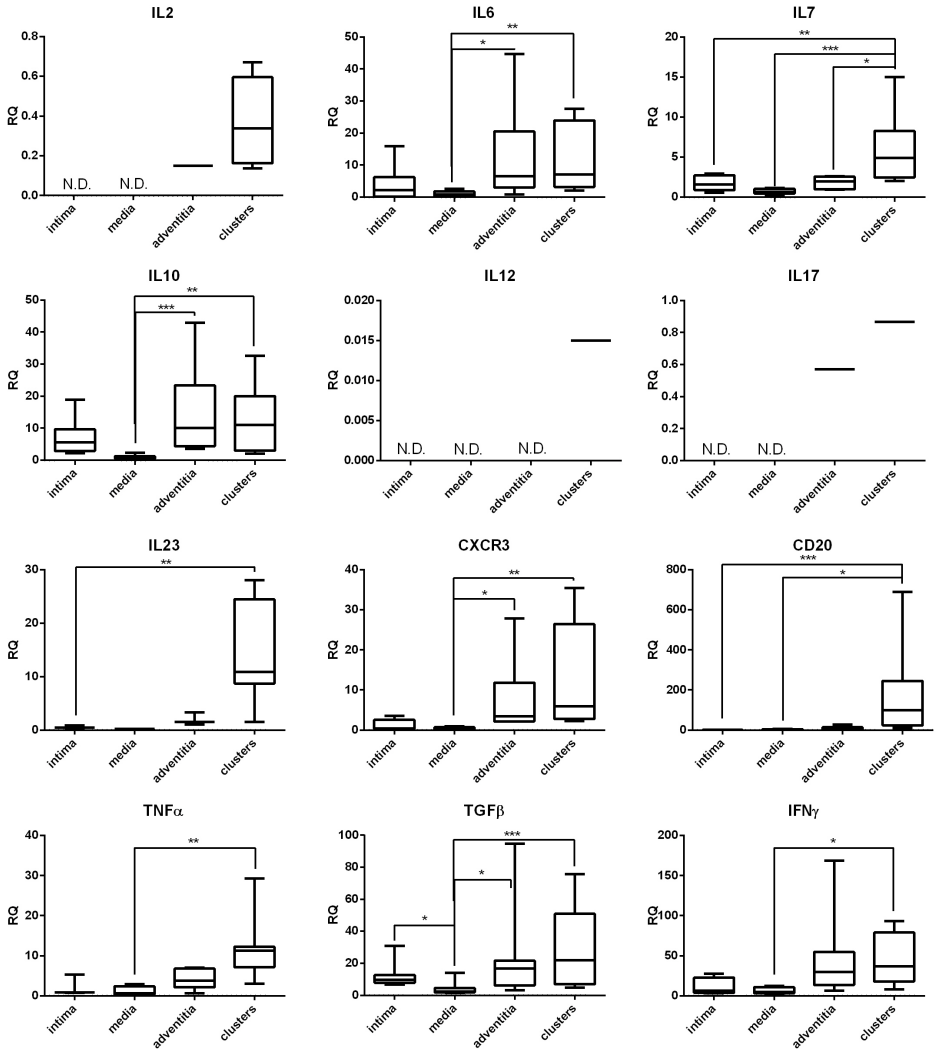

Figure 5. Cytokine expression in ELS compared to other areas within the vascular wall. IL2, IL4, IL12, and IL17 are not or expressed in low levels within all vascular layers and clusters (ELS), only a few patients show detectable levels with Q-PCR. All other markers are highly expressed in the ELS with lowest expression in the intima or media. RQ = relative quantity, N.D. = not determined. Boxplots display median with interquartile range. * p<0.050.

Discussion

To prolong the lives of transplanted grafts for as long as possible, more research into the causes of long-term cardiac graft rejection is needed. In this study, we examine cellular interaction leading to formation of ectopic lymphoid structures (ELS) and define the antigenic targets of antibodies produced in ELS surrounding coronary arteries after heart transplantation. Our previous work showed that the presence of ELS is associated with presence of CAV and time after transplant *(Chapter 4 Huibers et al 2014 JHLT accepted for publication)*. ELS contain B cells and plasma cells, suggesting an important role in humoral immune responses.

Antibody mediated rejection after cardiac transplantation is a topic not fully understood [19,20]. The origin of antibodies in antibody mediated rejection could be systemic or close to the site of action, that is within the transplanted organ. Local production of antibodies suggests a very effective local rejection process within the graft unfavorable for post-transplant outcomes. In kidney transplantation it was shown that intragraft antibodies were a better severity marker for antibody mediated rejection, than serum levels of antibodies alone [21]. If this is also the case in cardiac transplantation, patients with AMR may be missed when only serum DSAs are screened. Understanding the origin of antibody production may impact the diagnostic process to determine the presence of donor specific antibodies [22-24].

We hypothesized that ELS are very effective sites of local antibody production and contain characteristics of TLOs. One of the criteria for classification of lymphoid aggregates as TLOs is the presence of germinal centre activity, that can be detected through the presence of AID, an enzyme required for the process of somatic hypermutation in B cells (and therefore affinity maturation) and subsequent class switching [10,25]. The detection of AID in ELS in the present study indicated that active B cells class switches (from IgM to IgG) and antibody production takes place. These findings suggests that within ELS there may be germinal centre activity without the formation of distinct B cell germinal centres or paracortical T cell areas *(Chapter 4 Huibers et al 2014 JHLT accepted for publication)*.

In this study, the clonality of B cells in the ELS was analyzed, as a specific population of monoclonal B cells can be indicative of post-transplant lymphoproliferative disorder. The heterogeneity of the B cells and plasma cells in the ELS as assessed by examining kappa or lambda light chain regions demonstrated a polyclonal cell population, which corresponds to findings of others [26,27]. Multiple B cell lineages suggest that different clones are present in ELS and differentiate there. Within the ELS there are several attractant and survival signals for B cells as described in our previous paper (e.g. CXCL13, *Chapter 4 Huibers et al 2014 JHLT accepted for publication*), besides local proliferation of B cells cannot be excluded.

To study cellular activity and interactions within ELS cytokine expression was studied. In the media mRNA expression of cytokines is barely detected, which can be explained by the low numbers of mononuclear cells in these areas, corresponding to our previous findings [28,29]. Some cytokines are more prominently expressed in ELS, e.g. IL-6, IL-7, IL-23, IFNγ, TNFα and TGFβ, than in other areas. High expression of IL-6 indicates a pro- or anti-inflammatory reaction induced by T cells. The specific high expression of IL-23 in ELS might be caused by dendritic cells and macrophages that preferentially acts on $CD4^+$ T memory cells. The membrane markers CD20 and CXCR3 are positively correlated in the adventitia, meaning activation and entry of effector T cells [30] which can activate B cells leading to a humoral immune response. At these sites also high levels of TNFα and IFNγ were detected, which promote the inflammatory

process [31]. Although TGFβ is an anti-inflammatory cytokine, it controls proliferation and cellular differentiation at sites of infiltrating cells and might lead to a high cellular turnover. The high levels of IL-7 can induce CD20 on B cells and promote proliferation [32]. Also IL-10 and TGFβ, both anti-inflammatory cytokines, can enhance B cell survival, proliferation and antibody production. Besides, these cytokines cooperate in a regulatory T cell response [33] as previously described *(Chapter 4 Huibers et al 2014 JHLT accepted for publication)*.

It must be taken in account that immunosuppression therapy given to HTx patients represents a barrier to immune tolerance [34], because IL-2 formation is blocked by calcineurin inhibitors [35] which plays an important role in generating and maintaining regulatory T cells [36]. Many other cytokines are blocked by immune suppression, however in some way B cells [37] and ectopic lymphoid structures seem to escape.

To study antibodies in the epicardial ELS in more detail, tissue lysates were tested for the presence of IgG and IgM. These data show that more extensive clusters (ELS-2) have higher amounts of IgG and IgM. Besides, patients longer periods after transplantation (>6 months) tend to have higher amounts of antibodies, than shortly after transplantation, suggesting that the formation of antibodies is a long-term process.

High amounts of local antibodies may be irrelevant unless they are directed to transplant related targets. Therefore, we investigated whether these antibodies were directed against donor HLA. Four patients were positive for DSA, of which 3 patients were in het ELS-1 category and 1 patient in the ELS-2 category. This suggests that presence of ELS, but not the extensiveness of infiltration or time post-HTx determines the formation of DSAs. Besides, plasma of two patients early before death also contained DSAs. Plasma samples of the other two patients were taken long before death (as no other serum samples were available), suggesting that at earlier time points no DSAs were formed yet. Another possibility is that antibody production in tissue proceeds plasma DSAs. Interestingly, all DSAs found in tissue or plasma were directed towards HLA-II antigens; specifically HLA-DR or HLA-DQ. The importance of intra-graft antibodies was shown in kidney transplantation where patients with intra-graft DSAs were associated with a worse short-term graft outcome and lesions in the microcirculation, compared to patients without intra-graft DSAs. This relation was not found for plasma DSAs [21]. These results indicate that graft DSAs is a severity marker of the antibody-mediated pathogenic process.

Within our cohort of twenty-one HTx patients with ELS, only four showed antibodies directed towards the donor HLA-type. The question remained, towards what antigens are the other antibodies directed. Therefore, the presence of antibodies towards two non-HLA antigens, known to play a role in AMR (and/or CAV) after HTx, anti-vimentin [16,38,39] and anti-angiotensin II type-1 receptor [17], was tested. None of the controls (explanted hearts or HTx patients without ELS) had HLA or non-HLA antibodies. Within our HTx population with ELS none of the patients showed antibodies for vimentin, however eleven patients showed AT1R antibodies (52%). It is interesting to note that from the four patients with HLA DSAs, two cases also produced AT1R (non-HLA) antibodies. Previous data suggested that presence of another non-HLA antibody (MICA) could influence or even proceed HLA antibody production [40], which might explain our overlap between AT1R and HLA antibodies in these two cases.

This means that from all patients with ELS in 13 cases the target of antibody production (DSA or non-HLA directed) could be determined, explaining 62% of antibodies produced. In the cases the targets for the produced antibodies was not characterized, the detected antibodies may be directed towards other non-HLA antigens described in Heart

transplantation e.g. MICA [40], myosin [39], collagen-V, K-alpha1-tubulin 40, and/or endothelin-1 type A (ETAR; [18]).

C4d staining was studied to determine AMR. On first sight there seems no relation between extent of ELS, presence of DSAs, and pathological AMR status. However, all patients that were scored positive for pAMR (based on C4d) have antibodies within their epicardial tissue; 2 cases have donor specific HLA antibodies and 1 case had AT1R-antibodies.

The aim of this study was to investigate the humoral immune-related components of lymphoid clusters within the epicardial tissue of transplanted hearts. We demonstrated that ELS are not fully developed lymphoid structures (TLO), but with an relatively active cytokine production, that can activate and induce class switching in B cells. The antibodies detected in ELS and epicardial tissue are directed (in part) towards donor HLA or non-HLA antigens, which can influence graft survival. Taken together, this data has provided an important contribution to the field of cardiac rejection with respect to the role of antibody contribution and CAV.

Acknowledgements

We would like to thank Daniel Drop and Loes Plaisier for analysis of HLA antibodies by Luminex, and Tessa Vermeer for technical assistance with kappa/lambda ISH and IHC.

References

1. Mehra, M. R. et al. International Society for Heart and Lung Transplantation working formu-lation of a standardized nomenclature for cardiac allograft vasculopathy-2010. *J. Hear. lung Transplant.* **29**, 717–27 (2010).
2. Stehlik, J. et al. The Registry of the International Society for Heart and Lung Transplantation: Twenty-eighth Adult Heart Transplant Report--2011. *J. Hear. lung Transplant.* **30**, 1078–94 (2011).
3. Gareau, A., Hirsch, G., Lee, T. & Nashan, B. Contribution of B cells and antibody to cardiac allograft vasculopathy. *Transplantation* **88**, 470–477 (2009).
4. Valenzuela, N. M., McNamara, J. T. & Reed, E. F. Antibody-mediated graft injury: complement-dependent and complement-independent mechanisms. *Curr. Opin. Organ Transplant.* **19**, 33–40 (2014).
5. Angaswamy, N. et al. Interplay between immune responses to HLA and non-HLA self-antigens in allograft rejection. *Hum Immunol* **74**, 1478–1485 (2013).
6. Dragun, D., Philippe, A. & Catar, R. Role of non-HLA antibodies in organ transplantation. *Curr. Opin. Organ Transplant.* **17**, 440–5 (2012).
7. Wu, G. W. et al. Asymptomatic antibody-mediated rejection after heart transplantation predicts poor outcomes. *J. Hear. lung Transplant.* **28**, 417–22 (2009).
8. Thaunat, O. et al. Lymphoid neogenesis in chronic rejection: evidence for a local humoral alloimmune response. *Proc. Natl. Acad. Sci. U. S. A.* **102**, 14723–8 (2005).
9. Neyt, K., Perros, F., GeurtsvanKessel, C. H., Hammad, H. & Lambrecht, B. N. Tertiary lymphoid organs in infection and autoimmunity. *Trends Immunol.* **33**, 297–305 (2012).
10. Wehner, J. R. et al. B cells and plasma cells in coronaries of chronically rejected cardiac transplants. Transplantation **89**, 1141–8 (2010).
11. Berry, G. J. et al. The 2013 International Society for Heart and Lung Transplantation Working Formulation for the tandardization of nomenclature in the pathologic diagnosis of antibody-mediated rejection in heart transplantation. *J. Hear. Lung Transplant.* **32**, 1147–1162 (2013).
12. Stewart, S. et al. Revision of the 1990 working formulation for the standardization of nomenclature in the diagnosis of heart rejection. *J. Hear. lung Transplant.* **24**, 1710–20 (2005).
13. Berry, G. J. et al. The ISHLT working formulation for pathologic diagnosis of antibody-mediated rejection in heart transplantation: evolution and current status (2005-2011). *J. Hear. lung Transplant.* **30**, 601–11 (2011).
14. Mahesh, B. et al. Autoantibodies to vimentin cause accelerated rejection of cardiac allografts. *Am. J. Pathol.* **170**, 1415–27 (2007).
15. Jurcevic, S. et al. Antivimentin Antibodies Are An Independent Predictor of Transplant-Associated Coronary Artery Disease After Cardiac Transplantation. *Transplantation* **71**, 886–892 (2001).
16. Reinsmoen, N. L. et al. Increased negative impact of donor HLA-specific together with non-HLA-specific antibodies on graft outcome. *Transplantation* **97**, 595–601 (2014).
17. Hiemann, N. E. et al. Non-HLA antibodies targeting vascular receptors enhance alloimmune response and microvasculopathy after heart transplantation. *Transplantation* **94**, 919–24 (2012).
18. Fishbein, G. a & Fishbein, M. C. Morphologic and immunohistochemical findings in antibody-mediated rejection of the cardiac allograft. *Hum. Immunol.* **73**, 1213–7 (2012).
19. Chih, S., Tinckam, K. J. & Ross, H. J. A survey of current practice for antibody-mediated rejection in heart transplantation. *Am. J. Transplant* **13**, 1069–74 (2013).
20. Bachelet, T. et al. Kidney intragraft donor-specific antibodies as determinant of antibody-mediated lesions and poor graft outcome. *Am. J. Transplant.* **13**, 2855–64 (2013).
21. Lefaucheur, C. et al. Preexisting donor-specific HLA antibodies predict outcome in kidney transplantation. *J. Am. Soc. Nephrol.* **21**, 1398–1406 (2010).
22. Lefaucheur, C. et al. Antibody-mediated vascular rejection of kidney allografts: A population-based study. *Lancet* **381**, 313–319 (2013).
23. Otten, H. G., Verhaar, M. C., Borst, H. P. E., Hené, R. J. & Zuilen, A. D. Van. Pretransplant donor-specific HLA class-I and -II antibodies are associated with an increased risk for kidney graft failure. *Am. J. Transplant.* **12**, 1618–1623 (2012).
24. Perros, F. et al. Pulmonary lymphoid neogenesis in idiopathic pulmonary arterial hypertension. *Am. J. Respir. Crit. Care Med.* **185**, 311–321 (2012).
25. Wehner, J., Morrell, C. N., Reynolds, T., Rodriguez, E. R. & Baldwin 3rd, W. M. Antibody and complement in transplant vasculopathy. *Circ Res* **100**, 191–203 (2007).
26. Thaunat, O., Patey, N., Morelon, E., Michel, J.-B. & Nicoletti, A. Lymphoid neogenesis in chronic rejection: the murderer is in the house. *Curr. Opin. Immunol.* **18**, 576–9 (2006).
27. Hagemeijer, M. C. et al. T cells in cardiac allograft vasculopathy are skewed to memory Th-1 cells in the presence of a distinct Th-2 population. *Am J Transpl.* **8**, 1040–1050 (2008).
28. Huibers, M. et al. Intimal fibrosis in human cardiac allograft vasculopathy. *Transpl. Immunol.* **25**, 124–132 (2011).
29. Groom, J. R. & Luster, A. D. CXCR3 in T cell function. *Exp. Cell Res.* **317**, 620–31 (2011).

30. Dinarello, C. A. Proinflammatory cytokines. *Chest* **118**, 503–508 (2000).
31. Corfe, S. A. & Paige, C. J. The many roles of IL-7 in B cell development; Mediator of survival, proliferation and differentiation. *Semin. Immunol.* **24**, 198–208 (2012).
32. Jutel, M. et al. IL-10 and TGF-β cooperate in the regulatory T cell response to mucosal allergens in normal immunity and specific immunotherapy. *Eur. J. Immunol.* **33**, 1205–1214 (2003).
33. Noris, M. et al. Regulatory T cells and T cell depletion: role of immunosuppressive drugs. *J. Am. Soc. Nephrol.* **18**, 1007–1018 (2007).
34. Zeiser, R. et al. Inhibition of CD4+CD25+ regulatory T-cell function by calcineurin-dependent interleukin-2 production. *Blood* **108**, 390–399 (2006).
35. Malek, T. R. & Bayer, A. L. Tolerance, not immunity, crucially depends on IL-2. *Nat. Rev. Immunol.* **4**, 665–674 (2004).
36. Heidt, S. et al. Effects of immunosuppressive drugs on purified human B cells: evidence supporting the use of MMF and rapamycin. *Transplantation* **86**, 1292–1300 (2008).
37. Rose, M. L. & Smith, J. D. Clinical relevance of complement-fixing antibodies in cardiac transplantation. *Hum. Immunol.* **70**, 605–9 (2009).
38. Nath, D. S. et al. Characterization of immune responses to cardiac self-antigens myosin and vimentin in human cardiac allograft recipients with antibody-mediated rejection and cardiac allograft vasculopathy. *J. Hear. lung Transplant.* **29**, 1277–85 (2010).
39. Nath, D. S. et al. Donor-specific antibodies to human leukocyte antigens are associated with and precede antibodies to major histocompatibility complex class I-related chain A in antibody-mediated rejection and cardiac allograft vasculopathy after human cardiac transplantat. *Hum. Immunol.* **71**, 1191–6 (2010).
40. Nath, D. S. et al. A role for antibodies to human leukocyte antigens, collagen-V, and K-Đ1-Tubulin in antibody-mediated rejection and cardiac allograft vasculopathy. *Transplantation* **91**, 1036–43 (2011).
41. Huibers, M. M. H. et al. Distinct phenotypes of cardiac allograft vasculopathy after heart transplantation: A histopathological study. *Atherosclerosis* **236**, 353–359 (2014).

Supplemental data

Table S1. antibodies for immunohistochemistry

Marker		Species	Dilution	clone	Firm	Antigen retrieval	Secondary ab
CD20	B cell marker	Mouse monoclonal	1:50	L26	Abcam	citrate	polyclonal biotinylated anti-mouse 1:500
CD138	Plasma cell marker	Rabbit polyclonal	1:50	GR52674-1	Abcam	citrate	polyclonal biotinylated anti-mouse 1:500
IgG	Immunoglobulin G	Rabbit monoclonal	1:500	EPR4421	Abcam	citrate	polyclonal biotinylated anti-mouse 1:500
IgM	Immunoglobulin M	Rabbit monoclonal	1:500	EPR5539	Abcam	citrate	polyclonal biotinylated anti-mouse 1:500
AID	Activated Induced Cytodine Deaminase	Rat monoclonal	1:50	mAID-2	Ebioscience	citrate	polyclonal biotinylated goat anti-rat 1:500
C4d	Complement factor	Rabbit polyclonal	1:80 ventana	-	404A-16, Cellmarque	EDTA	Optiview DAB IHC Detection kit, Ventana
CD3	T cell marker	Rabbit plyclonal	1:400 ventana	-	A0452 DAKO	EDTA	Optiview DAB IHC Detection kit, Ventana

Table S2. AMR score according to ISHLT criteria. ELS = ectopic lymphoid structures, H-CAV = histological Cardiac Allograft Vasculopathy 41, F = female, M = male, HTx = heart transplantation, AMR = antibody mediated rejection, neg = negative, pos = positive.

ELS	H-CAV	Gender	Time post HTx (years)	C4d (%)	AMR	HLA	AT1R
0	3	F	10.02	1	neg	neg	neg
1	2	M	0.42	60	pos	pos	neg
1	2	M	1.02	0	neg	pos	pos
1	3	F	7.86	45	risk	neg	neg
1	3	M	7.01	2	neg	pos	neg
1	3	M	12.50	0	neg	neg	neg
1	3	M	17.80	1	neg	neg	pos
1	3	M	15.74	0	neg	neg	pos
1	3	M	3.50	10	neg	neg	risk
1	2	M	2.56	1	neg	neg	neg
1	2	M	0.89	0	neg	neg	risk
1	3	F	9.71	3	neg	neg	neg
1	3	M	3.93	0	neg	neg	risk
1	2	M	1.61	1	neg	neg	pos
1	2	M	5.33	5	neg	neg	risk
1	3	M	6.26	25	risk	neg	pos
1	3	M	11.55	0	neg	neg	neg
2	1	F	1.91	35	risk	neg	neg
2	1	F	0.33	80	pos	neg	pos
2	1	M	0.86	3	neg	neg	neg
2	2	M	2.54	70	pos	pos	risk

Table S3. Correlation between cytokine expression levels. Spearman correlation between the different vessel layers. Numbers display r-values with significant correlation in bold (* p<0.050, ** p<0.001). IL-2, IL-4, IL-12, and IL-17 were not or barely expressed so no correlation was calculated. N.D. = not determined due to small sample size.

		TNFα	TGFβ	IFNγ	IL6	IL7	IL10	IL23	CD20	CXCR3
TNFα	Intima									
	Media									
	Adventitia									
	ELS									
TGFβ	Intima	0.500								
	Media	0.800								
	Adventitia	**0.829***								
	ELS	0.429								
IFNγ	Intima	0.500	-0.400							
	Media	N.D.	0.600							
	Adventitia	**0.943****	**0.929****							
	ELS	0.071	0.690							
IL6	Intima	.	0.143	N.D.						
	Media	.	0.214	-0.500						
	Adventitia	0.429	0.467	0.714						
	ELS	0.250	**0.667***	0.048						
IL7	Intima	N.D.	0.071	0.600	0.500					
	Media	0.800	0.571	0.500	-0.200					
	Adventitia	0.600	0.600	0.100	-0.143					
	ELS	**0.893****	0.643	0.476	0.286					
IL10	Intima	N.D.	0.679	N.D.	0.400	0.600				
	Media	N.D.	0.750	0.400	0.300	0.486				
	Adventitia	0.486	0.617	0.750	0.600	0.086				
	ELS	0.393	**0.750***	0.429	0.533	0.333				
IL23	Intima	N.D.	N.D.	N.D.	N.D.	N.D.	N.D.			
	Media	.	.	.	.	.	.			
	Adventitia	N.D.	N.D.	N.D.	0.500	0.500	0.500			
	ELS	N.D.	0.286	0.643	-0.452	0.405	-0.214			
CD20	Intima	.	0.400	N.D.	0.400	N.D.	N.D.	N.D.		
	Media	N.D.	0.800	-0.500	N.D.	N.D.	0.500	.		
	Adventitia	0.657	**0.900****	0.714	0.550	0.771	0.550	0.500		
	ELS	0.679	**0.717***	0.619	0.500	**0.881***	0.267	0.333		
CXCR3	Intima	N.D.	0.700	0.500	N.D.	N.D.	0.800	N.D.	N.D.	
	Media	N.D.	0.700	0.500	N.D.	0.600	N.D.	.	N.D.	
	Adventitia	**0.900***	**0.943****	**0.829***	0.771	0.600	0.771	0.500	**0.886***	
	ELS	N.D.	0.800	N.D.	0.800	N.D.	N.D.	-0.800	0.600	

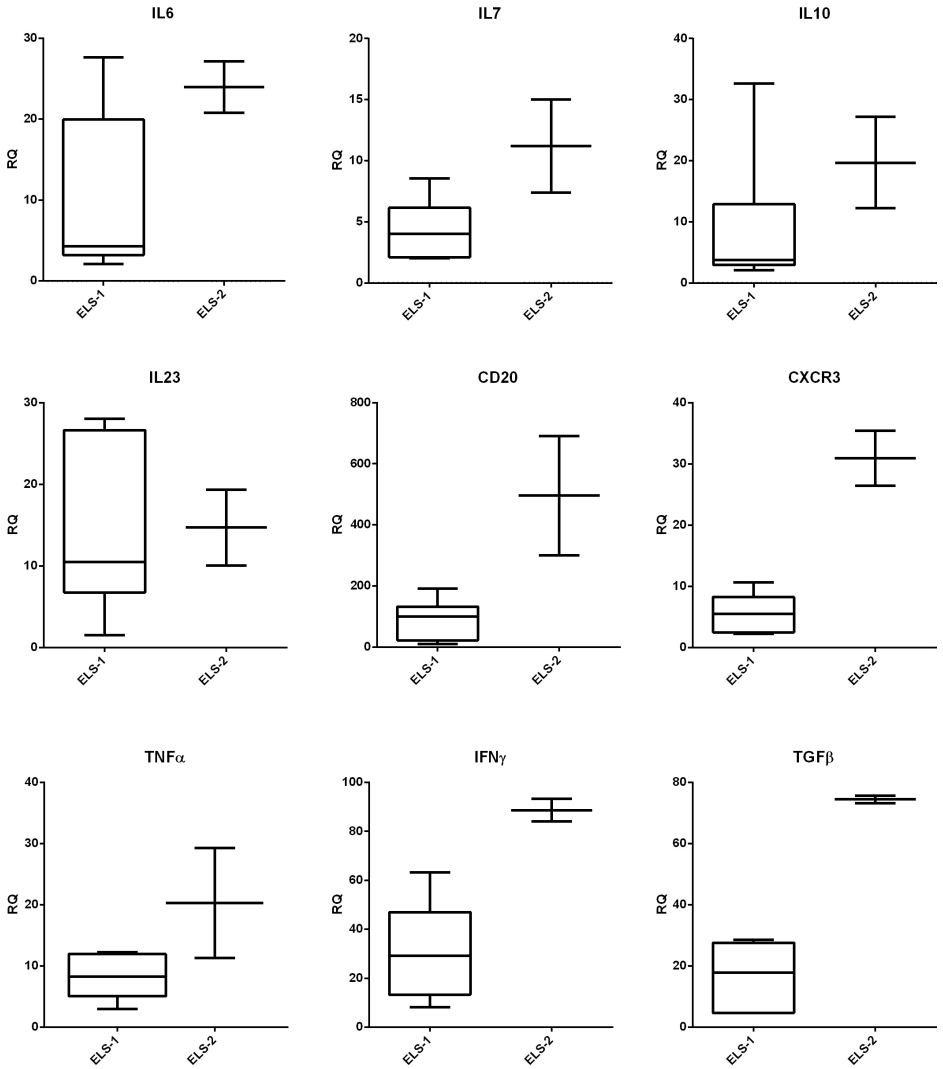

Figure S1. Cytokine expression differs between extent of ELS. Comparison of cytokine gene expression between ELS-1 (n=7) and ELS-2 (n=2) patients. ELS-2 patients have a higher cytokine gene expression profile than the ELS-1 patients. Boxplots display median with interquartile range. No statistics is performed due to low numbers. RQ = relative quantity.

Chapter 6.

CARDIAC ALLOGRAFT VASCULOPATHY: A DONOR OR RECIPIENT INDUCED PATHOLOGY?

*Patricia. van den Hoogen MSc [1,2] *, Manon M.H. Huibers MSc [2] *, Joost P.G. Sluijter PhD [1], Roel A. de Weger PhD [2]*

Departments of Cardiology, Experimental Cardiology laboratory [1], Pathology [2], University Medical Centre Utrecht, the Netherlands

** Authors contributed equally to the work*

Published
Journal of Cardiovascular Translational Research [Epub ahead of print] (2015)

Abstract

Cardiac allograft vasculopathy (CAV) is one of the main causes of late stage heart failure after heart transplantation. CAV is characterized by concentric luminal narrowing of the coronary arteries, but the exact pathogenesis of CAV is not elucidated. Many researchers show evidence of an allogeneic immune response of the recipient, whereas others show contradictory results in which donor-derived cells induce an immune response against the graft. In addition, fibrosis of the neo-intima can be induced by recipient-derived circulating cells or donor-derived cells. In this review, both donor and recipient sides of the story are described to obtain better insight in the pathogenesis of CAV. Dual outcomes were found regarding the contribution of donor and recipient cells in the initiation of the immune response and the development of fibrosis during CAV. Future research should focus more on the potential synergistic interaction of donor and recipient cells leading to CAV.

Introduction

Cardiac transplantation is often successfully applied in the treatment of end-stage heart failure[1]. Since 1982, more than 110,000 heart transplantations have been globally performed and these numbers are still rising[2]. Over the years, early survival rates of recipients, which received a heart transplantation, have significantly improved[2]. In the first months after transplantation, acute rejection of the transplanted heart can occur[3]. Much progress has been made in controlling this acute rejection phase, resulting in increased early survival rates[2]. However, chronic rejection is one of the major issues that affects long-term survival of heart transplant recipients[4].

One of the main causes of chronic rejection is cardiac allograft vasculopathy (CAV)[1–5]. CAV is an accelerated form of coronary artery disease[6] and affects both males and females[3]. The mechanism by which CAV develops is not fully elucidated, but it is estimated that 50% of heart transplantation recipients are developing CAV within five years after transplantation[7]. Hence, CAV is responsible for 10-15% of cardiac deaths after transplantation[8]. CAV affects the vasculature of the transplanted heart, resulting in congestive heart failure, arrhythmias, myocardial infarction or sudden cardiac death[1,9]. Multiple factors are involved in the development of CAV, although the immune system has shown to be the most important player[5,10]. CAV is characterized by diffuse intimal thickening leading to progressive narrowing of the coronary arteries[5,11]. There are different types of lesions in CAV patients, including intimal hyperplasia, atherosclerotic lesions and vasculitis[3]. Within the lesions of intimal hyperplasia , three histopathological phenotypes of CAV can be observed: 1) loose connective tissue with inflammatory cells, 2) lesions with smooth muscle cells and 3) fibrotic lesions (**figure 1**)[12]. Most commonly seen characteristic in CAV is fibromuscular hyperplasia of the intima, which also distinguishes CAV from atherosclerosis[8]. Ultimately, progressive narrowing of the coronary artery results in critical stenosis and ischemia of the graft[3].

The exact mechanism in which CAV is induced after heart transplantation is not elucidated, but it is known that both donor- and recipient cells are involved[13]. The question remains whether cells of the recipient react on cells of the donor heart or vice versa. Multiple researchers have investigated the mechanism of CAV and the results were often contradictory.

For example, one study revealed that donor dendritic cells (DCs) transmigrate through host secondary lymphoid organs, thereby promoting T-lymphocytes of the recipient, which may promote graft rejection[14]. However, others propose that allo-recognition of donor major histocompatibility complexes (MHC) by recipient immune cells leads to graft rejection[15]. The same holds true for the development of fibrosis: are recipient-derived endothelial progenitor cells or endothelial-mesenchymal transition of donor cells responsible for the progressive lesion formation[16,17]? The immune response could be the initial trigger for fibrosis, however, other mechanisms of fibrosis could be involved as well. In this overview, recipient and donor sides of the stories (immune response and fibrosis) are highlighted to obtain better insights in the pathogenesis of CAV.

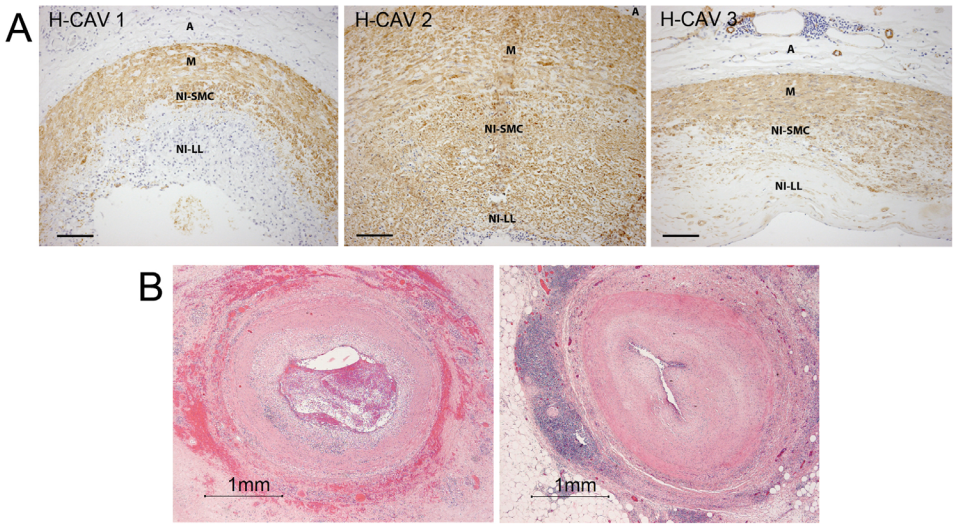

Figure 1. Microscopic pictures of the three histopathological phenotypes of CAV in the coronary artery of heart transplantation recipients. **A**. H-CAV 1 lesion, which shows infiltration of lymphocytes in the neo-intima layer. H-CAV 2 lesion, showing infiltration of lymphocytes together with infiltration of smooth muscle cells and formation of connective tissue. H-CAV 3 lesion, which shows a large fibrotic intimal lesion without inflammatory infiltrate (ĐSMA staining, magnification 100x, line indicates 100µm). **B**. Microscopic pictures of occluded coronary arteries by a thrombus or fibrotic tissue respectively (HE staining, magnification 20x, line indicates 1 mm).

Cardiac allograft vasculopathy: Immune response

Recipient-derived immune response

According to multiple research groups, CAV is initiated by the immune response of the recipient against the donor[3,5,9,18]. The hypothesis is that after the heart is transplanted, both cellular and humoral immune responses of the recipient are generated against the graft[3]. The immune response of the recipient can be triggered via a (1) direct- , an (2) indirect- or a (3) semi-direct pathway (**figure 2**)[18–21].

(1) In the direct pathway recipient T-lymphocytes are activated after recognition of allogeneic MHCs (with a foreign antigen) of donor antigen presenting cells (APCs)[18]. (2) The indirect pathway is activated by allo-recognition of processed foreign antigens by APCs of the recipient itself[19]. The recognition of donor antigens on recipient APCs leads to the activation and proliferation of T-lymphocytes. (3) The semi-direct pathway, a new pathway which may be involved, is activated by recipient APCs, presenting donor MHC molecules on their surface[20]. The hypothesis is that recipient APCs acquire donor MHC via cell-cell interaction (intercellular exchange) with donor cells or via the uptake of donor-derived exosomes[21]. The subsequent presentation of donor antigens by donor MHC molecules on recipient APCs will mount a host T-lymphocyte response, leading to the development of chronic rejection.

In all three pathways the activation of T-lymphocytes will lead to secretion of cytokines such as interleukin-2 (IL-2) and interferon-γ (IFN-γ)[22]. Cytotoxic T-lymphocytes, B-lymphocytes and macrophages are activated by these cytokines. In addition, endothelial cells are activated and start expressing vascular cell adhesion molecules, which leads to the recruitment of more immune cells[7]. The pro-inflammatory cytokines also enhance the proliferation of smooth muscle cells (SMCs)[15]. Activated B-lymphocytes begin to secrete donor-specific HLA antibodies. These antibodies are important mediators in the development of CAV[23,24]. They are able to bind the allo-antigens to enable complement factor binding, leading to the activation of the complement system. Furthermore, immune cells, such as macrophages, can bind the donor specific antibodies, which activates antibody-mediated lysis[18]. All of the indicated pathways will ultimately result in vascular injury, ischemia and damage to the allograft[9].

In addition, there is also evidence that "autoimmunity" plays an important role in the development of CAV[25]. For example, in lung transplant recipients, chronic allograft rejection developed even in the absence of human leukocyte antigen (HLA) antibodies[26]. An explanation for this phenomenon might be the presence of antibodies against non-HLA antigens[25], but the question remains which non-HLA antigens are involved. Recent studies showed that "auto-antibodies" against cardiac myosin and vimentin can be detected after heart transplantation[27,28]. These "auto-antibodies" are probably induced via antigen mimicry between the donor MHC peptides and auto-antigen peptides of the recipient[28]. T-lymphocytes, which are activated by an indirect allo-immune response, are able to induce chronic rejection via the recognition of these auto-antigens[29]. It has been shown in mouse models that induction of tolerance to cardiac myosin leads to a decrease in chronic rejection and an increase in long term survival after heart transplantation[30]. Therefore, reactivity of the T-lymphocytes towards auto-antigens is likely involved in the development of CAV[28].

Furthermore, the development of anti MHC-class-1-chain-related-A (MICA) antibodies may play a role in the development of CAV[23,25]. Normally, these antigens are expressed in fibroblasts, monocytes and endothelial cells[24]. In CAV there is an increase in MICA expression on endothelial cells[31]. In addition, allo-antibodies against MICA are detected, which actively induce an immune response and cause damage to the endothelium[23].

Cytomegalovirus (CMV) infection has also been known to affect transplantation outcome and CAV. Systemic replication of CMV is associated with increased risk of rejection of the graft and the development of CAV[32]. The hypothesis is that CMV infection induces inflammatory responses of the recipient, thereby contributing to vascular damage and accelerating the pathogenesis of CAV [33].

The trigger of these responses (direct-, indirect-, and semi-direct pathways, "autoimmunity" and CMV infection) ultimately leads to the proliferation of smooth muscle cells (SMCs), accumulation of extracellular matrix and hyperplasia of the intima of the vessel wall **(figure 2)**[15,22,23].

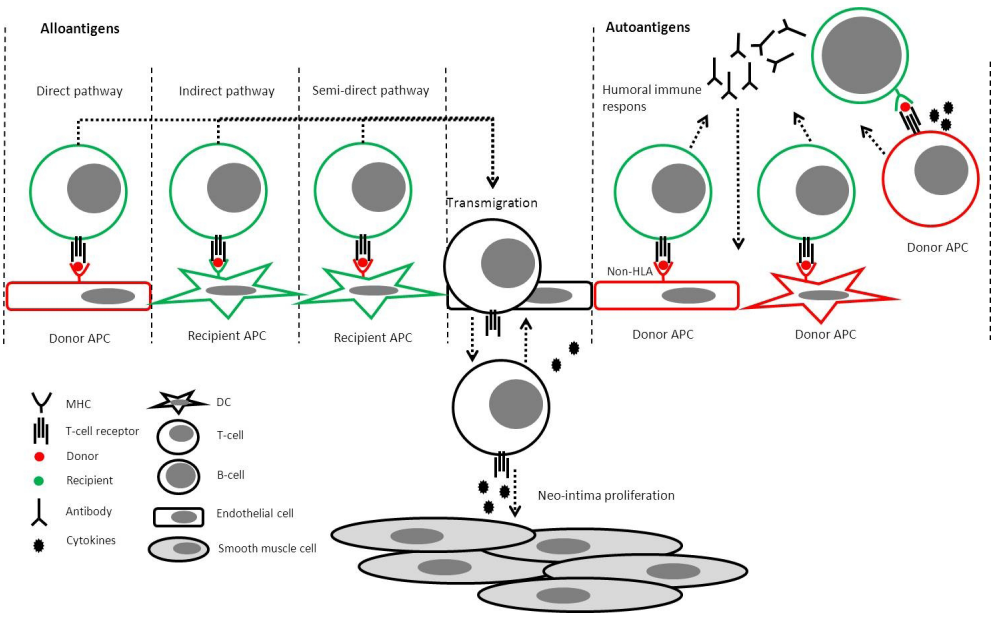

Figure 2. Pathways in recipient-derived immune response. Primary event is the recognition of allo-antigens by T-lymphocytes via one of the indicated pathways. The direct pathway is activated by the recognition of MHC complexes with a foreign HLA-antigen (red) presented by donor APCs (red). The indirect pathway is activated when T-lymphocytes recognize processed allo-antigens presented by recipient APCs (green). The semi-direct pathway is activated when T-lymphocytes recognize allo-antigens presented on donor MHC on recipient APCs. In addition, non-HLA antigens might be involved, which are bound by "auto-antibodies". This will lead to complement activation and T-lymphocyte activation. Activation of B-cells can be initiated by donor DCs and donor T-lymphocytes. All of the indicated pathways lead to activation of T-lymphocytes, which start to secrete pro-inflammatory cytokines such as IFN-γ. The secretion of IFN-γ recruits more immune cells, such as NK-cells and macrophages, and acts on SMCs. The proliferation of SMCs will ultimately result in proliferation of the intima and occlusion of the artery, which are the characteristics of CAV.

Donor-derived immune response

Next to the recipient-derived immune response, there is also evidence that donor cells are involved in the immune-pathogenesis of chronic rejection and CAV[34,35]. The current hypothesis is that remaining donor cells within the transplanted heart are able to actively induce an immune response of recipient immune cells[36,37]. It has been shown that donor-derived immune cells are able to migrate to lymph nodes of the recipient and locally present allo-antigens[38]. Heart-derived donor DCs can already be found three hours after transplantation in secondary lymphoid organs and are not as short-lived in recipients as previously thought[36]. A rodent animal study demonstrated that donor dendritic cells (DCs) can be found in T-lymphocyte areas of the host spleen and hepatic lymphnodes[35]. Hereby, cluster formation of donor DCs and host T-lymphocytes was initiated that activated T-lymphocyte proliferation[35]. These results suggest a donor-derived immune response, initiated by donor DCs.

In addition to donor DCs, the functional activity of donor CD4 T-lymphocytes was studied. In a mouse model the development of autoimmune reactions after heart transplantation and the contribution to CAV was analyzed[37]. Donor CD4 T-lymphocyte allo-recognition of MHC-II on recipient B-lymphocytes enhanced the production of auto-antibodies, thereby contributing to the development of CAV[37]. When donor CD4 T-lymphocytes were depleted, a significant decrease in both antibody and complement deposition was observed in the allograft[37]. Furthermore, transplant studies showed a mixture (chimerism) of donor and recipient leucocytes, including T-lymphocytes, in heart transplant recipients[39]. However, to what extent donor T-lymphocytes are contributing to CAV after heart transplantation is still unknown.

The expression of donor programmed death–ligand1 (PD-L1) is also involved in the development of CAV[40]. This ligand plays an important role in the regulation of an allo-immune response by regulating activation of CD4 and CD8 T-lymphocytes[41]. Donor deficiency of PD-L1 accelerates allograft rejection and the development of CAV compared to PD-L1 deficient recipients[40]. Deficiency of donor PD-L1 leads to the secretion of IFN-γ and proliferation of allo-reactive T-lymphocytes of the recipient, thereby promoting a recipient allo-immune response[41]. These findings show that PD-L1 expression on cardiac tissue or leukocytes of the donor is critical in the regulation of an allograft immune response in heart transplant recipients[40,41].

In addition, it has been shown that donor-derived selectins play an important role in the development of CAV[34]. Selectins are involved in adhesion of leukocytes to the endothelium of the vessel wall[34]. Donor-derived E and P-selectin, located on the endothelium of the graft, interact with L-selectin on recipient-derived leukocytes, thereby enhancing the attraction of immune cells[34]. In rats, there is a significant correlation between the amount of P-selectin expression and intimal thickening of the vessel wall[42]. Corresponding results were found in human recipients with a lung allograft[43]. Furthermore, an increased long-term graft survival with minimal vasculopathy was seen in recipients lacking donor-expressed selectins, indicating the importance of donor-derived selectins in the development of CAV[44].

According to this accumulating evidence, there is a donor-derived immune response causing the development of allograft vasculopathy and donor cells are involved in regulating the allo-immune response of the recipient. Since this is a relatively new insight, more focus on these aspects is needed to reveal the exact mechanism and to define all of the donor and recipient cells involved.

Differences in immune response in gender mismatch transplantations

Interesting differences in transplantation outcome have been reported between males receiving a female heart or females receiving a male heart, the so called donor-recipient gender mismatch transplantations[45]. Donor-recipient gender mismatch has been shown to influence the early pathogenesis of CAV[46]. At the vascular level, male recipients with a female allograft developed significantly higher amounts of intimal thickening within one year of transplantation[47]. Females receiving a male allograft only developed non-severe thickening of the intima[47]. The combination of male recipients receiving a female heart have been correlated with worse outcomes at several levels aside from CAV[48]. Which factors are involved is still under investigation, but there is evidence that smaller heart size, shear stress and loss of the estrogen-protected environment of the female heart are important factors[1,47]. All these factors also contribute to initial endothelial damage of the coronary arteries, thereby initiating CAV development. Furthermore, the vasculature of the female heart is thought to be immunologically more susceptible compared to male hearts[47]: a possible explanation is that the vasculature of the female heart expresses more HLA and non-HLA endothelial antigens than their male counterparts[49], which leads to triggering of the male immune system and thereby an earlier development of CAV[47].

At the organ level, contradictory studies showed higher incidents of rejection of female recipients receiving a male heart[50]. These high rejection rates might be explained by greater immuno-competence of the female by developing HLA antibodies against H-Y antigens, presented by cells of the male heart[50]. Presentation of these antigens can lead to an immune response followed by the formation of allogeneic antibodies[25]. The allogeneic immune response against H-Y antigens can lead to graft destruction and ultimately results in rejection of the male heart[51].

Based on these findings, donor-recipient gender mismatch in heart transplantation is followed by dual outcomes. Transplantation of male hearts into females is characterized by higher rejection rates, but in the end a higher long-term survival[50]. Transplantation of female hearts into males is characterized by an earlier development of CAV[50]. However, some of the studies were limited by the small numbers of gender mismatch transplantations available[46].

Cardiac allograft vasculopathy: Fibrosis

The before-mentioned immune reactions could be followed by fibrosis, which plays an important role in the progressive thickening of the neo-intima and subsequently in the development of CAV[52]. In some recipients, the neo-intima of the coronary arteries almost completely exists of fibrotic tissue[53]. It is known that some inflammatory cells of the recipient, such as T-lymphocytes and macrophages, are involved in the initiation of the fibrotic process[52]. The secretion of cytokines like IFN-γ and transforming growth factor-β (TGF-β) by T-lymphocytes leads to the activation of macrophages and fibroblasts respectively[25,54]. It has been shown that especially recipient-derived macrophages type 2 (M2) are increased in the neo-intima of CAV arteries[55,56]. These macrophages are involved in tissue remodeling and matrix deposition and play an important role in the development of fibrotic lesions[55,57]. They are known to infiltrate the allograft and produce growth factors, such as TGF-β, which increases neo-intimal proliferation[56]. However, more cell types are involved. Next to identified circulating cells of the recipient, there is again also evidence of the involvement of donor-derived cells[13,58].

Recipient-derived circulating cells

There is evidence emerging for the role of recipient endothelial progenitor cells (EPCs) in CAV[29]. EPCs ($CD133^+CD34^+Flk1$ [$VEGF\text{-}R1]^+$ in bone marrow, CD31 [$PECAM\text{-}1]^+CD146^+vWF^+NOS^+$ in circulation) are bone marrow-derived cells, which have endothelial regenerative properties[59]. Healthy endothelium of the vessel wall normally undergoes degeneration and regeneration[60]. By an imbalance in these processes, endothelial dysfunction occurs that can lead to injury of the vessel wall[60]. EPCs are able to adhere to the sides of injury and promote healing and repair[61]. Increased numbers of circulating EPCs have been shown to prevent cardiovascular diseases and to reduce neo-intimal hyperplasia in men[62]. However, upon heart transplantation, the protective role of EPCs changes and EPCs of the recipient may participate in the pathogenesis of CAV (**figure 3A**) [16,60,63]. Apparently, circulating EPCs attach to the vessel wall and start to proliferate as a result of a persistent allograft immune response[63]. The EPCs become uncontrolled, thereby contributing to chronic allograft rejection via accumulation of endothelial cells and SMCs, which in turn leads to occlusive narrowing of the coronary vessels[60]. Upon culturing mononuclear cells from blood, fewer colonies of circulating EPCs were found in heart transplantation recipients with vasculopathy during chronic rejection[16],compared to transplantation recipients without evidence of vasculopathy. Interestingly, there was also an increase of attached recipient EPCs in the coronary arties of the donor heart, where eventually CAV developed[16]. The hypothesis is that excessive numbers of recipient EPCs differentiate into endothelial cells and SMCs, and that an overload of these cells leads to hyperplasia of the neo-intima and fibrosis[16,63]. The number of circulating EPCs becomes depleted and thereby the protective effects, as mentioned before, are lost[16].

In addition to EPCs, there is also evidence for a role of recipient-derived extra-cardiac progenitor cells[64]. These extra-cardiac progenitor cells are thought to be derived from mesenchymal precursor cells and migrate towards to allograft where they differentiate into multiple cell lineages[65]. Engraftment of recipient-derived cells in the allograft, such as cardiac progenitor cells, resulted in chimerism of the transplanted heart, which can be beneficial by

repopulating the niches of rejected donor cells of the graft[61,66,67] However, chimerism of the transplanted heart by extra-cardiac progenitor cells has been shown to be linked to CAV and intimal fibrosis[65]. A possible explanation for this is that, during cell death of donor cells, an immune response is locally triggered leading to vascular damage of the coronary arteries[59]. In response to tissue injury, recipient-derived mesenchymal precursor cells are attracted and migrate towards the allograft and differentiate into fibroblasts[68]. In rats suffering from chronic allograft rejection, it has been shown that more than 65% of fibroblasts in the allograft are of recipient origin[68]. When these fibroblast are activated upon inflammation, they start to proliferate and produce extracellular matrix (ECM)[69]. Ongoing inflammation in chronic rejection leads to a continuous fibrogenic environment, which ultimately leads to fibrosis of the neo-intima in CAV[52,66,68,69].

Although the chimerism of the transplanted heart provides evidence for the involvement of recipient-derived circulating cells, the contribution of these cells in the pathogenesis of fibrosis in human CAV is still conflicting and remains to be elucidated.

Donor-derived cells

Besides the contribution of recipient-derived cells, there is also evidence that donor cells are involved in the formation of fibrosis[13,59] It is thought that especially donor-derived SMCs produce extracellular matrix and contribute to the formation of fibrotic lesions in the neo-intima[60]. In CAV, most of the cells in the neo-intima of coronary vessels express markers of SMCs[70]. In human CAV, the majority of these cells are derived from the graft and not from the host[13]. It is not known where these SMCs are originating from. It is possible that resident intimal SMCs expand in number upon inflammation or that they derive from the media and migrate towards the intima to sites with vascular damage (**figure 3B**) [9]. There is also evidence that these donor-derived SMCs are derived from endothelial mesenchymal transitions of donor cells[17]. However, the exact role of these donor-derived SMCs needs to be elucidated.

Endothelial-to-mesenchymal transition (Endo-MT) and epithelial-to-mesenchymal transition (EMT) have shown to be potential contributors to neo-intima formation[71–73]. Endo-MT is the trans-differentiation of endothelial cells into mesenchymal cells, such as SMCs and fibroblasts, whereas EMT represents the trans-differentiation of epithelial cells into mesenchymal cells[17,71]. This process normally occurs during certain stages of embryonic development of the heart under influence of TGF-β signaling and is implicated in fibrosis formation[71,74]. For example, biopsies of human kidney transplants with allograft vasculopathy showed a loss of epithelial markers and an increase in mesenchymal markers[75]. The same trend was observed in studies with cardiac fibrosis, where endo-MT significantly contributed to the development of fibrosis in chronic cardiac disease[76]. It is thought that both endothelial and epicardial-derived cells of the donor, located on the transplanted heart, use this mechanism to differentiate into SMCs and myofibroblasts, thereby contributing to the development of neo-intima fibrosis in CAV[71,76–78]. Although this hypothesis is increasingly gaining attention, it still needs to be elucidated where these donor-derived cells come from.

Donor-derived atherosclerotic plaques

Next to individual donor-derived cells, it has been suggested that atherosclerotic plaques in coronary vessels of the donor, pre-existing in the transplanted heart, influence the outcome of CAV in the recipient[79]. The atherosclerotic lesions make the intima and the endothelium of the donor coronary arteries more vulnerable for the development of fibrotic lesions during CAV[12]. In these arteries, the fibrotic process and proliferation of immune cells and SMCs was already ongoing in the plaque and could further develop in the transplanted heart, thereby causing neo-intima formation (**figure 3B**). It is also possible that these atherosclerotic lesions develop after transplantation, but there seems to be a correlation between pre-existing atherosclerotic lesions and a more fibrotic CAV outcome[8].

In conclusion, appears not only inflammatory cells of the donor are involved in the pathogenesis of CAV, but also donor-derived cells, such as endothelial cells, epicardial cells and smooth muscle cells. In addition, presence of atherosclerotic plaques might be correlated to fibrotic lesions in CAV. These findings provide new insights into a possible role for the donor in the development of neo-intima fibrosis in CAV, however, this is still under debate.

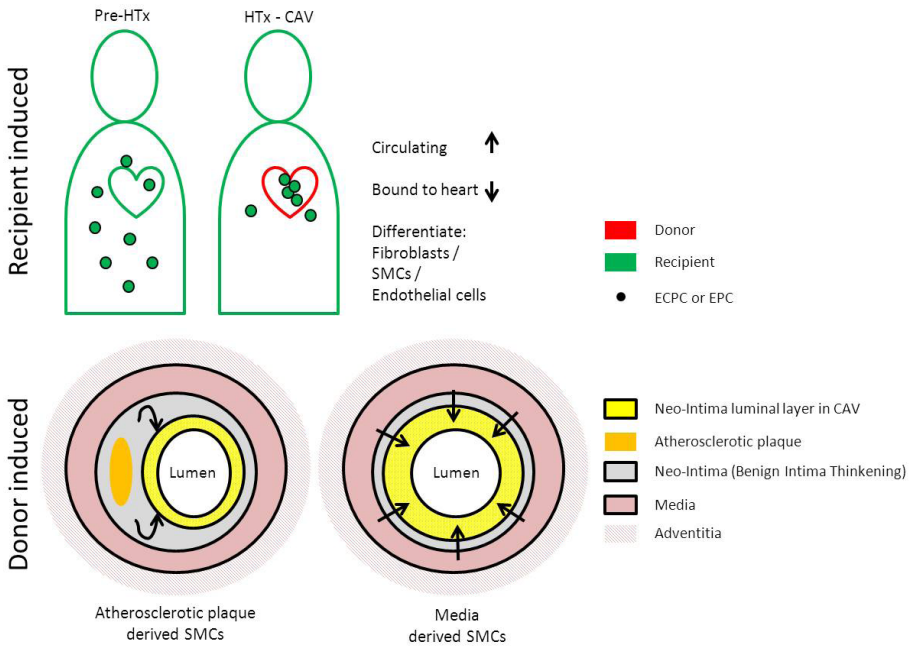

Figure 3. Role of recipient and donor-derived cells in concentric narrowing and fibrosis of the coronary artery. **A**. recipient-derived circulating cells, such as EPCs and ECPCs, contribute to concentric narrowing and fibrosis of the coronary arteries. Increased accumulation of circulating cells bound to the vessel wall induces differentiation of these cells towards fibroblasts, SMCs and endothelial cells, which enhances concentric narrowing of the coronary arteries. **B**. Donor-derived cells, such as SMCs, are migrating from atherosclerotic lesions or the media layer towards the neo-intima. Accumulation of donor-derived SMCs and production of ECM will lead to the expansion of the neo-intima resulting in narrowing and fibrosis of the coronary artery.

Interventions

Activation of the immune system of the recipient, for example by contact of donor- and recipient cells, should be avoided. Ideally, when transplanting a solid organ, there is no transfer of donor immune cells to trigger an immune response. In the future this might be achieved by, for instance, *ex vivo* perfusion of the donor organ, clearing all immune cells from the graft.[80].

Multiple prophylactic approaches have been used to prevent the development of CAV[81]. Modification of risk strategies may slow the progression of CAV[82], including the prevention of CMV infection and endothelial damage caused by the immune response in general. Environmental infection of CMV after transplantation can activate immune cells of donor and recipient[33]. However, most likely, this would not have an effect on the long-term fibrotic response.

Currently used therapeutic interventions, such as statins, angiotensin converting enzyme (ACE) inhibitors and immunosuppressive medications are not always successful in the treatment of CAV[81]. These therapies are not specifically developed for CAV, but are developed for cardiovascular diseases in general. Therefore, it is most likely that they do not specifically inhibit the immune- and fibrotic processes in CAV. The most advanced therapy is the use of proliferation inhibitors, a new class of immunosuppressants, such as everolimus and sirolimus[83]. These are able to reduce intimal thickening in CAV by inhibiting cell proliferation[84]. In CAV, proliferation of immune cells and SMCs is described, which would suggest that these proliferation inhibitors are effective as long proliferation of these cells would occur. These proliferation inhibitors already showed promising results in preliminary studies, however, remain not implicated in most clinical centers[85].

Conclusions

CAV is the leading cause of death after heart transplantation, although the pathogenesis is not fully elucidated[1]. Until recently, CAV has been considered to be induced by either a recipient-derived immune response or a donor-derived immune response[5]. However, more evidence point to the possibility of a dual action of both donor and recipient. By comparing both sides of the story, more knowledge about the pathogenesis of CAV will be obtained (see **table 1** for summary of presented findings).

In conclusion, CAV is a complex disease with an unrevealed pathogenesis. Presumably, CAV is not induced by only donor or only recipient. Based on current research, it is clear that both donor and recipient cells are involved[9,37,38]. It appears the immune system of the recipient is the most important player in the development of CAV, since immune activation of the recipient initiates allograft immune responses, which ultimately leads to vascular damage[10]. Also without the interference of donor-derived immune cells, CAV can probably develop. Donor immune cells, derived from the transplanted heart, are able to enhance the immune response of the recipient, but it seems that they are not able to induce CAV independently. Most likely, there is some kind of synergic interaction between recipient and donor cells, which accelerates the pathogenesis of CAV. More research is needed to fully identify the dual interaction of both donor and recipient cells, since some studies were using only animal experiments or experimental CAV. It would be interesting to investigate whether

the outcomes of animal studies are consistent in human CAV samples. The outcomes based on previous experimental models should in the future be extrapolated to the human transplant recipient to elucidate the potential enhancing role of donor cells in the pathogenesis of CAV.

Table 1. Summary based on recent findings of interacting cells derived from both donor and recipient in the pathogenesis of CAV.

Cardiac allograft vasculopathy: Immune response

Recipient-derived immune response	**Donor-derived immune response**
Alloimmune response [1] direct pathway [2] indirect pathway [3] semi-direct pathway alloantibodies MICA	*Alloimmune response* donor DCs donor CD4+ T-lymphocytes donor-derived selectin expression donor-derived PD-L1 expression
Auto-immune response autoantibodies	

Cardiac allograft vasculopathy: Fibrosis

Recipient-derived circulating cells	**Donor-derived cells**
Circulating cells T-lymphocytes macrophages type-2 fibroblasts	*Donor cells* smooth muscle cells myofibroblasts
Progenitor cells endothelial progenitor cells extra-cardiac progenitor cells	*Mesenchymal transitions* Endothelial > mesenchymal cells Epicardial > mesenchymal cells
	Presence of donor-derived atherosclerotic plaques

Acknowledgements

We would like to thank Frederieke van den Akker for proofreading of the manuscript.

References

1. Behrendt, D., Ganz, P. & Fang, J. Cardiac allograft vasculopathy. *Curr. Opin. Cardiol.* **78229**, 10–16 (2000).
2. Lund, L. H. et al. The Registry of the International Society for Heart and Lung Transplantation: Thirtieth Official Adult Heart Transplant Report--2013; focus theme: age. *J. Heart Lung Transplant.* **32**, 951–64 (2013).
3. Seki, A. & Fishbein, M. C. Predicting the development of cardiac allograft vasculopathy. *Cardiovasc. Pathol.* (2014). doi:10.1016/j.carpath.2014.05.001
4. Suzuki, J., Ogawa, M., Hirata, Y., Nagai, R. & Isobe, M. Effects of immunoglobulin to prevent coronary allograft vasculopathy in heart transplantation. *Expert Opin. Ther. Targets* **16**, 783–9 (2012).
5. Costello, J. Mechanisms of chronic cardiac allograft rejection. *Texas Hear. Inst. ...* **40**, 395–399 (2013).
6. Kobashigawa, J. What is the optimal prophylaxis for treatment of cardiac allograft vasculopathy? *Curr. Control. Trials Cardiovasc. Med.* **1**, 166–171 (2000).
7. Daly, K. P. et al. VEGF-C, VEGF-A and related angiogenesis factors as biomarkers of allograft vasculopathy in cardiac transplant recipients. *J. Heart Lung Transplant.* **32**, 120–8 (2013).
8. Lu, W. et al. Diverse morphologic manifestations of cardiac allograft vasculopathy: a pathologic study of 64 allograft hearts. *J. Heart Lung Transplant.* **30**, 1044–50 (2011).
9. Pober, J. S., Jane-Wit, D., Qin, L. & Tellides, G. Interacting Mechanisms in the Pathogenesis of Cardiac Allograft Vasculopathy. Arterioscler. *Thromb. Vasc. Biol.* 1609–1614 (2014). doi:10.1161/ ATVBAHA.114.302818
10. Mitchell, R. N. Graft vascular disease: immune response meets the vessel wall. *Annu. Rev. Pathol.* **4**, 19–47 (2009).
11. Safa Kalache, Rajani Dinavahi, Sean Pinney, Anita Mehrotra, Madeleine W Cunningham, P. S. H. Anti-cardiac myosin immunity and chronic allograft vasculopathy in heart transplant recipients. *J. Immunol.* **187**, 1023–1030 (2011).
12. Huibers, M. M. H. et al. Distinct phenotypes of cardiac allograft vasculopathy after heart transplantation: A histopathological study. *Atherosclerosis* **236**, 353–359 (2014).
13. Atkinson, C. et al. Neointimal smooth muscle cells in human cardiac allograft coronary artery vasculopathy are of donor origin. *J. Heart Lung Transplant.* **23**, 427–35 (2004).
14. Ueta, H. et al. Systemic transmigration of allosensitizing donor dendritic cells to host secondary lymphoid organs after rat liver transplantation. *Hepatology* **47,** 1352–62 (2008).
15. Benatti, R. D. & Taylor, D. O. Evolving concepts and treatment strategies for cardiac allograft vasculopathy. *Curr. Treat. Options Cardiovasc. Med.* **16**, 278 (2014).
16. Simper, D. et al. Endothelial progenitor cells are decreased in blood of cardiac allograft patients with vasculopathy and endothelial cells of noncardiac origin are enriched in transplant atherosclerosis. *Circulation* **108**, 143–9 (2003).
17. Borthwick, L. a et al. Epithelial to mesenchymal transition (EMT) and airway remodelling after human lung transplantation. *Thorax* **64**, 770–7 (2009).
18. Eisen, H. Heart Transplantation: Graft Rejection Basics. *John Hopkins Adv. Stud. Med.* **8**, 174–181 (2008).
19. Colvin-Adams, M., Harcourt, N. & Duprez, D. Endothelial dysfunction and cardiac allograft vasculopathy. *J. Cardiovasc. Transl. Res.* **6**, 263–77 (2013).
20. Smyth, L. a. et al. The Relative Efficiency of Acquisition of MHC:Peptide Complexes and Cross-Presentation Depends on Dendritic Cell Type. *J. Immunol.* **181**, 3212–3220 (2008).
21. Dolan, B. P., Gibbs, K. D. & Ostrand-Rosenberg, S. Tumor-Specific CD4+ T Cells Are Activated by "Cross-Dressed" Dendritic Cells Presenting Peptide-MHC Class II Complexes Acquired from Cell-Based Cancer Vaccines. *J. Immunol.* **176**, 1447–1455 (2006).
22. Jones, N. D. et al. T-cell activation, proliferation, and memory after cardiac transplantation in vivo. *Ann. Surg.* **229**, 570–8 (1999).
23. Zhang, Q., Cecka, J., Gjertson, D. & Ge, P. HLA and MICA: targets of antibody-mediated rejection in heart *transplantation. ...* **91**, 1153–1158 (2011).
24. Angaswamy, N. et al. Interplay between immune responses to HLA and non-HLA self-antigens in allograft rejection. *Hum. Immunol.* **74**, 1478–85 (2013).
25. Nath, D., Basha, H. & Mohanakumar, T. Anti-human leukocyte antigen antibody induced autoimmunity: role in chronic rejection. *Curr. Opin. organ ...* **15**, 16–20 (2010).
26. Hachem, R. R. Lung allograft rejection: diagnosis and management. *Curr. Opin. Organ Transplant.* **14**, 477–82 (2009).
27. Gilles Benichou, Alessandro Alessandrini, Rachida-Sihem Charrad, D. S. W. Induction of autoimmunity after allotransplantation. *Front. Biosci.* **12**, 4362–4369 (2007).
28. Rolls, H. K. et al. T-cell response to cardiac myosin persists in the absence of an alloimmune response in recipients with chronic cardiac allograft rejection. *Transplantation* **74**, 1053–7 (2002).
29. Weiss, M. J., Madsen, J. C., Rosengard, B. R. & Allan, J. S. Mechanisms of chronic rejection in cardiothoracic transplantation. *Front. Biosci.* **13**, 2980–8 (2008).
30. Fedoseyeva, E. V. et al. Modulation of Tissue-Specific Immune Response to Cardiac Myosin Can Prolong Survival of Allogeneic Heart Transplants. *J. Immunol.* **169**, 1168–1174 (2002).
31. Nath, D., Angaswamy, N. & Basha, H. With And Precede Antibodies To MICA In Antibody Mediated Rejection And Cardiac

Allograft Vasculopathy Following Human Cardiac Transplantation. *Hum. ...* **71**, 1191–1196 (2010).
32. Bij, W. Van Der & Speich, R. Management of Cytomegalovirus Infection and Disease after Solid-Organ Transplantation. *Clin. Infect. Dis.* **33**, s32–s37 (2001).
33. Potena, L. & Valantine, H. a. Cytomegalovirus-associated allograft rejection in heart transplant patients. *Curr. Opin. Infect. Dis.* **20**, 425–31 (2007).
34. Izawa, A. et al. Importance of donor- and recipient-derived selectins in cardiac allograft rejection. *J. Am. Soc. Nephrol.* **18**, 2929–36 (2007).
35. Saiki, T., Ezaki, T. & Ogawa, M. In vivo roles of donor and host dendritic cells in allogeneic immune response: cluster formation with host proliferating T cells. *J. Leukoc. ...* **69**, 705–712 (2001).
36. Ueno, T. et al. Divergent role of donor dendritic cells in rejection versus tolerance of allografts. *J. Am. Soc. Nephrol.* **20**, 535–44 (2009).
37. Win, T. S. et al. Donor CD4 T cells contribute to cardiac allograft vasculopathy by providing help for autoantibody production. *Circ. Heart Fail.* **2**, 361–9 (2009).
38. Larsen, C., Morris, P. & Austyn, J. Migration of dendritic leukocytes from cardiac allografts into host spleens. A novel pathway for initiation of rejection. *J. Exp. ...* **171**, 307–314 (1990).
39. Starzl, T., Murase, N., Ildstad, S. & Ricordi, C. Cell migration, chimerism, and graft acceptance. *Lancet* **339**, 1579–1582 (1992).
40. Yang, J. et al. Critical role of donor tissue expression of programmed death ligand-1 in regulating cardiac allograft rejection and vasculopathy. *Circulation* **117**, 660–9 (2008).
41. Tanaka, K. et al. PDL1 Is Required for Peripheral Transplantation Tolerance and Protection from Chronic Allograft Rejection. *J. Immunol.* **179**, 5204–5210 (2007).
42. Koskinen, P. K. & Lemstro, K. B. Adhesion Molecule P-Selectin and Vascular Cell Adhesion Molecule–1 in Enhanced Heart Allograft Arteriosclerosis in the Rat. *Circulation* **95**, 191–196 (1997).
43. Shreeniwas, R. Adhesion molecules (E-selectin and ICAM-1) in pulmonary allograft rejection. *CHEST ...* **110**, 1143–1149 (1996).
44. Sarraj, B. et al. Impaired selectin-dependent leukocyte recruitment induces T-cell exhaustion and prevents chronic allograft vasculopathy and rejection. *Proc. Natl. Acad. Sci. U. S. A.* (2014). doi:10.1073/pnas.1303676111
45. Khush, K. K., Kubo, J. T. & Desai, M. Influence of donor and recipient sex mismatch on heart transplant outcomes: analysis of the International Society for Heart and Lung Transplantation Registry. *J. Heart Lung Transplant.* **31**, 459–66 (2012).
46. Schlechta, B. et al. Impact of gender mismatch on the outcome of heart transplantation. *Transplant. Proc.* **31**, 3340–2 (1999).
47. Mehra, M. R. Crossing the vasculopathy bridge from morphology to therapy: a single center experience. *J. Heart Lung Transplant.* **19**, 522–8 (2000).
48. Reed RM, Netzer G, Hunsicker L, Mitchell BD, Rajagopal K, Scharf S, E. M. Cardiac Size and Sex-Matching in Heart Transplantation: Size Matters in Matters of Sex and the Heart. *Am. Coll. Cardiol. Found. Hear. Fail.* **2**, 73–83 (2014).
49. Zeier, M. The Effect of Donor Gender on Graft Survival. *J. Am. Soc. Nephrol.* **13**, 2570–2576 (2002).
50. Welp, H. et al. Sex mismatch in heart transplantation is associated with increased number of severe rejection episodes and shorter long-term survival. *Transplant. Proc.* **41**, 2579–84 (2009).
51. Tan, J., Wadia, P. & Coram, M. HY antibody development associates with acute rejection in female patients with male kidney transplants. *Transplantation* **86**, 75–81 (2008).
52. Huibers, M. et al. Intimal fibrosis in human cardiac allograft vasculopathy. *Transpl. Immunol.* **25**, 124–32 (2011).
53. Rahmani, M., Cruz, R. P., Granville, D. J. & McManus, B. M. Allograft vasculopathy versus atherosclerosis. *Circ. Res.* **99**, 801–15 (2006).
54. Zeng, Q. et al. B cells mediate chronic allograft rejection independently of antibody production. *J. ...* (2014). doi:10.1172/JCI70084DS1
55. Koning, E. de et al. 237: M2 macrophages: Keyplayers in the fibro-proliferative response in cardiac allograft vasculopathy. *J. Hear. Lung Transplant.* **26**, S145 (2007).
56. Kitchens, W. H. et al. Macrophage depletion suppresses cardiac allograft vasculopathy in mice. *Am. J. Transplant* **7**, 2675–82 (2007).
57. Mantovani, A. et al. The chemokine system in diverse forms of macrophage activation and polarization. *Trends Immunol.* **25**, 677–86 (2004).
58. Quaini, F. & Urbanek, K. Chimerism of the transplanted heart. *... Engl. J. ...* **346**, 5–15 (2002).
59. Hillebrands, J.-L., Onuta, G. & Rozing, J. Role of progenitor cells in transplant arteriosclerosis. T*rends Cardiovasc. Med.* **15**, 1–8 (2005).
60. Hillebrands, J.-L., Klatter, F. a & Rozing, J. Origin of vascular smooth muscle cells and the role of circulating stem cells in transplant arteriosclerosis. *Arterioscler. Thromb. Vasc. Biol.* **23**, 380–7 (2003).
61. D'Alessandro, D. a et al. Progenitor cells from the explanted heart generate immunocompatible myocardium within the transplanted donor heart. *Circ. Res.* **105**, 1128–40 (2009).
62. Hill, J. & Zalos, G. Circulating endothelial progenitor cells, vascular function, and cardiovascular risk. *... Engl. J. ...* **348**, 593–600 (2003).
63. Sathya, C. J. et al. Correlation between circulating endothelial progenitor cell function and allograft rejection in heart transplant patients. *Transpl. Int.* **23**, 641–8 (2010).

64. Minami, E., Laflamme, M. a, Saffitz, J. E. & Murry, C. E. Extracardiac progenitor cells repopulate most major cell types in the transplanted human heart. *Circulation* **112**, 2951–8 (2005).
65. Wu, G. D. et al. Migration of mesenchymal stem cells to heart allografts during chronic rejection. *Transplantation* **75**, 679–85 (2003).
66. Bittmann, I. et al. Cellular chimerism of the lung after transplantation. An interphase cytogenetic study. *Am. J. Clin. Pathol.* **115**, 525–33 (2001).
67. De Weger, R. a et al. Stem cell-derived cardiomyocytes after bone marrow and heart transplantation. *Bone Marrow Transplant.* **41**, 563–9 (2008).
68. Wu, G. D. et al. Evidence for recipient derived fibroblast recruitment and activation during the development of chronic cardiac allograft rejection. *Transplantation* **76**, 609–14 (2003).
69. Pichler, M., Rainer, P. P., Schauer, S. & Hoefler, G. Cardiac fibrosis in human transplanted hearts is mainly driven by cells of intracardiac origin. *J. Am. Coll. Cardiol.* **59**, 1008–16 (2012).
70. Salomon, R. & Hughes, C. Human coronary transplantation-associated arteriosclerosis. Evidence for a chronic immune reaction to activated graft endothelial cells. *Am. J. ...* **4**, 791–798 (1991).
71. Chen, P., Qin, L., Barnes, C., Charisse, K. & Yi, T. FGF Regulates TGF-β Signaling and Endothelial-to-Mesenchymal Transition via Control of let-7 miRNA Expression. *Cell Rep.* **2**, 1684–1696 (2012).
72. Kovacic, J. C., Mercader, N., Torres, M., Boehm, M. & Fuster, V. Epithelial-to-mesenchymal and endothelial-to-mesenchymal transition: from cardiovascular development to disease. *Circulation* **125**, 1795–808 (2012).
73. Gise, A. von & Pu, W. Endocardial and epicardial epithelial to mesenchymal transitions in heart development and disease. *Circ. Res.* **110**, 1628–1645 (2012).
74. Piera-Velazquez, S. & Jimenez, S. a. Molecular mechanisms of endothelial to mesenchymal cell transition (EndoMT) in experimentally induced fibrotic diseases. *Fibrogenesis Tissue Repair* **5**, S7 (2012).
75. Vongwiwatana, A., Tasanarong, A., Rayner, D. C., Melk, A. & Halloran, P. F. Epithelial to mesenchymal transition during late deterioration of human kidney transplants: the role of tubular cells in fibrogenesis. *Am. J. Transplant* **5**, 1367–74 (2005).
76. Zeisberg, E. M. et al. Endothelial-to-mesenchymal transition contributes to cardiac fibrosis. *Nat. Med.* **13**, 952–61 (2007).
77. Zhou, B. & Pu, W. T. Epicardial epithelial-to-mesenchymal transition in injured heart. *J. Cell. Mol. Med.* **15**, 2781–3 (2011).
78. Chen, S., Cheng, A. & Mehta, K. A review of telemedicine business models. *Telemed. J. E. Health.* **19**, 287–97 (2013).
79. Hernandez, J. M. D. L. T. et al. Virtual histology intravascular ultrasound assessment of cardiac allograft vasculopathy from 1 to 20 years after heart transplantation. *J. Heart Lung Transplant.* **28**, 156–62 (2009).
80. Machuca, T. N. & Cypel, M. Ex vivo lung perfusion. *J. Thorac. Dis.* **6**, 1054–62 (2014).
81. S.-S. Wang. Treatment and Prophylaxis of Cardiac Allograft Vasculopathy. *Transplant. Proc.* **40**, 2609–2610 (2008).
82. Valantine, H. Cardiac allograft vasculopathy after heart transplantation: risk factors and management. *J. Heart Lung Transplant.* **23**, S187–93 (2004).
83. Segovia, J., Gómez-Bueno, M. & Alonso-Pulpón, L. Treatment of allograft vasculopathy in heart transplantation. *Expert Opin. Pharmacother.* **7**, 2369–83 (2006).
84. Delgado, J. F. et al. The use of proliferation signal inhibitors in the prevention and treatment of allograft vasculopathy in heart transplantation. *Transplant. Rev.* **23**, 69–79 (2009).
85. Kobashigawa, J. et al. Everolimus for the Prevention of Allograft Rejection and Vasculopathy in Cardiac- Transplant Recipients. *N. Engl. J. Med.* **349**, 847–858 (2003).

Chapter 7.

HUMANIZED MOUSE MODELS IN TRANSPLANTATION RESEARCH

M.C.H. Hogenes MD, M.M.H. Huibers MSc*, C. Kroone MSc, R.A. de Weger PhD*

**Authors contributed equally to the work.*

Published
Transplantation Reviews. 28(3):103-110 (2014).

Abstract

The interest in the use of humanized mouse models for research topics like Graft versus Host Disease (GvHD), allograft studies and other studies to the human immune system is growing. The design of these models is still improving and enables even more complicated studies to these topics. For researchers it can be difficult to choose the best option from the current pool of available models. The decision will depend on which hypothesis needs to be tested, in which field of interest, and therefore 'the best model' will differ for one to another.

In this review, we provide a guide to the most common available humanized mouse models, with regards to different mouse strains, transplantation material, transplantation techniques, pre- and post-conditioning and references to advantages and disadvantages. Also, an evaluation of experiences with humanized mouse models in studies on GvHD and allograft rejection is provided.

Introduction

In many studies on human immunity and cancer, there is a growing interest for the use of (small sized) humanized animal models. The benefit is that one can test parameters of human cells directly and theoretically the results do not have to be translated from another (donor) species. However, the formation of a xeno-transplantation-situation can make the interpretation of results difficult, as it is not known whether the human cells will behave exactly the same as in a human recipient.

Although 'the perfect' mouse strain to study the human immune system is still to be found, the current available strains do give the opportunity to study parts of the human immune system in a set context. Many of these strains come with disadvantages, which might severely hamper their suitability for specific studies.

This review provides an overview of the most common currently available strains of immune compromised or -deficient mice, an outline of the human material transplants and transplantation techniques, including their benefits and restrictions with a summarizing flow chart (**Figure 1**). We will guide researchers along the most well-known humanized mouse models, to enable them to make a suitable choice for their studies in graft versus host disease and/or allograft (transplant) rejection.

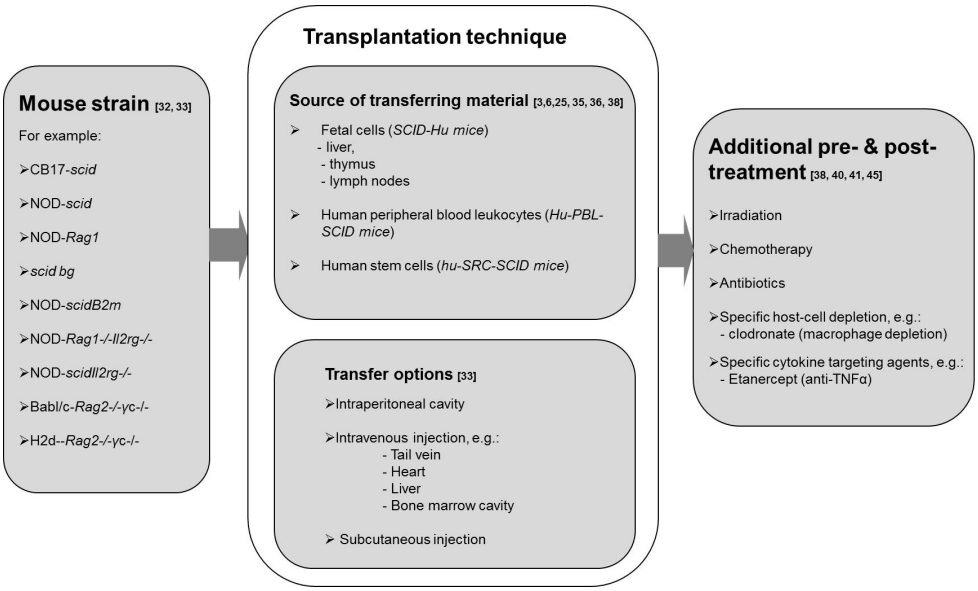

Figure 1. Flowchart for designing a humanized mouse model. This flow charts shows an easy overview of usable murine strains, sources and transfer techniques and possible pre- and post-treatment options that might be used to design a humanized mouse model for either GvHD or allograft rejection research, including references.

7

Mouse strains

One of the first gene-mutations found resulting in severe combined immunodeficiency in mice was the Prkdc^{scid} mutation in a CB17-mouse strain. These mice have a loss-of-function mutation of the Prkdc gene. This gene encodes the catalytic subunit of a DNA dependent protein kinase with a role in resolving the DNA double strand breaks that occur during V(D)J recombination. In the absence of V(D)J recombination, the T cell receptor (TCR) gene in T cells and the immunoglobulin (Ig) gene in B cells are not expressed. This Prkdc^{scid} mutation made it impossible for these mice to produce mature T- and B-cells with functional surface receptors [1,2], but first reports often showed only low level engraftment when introducing human cells in these mice [3-5]. Human T-cells became anergic and/or xenospecific selection of the T-cell repertoire occurred [3,6,7]. The CB17-scid mice also showed leakiness of T- and B-cells. Some improvement was achieved with the use of γ-irradiation [8,9] destroying almost all murine stem- and haematopoietic cells, but the scid mutation results in an overall defect in DNA repair and causes more radiation sensitivity. A second injection of human cells a few days after the initial injection and chemical macrophage depletion has been suggested to improve engraftment [10-12]. Nevertheless, the most fundamental approach to improve human cell engraftment and to overcome still existing innate immunity has been the alteration of strain background and addition of mutations.

Balb/*c-scid* bg and CB57BL/6*J-scid* bg mice both contain the Prkdc^{scid} as well as a mutation in lysosome trafficking regulator (Lyst^{bg}). This resulted in strains with no B- or T-cells, neutropenia/granulocyte defects and decreased NK-cell activity. The Balb/*c-scid*

bg was also radiosensitive [13,14]. However, leakiness remained a problem in these *scid bg* strains. None-obese diabetic (NOD) mice with scid mutation (Prkdc^{scid}) showed an altered antigen expression, imperfect myeloid lineage production, lack of complement and low NK cell activity, with better engraftment levels of human cells compared to the CB17-*scid*. This strain has been crossed further to become NOD/LtSz-*scid*, which remained diabetes-free and has often been abbreviated as NOD-*scid* in literature. The NOD-*scid* mice were highly radiosensitive [8,15,16]. Although these NOD-*scid* mice are still known as the 'golden standard' for xeno-transplantation studies, leakiness limit their usage and 70% of these mice develop thymic lymphomas, severely decreasing their life span [15,17]. A knock-out of β2-microglobuline in NOD-*scid* mice (NOD-*scid*-*B2m*$^{-/-}$) showed an improved engraftment rate compared to the usual NOD-scid mice. In these mice homozygosity for the *B2m*$^{-/-}$ allele resulted in the absence of MHC class I expression and thereby loss of NK cell activity [18]. Unfortunately, the NOD-scid-*B2m*$^{-/-}$ mice developed lymphomas even faster compared to previously described strains [18] and mice with *B2m*$^{-/-}$ were prone to develop haemachromatosis [19].

Introduction of a *Rag1* or *Rag2* mutation in NOD-*scid* mice solved the leakiness-problem, but engraftment levels in these Rag-mice remained low [5,20,21] and problems with development of lymphomas, as described in earlier models with NOD-*scid*, persisted [17,22]. Mice with a knockout of either *Rag1* or *Rag2* have a very similar phenotype to scid-knockout mice in the immune system (elimination of T and B cells), but they do not have the side effect of radiation sensitivity. Combining a *Rag* mutation on a NOD strain background only (NOD-*Rag1*$^{-/-}$) had an engraftment rate comparable to NOD-*scid* mice with better survival rates [22]. Rag mice however were more resistant to radiation than NOD-*scid* [8,22] and needed additional conditioning to attenuate their innate immunity before injecting human cells [5]. In addition, NOD-*Rag*$^{-/-}$ mice still showed late onset of lymphomas like follicular centre cell and thymic lymphomas [22].

Introduction of mutations in the common cytokine receptor y-chain led to more essential improvements. The interleukin 2 receptor gamma (IL-2Rγ) is responsible for correct signal transmission within the αβγ-complex of interleukins. A complete null mutation of this *Il2rg* fully eliminates the possibility to signal through the y-chain [23] and impairs NK cell development [24]. The generation of NOD-*scid*-*Il2rg*$^{-/-}$ mice created a model with high engraftment levels without development of thymic lymphomas [23,25]. Knock-outs with either a truncated *Il2rg*$^{-/-}$ (NOG-mice) or null mutation of this gene (NSG-mice) are known. NSG mice were more efficiently engrafted than NOG mice which indicates that the presence of the extracellular domain of IL2Rγ-chain in NOG mice might negatively affect human cell engraftment [26]. The combination of both NOD and *Il2rg* mutation also made the mice less prone to 'leakiness' [27]. Combining a NOD-*Rag1*$^{-/-}$ mouse with *Il2rg*$^{-/-}$ provided a model (NRG-mice) comparable to NOD-*scid*-*Il2rg*$^{-/-}$. However, NRG-mice do not have the same sensitivity to DNA damage as NSG-mice do. This makes it a suitable model in any application that requires high doses of radiation [28]. The H2^{d}-*Rag2*$^{-/-}$*Il2rg*$^{-/-}$ mice (also referred to as *Rag2*$^{-/-}$γ*c*$^{-/-}$ mice) had no T and B-cells and no NK cells. These mice showed neither leakiness nor thymic lymphoma development; even though they were not based on the more commonly used CB17-scid or NOD-*scid* background [29]. Their main benefit was the possibility to introduce human cells intravenously, while maintaining high engraftment levels. This reduced the amount of human cells that needed to be injected for response considerably, compared to other strains.

Although strains for humanized mouse models were greatly improved in the past, the perfect strain still remains to be found. Recent studies with HLA transgenic mice show

promising results to generate new models with high engraftment rates and prolonged survival [30,31].

Table 1 shows an overview of mutations in the common strains mentioned above, including phenotype, known limitations, reconstitution materials and known usage for either GvHD or allograft studies. A detailed overview of the advantages and disadvantages of most of these strains has also recently been reviewed by Shultz et al [32,33].

Table 1. Overview of common humanized mouse strains, phenotype, limitations, known use and reconstitution material.

Mouse comon name	Mutation(s)	Phenotype	Limitations	Known study subjects	Known reconstitution	Reference
CB17-*scid*	*Prkdc*^{scid}	No mature T-cell No mature B-cell Radiosensitive	Low level engraftment of human cells Anergic human T-cells Xenospecific selection T-cell repertoire Leakiness of T- and B-cells Enhanced innate immune system	Acute GvHD Allograft studies	Surgical implantation or intravenous injection of human fetal thymus, liver, lymphnode and spleen tissue Human bone marrow transplant with additional EPO, hu-MGFor PIXY321 Intraperitoneal injection of huPBL Human fetal lung tissue transplant	3-7, 46, 76
NOD-*scid*	*Prkdc*^{scid}	No mature T-cells No mature B-cells Radiosensitive Decreased innate immunity Decreased NK-cell activity Defective macrophages	Leakiness of T- and B-cells Thymic lymphoma development Better engraftment when injected in bone marrow compared to intravenous injection	Possible GvHD (not further specified)	Intra peritoneal injection of huPBL (with or without antiCD122) Intravenous injection of human T lymphoblastoid cells Intrafemoral injection of huCD34+ cord blood cells	5, 7, 15, 16, 26, 43
NOD-*Rag1*	*Rag1*	No mature T-cells No mature B-cells Radiation resistant	Low and/or variable engraftment of human cells Late onset lymphoma development Might need additional conditioning to attenuate innate immunity		Intra peritoneal injection of huPBL	5, 17, 22
NOD-*Rag2*	*Rag2*	No mature T-cells No mature B-cells Radiation resistant	Low and/or variable engraftment of human cells (especially after i.p. injection) Late onset lymphoma development Might need additional conditioning		Human thyroid tissue transplant Intra peritoneal injection of huPBL	20, 21
Balb/*c-scid bg*	*Prkdc*^{scid} *Lyst*^{bg}	No mature T-cells No mature B-cells Neutropenia Decreased NK activity Radiosensitive	Leakiness Low level engraftment of human cells	Allograft studies	Intravenous injection of thymocytes Human internal mammary artery graft (with or without intra peritoneal huPBL injection)	13-15, 52, 66, 67, 69
NOD-*scid B2m*$^{-/-}$	*Prkdc*^{scid} β2-microglobuline	No mature T-cells No mature B-cells Lack of MHC class I expression Low NK cell function Radiation sensitive	Rapid lymphoma development haemochromatosis	Acute GvHD	intravenous injection of human T (blastoid) cells	18, 44, 48

NRG (NOD-*Rag1*$^{-/-}$ *IL2rg*$^{-/-}$)	*RAG1* *Il2rg*	No mature T-cells No mature B-cells Impared NK cell development Radioresistant	Comparable to NOD-*scid IL2rg*$^{-/-}$)	GvHD (not further specified)	Intravenous injection of huPBL	28, 30
NSG (NOD-*Rag1*$^{-/-}$ *IL2rg*$^{-/-}$)	*Prkdc*^{scid} *Il2rg (null mutation)*	No mature T-cells No mature B-cells Impared NK cell development Radioresistant	Higher engraftment levels of human cells in newborns compared to adults Xenospecific selection of human T-cells might occur However: high engraftment without irradiation is possible	Acute GvHD Sclerotic chronic GvHD	Intravenous injection of huCD34+ cord blood cells Intrafemoral injection of huCD34+ cord blood cells Intravenous injection of huPBL	23, 25, 26, 45, 50, 43
NOG (NOD-*scid* *IL2rg*$^{-/-}$)	*Prkdc*^{scid} *Il2rg (truncated)*	No mature T-cells No mature B-cells Impared NK cell development	Less efficient engraftment of human cells compared to NSG mice	GvHD (not further specified) Allograft studies	Intrafemoral injection of huCD34+ cord blood cells Human liver transplantation	24, 26, 43, 74
(Balb/c or H2d) *Rag2*$^{-/-}$ *yc*$^{-/-}$	*Rag2 Il2rg*	No mature T-cells No mature B-cells No NK-cells Radioresistant	Additional conditioning might be necessary Variable human cell engraftment has been described More constant model for allograft studies	Sclerotic chronic GvHD Allograft studies	Intravenous injection of huCD34+ fetal liver cells (with or without human thymus transplant) Intravenous injection of huPBL Human internal mammary artery with intra peritoneal huPBL injection Human internal mammary artery branch with intravenous human CD25-CD4+ T-cells	29, 32, 40, 51, 59, 61, 68

Reconstitution

Material choice

In the development of a humanized mouse model an adequate source should be chosen to create an actual immune system in the immunodeficient animals. So far, a few sources to repopulate these mice are known: (1) fetal cells, (2) human peripheral blood leukocytes, (3) human stem cells, and (4) induced pluripotent stem cells (iPSCs).

The first technique consists of transplanting human fetal liver cells, human fetal thymus and human fetal lymph nodes and was first developed in *scid*-mice. The fetal liver holds all the progenitors for myelomonocytic, erythroid and lymphoid lineages. As the cells are obtained early in fetal stage, the T-cells are not yet committed to self and non-self recognition. This results in donor human T-cells which fail to provoke a graft versus host (GvH) response. The fetal thymus is necessary to induce central tolerance for immature human T-cells. Finally, the addition of fetal human lymph nodes promotes human B-cell development. These so called SCID-Hu mice have human $CD4^+$ and $CD8^+$ T-cells and their circulation contains human IgG. However, usage of this model requires high surgical skills [3].

The second technique uses injection of human Peripheral Blood Leukocytes (huPBLs) and is much easier. The level of engraftment appears to be higher compared to the SCID-Hu model [34]. Injection of PBLs ip in *scid*-mice resulted in a transfer of various cell types, including human haematopoietic stem cells (HSCs) and mature T and B-cells. These cells are able to generate a functional immune response [6]. Due to the mature portion of immune cells injected, this model provides a fast way to study the human immune system *in vivo* [28].

The third technique includes injecting of human HSCs. Sources for human HSCs are umbilical cord blood (UCB), bone marrow, cytokine-mobilized peripheral blood, or fetal liver [25]. Known examples of this technique are injection of early haematopoetic stem cells (CD34+) of huUCB in the liver of *Rag2*$^{-/-}$*yc*$^{-/-}$ [35], injecting human UCB cells via the facial vein into sub-lethally irradiated NOD-*scid Il2rg*$^{-/-}$ new-born mice [23] and NOD-*scid Il2rg*$^{-/-}$ mice injected with cytokine-mobilized peripheral blood stem cells [25,36].

In addition, Nakauchi H et al. has recently reported that *in vitro* generation of hematopoietic stem cells from induced pluripotent stem cells has the potential to provide a novel approach for developing humanized mice [37].

Transfer options

The transfer route of the human cells into the mice is a critical determinant for establishing a suitable humanized mouse model [34]. A widely used method is injection of human cells into the peritoneal cavity. Other options are intravenous injection in tail vein, heart or liver. Less commonly, injection in the bone marrow cavity has been applied. When SCID mice were injected in the peritoneal cavity with human PBLs, cells could be detected in that area for minimally 3 weeks. In other organs, cells were detected after one month, predominantly T-cells (96-100%, $CD4^+$ or $CD8^+$), with a peak between one and two months. The amount of cells declined at five months [6]. Mainly spleen and bone marrow, and to a lesser extent lung

and liver, were infiltrated, but too many cells in these organs causes (un)desired illness e.g. graft versus host disease.

T-cells appeared to be an important cell type to create an immune system *in vivo*. However, accessory cells were necessary. When injected solely, T-cells could not populate *scid*-mice. This indicates that human accessory cells, like dendritic cells and macrophages, present in the PBL mixture play an important role in immune activation [5]. This was also indicated by injection of PBLs intravenously (i.v.). Apparently, it is harder to get proper bystander help from accessory cells to activate T-cells when injecting i.v. [6]. Comparable to the i.v. route via the tail vein in adult animals is the intravenous method via the cardiac route in new-born animals [38]. Intracardiac injection of huHSCs in newborn *Il2rg*$^{-/-}$ mice showed more efficient engraftment than injection via the same route in adult mice [39].

Bearing the importance of accessory cells in mind some other routes of injection have been studied but are less frequently used, like an intrahepatic injection route in conditioned newborn *Rag2*$^{-/-}$*yc*$^{-/-}$ mice with CD34^{+} human cord blood cells [35] and direct delivery of huHSCs into the bone marrow cavity of the femur [26].

Pre- and post-treatment options

Pre- or post-treatment of the mice might be added. Known basic pre-treatment regiments include radiation (for example total body irradiation), chemotherapy or a mix of both. Other pre-treatment options are targeting the remaining murine cells or introduced donor derived cells, e.g. the depletion of macrophages with clodronate-containing liposomes [40], additional EPO, human mast cell growth factor (hu-MGF), PIXY321 (a fusion protein of IL-3 and GM-CSF) or anti-CD122 mAb for NK cell depletion [4,5]. Nevozhay et al [41] provided an overview of some protocols, including irradiation protocols with known effective doses in different murine models based on currently described protocols [38]. Post-treatment options include e.g. antibiotics, to prevent infections or other medication to prevent GvH reaction.

Applications

Graft-versus-Host disease

Humanized mouse models can serve as excellent models for Graft-verus Host disease (GvHD) related research, especially when focussing on treatment with e.g. specific cell-targeting medication to reduce the GvHD.

GvHD is a major complication occurring after allogeneic bone marrow transplantation (BMT) or donor lymphocyte infusions in immunodeficient recipients that may lead to severe morbidity or even death. Since the 'perfect model' to study the complete GvH responses remains lacking, knowledge of the exact pathogenesis of GvH responses still relies on picking the right model for the right experiments. General considerations important for selecting a proper model for GvHD research from the current pool of immunodeficient strains have well been outlined earlier by Schoeder *et al* [42]. One of the benefits of an humanized mouse model is the possibility to differentiate between host- or donor related reactions, e.g. by differentiating between species specific cytokines or cells.

Due to different kinetics, the distinction between acute and chronic GvHD (aGvHD and cGvHD respectively) in mice cannot be based on time. Differentiation between acute and chronic GvH relies on comparison of the symptoms and morphological aspects to the human GvH equivalent. For chronic GvHD, one can differentiate between a sclerotic and an auto-antibody mediated variant. In mice the differentiation between aGvHD and cGvHD is primarily made on the predominant T-cell subset (Th1 in acute GvH and Th2 in chronic GvH), specific cytokine production (e.g. TGF-alpha, IL1 in aGvHD or TGF-beta in cGvHD) and/or the presence of for example auto-antibody production and/or systemic fibrosis [42].

Humanized mouse models known to be used in GvH research are NOG [43], NOD-*scid* [43], NOD-*scid-B2m*$^{-/-}$ [44], NOD-*scid Il2rg*$^{-/-}$ [45] and the *Rag2*$^{-/-}$*yc*$^{-/-}$ mice [40]. Although many of the earlier discussed humanized mouse models have been presented with an analysis of the specific cell subtype in the human infiltrate, less effort was often made to differentiate them as a specific model for aGvHD or sclerotic versus auto-antibody mediated cGvHD.

For aGvHD the CB17-scid with i.p. huPBL injection has been suggested. In this model the similarity to the huGvHD equivalent was based on the production of macrophages migration inhibitory factor (MIF) [46], although the suggestion of MIF to relate to acute huGvHD has been made on a mouse-mouse based model [47]. NOD-*scid Il2rg*$^{-/-}$ was suggested as a model for aGvHD as well, based on the presented delaying effects of etanercept (an anti-TNFα agent) on the onset of the GvHD symptoms in this model [45]. Intravenous injection is possible in these mice, in which a small number of huPBL's is efficient to induce GvHD and total body irradiation was not always necessary[43]. Furthermore, the NOD-*scid-B2m*$^{-/-}$ model injected with human T-cells could be considered a model for aGvHD and is one of the few models with a specified scoring system for the occurring acute reaction [44,48].

The auto-antibody mediated variant of chronic GvHD is not common in humanized mouse models, since humanized mouse models usually lack the ability to produce (autoreactive and other) T-cells due to the lack of thymic tissue. More often, humanized mouse models with auto-antibody production have been used to study other auto-immune diseases like SLE [49]. *Rag2*$^{-/-}$*yc*$^{-/-}$ injected with huPBL from a donor suffering from SLE or huPBL injection in CB17-

scid or CB57BL/6J-*Il2rg*$^{-/-}$ mice after human thyroid engraftment [21] have been used to study human auto-immune thyroiditis, both containing auto-reactive antibodies from the donor.

For sclerotic cGvHD the NOD-*scid Il2rg*$^{-/-}$ and the *Rag2*$^{-/-}$*yc*$^{-/-}$ have been used previously [40,50]. The morphologic changes are best known for the *Rag2*$^{-/-}$*yc*$^{-/-}$ mice [51].

In general, in a humanized model for GvHD research the choice of material-transfer will influence the developing GvH response; injection of huPBLs is said to represent a more acute GvHD model (even though sclerotic cGvHD could be achieved using appropriate conditions), whereas the transplantation of bone marrow, thymus and liver represents a more chronic model [50,51]. The rate and severity of the reaction will depend on several items. Mice injected with HSCs depleted of human T-cells showed less GvHD development [38]. Also, SCID and NOD-*scid* mice usually showed low engraftment, whereas models incorporating other mutations, sometimes combined with extra preconditioning, lead to higher engraftment levels of human cells and therefore more GvH response [40,45]. NOD-*scid Il2rg*$^{-/-}$ mice showed high levels of engraftment even with low amounts of huPBL injection i.v. and *Rag2*$^{-/-}$γ*c*$^{-/-}$mice injected intravenously with huPBL also produced a stable model with development of systemic GvHD symptoms. In virtually all mice the morphology and rate of the GvHD symptoms could be influenced with macrophage-depletion as preconditioning. Macrophage depleted mice developed severe, more acute symptoms and non-macrophages-depleted mice showed a slower development of a more sclerotic GvH response [40].

Keep in mind that although high engraftment levels in your model comes with more intense clinical GvHD symptoms [5], the symptoms might not correlate with the human GvHD phenotype. It is only proof that the injection of human cells in an immunodeficient mouse induces a GvH reaction. With the difficulties in translation of the induced GvH reaction in a comparable acute and chronic equivalent of human GvHD, the use of histology, cytokine analysis and infiltration analysis remains essential in every GvHD study using a humanized model.

Host-versus-Graft Disease (allograft rejection)

Solid organ transplantation often suffers rejection of the donor organ by the host, known as a 'host versus graft' response (HvG) or allograft rejection. Despite immunosuppressive medication, rejection remains a problem that restricts long term success of graft survival [52,53]. One aim of immunologists in transplantation research is realizing graft survival without chronic immunosuppression [54,55]. To achieve this goal humanized mouse models can be used in experimental studies, to analyse the underlying mechanisms of rejection and to evaluate several reagents, because of closer resemblance to the human immune system than other models. For example in allograft vasculopathy; mouse-mouse/rat-rat transplantation models provided a different mechanism with influx of smooth muscle cells [56-58] compared to the humanized mouse models which showed influx of mononuclear cells [59-61]. Non-humanized models give us insight in the process, but do not mimic the human immune response as humanized mouse models do.

The immunodeficient mice described before, tolerated allogeneic grafts (from a different mouse of the same species) and even xenogeneic grafts (different species) [3] and allowed engraftment of human immune cells. Together, these properties made them suitable models for HvG rejection research. A recent review by Brehm and Shultz described the

historical perspective of humanized mice in allograft rejection studies [62]. They discussed skin and islet allografts in detail [63-65] and to a lesser extent other allografts. This paragraph will focus on rejection studies of solid organ transplantation, but also vessel rejection studies shall be included.

One of the first 'humanized' mouse models used for transplantation studies was the SCID/bg (Balb/c-*scid* bg) mouse, with pig epicardial coronary arteries inserted into the murine infrarenal aorta [66]. Also human arteries have been successfully transplanted [67]. When mice transplanted with human arteries were also engrafted with huPBLs from an allogeneic donor an immune response against the arterial graft occurs *in vivo*. This model made it possible to study aspects of post-transplant graft arteriosclerosis with close resemblance to human graft arteriosclerosis [52]. When comparing the *Rag2*$^{-/-}$*y*$_c^{-/-}$ model to the well-established SCID/bg model for vascular allograft rejection, *Rag2*$^{-/-}$*y*$_c^{-/-}$ mice were advantageous on both engraftment of human artery as well as engraftment of huPBLs. These mice did not become leaky, as they do not involve the SCID mutation. *Rag2*$^{-/-}$*y*$_c^{-/-}$ mice provided a more constant model, with only some discrete intima changes preceding the huPBL injection compared to SCID/bg [59,61,68]. However, a limitation of the hu-PBL-SCID model is that from all injected human cells only T-cells and a few B-cells survive.

For studying macrophages in allograft rejection a new model was introduced. HSCs were isolated from adult human peripheral blood enriched for CD34$^+$. Two strains (NOD-*scid Il2rg*$^{-/-}$ and SCID/bg mice) have been compared for their ability to support human skin, artery and HSC engraftment. SCID/bg animals were advantageous over NOD-*scid Il2rg*$^{-/-}$ for the engraftment of human skin and artery, but engraftment levels of HSCs were higher for NOD-*scid Il2rg*$^{-/-}$. This was disappointing, because a proper working model needs all engraftments on a relative high level to show human macrophages inside skin or artery. Creating a model in which both macrophages and T-cells can be transferred, lead to artery engraftment in SCID/bg mice with only HSC injection. The intima of the graft in SCID/bg animals showed proliferation and presence of macrophages, enabling it as a model to study the role of macrophages [69].

Looking at the history of humanized mouse models used in allograft studies, one will notice that most models used for transplantation studies were developed in the field of microbiology and cancer research. Instead of transplanting a human artery one might consider transplanting parts of solid organs. However, this is a whole new field of organ rejection studies since complete solid organs will not fit the size of a mouse. An example of humanized mouse model usage in microbiology research using solid organ tissue is the model constructed for liver research. In this model mouse hepatocytes were replaced by human hepatocytes [70]. This model was used to study hepatitis B [71] and hepatitis C virus [72]. Functional analysis of human liver was assessed within these models in Ncr-Nude mice [73] and NOG mice [74]. Another example is the model from the Crombleholme group in which a human fetal trachea was transplanted on the flank of SCID or SCID/bg mice [75-78]. They showed development of human airway epithelium and submucosal gland [79]. This model is now used to study gene therapy for cystic fibrosis. Rejection in lung transplantation is now studied with mouse models in which a trachea is transplanted from one mouse to another [80]. These models for lung and liver transplantation might eventually be used for transplant rejection studies as well.

Discussion

In the past few decades, a lot of progress has been made on the development of humanized mouse models to study the human immune system in transplantation [33,62].

Despite the major improvements so far to enable both GvHD and allograft rejection studies, lots of improvement maintains necessary, before all transplantation processes and different organs of interest for transplantation (like e.g. human brain, lung, and gut) can be studied within such a model [81].

The pathogenesis of GvHD remains very complex and new insights in the effects of many different cell-subsets and their relations in the development of GvHD are still uncovered. An important issue that still needs to be addressed in humanized mouse models for GvHD is the lack of auto-reactive antibody production by the recipient. Also, extra effort will have to be made to ensure stability of engraftment levels and clinical symptoms in the models. More insight in the morphological comparisons and differences of the humanized models to acute and chronic (sclerotic or auto-antibody induced) huGvHD needs to be obtained. This includes improvement of our knowledge of migrational patterns of donor cells within the murine organs with histopathological studies. We quite often assume that the morphological aspects of the reaction are in line with the severity of the clinical aspects, but when studying huGvHD, proper evaluations of histological severity of the reaction versus actual clinical outcome are quite rare. For evaluation of this aspect in a murine model, grading systems for the morphology of the induced GvH reactions in humanized models are currently scarce.

Within the research field of allograft rejection there are size limitations to study human organs. One cannot transplant a human kidney or lung within a mouse and is therefore limited to little pieces or parts of the organ. Currently, parts of the rejection process (e.g. artery or skin) can be studied and although these are well established models, they are still just little components of the complete rejection pathogenesis. In artery transplantation and huPBL infusion a fierce lymphocytic rejection process is mimicked, but the role of the humoral immune system or chronic fibrotic processes are excluded.

With the newest immune deficient mice, new techniques for engraftment of the human immune system and improvements on transplantation techniques better models will be created. For both clinical transplantation research and GvHD research this is very important, since well-established models will improve our knowledge about the pathogenesis and new therapeutics can be tested. For this reason, it is important that the field of basic science collaborates with clinical scientists and that together they try to overcome rejection difficulties.

When choosing a model for your research, you should strongly focus on the hypothesis you want to test. In this review we outline known phenotypes, limitations and known usage for common strains of humanized mouse models in GvHD and allograft studies (summarized in **Table 1**) and the methods to create these models with regard to reconstitution material and transplantation methods (summarizing the steps to take in **Figure 1**), that will help researchers to choose the right model for their research in either GvHD or allograft studies. From the very beginning you should look for a model that mimics the process you would like to study as close as virtually possible with regards to the current limitations that remain in humanized models. One should realize that using a humanized mouse model mimics the human situation as closely as possible, but still does not include all facets of the human system and is based

on a combination of two different species. However, when the right model is chosen, you are just one step away to contribute to the improvement on current knowledge about allograft rejection and graft versus host rejection.

References

1. Malynn, B.A., et al. The scid defect affects the final step of the immunoglobulin VDJ recombinase mechanism. *Cell* **54**, 453-460 (1988).
2. Schuler, W., et al. Rearrangement of antigen receptor genes is defective in mice with severe combined immune deficiency. *Cell* **46**, 963-972 (1986).
3. McCune, J.M., et al. The SCID-hu mouse: murine model for the analysis of human hematolymphoid differentiation and function. *Science* **241**, 1632-1639 (1988).
4. Lapidot, T., et al. Cytokine stimulation of multilineage hematopoiesis from immature human cells engrafted in SCID mice. *Science* **255**, 1137-1141 (1992).
5. Berney, T., et al. Patterns of engraftment in different strains of immunodeficient mice reconstituted with human peripheral blood lymphocytes. *Transplantation* **72**, 133-140 (2001).
6. Tary-Lehmann, M., Saxon, A. & Lehmann, P.V. The human immune system in hu-PBL-SCID mice. *Immunol Today* **16**, 529-533 (1995).
7. Garcia, S., Dadaglio, G. & Gougeon, M.L. Limits of the human-PBL-SCID mice model: severe restriction of the V beta T-cell repertoire of engrafted human T cells. *Blood* **89**, 329-336 (1997).
8. Greiner, D.L., Hesselton, R.A. & Shultz, L.D. SCID mouse models of human stem cell engraftment. *Stem Cells* **16**, 166-177 (1998).
9. Fulop, G.M. & Phillips, R.A. The scid mutation in mice causes a general defect in DNA repair. *Nature* **347**, 479-482 (1990).
10. Shiroki, R., et al. Human peripheral blood lymphocyte reconstituted severe combined immunodeficient (hu-PBL-SCID) mice. A model for human islet allograft rejection. *Transplantation* **57**, 1555-1562 (1994).
11. Olive, C., Cheung, C. & Falk, M.C. T cell engraftment in lymphoid tissues of human peripheral blood lymphocyte reconstituted SCID mice with or without prior activation of cells. *Immunol Cell Biol* **76**, 520-525 (1998).
12. Shibata, S., et al. Peritoneal macrophages play an important role in eliminating human cells from severe combined immunodeficient mice transplanted with human peripheral blood lymphocytes. *Immunology* **93**, 524-532 (1998).
13. Christianson, S.W., et al. Role of natural killer cells on engraftment of human lymphoid cells and on metastasis of human T-lymphoblastoid leukemia cells in C57BL/6J-scid mice and in C57BL/6J-scid bg mice. *Cell Immunol* **171**, 186-199 (1996).
14. Mosier, D.E., Stell, K.L., Gulizia, R.J., Torbett, B.E. & Gilmore, G.L. Homozygous scid/scid;beige/beige mice have low levels of spontaneous or neonatal T cell-induced B cell generation. *J Exp Med* **177**, 191-194 (1993).
15. Shultz, L.D., et al. Multiple defects in innate and adaptive immunologic function in NOD/LtSz-scid mice. *J Immunol* **154**, 180-191 (1995).
16. Greiner, D.L., et al. Improved engraftment of human spleen cells in NOD/LtSz-scid/scid mice as compared with C.B-17-scid/scid mice. *Am J Pathol* **146**, 888-902 (1995).
17. Prochazka, M., Gaskins, H.R., Shultz, L.D. & Leiter, E.H. The nonobese diabetic scid mouse: model for spontaneous thymomagenesis associated with immunodeficiency. *Proc Natl Acad Sci U S A* **89**, 3290-3294 (1992).
18. Christianson, S.W., et al. Enhanced human CD4+ T cell engraftment in beta2-microglobulin-deficient NOD-scid mice. *J Immunol* **158**, 3578-3586 (1997).
19. de Sousa, M., et al. Iron overload in beta 2-microglobulin-deficient mice. *Immunol Lett* **39**, 105-111 (1994).
20. Steinsvik, T.E., Gaarder, P.I., Aaberge, I.S. & Lovik. Engraftment and humoral immunity in SCID and RAG-2-deficient mice transplanted with human peripheral blood lymphocytes. *Scand J Immunol* **42**, 607-616 (1995).
21. Martin, A., et al. Engraftment of human lymphocytes and thyroid tissue into scid and rag2-deficient mice: absent progression of lymphocytic infiltration. *J Clin Endocrinol Metab* **79**, 716-723 (1994).
22. Shultz, L.D., et al. NOD/LtSz-Rag1null mice: an immunodeficient and radioresistant model for engraftment of human hematolymphoid cells, HIV infection, and adoptive transfer of NOD mouse diabetogenic T cells. *J Immunol* **164**, 2496-2507 (2000).
23. Ishikawa, F., et al. Development of functional human blood and immune systems in NOD/SCID/IL2 receptor {gamma} chain(null) mice. *Blood* **106**, 1565-1573 (2005).
24. Cao, X., et al. Defective lymphoid development in mice lacking expression of the common cytokine receptor gamma chain. *Immunity* **2**, 223-238 (1995).
25. Shultz, L.D., et al. Human lymphoid and myeloid cell development in NOD/LtSz-scid IL2R gamma null mice engrafted with mobilized human hemopoietic stem cells. *J Immunol* **174**, 6477-6489 (2005).
26. McDermott, S.P., Eppert, K., Lechman, E.R., Doedens, M. & Dick, J.E. Comparison of human cord blood engraftment between immunocompromised mouse strains. *Blood* **116**, 193-200 (2010).
27. Katano, I., Ito, R., Eto, T., Aiso, S. & Ito, M. Immunodeficient NOD-scid IL-2Rgamma(null) mice do not display T and B cell leakiness. *Exp Anim* **60**, 181-186 (2011).
28. Pearson, T., et al. Non-obese diabetic-recombination activating gene-1 (NOD-Rag1 null) interleukin (IL)-2 receptor common gamma chain (IL2r gamma null) null mice: a radioresistant model for human lymphohaematopoietic engraftment. *Clin Exp Immunol* **154**, 270-284 (2008).
29. Weijer, K., et al. Intrathymic and extrathymic development of human plasmacytoid dendritic cell precursors in vivo. *Blood* **99**, 2752-2759 (2002).

30. Buchner, S.M., et al. Delayed onset of graft-versus-host disease in immunodeficent human leucocyte antigen-DQ8 transgenic, murine major histocompatibility complex class II-deficient mice repopulated by human peripheral blood mononuclear cells. *Clin Exp Immunol* **173**, 355-364 (2013).
31. Suzuki, M., et al. Induction of human humoral immune responses in a novel HLA-DR-expressing transgenic NOD/Shi-scid/gammacnull mouse. *International immunology* **24**, 243-252 (2012).
32. Shultz, L.D., Ishikawa, F. & Greiner, D.L. Humanized mice in translational biomedical research. *Nat Rev Immunol* **7**, 118-130 (2007).
33. Shultz, L.D., Brehm, M.A., Garcia-Martinez, J.V. & Greiner, D.L. Humanized mice for immune system investigation: progress, promise and challenges. *Nat Rev Immunol* **12**, 786-798 (2012).
34. Mosier, D.E., Gulizia, R.J., Baird, S.M. & Wilson, D.B. Transfer of a functional human immune system to mice with severe combined immunodeficiency. *Nature* **335**, 256-259 (1988).
35. Traggiai, E., et al. Development of a human adaptive immune system in cord blood cell-transplanted mice. *Science* **304**, 104-107 (2004).
36. Lepus, C.M., et al. Comparison of human fetal liver, umbilical cord blood, and adult blood hematopoietic stem cell engraftment in NOD-scid/gammac$^{-/-}$, Balb/c-Rag1$^{-/-}$gammac$^{-/-}$, and C.B-17-scid/bg immunodeficient mice. *Hum Immunol* **70**, 790-802 (2009).
37. Suzuki, N., et al. Generation of engraftable hematopoietic stem cells from induced pluripotent stem cells by way of teratoma formation. *Molecular therapy : the journal of the American Society of Gene Therapy* **21**, 1424-1431 (2013).
38. Pearson, T., Greiner, D.L. & Shultz, L.D. Creation of "humanized" mice to study human immunity. *Curr Protoc Immunol Chapter* **15**, Unit 15 21 (2008).
39. Brehm, M.A., et al. Parameters for establishing humanized mouse models to study human immunity: analysis of human hematopoietic stem cell engraftment in three immunodeficient strains of mice bearing the IL2rgamma(null) mutation. *Clin Immunol* **135**, 84-98 (2010).
40. van Rijn, R.S., et al. A new xenograft model for graft-versus-host disease by intravenous transfer of human peripheral blood mononuclear cells in RAG2$^{-/-}$ gammac$^{-/-}$ double-mutant mice. *Blood* **102**, 2522-2531 (2003).
41. Nevozhay, D. & Opolski, A. Key factors in experimental mouse hematopoietic stem cell transplantation. *Arch Immunol Ther Exp (Warsz)* **54**, 253-269 (2006).
42. Schroeder, M.A. & DiPersio, J.F. Mouse models of graft-versus-host disease: advances and limitations. *Dis Model Mech* **4**, 318-333 (2011).
43. Ito, R., et al. Highly sensitive model for xenogenic GVHD using severe immunodeficient NOG mice. *Transplantation* **87**, 1654-1658 (2009).
44. Nervi, B., et al. Factors affecting human T cell engraftment, trafficking, and associated xenogeneic graft-vs-host disease in NOD/SCID beta2mnull mice. *Exp Hematol* **35**, 1823-1838 (2007).
45. King, M.A., et al. Human peripheral blood leucocyte non-obese diabetic-severe combined immunodeficiency interleukin-2 receptor gamma chain gene mouse model of xenogeneic graft-versus-host-like disease and the role of host major histocompatibility complex. *Clin Exp Immunol* **157**, 104-118 (2009).
46. Chen, X., et al. Prevention of acute graft-versus-host disease in a xenogeneic SCID mouse model by the humanized anti-CD74 antagonistic antibody milatuzumab. *Biol Blood Marrow Transplant* **19**, 28-39 (2013).
47. Toubai, T., et al. Effect of macrophage migration inhibitory factor (MIF) on acute graft-versus-host disease in a murine model of allogeneic stem cell transplantation. *Transpl Immunol* **16**, 117-124 (2006).
48. Krenger, W., et al. Transplantation of polarized type 2 donor T cells reduces mortality caused by experimental graft-versus-host disease. *Transplantation* **62**, 1278-1285 (1996).
49. Andrade, D., et al. Engraftment of peripheral blood mononuclear cells from systemic lupus erythematosus and antiphospholipid syndrome patient donors into BALB-RAG-2-/- IL-2Rgamma-/- mice: a promising model for studying human disease. *Arthritis Rheum* **63**, 2764-2773 (2011).
50. Greenblatt, M.B., et al. Graft versus host disease in the bone marrow, liver and thymus humanized mouse model. *PLoS One* **7**, e44664 (2012).
51. Hogenes, M.C., et al. Histological assessment of the sclerotic graft-versus-host response in the humanized RAG2$^{-/-}$gammac$^{-/-}$ mouse model. *Biol Blood Marrow Transplant* **18**, 1023-1035 (2012).
52. Pober, J.S., et al. Immunopathology of human T cell responses to skin, artery and endothelial cell grafts in the human peripheral blood lymphocyte/severe combined immunodeficient mouse. *Springer Semin Immunopathol* **25**, 167-180 (2003).
53. Stehlik, J., et al. The Registry of the International Society for Heart and Lung Transplantation: 29th official adult heart transplant report--2012. *J Heart Lung Transplant* **31**, 1052-1064 (2012).
54. Auchincloss, H., Jr. & Sachs, D.H. Xenogeneic transplantation. *Annu Rev Immunol* **16**, 433-470 (1998).
55. Waldmann, H. Transplantation tolerance-where do we stand? *Nat Med* **5**, 1245-1248 (1999).
56. Soleimani, B., et al. Smooth muscle cell proliferation but not neointimal formation is dependent on alloantibody in a murine model of intimal hyperplasia. *Clin Exp Immunol* **146**, 509-517 (2006).
57. Mitchell, R.N. Graft vascular disease: immune response meets the vessel wall. *Annu Rev Pathol* **4**, 19-47 (2009).
58. Onuta, G., et al. Development of transplant vasculopathy in aortic allografts correlates with neointimal smooth muscle cell proliferative capacity and fibrocyte frequency. *Atherosclerosis* **209**, 393-402 (2010).

59. Abele-Ohl, S., et al. Rag2-/- gamma-chain-/- mice as hosts for human vessel transplantation and allogeneic human leukocyte reconstitution. *Transpl Immunol* **23**, 59-64 (2010).
60. Lebastchi, A.H., et al. Transforming growth factor beta expression by human vascular cells inhibits interferon gamma production and arterial media injury by alloreactive memory T cells. *Am J Transplant* **11**, 2332-2341 (2011).
61. Nadig, S.N., et al. In vivo prevention of transplant arteriosclerosis by ex vivo-expanded human regulatory T cells. *Nat Med* **16**, 809-813 (2010).
62. Brehm, M.A. & Shultz, L.D. Human allograft rejection in humanized mice: a historical perspective. *Cell Mol Immunol* **9**, 225-231 (2012).
63. Anam, K., et al. Amnion-derived multipotent progenitor cells support allograft tolerance induction. *Am J Transplant* **13**, 1416-1428 (2013).
64. Coluccio, A., et al. Targeted gene addition in human epithelial stem cells by zinc-finger nuclease-mediated homologous recombination. Molecular therapy : the journal of the American Society of Gene *Therapy* **21**, 1695-1704 (2013).
65. Wu, J.M., Thoburn, C.J., Wisell, J., Farmer, E.R. & Hess, A.D. CD20, AIF-1, and TGF-beta in graft-versus-host disease: a study of mRNA expression in histologically matched skin biopsies. *Mod Pathol* **23**, 720-728 (2010).
66. Tellides, G., et al. Interferon-gamma elicits arteriosclerosis in the absence of leukocytes. *Nature* **403**, 207-211 (2000).
67. Lorber, M.I., et al. Human allogeneic vascular rejection after arterial transplantation and peripheral lymphoid reconstitution in severe combined immunodeficient mice. *Transplantation* **67**, 897-903 (1999).
68. Feng, G., et al. Functional regulatory T cells produced by inhibiting cyclic nucleotide phosphodiesterase type 3 prevent allograft rejection. *Sci Transl Med* **3**, 83ra40 (2011).
69. Kirkiles-Smith, N.C., et al. Development of a humanized mouse model to study the role of macrophages in allograft injury. *Transplantation* **87**, 189-197 (2009).
70. Tateno, C., et al. Near completely humanized liver in mice shows human-type metabolic responses to drugs. *Am J Pathol* **165**, 901-912 (2004).
71. Tsuge, M., et al. Infection of human hepatocyte chimeric mouse with genetically engineered hepatitis B virus. *Hepatology* **42**, 1046-1054 (2005).
72. Ohira, M., et al. Adoptive immunotherapy with liver allograft-derived lymphocytes induces anti-HCV activity after liver transplantation in humans and humanized mice. *J Clin Invest* **119**, 3226-3235 (2009).
73. Chen, A.A., et al. Humanized mice with ectopic artificial liver tissues. *Proc Natl Acad Sci U S A* **108**, 11842-11847 (2011).
74. Hasegawa, M., et al. The reconstituted 'humanized liver' in TK-NOG mice is mature and functional. *Biochem Biophys Res Commun* **405**, 405-410 (2011).
75. Goldman, M.J., Yang, Y. & Wilson, J.M. Gene therapy in a xenograft model of cystic fibrosis lung corrects chloride transport more effectively than the sodium defect. *Nat Genet* **9**, 126-131 (1995).
76. Peault, B., et al. Gene transfer to human fetal pulmonary tissue developed in immunodeficient SCID mice. *Hum Gene Ther* **5**, 1131-1137 (1994).
77. Lim, F.Y., et al. Human fetal trachea-SCID mouse xenografts: efficacy of vesicular stomatitis virus-G pseudotyped lentiviral-mediated gene transfer. *J Pediatr Surg* **38**, 834-839 (2003).
78. Keswani, S.G., et al. Pseudotyped AAV vector-mediated gene transfer in a human fetal trachea xenograft model: implications for in utero gene therapy for cystic fibrosis. *PLoS One* **7**, e43633 (2012).
79. Keswani, S.G., et al. Submucosal gland development in the human fetal trachea xenograft model: implications for fetal gene therapy. *J Pediatr Surg* **46**, 33-38 (2011).
80. Wagnetz, D., et al. Rejection of tracheal allograft by intrapulmonary lymphoid neogenesis in the absence of secondary lymphoid organs. *Transplantation* **93**, 1212-1220 (2012).
81. Su, L. Studying human immunology and immunopathology in humanized mice transplanted with human lymphoid tissues and immune cells. *Cell Mol Immunol* **9**, 191-192 (2012).

Chapter 8.

ALTERATIONS IN HUMAN CORONARY ARTERY microRNA PROFILE DURING CARDIAC ALLOGRAFT VASCULOPATHY ARE NOT REFLECTED BY CIRCULATING microRNAS

M.M.H. Huibers MSc [1], H. Vroman MSc [1], B. van Holthe tot Echten BSc [1], J. van Kuik BSc [1], E. Siera-De Koning BSc [1], A.L.M. Peeters BSc [1], A. Vink MD PhD [1], J.R. Lahpor MD PhD [2], N. de Jonge MD PhD [3], and R.A. de Weger PhD [1]

Department of Pathology [1], Cardiothoracic surgery [2], and Cardiology [3], University Medical Center Utrecht, the Netherlands

Manuscript submitted

Abstract

Objective:
After heart transplantation (HTx) coronary arteries are affected by cardiac allograft vasculopathy (CAV). The role of microRNAs (miRs) is not described in CAV. Our aim was to determine miR expression changes in CAV and see whether these are reflected in plasma post-HTx.

Approach and results:
From CAV and control arteries the intimal layer was isolated by laser microdissection. MiR screening in intimal tissue (n=6) was done using arrays (754 miRs) where 8 miRs were selected. Q-PCR assays (n=15) confirmed 5 miRs as significantly up- (miR-21, -223, and -146b-5p) or down-regulated (miR-886-5p and -214). The same procedure for miR screening and validation on first year plasma of HTx patients (n=6) was performed; 1 miR was up-regulated over time (miR-132; n=15). No overlap was detected in the top-8 miRs of intima and plasma analysis. Localization of the 5 tissue-miRs was confirmed by in situ hybridization on CAV arteries (n=20) and localized in either (myo)fibroblast-like or immune cells.

Conclusions:
MiR expression alter both in intima and plasma of CAV patients. However, alterations in the intima are not reflected in plasma. Localization of tissue-miRs suggested a role in immune regulation or fibrosis. If these miRs have a role in CAV development they could be considered potential therapeutic targets.

Introduction

Heart transplantation (HTx) is still the best curative therapy for patients with end stage heart failure. Acute rejection, which severely limited survival in the past, can now largely be prevented by the present immunosuppressive therapy. However, long-term mortality has remained relatively constant in the past two decades, mainly due to cardiac allograft vasculopathy (CAV) as one of the unsolved problems[1]. CAV is characterized by concentric hyperplasia of the neo-intimal layer of coronary arteries. Hyperplasia of the neo-intima is due to infiltration of lymphocytes that induce smooth muscle cell (SMC) proliferation and formation of extra cellular matrix (ECM)[2, 3]. Neo-intima hyperplasia causes diffuse luminal narrowing of the coronary arteries with ensuing cardiac ischemia resulting in congestive heart failure, ventricular arrhythmias and even sudden cardiac death[4].

The International Society for Heart and Lung Transplantation formulated a recommended nomenclature for diagnosis of clinical CAV detected by angiography[5] and recently we described different histological types of CAV[6] which corresponds to findings of others[7]. The clinical diagnosis of CAV is mostly done by angiography[8] although this technique only visualizes the lumen. Intravascular ultrasound is able to visualize different vessel layers and is thereby of greater diagnostic value[9]. It is however, expensive and not able to examine smaller, more distal vessels (where CAV presents first)[10]. Therefore, other options, for the early diagnosis of CAV are sought for[11,12]. Some biomarkers have provided insight in the pathogenesis of CAV but none of these have been introduced as diagnostics[8].

MicroRNAs (miRs) have been described as promising biomarkers[13]. These are small noncoding RNAs (18-22 nucleotides long) that regulate the translation of mRNA into protein. One miR can inhibit the translation of multiple target genes and they are present both in tissue and blood[14]. In the circulation miRs are packed in exosomes or present in a free form in case they originate from apoptotic/necrotic cells. Via the circulation they can exert distant cell to cell signaling[15].

In multiple vascular diseases like atherosclerosis or post-angioplasty restenosis it has been shown that miRs exert important roles in essential processes[16-18]. Previously, a few studies focused on miRs in transplantation, but only in kidney[19,20], small-bowel[21] and liver transplantation[22]. Several up- and/or down-regulated miRs were identified that could influence immune responses involved in rejection after transplantation[23]. Only one study on miRs in plasma of HTx patients is performed, but this included acute rejection samples24. Profiling miR expression in plasma after HTx could give information about the onset and progression of CAV. Besides, miRs could help us to understand the development of CAV and serve as therapeutic targets.

The aim of this study is to determine changes in miR expression in the neo-intima of CAV and see whether these are reflected by circulating miRs that could function as biomarker for CAV development.

Materials and Methods

Patient population

Patients that underwent HTx 1985-2012 were included in this study. Characteristics are summarized in **Table 1**. Selection was based on the availability of plasma samples and coronary arteries (obtained at autopsy). Informed consent of all patients was obtained prior to HTx. The human material used in this study was obtained at explanation or autopsy and followed the code of proper use of human material in the Netherlands. HTx patients were treated with a triple immunosuppressive therapy of cyclosporine/azathioprine/prednisone or tacrolimus/mycophenolate mofetil/prednisone.

Selection of tissue and plasma

CAV development after HTx was determined based on histology of the coronary arteries obtained at autopsy (H-CAV0, 1, 2, or 3[6], **Figure 6**). HTx patients with severe atherosclerotic plaque formation in the coronary vessels were excluded from the study. Experiments were performed according to the workflow depicted in **Figure 1**.

MiR selection in tissue, relevant for CAV was performed on formalin fixed paraffin embedded (FFPE) coronary arteries of 4 HTx patients (H-CAV1 n=1; H-CAV2 n=2; H-CAV3 n=1) and 2 explanted hearts with dilated cardiomyopathy (controls, H-CAV0, n=2). To confirm and validate these results the cohort of coronary arteries was extended to 15 HTx patients (H-CAV1 n=5; H-CAV2 n=5; H-CAV3 n=5) and 5 explanted hearts (controls, H-CAV0 n=5; **Table 1**).

MiR selection in plasma was performed in HTx patients at 6 weeks and 12 months post transplantation and was compared to plasma of healthy controls. At 6-weeks and 12-months two pools both consisting of 3 patients were analyzed. For control plasma two pools consisting of 5 subjects were used. Validation of the selected miRs in individual matched plasma samples was performed using 15 individual HTx patients and 10 healthy individuals. Furthermore, for the plasma analysis, additional time points before and after HTx (pre-HTx, 6-weeks, 3-months, 6-months, and 12-months) were analyzed separately and compared to controls (**Table 1**).

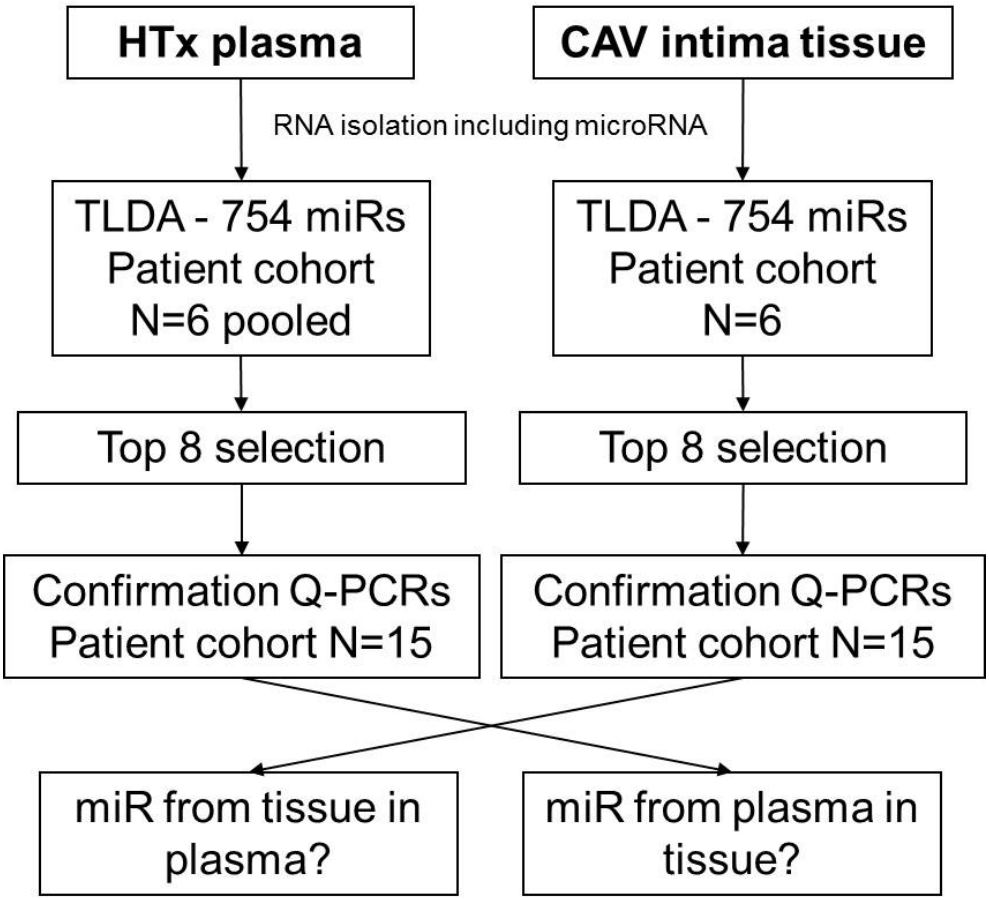

Figure 1. Work flow. This study is executed as two main tracks. First, miRs were screened in tissue and plasma by TLDA (Tissue Low Density Array). Then, from this screening 8 miRs were selected based on Cq-values <32, reliable amplification plots (shape of the curve), and the miR should be detectable in all samples. These selected miRs were confirmed by individual Q-PCR experiments on tissue and plasma samples. To compare both validation cohorts cross analysis was performed.

Table 1. Patient characteristics. * H-CAV=histological CAV type as explained in legends Figure 6, † samples used for miR screening, ‡ plasma samples pooled for miR screening, HTx = heart transplantation, M = male, F = female, CAV = cardiac allograft vasculopathy, MI = myocardial infarction, wk = week, mn = month, X = included in that part of the study

Patient	Gender (M/F)	Age at HTx (years)	Survival post HTx (years)	H-CAV type*	Cause of death	Intima screening †	Intima validation	Plasma screening ‡ (time point / pool nr)	Plasma validation	Locating miRs
HTx 1	M	44	1.6	2	CAV	X	X	6-wk 1		
HTx 2	F	52	0.1	1	Heart failure			6-wk 1		
HTx 3	M	54	0.9	2	Brachycardia		X	6-wk 1		
HTx 4	F	61	1.2	3	Lung infarction			6-wk 2		
HTx 5	F	18	0.3	1	Acute rejection + CAV		X	6-wk 2		X
HTx 6	M	44	0.1	1	Acute rejection + CMV infect.			6-wk 2		
HTx 7	F	40	9.7	3	CAV + atherosclerosis		X	12-mn 1	X	X
HTx 8	M	57	7.0	3	CAV + thrombosis			12-mn 1	X	X
HTx 9	F	15	1.3	2	Ventricle fibrillation			12-mn 1	X	
HTx 10	F	50	7.9	3	Sepsis and heart failure			12-mn 2	X	
HTx 11	M	35	2.5	2	CAV + atherosclerosis			12-mn 2	X	
HTx 12	M	60	6.3	3	Heart + lung failure	X	X	12-mn 2	X	X
HTx 13	M	54	1.4	1	CAV + cellular rejection				X	
HTx 14	F	51	7.0	1	CAV				X	
HTx 15	M	60	13.3	3	MI atherosclerosis		X		X	
HTx 16	M	41	2.6	2	CAV + acute rejection				X	
HTx 17	M	63	1.0	2	CAV + cellular rejection				X	
HTx 18	F	53	10.0	1	Pneumonia	X	X		X	X
HTx 19	M	59	3.9	3	CAV + MI		X		X	
HTx 20	M	38	5.3	2	CAV + MI		X		X	X
HTx 21	F	36	1.9	1	Acute rejection		X		X	X
HTx 22	M	57	7.0	2	Adenocarcinoma	X	X			
HTx 23	M	30	0.0	1	Sepsis		X			
HTx 24	M	55	0.0	1	Sepsis		X			
HTx 25	F	48	2.6	2	CAV		X			X

HTx 27	M	28	0.0	0	Graft failure				X
HTx 28	M	49	0.0	0	Graft failure				X
HTx 29	M	45	0.7	1	Acute rejection				X
HTx 30	M	49	0.9	1	Acute rejection				X
HTx 31	M	58	17.8	3	CAV				X
Explant 1	F	26	-	0	Dilated cardiomyopathy	X	X		X
Explant 2	F	50	-	0	Dilated cardiomyopathy	X	X		X
Explant 3	M	27	-	0	Dilated cardiomyopathy		X		
Explant 4	M	43	-	0	Dilated cardiomyopathy		X		X
Explant 5	F	49	-	0	Dilated cardiomyopathy		X		X
Explant 6	M	16	-	0	Dilated cardiomyopathy				X
Explant 7	F	61	-	0	Dilated cardiomyopathy				X
Explant 8	F	62	-	0	Dilated cardiomyopathy				

RNA isolation

RNA form the neo-intima of CAV arteries was isolated from FFPE tissue sections after laser micro dissection (LMD) using the RNeasy FFPE kit (Qiagen Inc, Valencia, CA). Plasma RNA was isolated using the miRVana™Paris kit (Applied Biosystems/Ambion, Austin, TX, USA). Further details on RNA isolation are described in the supplemental data (RNA isolation).

Screening; Taqman low density array

Reverse transcription of total RNA was performed using the TaqMan® microRNA Reverse Transcription kit and the MegaPlex™ Reverse Transcription Primer Pool set v3.0. Pre-amplification (prior to Q-PCR) was performed using the MegaPlex™ PreAmp Primer Pool Set v3.0 and the TaqMan® PreAmp Master Mix. Reverse transcription and pre-amplification were performed using a 96-well GeneAmp® PCR system 9700. For Q-PCR array analysis, TaqMan® Array Human MicroRNA A+B card sets v3.0 and Taqman® Universal master mix was used. This array analysis measures the expression of 754 different miRs in total. Q-PCR was performed using the ABI PRISM 7900 HT real time PCR sequence detection system. All steps within the Taqman low density array study were executed according to manufacturer's instructions (all Applied Biosystems/Ambion). Thermal cycling included a denaturation step at 95ºC for 10min, followed by 40 cycles of 95ºC for 15sec and 60ºC for 1 min.

Array data was analyzed using SDS 2.4, RQ manager 1.2.1 and Data Assist v3.0 (all Applied Biosystems/Ambion). In RQ manager 1.2.1 multiple arrays were combined and raw data was analyzed on quality of the amplification plots. In Data Assist v3.0 normalization was done using the global normalization method[25]. Within Data Assist v3.0 also selection of an endogenous control target was made for further validation studies. For validation studies 8 miRs were selected from the array analysis; the 4 most up- and the 4 most down regulated miRs. Criteria for selection were: Cq-values <32, reliable amplification plots (shape of the curve), and the miR should be detectable in all samples.

Expression patterns of all detected miRs in plasma and tissue were visualized with Cluster 3.0 (http://bonsai.hgc.jp/~mdehoon/software/cluster/software.htm) and Java Tree View software (http://jtreeview.sourceforge.net/), using average linkage and Spearman rank correlation as an instrument for similarity.

Validation; Taqman assay validation

For validation of the array data, single Q-PCR analysis of the selected miRs was performed. Reverse Transcription was performed using the TaqMan® microRNA Reverse Transcription kit and Q-PCR was done using TaqMan® miRNA assays (**Supplemental Table I**) and TaqMan® Universal Master Mix. PCR reactions were performed on the ViiA™ 7 Real-Time PCR system. All steps within the Taqman assay validation study were executed according to manufacturer's instructions (all Applied Biosystems/Ambion). Thermal cycling conditions consisted of a denaturation step at 95°C for 10min, followed by 40 cycles of 95°C for 15sec and 60°C for 1min. The single miR assays were analyzed using ViiA™ 7 RUO Software (Applied Biosystems/

Ambion). Cq values above 35 were defined as negative. A stable miR from the previously performed array on plasma or tissue was used as reference. The software was used to check the stability of the selected endogenous controls; within one experiment the Cq values of the endogenous control should be within mean +/-2x standard deviation. If this was not the case, this sample was excluded from analysis. Relative Quantity (RQ) values were calculated as follows: $RQ=2^{-\Delta\Delta Cq}$.

In Situ Hybridization

Localization of the tissue microRNAs was visualized by *in situ* hybridization (ISH). ISH was performed using the mercury LNA™ microRNA ISH optimization kit (FFPE) (Exiqon, Vadbaek, Denmark) following the corresponding protocol with some minor modifications (Supplemental data *In Situ* Hybridization).

Statistical Analysis

The normality assumption of variables was tested using a Kolmogorov-Smirnov test. When necessary, a log-transformation was performed to meet the normality assumption. An unpaired T-test was used when two groups were compared (control versus CAV) and one-way analysis of variance (ANOVA) when more groups were compared. Post-hoc tests with Bonferroni correction were done in one-way ANOVA statistics. If one patient was measured at multiple time points (plasma pre and post HTx) a Mixed Model analysis was performed with time as fixed effect (without random effects). Data were analyzed using SPSS version 20.0. P-values <0.05 (two-tailed) were considered statistically significant for all analyses.

Results

Screening of miRs; CAV tissue

On array card A (H-CAV0 n=2; H-CAV1 n=1; H-CAV2 n=2; H-CAV3 n=1) 37 miRs showed expression within all samples. From these miRs the four most up- and down-regulated (8 in total) were selected to test in the validation study (**Figure 2A & Supplemental Table II**, expressed in bold). Besides, from these 37 miRs, the one with reliable amplification plots and most stable Cq-values amongst all samples (lowest standard deviation) was selected as endogenous control which resulted in miR-191 (**Supplemental Table II**). Analysis of array card B on 2 FFPE coronary arteries (1x H-CAV0 and 1x H-CAV3) only showed 17 miRs detected in all samples without significant changes, therefore we only focused on card A.

Screening of miRs; plasma

The correlation between the two plasma pools at each time point (6-weeks, 12-months, or control) was checked, to determine whether it was correct to group these pools and analyze them as one (**Supplemental Table IV**). The pools showed very high correlation coefficients ($r>0.7921$), which confirmed that the two plasma pools showed similar expression patterns. Of the total amount of 377 miRs analyzed on array card A, 110 miRs were detectable in all the groups. Forty miRs remain when only the miRs with a $\log2(RQ)>2$ are taken into account. Only 34 miRs from card B showed expression within all samples, and not more than 12 miRs remain with $\log2(RQ)>2$. Overall expression levels of card B were lower than card A, therefore only card A was used for the miR selection. The 8 miRs that showed the largest change of expression (4 up- and 4 down-regulated) compared to control were selected (**Figure 2B & Supplemental Table V**, expressed in bold). For Q-PCR validation, the miR with the most stable Cq-values among all samples (lowest standard deviation) was chosen as endogenous control (**Supplemental Table III**). For plasma samples this was miR-195.

Cluster analysis

As stated before, from tissue array analysis 37 miRs and from the plasma array analysis 110 miRs were detected in all samples. Clustering of these miRs revealed distinct expression patterns between control and HTx patient plasma (**Supplemental Figure IA**). Control versus CAV vessels clustered less clearly but did show an interesting pattern in which H-CAV0 is clearly separated from H-CAV3 (**Supplemental Figure IB**). The relative expression of each sample is displayed using one of the control samples as reference.

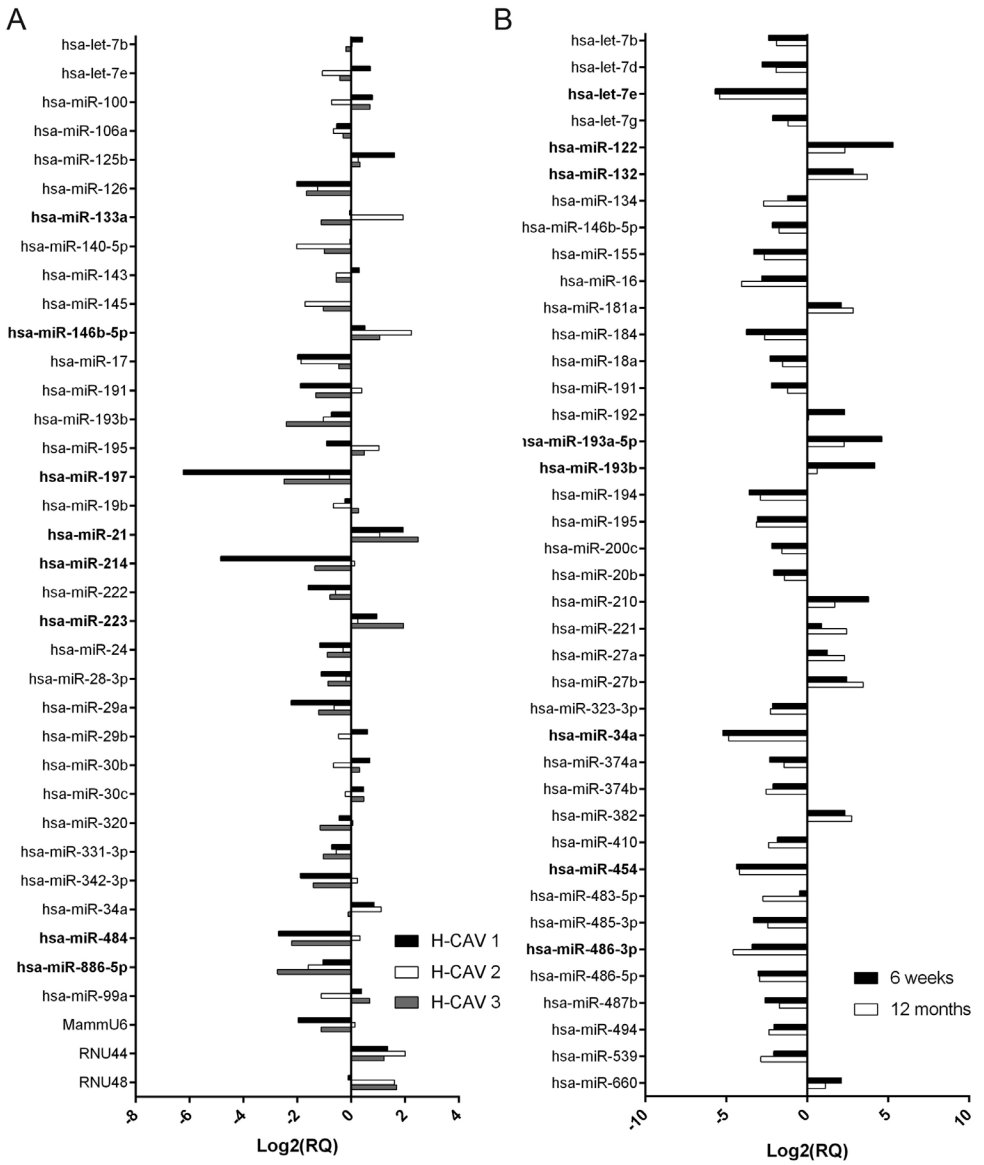

Figure 2. miR expression screening of tissue and plasma. Expression of miRs in samples normalized with global normalization as indicated in the methods section. MiRs selected for validation analysis are displayed in bold. **(A)** Tissue array (n=6): 37 miRs are displayed that were differentially expressed (H-CAV1, 2, 3 compared to H-CAV0 which was used as reference). **(B)** Plasma array (n=6): 34 miRs are displayed that were differentially expressed with a Log2(RQ)>2 (6 weeks and 12 months compared to control which was used as reference). hsa = homo sapiens, miR = microRNA, RQ = relative quantity.

Validation of miRs; CAV tissue

Five (out of eight) selected miRs from the array analysis were confirmed in the validation study. Similar to the array analysis, three miRs showed an up-regulation (miR-146b-5p, -21, and -223) and two a down-regulation (miR-214 and -886-5p) when CAV intima (H-CAV1, 2, and 3 combined) was compared to control intima (**Figure 3A**). The expression pattern of these miRs analyzed in the four separate H-CAV types showed to be significant for miR-146b-5p (p=0.038) and -214 (p=0.001), but not for miR-21 (p=0.054), -223 (p=0.102), and -886-5p (p=0.088) (**Figure 3B**). Analysis of the separate H-CAV types showed little significance due to small sample sizes, but does give an indication of the expression pattern in these different histological appearances of CAV.

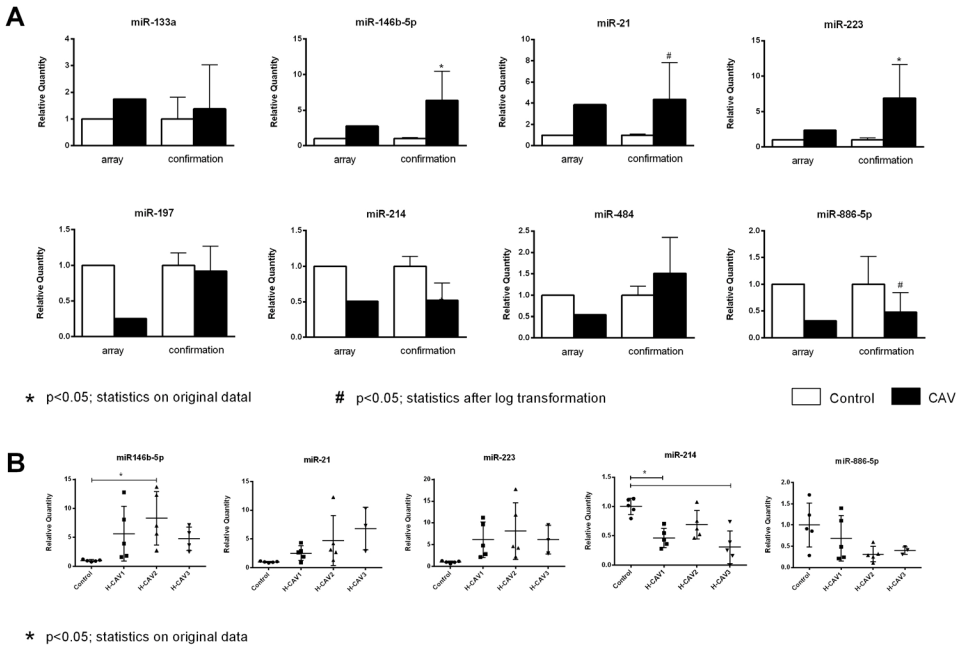

Figure 3. Validation of selected miRs in intimal tissue. All 8 selected miRs showed different expression patterns in array analysis between control intima and CAV intima. **(A)** TLDA results (n=6) are plotted next to the results of the validation study (confirmation, n=20). From the 8 miRs tested, 5 showed the same expression pattern and a significant up- (miR-146b-5p, -21, and -223) or down-regulation (miR-214 in separate H-CAV types and -886-5p) in CAV. **(B)** CAV arteries are separated based on histology, which showed a significant up-regulation for miR-146b-5p in H-CAV2 and a significant down-regulation of miR-214 in H-CAV1 and 3 compared to control. The others miRs did not show significant changes due to small sample size. * p<0.05; statistics on original data.

Validation of miRs; plasma

The top 8 miRs detected in pooled plasma samples by the array analysis were validated by Q-PCR in 15 individual patient samples and compared to 5 controls. Four out of the 8 miRs showed significant changes in Q-PCR validation between control, 6-weeks and 12-months plasma levels. Two miRs showed the same pattern as was found in the array analysis (miR-132 and miR-193a-5p), whereas two others displayed a pattern that was different from that in the array analysis (miR-486-3p and miR-34a) (**Figure 4A**). Verification of these 4 miRs in matched plasma samples taken at various times after HTx showed significant changes over time and/or compared to control (**Figure 4B**); miR-132 (p=0.010), -193a-5p (p=0.006), -486-3p (p=0.005), and -34a (p<0.001). When controls are excluded and a Mixed Model analysis is performed, time has a significant effect on log-transformed miR-132 (p=0.018 quadratic polynomial), miR-486-3p (p=0.003 quadratic polynomial), and miR-34a (p=0.029 quadratic polynomial), but not on miR-193a-5p (p=0.614 linear polynomial). This means that time after HTx has a significant effect on the expression of miR-132, -486-3p, and 34a in plasma.

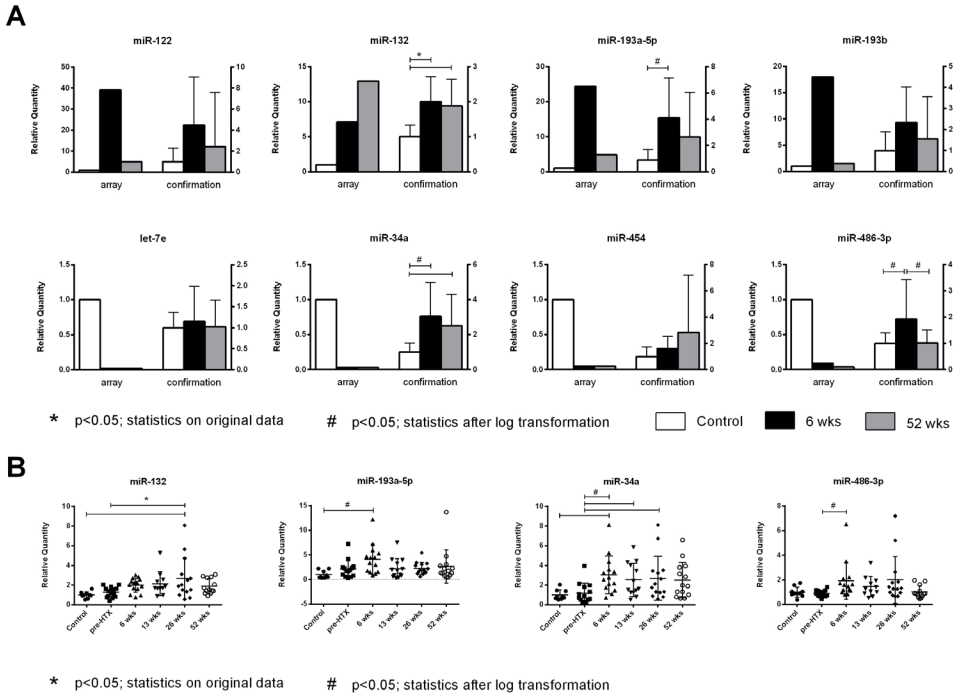

Figure 4. Validation of selected miRs in plasma. Eight miRs showed significant changes in array analysis between control, 6-week and 12 month plasma samples. **(A)** TLDA results (n=6) are plotted next to the results of the validation study (confirmation, n=15). After confirmation, four miRs showed a significant change in plasma (miR-132, -193a-5p, -34a, and -486-3p). **(B)** These four miRs showed significant expression changes over time post transplantation. wks = weeks, * p<0.05; statistics on original data, # p<0.05; statistics on log transformation.

Comparison of tissue and plasma miRs

A cross-analysis was done for two reasons. First, to see whether the miRs that showed changes in the intima of CAV arteries (miR-146b-5p, -21, -214, and -886-5p) could be detected in plasma samples and if they would represent the same expression pattern as seen in tissue. Secondly the cross-analysis was done to study whether the miRs that showed significant changes in plasma (miR-132, -193a-5p, -34a and -486-3p) could also be detected in tissue and if they show the same expression pattern.

All four miRs that revealed significant changes in the CAV lesions could be detected in plasma. Cross-analysis in plasma revealed only miR-21 ($p=0.017$) and -214 ($p<0.001$) to be significantly changing compared to control plasma (**Figure 5A**). MiR-21 was up-regulated in CAV lesions, which corresponds with the plasma findings; it is elevated after transplantation. The CAV lesions expressed less miR-214 than control intima, whereas in plasma after HTx first an up-regulation was found (6 weeks) after which the levels returned to normal. Although miR-146b-5p does show a trend in up-regulation in plasma post HTx ($p=0.048$, also up-regulated in CAV lesions), a post-hoc test did not show specific changes.

In plasma significant changes were detected for miR-132, -193a-5p, -34a and -486-3p. The tissue array data showed that from these four miRs, only miR-132 was detected (**Figure 5B**). For practical reasons three extra miRs were validated which were initially not selected due to previously described criteria (absent signals in some samples or not within top 8 up/down-regulation). Based on absent expression in control and high expression in CAV intima miR-212 and -376c were selected. Finally, miR-125b was chosen because it was the 6th most up-regulated miR from tissue array analysis. Although changes were observed in plasma post-HTx, none of the miRs showed significant changes in CAV lesions.

Locating miRs by *In Situ* Hybridization (ISH)

To localize the expression of the miRs selected from neo-intima tissue, ISH was performed (**Figure 6**). All control probes showed the expected effect; U6 probe was positive in most nuclei and scramble probe showed no positive signal at all. Control (H-CAV0) and two H-CAV types (H-CAV1 and H-CAV3) were selected for their different cellular composition (mononuclear cell infiltrate and fibrosis respectively). Most miRs showed no (miR-21, -223, -146b-5p) or little expression (miR-214, -886-5p) in the intima of healthy coronary arteries. In intima of CAV arteries miR-21 and -214 were detected in elongated spindle shaped-like cells, probably (myo) fibroblasts (especially in H-CAV1). In the fibrotic CAV type (H-CAV3) miR-214 is abundantly present in fibroblast like cells. MiR-223 is mainly expressed in endothelial cells en cells close to endothelial layer. MiR-146b-5p is expressed in specific immune cells within the intima of H-CAV1 and almost not detected in H-CAV3. The fifth miR, miR-886-5p, is present in many (but not all) infiltrating cells within the intimal layer of H-CAV1 and 3, these cells have a large phenotype which might represent macrophages.

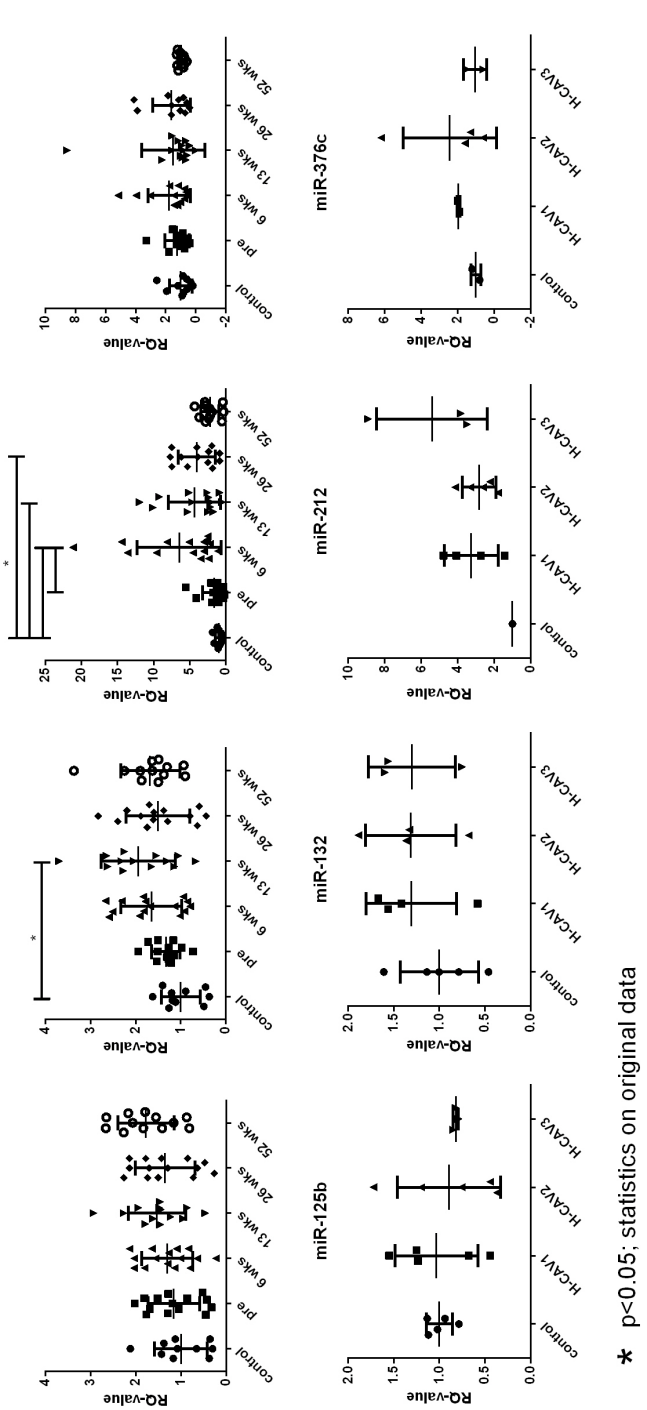

Figure 5. Cross-analysis of miRs from tissue and plasma. (A) Four miRs that were confirmed in CAV intima were analyzed in plasma (n=15) over time post transplantation. Only miR-21 and miR-214 showed changes over time. **(B)** One miR that was confirmed in plasma analysis (miR-132) and three other miRs did not show changes between the histological CAV stages (n=20). wks = weeks, * p<0.05; statistics on original data.

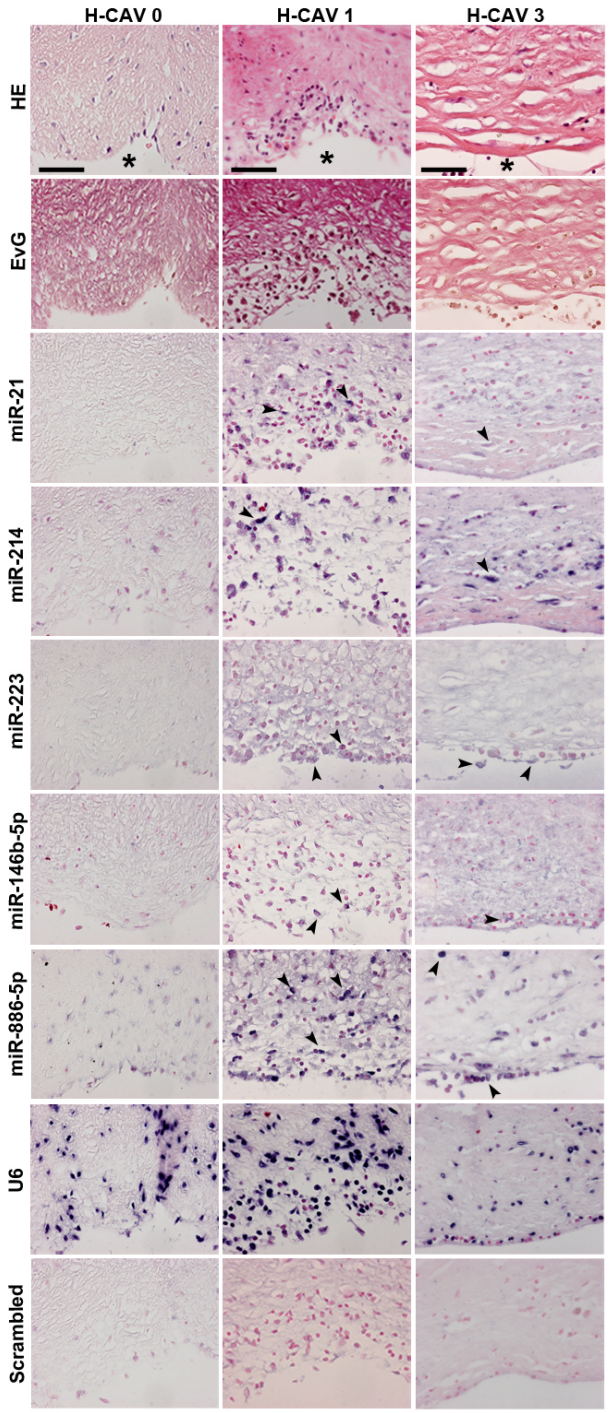

Figure 6. Localization of miRs in CAV arteries with In Situ Hybridization. The histological different CAV types (H-CAV0, 1, and 3) show different expression of the selected miRs in the intimal layer (n=20). Only benign intima thickening (BIT) is observed in H-CAV0(7). In H-CAV1 a layer of loose connective tissue containing mononuclear cells (MNC) is formed on top of the BIT. In H-CAV2 this layer becomes denser and is replaced by smooth muscle cells and less MNCs (not shown). In H-CAV3 this layer is completely fibrotic(6). Every miR shows a different staining pattern amongst the different cell types. Some miRs are mainly expressed in spindle-shaped cells and others predominantly in infiltrated mononuclear cells. Arrowheads indicate positive cells for specific miR probes. Scale bar represents 50μm. * = lumen of vessel, BIT = benign intima thickening, MNC = mononuclear cells, HE = Hematoxilin Eosin, EvG = Elastica von Gieson, H-CAV = Histological CAV stage.

Discussion

To understand the molecular mechanism of CAV development after HTx, microRNA expression within the neo-intima was studied. Not only may this lead to new therapeutic targets for this important medical problem, but it could also result in potential new biomarkers to detect the onset of CAV.

To this goal, first the miR levels were measured in the intima of arteries with CAV and in pooled plasma samples by an array approach. Subsequently, the miRs that showed significant changes in these arrays were validated in single Q-PCR assays in a larger cohort of tissue and matched plasma samples. Both, the plasma and tissue validation did not show 100% concordance with the array findings. This showed that miR arrays should be interpreted carefully, because they may give an over/under estimation. Validation studies are necessary to confirm array results[26]. In our study a higher concordance was reached in validation of miRs from intimal tissue (selected piece of affected tissue by laser micro dissection) compared to plasma (high background signals and influenced by many other organs).

After validation neo-intimal tissue demonstrated 5 (out of 8 miRs from screening) to be significantly different in CAV compared to controls; 3 were up-regulated (miR-146b-5p, -21, and -223) and 2 were down-regulated (miR-214 and -886-5p). The complete function of these miRs is not elucidated yet in vascular disease and transplantation, however we can speculate on their possible role in CAV.

In CAV it is generally accepted that immune responses induce intimal fibrosis[3, 27]. So, miRs involved in either of the two processes might be important. MiR-21 plays a major role in neo-intimal fibrosis of pulmonary arterial hypertension[28, 29] and vein grafts[30]. Also, mechanical injury of large vessels causes neo-intima formation and up-regulation of miR-21 in SMCs, restoration of miR-21 levels prevented restenosis[31]. The latter study demonstrates that miR-21 regulation could be a target for treatment in SMC proliferation and fibrosis. On the other hand, miR-223 is up-regulated in acute renal rejection and shows a positive association with intra-graft CD3 and CD20 mRNA[19]. Besides, it has a role in T-cell differentiation, the innate immune response[32], and macrophage polarization[33]. Also miR-146 is related to the immune system[34], it influences the TLR/IL-1β and TNFα signaling pathway in chronic inflammatory diseases[32, 35]. In transplantation miR-146b-5p (and miR-146a) is up-regulated in acute rejection after small bowel[36] and kidney[19] transplantation and influences the Th1/Th2 shift[36]. MiR-214 and -886-5p are not studied as often as the before mentioned miRs, which does not make their role less important in CAV. MiR-214 protects cardiac ischemic injury by controlling Ca^{2+} overload and cell death[37] and is described to inhibit angiogenesis[38]. Finally, miR-886-5p was in our study, as it was in others[36], considered a miR but is also described as 'vault RNA'[39, 40]. These previous studies on the 5 detected miRs in our study, suggest a role for them either in fibrosis and SMC proliferation, or immune regulation, which are both important processes in CAV development.

In plasma, 8 miRs were selected from the array analysis for validation where 2 showed the same pattern (miR-132 and miR-193a-5p) and 2 a different pattern (miR-486-3p and miR-34a). MiR-193a-5p and -486-3p showed an incline at 6 weeks post-HTx but a decrease thereafter. These changes are possibly due to the surgical procedure, but do not persist and may therefore not be related to chronic processes. The other two, miR-132 and -34a, do alter over time until one-year post transplantation.

MiR-34a is described to regulate aging of the heart and by inhibition of miR-34a cell

death and fibrosis could be reduced[41]. The role of miR-132 has been described in vascular changes as it activates the endothelium to facilitate angiogenesis[42], and therefore helps to repair the heart after myocardial infarction[43]. Besides its role in vascular processes, miR-132 appears to have a role in immunity[44]. These previously described functions of miR-132 and -34a suggest that these miRs might be potential biomarkers for the onset of CAV. To determine if these miRs are in fact CAV related, they were studied in the intima of CAV arteries. MiR-34a was not detected in tissue array analysis and therefore not further investigated. MiR-132 was detected in the neo-intima of CAV arteries but did not show significant changes in comparison to controls. The fact that this miR is confirmed in plasma and changes after transplantation suggests that it is involved in other transplantation related process, and for that it may be an interesting biomarker. Further research for the potential origin may provide more information about the role of this miR in plasma.

As indicated, many of the selected miRs in the present study are possibly involved in the mechanism of CAV, but have not yet been described in all forms of chronic rejection in transplantation of other organs. A study on serum biomarkers for detection of injury after liver transplantation[22] described completely different miRs. Also biomarker research on chronic rejection after kidney transplantation[45] and acute rejection in heart transplantation[24] did not show overlap with our presented miRs. These differences could be caused by the techniques used to detect miRs, the differences of specimen (serum / urine or liver / kidney / heart) and underlying disease processes. Especially, miRs in plasma may be completely different due to the impact of heart or liver transplantation on the total physiology of the patient.

The miRs found in neo-intimal tissue of coronary arteries could be potential therapeutic targets to prevent or slow down the process of CAV. To see what cell types express these five tissue-miRs in situ hybridization was performed. Previous studies and our ISH results suggest two main cell categories that could express these miRs; miR-146b and -223 were mainly detected in immune cells and miR-21, -214, and -886-5p mainly in fibroblasts, smooth muscle, and/or endothelial cells. The type of cells expressing a certain miR did not change as CAV progresses, but because the cellular profile in the arterial wall changes in relation to the different types of CAV, miR expression patterns also change. The localization by ISH confirms that these miRs might play a role in the immunological and/or fibrotic process of CAV. The functional role of these miRs in CAV development has to be determined and should be tested in experimental models to see whether they could serve as therapeutic targets.

In conclusion, miR levels alter in HTx patients both in the intima of CAV arteries and in plasma. This study shows that one should be careful by drawing conclusions from array analysis and stresses the importance of subsequent validation studies. Furthermore, miR expression in the intima is not reflected in the plasma which may question the role as biomarker for the described miRs in CAV. Localization of the tissue miRs underlines their function in immunological and/or fibrotic processes. According to our knowledge this is the first study that shows miR expression changes in CAV patients. The miRs selected from the neo-intimal layer might have a role in CAV development and could be considered potential therapeutic targets in the future.

Study limitations

This study is based on autopsy material and therefore relates to patients with end-stage disease. Furthermore, the patient population is biased by the fact that autopsy is mainly performed on hospitalized patients, which skews our population to time intervals early after transplantation. Therefore, the presented data on miR expression probably cannot be extrapolated to the whole population of patients with CAV but could be indicative for the disease process.

References

1. Stehlik,J. et al. The Registry of the International Society for Heart and Lung Transplantation: 29th official adult heart transplant report--2012. *J. Heart Lung Transplant.* **31**, 1052-1064 (2012).
2. Rahmani,M., Cruz,R.P., Granville,D.J., & McManus,B.M. Allograft vasculopathy versus atherosclerosis. *Circ. Res.* **99**, 801-815 (2006).
3. Huibers,M. et al. Intimal fibrosis in human cardiac allograft vasculopathy. *Transpl. Immunol.* **25**, 124-132 (2011).
4. Weis,M. & von,S.W. Cardiac allograft vasculopathy: a review. *Circulation* **96**, 2069-2077 (1997).
5. Mehra,M.R. et al. International Society for Heart and Lung Transplantation working formulation of a standardized nomenclature for cardiac allograft vasculopathy-2010. *J. Heart Lung Transplant.* **29**, 717-727 (2010).
6. Huibers,M.M. et al. Distinct phenotypes of cardiac allograft vasculopathy after heart transplantation: A histopathological study. *Atherosclerosis* **236**, 353-359 (2014).
7. Devitt,J.J. et al. Impact of donor benign intimal thickening on cardiac allograft vasculopathy. *J. Heart Lung Transplant.* **32**, 454-460 (2013).
8. Colvin-Adams,M. & Agnihotri,A. Cardiac allograft vasculopathy: current knowledge and future direction. *Clin. Transplant.* **25**, 175-184 (2011).
9. Logani,S., Saltzman,H.E., Kurnik,P., Eisen,H.J., & Ledley,G.S. Clinical utility of intravascular ultrasound in the assessment of coronary allograft vasculopathy: a review. *J. Interv. Cardiol.* **24**, 9-14 (2011).
10. Nissen,S.E., Gurley,J.C., Booth,D.C., & DeMaria,A.N. Intravascular ultrasound of the coronary arteries: current applications and future directions. *Am. J. Cardiol.* **69**, 18H-29H (1992).
11. Labarrere,C.A. et al. C-reactive protein, arterial endothelial activation, and development of transplant coronary artery disease: a prospective study. *Lancet* **360**, 1462-1467 (2002).
12. Martinez-Dolz,L. et al. Follow-up study on the utility of von Willebrand factor levels in the diagnosis of cardiac allograft vasculopathy. *J. Heart Lung Transplant.* **27**, 760-766 (2008).
13. Gilad,S. et al. Serum microRNAs are promising novel biomarkers. *PLoS. One.* **3**, e3148 (2008).
14. Garzon,R., Marcucci,G., & Croce,C.M. Targeting microRNAs in cancer: rationale, strategies and challenges. *Nat. Rev. Drug Discov.* **9**, 775-789 (2010).
15. McDonald,J.S., Milosevic,D., Reddi,H.V., Grebe,S.K., & Algeciras-Schimnich,A. Analysis of circulating microRNA: preanalytical and analytical challenges. *Clin. Chem.* **57**, 833-840 (2011).
16. Leptidis,S. et al. A deep sequencing approach to uncover the miRNOME in the human heart. *PLoS. One.* **8**, e57800 (2013).
17. Small,E.M. & Olson,E.N. Pervasive roles of microRNAs in cardiovascular biology. *Nature* **469**, 336-342 (2011).
18. Zhang,C. MicroRNAs in vascular biology and vascular disease. *J. Cardiovasc. Transl. Res.* **3**, 235-240 (2010).
19. Anglicheau,D. et al. MicroRNA expression profiles predictive of human renal allograft status. *Proc. Natl. Acad. Sci. U. S. A* **106**, 5330-5335 (2009).
20. Sui,W. et al. Microarray analysis of MicroRNA expression in acute rejection after renal transplantation. *Transpl. Immunol.* **19**, 81-85 (2008).
21. Sotolongo,B. et al. Gene expression profiling of MicroRNAs in small-bowel transplantation paraffin-embedded mucosal biopsy tissue. *Transplant. Proc.* **42**, 62-65 (2010).
22. Farid,W.R. et al. Hepatocyte-derived microRNAs as serum biomarkers of hepatic injury and rejection after liver transplantation. *Liver Transpl.* **18**, 290-297 (2012).
23. Shan,J. et al. MicroRNAs: potential biomarker in organ transplantation. *Transpl. Immunol.* **24**, 210-215 (2011).
24. Sukma Dewi,I., Torngren,K., Gidlof,O., Kornhall,B., & Ohman,J. Altered serum miRNA profiles during acute rejection after heart transplantation: Potential for non-invasive allograft surveillance. *J. Heart Lung Transplant.* (2013).
25. D'haene,B., Mestdagh,P., Hellemans,J., & Vandesompele,J. miRNA expression profiling: from reference genes to global mean normalization. *Methods Mol. Biol.* **822**, 261-272 (2012).

26. Tijsen,A.J. et al. MiR423-5p as a circulating biomarker for heart failure. *Circ. Res.* **106**, 1035-1039 (2010).
27. van Loosdregt,J. et al. The chemokine and chemokine receptor profile of infiltrating cells in the wall of arteries with cardiac allograft vasculopathy is indicative of a memory T-helper 1 response. *Circulation* **114**, 1599-1607 (2006).
28. Bockmeyer,C.L. et al. Plexiform vasculopathy of severe pulmonary arterial hypertension and microRNA expression. *J. Heart Lung Transplant.* **31**, 764-772 (2012).
29. Caruso,P. et al. Dynamic changes in lung microRNA profiles during the development of pulmonary hypertension due to chronic hypoxia and monocrotaline. *Arterioscler. Thromb. Vasc. Biol.* **30**, 716-723 (2010).
30. McDonald,R.A. et al. miRNA-21 is dysregulated in response to vein grafting in multiple models and genetic ablation in mice attenuates neointima formation. *Eur. Heart J.* (2013).
31. Ji,R. et al. MicroRNA expression signature and antisense-mediated depletion reveal an essential role of MicroRNA in vascular neointimal lesion formation. *Circ. Res.* **100**, 1579-1588 (2007).
32. Sonkoly,E., Stahle,M., & Pivarcsi,A. MicroRNAs and immunity: novel players in the regulation of normal immune function and inflammation. Semin. *Cancer Biol.* **18**, 131-140 (2008).
33. Zhuang,G. et al. A novel regulator of macrophage activation: miR-223 in obesity-associated adipose tissue inflammation. *Circulation* **125**, 2892-2903 (2012).
34. Harris,A., Krams,S.M., & Martinez,O.M. MicroRNAs as immune regulators: implications for transplantation. *Am. J. Transplant.* **10**, 713-719 (2010).
35. Ichii,O. et al. Altered expression of microRNA miR-146a correlates with the development of chronic renal inflammation. Kidney Int. 81, 280-292 (2012).
36. Asaoka,T. et al. MicroRNA signature of intestinal acute cellular rejection in formalin-fixed paraffin-embedded mucosal biopsies. *Am. J. Transplant.* **12**, 458-468 (2012).
37. Aurora,A.B. et al. MicroRNA-214 protects the mouse heart from ischemic injury by controlling Ca(2)(+) overload and cell death. *J. Clin. Invest* **122**, 1222-1232 (2012).
38. van Mil,A. et al. MicroRNA-214 inhibits angiogenesis by targeting Quaking and reducing angiogenic growth factor release. *Cardiovasc. Res.* **93**, 655-665 (2012).
39. Persson,H. et al. The non-coding RNA of the multidrug resistance-linked vault particle encodes multiple regulatory small RNAs. *Nat. Cell Biol.* **11**, 1268-1271 (2009).
40. Stadler,P.F. et al. Evolution of vault RNAs. *Mol. Biol. Evol.* **26**, 1975-1991 (2009).
41. Boon,R.A. et al. MicroRNA-34a regulates cardiac ageing and function. *Nature* **495**, 107-110 (2013).
42. Anand,S. et al. MicroRNA-132-mediated loss of p120RasGAP activates the endothelium to facilitate pathological angiogenesis. *Nat. Med.* **16**, 909-914 (2010).
43. Katare,R. et al. Transplantation of human pericyte progenitor cells improves the repair of infarcted heart through activation of an angiogenic program involving micro-RNA-132. *Circ. Res.* **109**, 894-906 (2011).
44. Lagos,D. et al. miR-132 regulates antiviral innate immunity through suppression of the p300 transcriptional co-activator. *Nat. Cell Biol.* **12**, 513-519 (2010).
45. Scian,M.J. et al. MicroRNA profiles in allograft tissues and paired urines associate with chronic allograft dysfunction with IF/TA. *Am. J. Transplant.* **11**, 2110-2122 (2011).

Supporting information

RNA isolation

MiR expression was first determined using a Q-PCR based Taqman Low Density Array (TLDA) and later validated with single Q-PCRs.

To isolate RNA from CAV lesions in the vessels wall, 5 µm FFPE sections of coronary arteries were placed on 1.0 PEN-membrane slides (Carl Zeiss Micro Imaging, Munich, Germany). The slides were heated for 20 min at 59 °C and deparaffinized in xylene. Slides were then shortly stained with haematoxylin, dehydrated and air dried before use. Using tissue laser micro dissection (LMD) the neo-intima of the coronary arteries ($12*10^6$ μm^2) was dissected using the P.A.L.M MicroBeam System (Carl Zeiss Micro Imaging) and collected in LPC microfuge tubes. Atherosclerotic lesions were avoided. Total RNA isolation was performed using the RNeasy FFPE kit (Qiagen Inc, Valencia, CA). In the screening TLDA study the total yield of RNA was precipitated and used in the sequential megaplex RT reaction. For the validation of the array findings, for each patient at least $12*10^6$ μm^2 of intima tissue was dissected from coronary arteries and RNA was isolated as described above.

For the screening TLDA analysis of plasma, total RNA was extracted from 500 µl of pooled plasma using the miRVana™Paris kit (Applied Biosystems/Ambion, Austin, TX, USA). The total yield of RNA was precipitated and used in the sequential megaplex RT reaction. For the plasma validation study, total RNA was isolated from 500 µl plasma per time point with the miRVana™Paris kit.

In Situ Hybridization

Localization of the tissue microRNAs was visualized by in situ hybridization (ISH). RNAse-free conditions were maintained during all steps throughout the protocol. ISH was performed using the mercury LNA™ microRNA ISH optimization kit (FFPE) (Exiqon, Vadbaek, Denmark) following the corresponding protocol with some minor modifications. In short; FFPE tissue was first deparaffinized in xylene, rehydrated, fixed with 4% formaldehyde for 10 min, re-fixed with Karnovsky for 15 min, treated with 12 µg/ml Proteinase K for 10 min at 37°C, and dehydrated with ethanol. Slides are hybridized in a ThermoBrite (Abbott Molecular, Des Plaines, IL, USA) for 5 h with 3' and 5' Digoxigenin (DIG) LNA modified probes for miR-21 (250nM, 54°C), miR-214 (167nM, 54°C), miR-223 (250nM, 53°C), miR-146b-5p (625nM, 54°C), or miR-886-5p (250nM, 63°C). As controls a scrambled probe (250nM, probes hybridization temp) and U6 probe (250nM, 54°C) was used. Slides were then stringently washed at hybridization temperature with 5x SSC (twice), 1x SSC (twice), 0.2xSSC (twice), and once with 0.2xSSC at room temperature. Then slides were incubated overnight with sheep-anti-DIG-AP antibody (Roche, Mannheim, Germany) diluted 1:800 in 1%BSA and sheep serum. For staining, an NBT/BCIP-tablet (Roche) and levamisol were dissolved in 10 ml aqua dest, this solution was applied to the slides and incubated for 6 h at 30°C. Slides were counterstained with nuclear fast red, dehydrated and mounted with pertex.

Table S I: Selected miRs for assay validation in plasma and tissue. The eight selected miRs for the tissue and plasma with their selected endogenous controls. Alls assay ID numbers correspond to information from Applied Biosystems (Applied Biosystems/Ambion, Austin, TX, USA).

Plasma			Tissue		
Assay name	**Assay ID**	**Target**	**Assay name**	**Assay ID**	**Target**
miR-122	002245	Up-regulated miR	miR-21	000397	Up-regulated miR
miR-132	000457	Up-regulated miR	miR-223	002295	Up-regulated miR
miR-193a-5p	002281	Up-regulated miR	miR-146b-5p	001097	Up-regulated miR
miR-193b	002367	Up-regulated miR	miR-133a	002246	Up-regulated miR
let7e	002406	Down-regulated miR	miR-197	000497	Down-regulated miR
miR-486-3p	002093	Down-regulated miR	miR-886-5p	002193	Down-regulated miR
miR-34a	000426	Down-regulated miR	miR-214	002306	Down-regulated miR
miR-454	002323	Down-regulated miR	miR-484	001821	Down-regulated miR
miR-195	000494	Endogenous control	miR-191	002299	Endogenous control
U6 snRNA	001973	Endogenous control	U6 snRNA	001973	Endogenous control

Table S II: Taqman Low Density Array analysis of tissue. MiR expression in neointima tissue was analyzed by low density array and shows different expression between the H-CAV stages. Form these data 37 miRs on card A and 17 miRs on card B were expressed in all samples. The miRs in bold are selected for further validation studies based on expression levels.

		RQ				log2(RQ)			
	Assay	**H-CAV 0**	**H-CAV 1**	**H-CAV 2**	**H-CAV 3**	**H-CAV 0**	**H-CAV 1**	**H-CAV 2**	**H-CAV 3**
Card A									
	hsa-let-7b	1	1,34	1,02	0,87	0	0,42	0,03	-0,20
	hsa-let-7e	1	1,63	0,48	0,75	0	0,71	-1,07	-0,42
	hsa-miR-100	1	1,74	0,61	1,62	0	0,79	-0,72	0,70
	hsa-miR-106a	1	0,69	0,63	0,81	0	-0,54	-0,66	-0,30
	hsa-miR-125b	1	3,06	1,20	1,26	0	1,61	0,26	0,33
	hsa-miR-126	1	0,25	0,42	0,32	0	-2,02	-1,25	-1,66
	hsa-miR-133a	**1**	**0,96**	**3,81**	**0,46**	**0**	**-0,06**	**1,93**	**-1,11**
	hsa-miR-140-5p	1	0,97	0,25	0,50	0	-0,05	-2,02	-0,99
	hsa-miR-143	1	1,23	0,68	0,68	0	0,30	-0,55	-0,55
	hsa-miR-145	1	1,01	0,31	0,49	0	0,02	-1,71	-1,03
	hsa-miR-146b-5p	**1**	**1,42**	**4,73**	**2,08**	**0**	**0,51**	**2,24**	**1,06**
	hsa-miR-17	1	0,25	0,28	0,72	0	-1,99	-1,86	-0,46
	hsa-miR-191	1	0,27	1,31	0,40	0	-1,88	0,39	-1,31
	hsa-miR-193b	1	0,60	0,48	0,19	0	-0,74	-1,04	-2,41
	hsa-miR-195	1	0,53	2,04	1,40	0	-0,91	1,03	0,49
	hsa-miR-197	**1**	**0,01**	**0,57**	**0,18**	**0**	**-6,23**	**-0,80**	**-2,49**
	hsa-miR-19b	1	0,85	0,63	1,21	0	-0,23	-0,66	0,27
	hsa-miR-21	**1**	**3,81**	**2,09**	**5,63**	**0**	**1,93**	**1,06**	**2,49**
	hsa-miR-214	**1**	**0,04**	**1,10**	**0,39**	**0**	**-4,84**	**0,13**	**-1,35**
	hsa-miR-222	1	0,33	0,67	0,58	0	-1,59	-0,58	-0,79
	hsa-miR-223	**1**	**1,93**	**1,19**	**3,84**	**0**	**0,95**	**0,25**	**1,94**
	hsa-miR-24	1	0,44	0,81	0,54	0	-1,17	-0,30	-0,89
	hsa-miR-28-3p	1	0,46	0,87	0,55	0	-1,11	-0,20	-0,86
	hsa-miR-29a	1	0,21	0,64	0,43	0	-2,23	-0,64	-1,21
	hsa-miR-29b	1	1,51	0,72	1,00	0	0,60	-0,47	0,00
	hsa-miR-30b	1	1,61	0,63	1,24	0	0,69	-0,66	0,31
	hsa-miR-30c	1	1,38	0,86	1,38	0	0,46	-0,22	0,47
	hsa-miR-320	1	0,73	1,04	0,45	0	-0,45	0,06	-1,15
	hsa-miR-331-3p	1	0,61	0,68	0,48	0	-0,72	-0,55	-1,04
	hsa-miR-34a	1	1,80	2,15	0,93	0	0,85	1,11	-0,11
	hsa-miR-484	**1**	**0,15**	**1,26**	**0,22**	**0**	**-2,70**	**0,33**	**-2,21**
	hsa-miR-886-5p	**1**	**0,48**	**0,33**	**0,15**	**0**	**-1,05**	**-1,59**	**-2,74**
	hsa-miR-99a	1	1,30	0,46	1,61	0	0,38	-1,11	0,69
	MammU6	1	0,26	1,11	0,46	0	-1,97	0,14	-1,12
	RNU44	1	2,54	4,03	2,33	0	1,35	2,01	1,22
	RNU48	1	0,93	3,05	3,24	0	-0,11	1,61	1,69
Card B									
	hsa-miR-1260	1			0,31	0			-1,70
	hsa-miR-1274A	1			3,84	0			1,94
	hsa-miR-1274B	1			1,02	0			0,03
	hsa-miR-1275	1			0,50	0			-1,01
	hsa-miR-145#	1			2,45	0			1,29
	hsa-miR-181a-2#	1			1,70	0			0,76
	hsa-miR-21#	1			3,19	0			1,67
	hsa-miR-30a-3p	1			4,63	0			2,21
	hsa-miR-30a-5p	1			1,68	0			0,75
	hsa-miR-30d	1			2,02	0			1,01
	hsa-miR-30e-3p	1			4,21	0			2,07
	hsa-miR-320B	1			1,62	0			0,69
	hsa-miR-409-3p	1			2,40	0			1,26
	hsa-miR-572	1			1,81	0			0,86
	hsa-miR-720	1			0,54	0			-0,90
	RNU44	1			24,83	0			4,63
	RNU48	1			29,39	0			4,88
	U6 snRNA	1			14,86	0			3,89

Table S III: Selection of endogenous control miRs. From the array analysis the most stable miRs were selected to serve as endogenous control for the validation studies. The most stable miRs were selected on their small standard deviations (SD) of their Cq values over the samples. MiR-484 was not selected as endogenous control because of unreliable amplification plots within the taqman low density array.

	Tissue		**Plasma**	
	miR	SD of Cq values	miR	SD of Cq values
1	hsa-miR-484	1,01	**hsa-miR-195**	1,11
2	**hsa-miR-191**	1,06	hsa-miR-34a	1,55
3	hsa-miR-342-3p	1,21	hsa-miR-194	1,65
4	MammU6	1,36	hsa-let-7b	1,64
5	hsa-miR-29a	1,55	has-miR-155	1,57

Table S IV: Correlation between two plasma pools. On each time point in the plasma array analysis two pools of samples were made. These two pools correlated very well according to their r values.

	Plasma pools	**r**
Card A	control pool 1 - control pool 2	0.9414
	6-week pool 1 - 6-week pool 2	0.8686
	12-month pool 1 - 12 month pool 2	0.9169
Card B	control pool 1 - control pool 2	0.9363
	6-week pool 1 - 6-week pool 2	0.8201
	12-month pool 1 - 12 month pool 2	0.7921

Table S V: Taqman Low Density Array analysis of plasma. MiR expression in plasma was analyzed by low density array and changes over time post transplantation appear when compared to control. Only miRs with an expression pattern of log2(RQ)>2 between control samples and 6 weeks and/or 12 months are displayed. This resulted in 40 miRs on card A and 12 miRs on card B. The miRs in bold were selected for further validation studies based on the criteria mentioned in the methods.

		RQ			log2(RQ)		
	Assay	**Control**	**6 weeks**	**12 months**	**Control**	**6 weeks**	**12 months**
Card A							
	hsa-let	1	0,19	0,27	0	-2,38	-1,90
	hsa-let-7d	1	0,15	0,26	0	-2,78	-1,93
	hsa-let-7e	**1**	**0,02**	**0,02**	**0**	**-5,70**	**-5,42**
	hsa-let-7g	1	0,23	0,44	0	-2,14	-1,18
	hsa-miR-122	**1**	**39,14**	**5,03**	**0**	**5,29**	**2,33**
	hsa-miR-132	**1**	**7,11**	**12,93**	**0**	**2,83**	**3,69**
	hsa-miR-134	1	0,43	0,15	0	-1,22	-2,70
	hsa-miR-146b-5p	1	0,22	0,30	0	-2,16	-1,75
	hsa-miR-155	1	0,10	0,16	0	-3,30	-2,66
	hsa-miR-16	1	0,14	0,06	0	-2,80	-4,06
	hsa-miR-181a	1	4,31	7,09	0	2,11	2,83
	hsa-miR-184	1	0,07	0,16	0	-3,76	-2,64
	hsa-miR-18a	1	0,20	0,35	0	-2,31	-1,53
	hsa-miR-191	1	0,21	0,43	0	-2,22	-1,22
	hsa-miR-192	1	4,97	1,06	0	2,31	0,08
	hsa-miR-193a-5p	**1**	**24,43**	**4,81**	**0**	**4,61**	**2,27**
	hsa-miR-193b	**1**	**18,00**	**1,53**	**0**	**4,17**	**0,62**
	hsa-miR-194	1	0,08	0,13	0	-3,58	-2,90
	hsa-miR-195	1	0,12	0,11	0	-3,08	-3,15
	hsa-miR-200c	1	0,22	0,34	0	-2,20	-1,56
	hsa-miR-20b	1	0,24	0,37	0	-2,08	-1,42
	hsa-miR-210	1	13,75	3,24	0	3,78	1,69
	hsa-miR-221	1	1,83	5,40	0	0,87	2,43
	hsa-miR-27a	1	2,37	4,89	0	1,24	2,29
	hsa-miR-27b	1	5,43	10,92	0	2,44	3,45
	hsa-miR-323-3p	1	0,23	0,21	0	-2,15	-2,28
	hsa-miR-34a	**1**	**0,03**	**0,03**	**0**	**-5,22**	**-4,86**
	hsa-miR-374a	1	0,20	0,37	0	-2,32	-1,44
	hsa-miR-374b	1	0,23	0,17	0	-2,12	-2,54
	hsa-miR-382	1	5,01	6,67	0	2,32	2,74
	hsa-miR-410	1	0,28	0,19	0	-1,85	-2,39
	hsa-miR-454	**1**	**0,05**	**0,05**	**0**	**-4,36**	**-4,19**
	hsa-miR-483-5p	1	0,72	0,15	0	-0,48	-2,75
	hsa-miR-485-3p	1	0,10	0,19	0	-3,33	-2,43
	hsa-miR-486-3p	**1**	**0,09**	**0,04**	**0**	**-3,40**	**-4,58**
	hsa-miR-486-5p	1	0,12	0,13	0	-3,04	-2,95
	hsa-miR-487b	1	0,16	0,30	0	-2,62	-1,73
	hsa-miR-494	1	0,24	0,19	0	-2,06	-2,37
	hsa-miR-539	1	0,24	0,14	0	-2,07	-2,87
	hsa-miR-660	1	4,29	2,18	0	2,10	1,13
Card B							
	hsa-miR-1227	1	0,16	0,43	0	-2,60	-1,20
	hsa-miR-1274A	1	37,72	2,88	0	5,24	1,53
	hsa-miR-1274B	1	8,74	3,82	0	3,13	1,93
	hsa-miR-30a-5p	1	8,08	4,34	0	3,01	2,12
	hsa-miR-30d	1	7,29	3,82	0	2,87	1,94
	hsa-miR-320B	1	8,26	9,06	0	3,05	3,18
	hsa-miR-520c-3p	1	0,34	0,15	0	-1,57	-2,76
	hsa-miR-625#	1	0,14	0,42	0	-2,80	-1,26
	hsa-miR-629	1	0,53	0,13	0	-0,91	-2,92
	hsa-miR-720	1	10,68	9,32	0	3,42	3,22
	hsa-miR-769-5p	1	7,44	6,18	0	2,89	2,63
	U6 snRNA	1	8,97	1,73	0	3,17	0,79

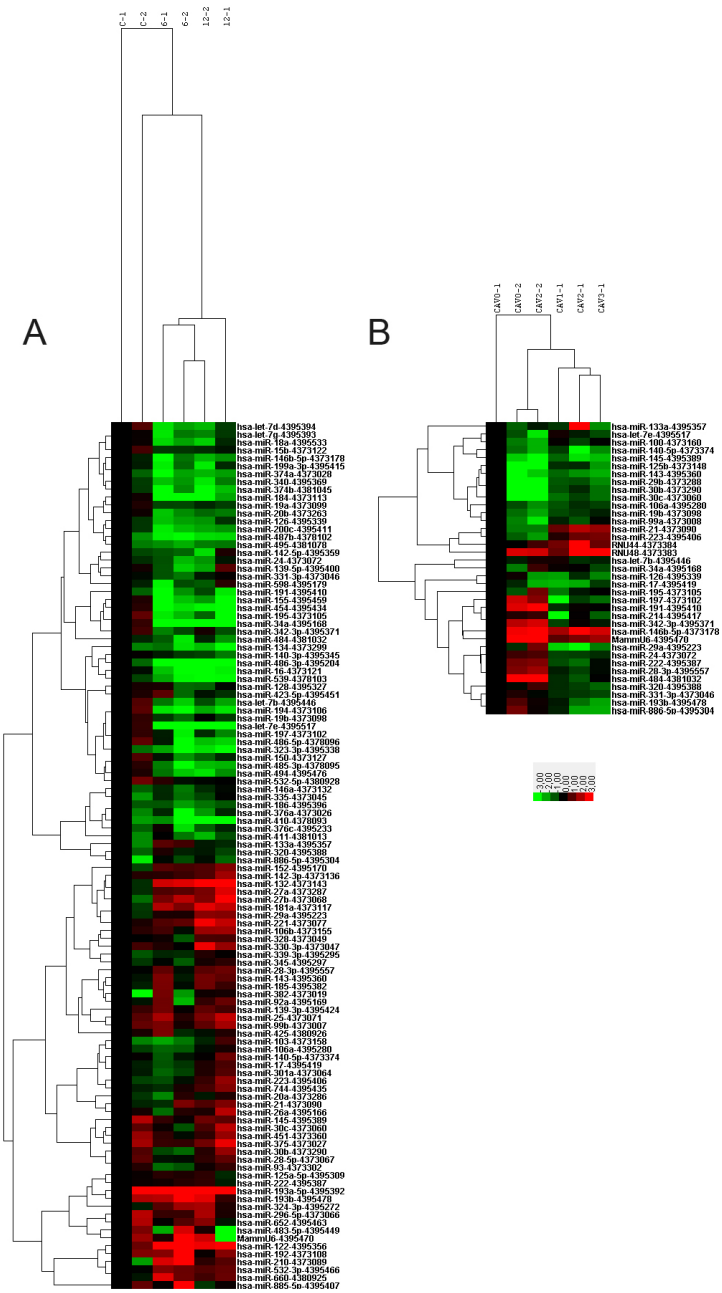

Figure S I: Cluster analysis of miR array results. Expression (Log2) of miRs in individual samples from card A normalized with global normalization. Relative expression is displayed using one of the control samples as reference. **(A)** Plasma: control versus HTx patients at 6weeks or 12months (C-1 = control plasma 1). **(B)** Tissue: control vs CAV intima (CAV0-1 = H-CAV 0 number 1).

Chapter 9.

FUNCTIONAL ANALYSIS OF microRNAS IN CARDIAC ALLOGRAFT VASCULOPATHY

Manon Huibers MSc [1], Roel de Weger PhD [1], Joost Sluijter PhD [2], Nicolaas de Jonge MD PhD [3], Joyce van Kuik BSc [1], Erica Siera-de Koning BSc [1], Jaap Lahpor MD PhD [4], Lingfeng Qin MD PhD [5], George Tellides MD PhD [5]

Department of Pathology [1], Experimental Cardiology laboratory [2], Cardiology [3], Cardiothoracic Surgery[4], University Medical Center Utrecht, the Netherlands and Department of Cardiovascular surgery [5], Yale School of Medicine, New Haven, United States of America.

Manuscript in preparation

Abstract

Background:
A major limitation of long-term survival after heart transplantation (HTx) is Cardiac allograft vasculopathy (CAV), characterized by concentric intima hyperplasia in epicardial coronary arteries. Although more knowledge is gained about the molecular process, no clinical treatment is implemented yet. MicroRNA (miR) regulation might be a new approach to target CAV. The aim of this study was to determine whether selected miRs that change during CAV development in humans can be studied in the huSCID/bg model.

Methods:
Expression levels of the selected miRs (miR-21, -146b-5p, 214, -223, -886-5p) were determined in autopsy material of 10 HTx patients by Q-PCR in specific vessel layers (intima, media, and adventitia). Expression of three mRNA targets (STAT3, TIMP3, PDCD4) of miR-21 were determined in the same samples. Within the humanized Allograft Vasculopathy mouse model, expression of the same miRs was measured by Q-PCR in whole artery grafts and the specific vessel layers.

Results:
In human CAV many of the detected immunologically oriented miRs (miR-223, -146b-5p, -21) were significantly correlated. Interestingly, downstream mRNA targets for miR-21 were low in areas where miR-21 expression was high. MiR-214 showed resemblance between the human CAV arteries and the mouse AV grafts; both significantly downregulated compared to controls. Although not significant, miR-146b-5p showed a upregulating trend in AV grafts compared to controls.

Conclusion:
When targeting a specific miR in vivo, one should take model specific expression levels into account. The AV huSCID/bg model shows similarities with human CAV regarding miR expression levels, making this an appropriate model to study AV. The molecular process of CAV is two sided, with miR-146b-5p as immune and miR-21 as fibrosis modulator with downstream mRNA effects. Targeting these two processes in vivo could offer a new therapeutic approach for CAV.

Introduction

Cardiac Allograft Vasculopathy (CAV) is the main cause of death in long-term survivors after Heart transplantation (HTx) [1]. CAV is characterized as a concentric intima thickening in the coronary arteries of the transplanted heart. This intima formation is caused by a proliferative immunological response of mononuclear cells (MNC) that eventually induce fibrosis of the vessel wall. Histological characterization of these human samples showed different phenotypes [2]. The major component of the MNC infiltrates were activated memory T-helper 1 cells, yet a minor population of T-helper 2 cells and M2-macrophages was detected as well. Interferon-γ (IFNγ) and Transforming Growth Factor-β (TGFβ) are the main cytokines expressed in the CAV vessel wall [3–5].

The most suitable model to study CAV uses a microsurgical approach; a human artery is transplanted in an immune deficient mouse after which a human immune system is introduced (reconstitution). Intima formation in this model has great concordance with human CAV 6. The main MNC component of this intima are memory T-cells with IFNγ and TGFβ as the main cytokines responsible for intima proliferation [7–12].

Although more knowledge is gained through human and animal studies about the molecular process of allograft vasculopathy, no clinical treatment is implemented yet. New approaches are necessary to tackle this disease process. MicroRNAs (miRs) are important regulators in immunological and (cardio)vascular diseases. Previous publications showed the therapeutic potential of influencing miRs *in vivo* [17,18]. In 2013, the role of miRs in transplantation was described [13] without any study in cardiac transplantation. More recently, the role of miRs in acute cellular rejection after heart transplantation was reported [14–16]. Despite these developments, cardiac allograft vasculopathy was never studied for miR expression patterns. We previously reported a miR selection in CAV arteries based on an array inventory of miRs isolated from microdissected neo-intima tissue of HTx patients and controls *(Huibers et al submitted for publication, Chapter 8)*. Of the selected miRs, 5 were confirmed to be significantly different. To study the *in vivo* effect of the selected miRs, a well-established humanized mouse model was used in the present study.

We aimed to determine which of the human selected miRs are present in the intima of the huSCID/bg model (T-cell focused intima formation). By influencing the miR levels in this model we aim to inhibit intima proliferation in the human arterial graft. This study is the first to determine the role of miRs in allograft vasculopathy in an experimental animal model which might lead to new therapeutic strategies.

Methods

Humanized mouse model

The previously described humanized mouse model was used to study allograft vasculopathy (AV) [19–21]. Segments of human coronary arteries were obtained from explanted donor hearts (unsuitable for cardiac transplantation) or mammary arteries during bypass surgery and directly stored in ice cold saline. Research protocols were approved by the Yale Human Investigators Committee and the New England Organ Bank. The arterial segments were interposed within 6 hours after harvesting into the infrarenal aortae of 8-12 weeks old C.B.-17 SCID/beige-RAG1$^{-/-}$ mice using an end-to-end anastomotic continuous suture technique (n=14; **Supplemental figure 1**). The mice were transplanted in pairs (n=7 pairs); one serving as a control (no peripheral blood mononuclear cells (PBMCs)) and in the other AV would be induced (i.p. injection of PBMCs). The amount of PBMCs to inject was previously determined on reconstitution rates measured in the blood by Fluorescence Activated Cell Sorting (FACS) analysis (ratio humanCD3 / mouseCD45 = 5-25%). After 4-6 weeks the mice were sacrificed and the transplanted arterial graft was embedded in Tissue-Tek O.C.T. (optimal cutting temperature) and frozen at -80°C.

Histology and Immunohistochemistry

On frozen sections (6µm) Hematoxilin and Eosin (HE) and Elastic van Giesson (EvG) staining was performed to determine if intima proliferation was present. The EvG stained slides were used to measure lumen, intima, media, and total vessel (external elastic lamina) area in mm^2. Subsequently, the grafts were analyzed by immunohistochemistry (IHC) for the characterization of infiltrated cells (αSMA, CD45, CD3, and CD68; **Supplemental table 1**) according to previously described protocols *(Chapter 4, Huibers et al JHLT 2014 accepted for publication)*. In short, snap frozen grafts were sectioned at 6 µm, fixed in acetone and stained with the antibody of interest. Positive (heart tissue) and negative (without primary antibody) controls were taken along each staining method. Secondary antibodies were species specific and contained an HRP label. Detection of enzymatic activity was performed with diaminobenzidine (DAB) solution.

Laser microdissection and RNA isolation

The presence and location of the specific miR was analyzed by quantitative polymerase chain reaction (Q-PCR) on laser microdissected material. Laser microdissection (LMD) was performed on the grafts to separate the different vessel layers. Fifteen sections of 10 µm thickness were cut per vessel and transferred onto glass slides that contain a polyethylene naphthalate membrane (membrane slide 1.0 PEN, Carl Zeiss Microscopy Gmbh, Göttingen, Germany). Micro dissection was done using the P.A.L.M. Microlaser Technologies MB03223 attached to a Carl Zeiss Axiovert 200M microscope and operated with the P.A.L.M. RoboSoftware

(P.A.L.M. Microlaser Technologies AG, Bernried, Germany). The vessel layers of the graft were dissected and collected separately. From each layer $1*10^6$ μm^2 was collected and total RNA was isolated using the miRNeasy micro kit according to manufacturer's instructions (Qiagen Gmbh, Hilden, Germany).

cDNA synthesis and Q-PCR analysis

Total RNA (including mRNA and microRNA) was used to perform expression analysis using Q-PCR. For mRNA expression analysis, RNA was converted to cDNA using a previously described protocol [5] *(Chapter 4, Huibers et al JHLT 2014 accepted for publication)*. Specific Taqman probes for genes of interest (CD3, CD31, TGFβ, MYH11, and Col1A1) were used for Q-PCR analysis. For miR expression analysis, RNA was converted to specific cDNA for each microRNA (miR-146b, miR-21, miR-214, miR-223 and miR-886) and an endogenous control (U6) with the Taqman microRNA reverse transcription kit (Life technologies, Carlsbad, California, USA). Quantification of cDNA for mRNA and miR was performed using Taqman reagents on the Viia 7 Real time PCR System (Life technologies). Analysis of the Q-PCR results was done with the Viia 7 software (version 1.2.1).

Anti-miR treatment in a humanized mouse model for AV

The presence of the 5 human-based miRs (miR-146b-5p, -21, -223, -214, and -886-5p; *Huibers et al submitted for publication, Chapter 8*) was studied in the established model for allograft vasculopathy. Two miRs (miR-146b-5p and -21) were chosen to test for therapeutic effects in AV. In the transplanted arteries AV develops within four weeks after PBMC injection. Mice are treated with the selected miR blockers or its control (scramble miR). Three experimental groups were formed: (1) transplantation + PBMCs + miR-146b-5p inhibition treatment, (2) transplantation + PBMCs + miR-21 inhibition treatment, and (3) transplantation + PBMCs + scramble miR treatment. At 0.5 and 1.5 weeks after reconstitution, miR LNA inhibitors (Exiqon, Vedbaek, Denmark) were given (**Supplemental Figure 2**). Per dose 25 mg/kg (25ug/g) miR therapeutic in PBS were injected intra peritoneal. The main read-out parameter is the increase or decrease in size of the intima of the transplanted arteries in the different experimental groups (paired analysis).

Statistics

Data of the humanized mouse model is analyzed using paired analysis of reconstituted mice (PBMCs) and controls (control) using a paired t-test (**Figure 1A and 2A-C**; Graphpad Prism Version 6, San Diego, USA). To see whether the four different vessels layers (intima, media, adventitia, and ectopic lymphoid structures) show different expression levels, a Kruskall-Wallis test and post-hoc analysis was done with Dunn's multiple comparison (**Figure 3A**; Graphpad Prism). Correlation analysis was done using the Spearman correlation coefficients (**Figure 3B**; IBM SPSS Statistics 20, New York, USA). Values of $p<0.05$ were considered significant.

Results

MicroRNA expression in human CAV differs per vessel layer

To determine whether the human CAV specific miRs (selected in CAV versus control intima tissue) were only expressed in the intima or also in other vessel layers, the areas of interest were isolated by laser microdissection and expression levels were measured (**Figure 1A**). The areas of interest were the intima, media, adventitia and ectopic lymphoid structures (ELS) which are lymphoid areas surrounding CAV arteries possibly involved in the immune reaction *(Chapter 4, Huibers et al 2014 JHLT accepted for publication)*. MiR-21 and -214 showed highest expression in the intima and lowest expression in the ELS with an overall significant difference between all four groups (p=0.0118 and p=0.0002, respectively). The expression pattern of miR-146b-5p and miR-223 were very similar and significantly different amongst the four areas (p=0.0194 and p=0.0176, respectively). Both miRs were highly expressed in the adventitia and had low expression in the media. MiR-886-5p, displayed a completely different pattern with a high expression in the intima and media, and low expression in the adventitia and ELS (p=0.0043).

To test whether the five miRs were related to each other within the specific areas, Spearman correlation analysis was performed on their expression levels (**Supplemental table 2**). All miRs show a positive correlation, meaning that if one miR is upregulated another one is upregulated too (and not down regulated; **Figure 1B**). Interestingly, miR-146b-5p and miR-223 expression are always correlated regardless their location; intima (r=0.636 p=0.048), media (r=0.806 p=0.005), adventitia (r=0.855 p=0.002), and ELS (r=0.786 p=0.021). Suggesting they have a similar function or are expressed by the same cells. Besides, miR-21 is in most areas with immune cells correlated to miR-223 (intima r=0.636 p=0.048, adventitia r=0.806 p=0.005, ELS r=0.810 p=0.015) and miR-146b-5p (adventitia r=0.879 p=0.001, ELS r=0.952 p<0.001).

Figure 1. MicroRNA expression in human cardiac allograft vasculopathy: per vessel layer. Relative quantification (RQ) values of miR-21, -146b-5p, -214, -223, and -886-5p to determine expression levels in human CAV vessels. (A) Human CAV miR expression in the intima, media, adventitia and Ectopic lymphoid structures (ELS). Kruskall wallis test and Dunn's multiple comparison analysis. (B) Spearman correlation coefficients (r-value) of a selection of significantly correlated miRs.

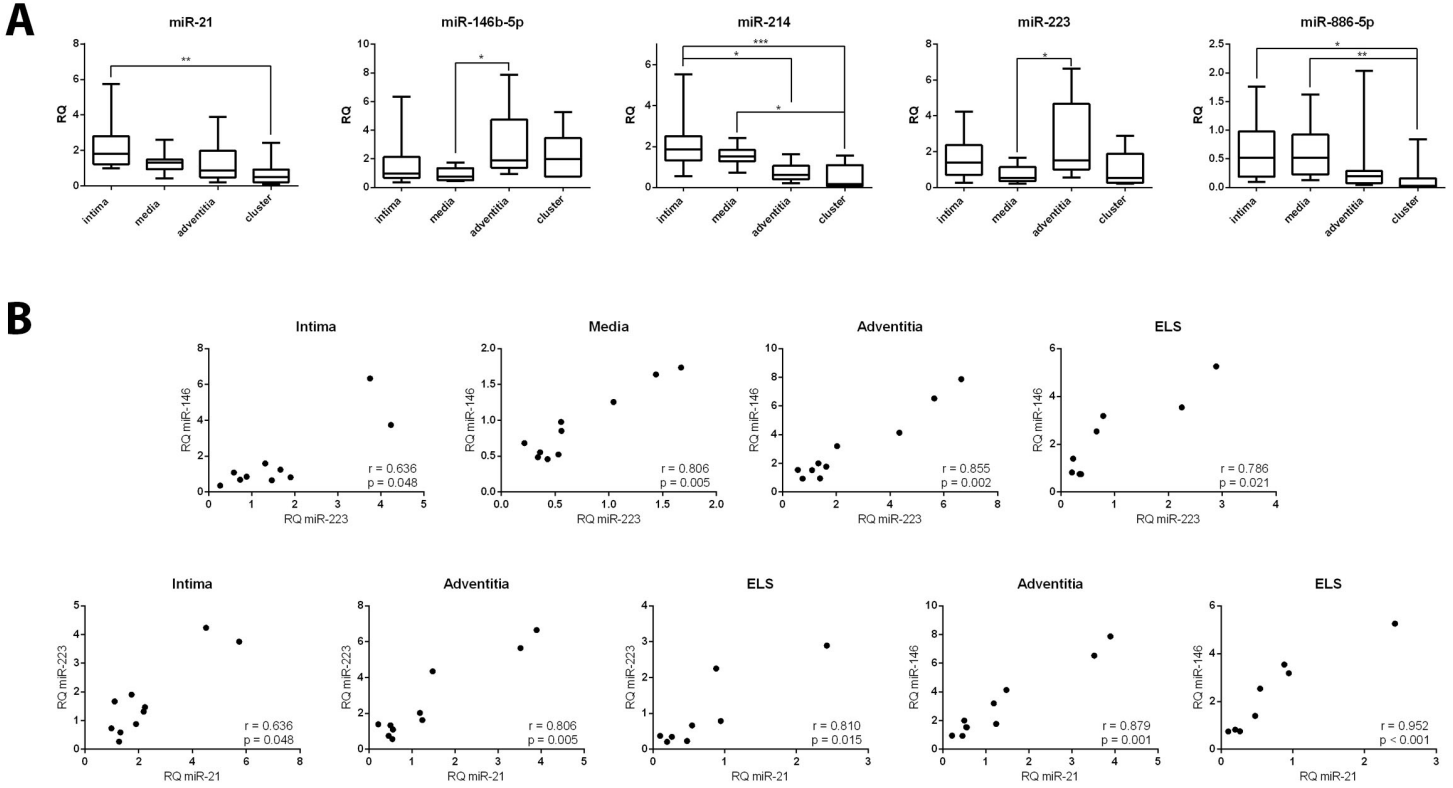

Messenger RNA targets of miR-21 in human CAV arteries

To analyze whether a miR found in CAV has a downstream effect, four validated mRNA targets of miR-21 (STAT3, TIMP3, and PDCD4) were selected to determine their expression level in human CAV vessels[22-25]. As presented above, miR-21 expression in highest in the intima and lowest in ELS surrounding CAV arteries with intermediate expression in the media and adventitia (p=0.0118). Interestingly, an opposite trend was seen for its mRNA targets (**Figure 2**). STAT3 expression was highest in the ELS and lowest in the media (p=0.0011), with lower (not significant) levels in the intima. TIMP3 expression was lowest in the intima with a significantly higher expression in the ELS and adventitia (p=0.0004). The expression pattern of PDCD4 was even more striking with barely any expression in the intima and media, intermediate expression in the adventitia, and high expression in ELS (p<0.0001). All three markers were high when miR-21 levels were low and vice versa.

MicroRNA expression changes dramatically between cell types

With intima proliferation in CAV arteries many cell types are involved that could potentially express the miRs of interest. Therefore, the four main cell types in CAV (endothelial cells, fibroblasts, smooth muscle cells, and immune cells) were cultured to measure their miR expression pattern (**Figure 3**). MiR-21 was highly present in smooth muscle cells (SMCs), showed intermediate expression in fibroblasts and human umbilical vein endothelial cells (HUVECs), and was barely detected in peripheral blood mononuclear cells (PBMCs). The same pattern was seen for miR-886-5p; expressed in HUVEC, fibroblasts, and SMCs, but not detected in PBMCs. MiR-214 was predominantly expressed by fibroblasts, showed intermediate expression in SMCs, low expression in HUVECs, and could not be detected in PBMCs. A complete different pattern was seen for miR-146b-5p and miR-223. They were both highly expressed in PBMCs, showed intermediate/low expression in SMCs and low/no expression in fibroblasts and HUVECs. MiR-223 was specifically expressed in PBMCs without any expression detected by Q-PCR in HUVECs or fibroblasts. These data show that miRs are highly cell specific and can be divided in immune (miR-146b-5p and -223) or myofibroblast specific miRs (miR-21, -214, and -886-5p). None of these microRNAs are truly endothelial cell specific (only present in HUVECs).

Figure 2. Targets of miR-21 in human CAV arteries. Relative quantification (RQ) values of miR-21 and its mRNA targets STAT3, TIMP3, and PDCD4 in human CAV intima, media, adventitia and Ectopic lymphoid structures (ELS). Statistics performed with Kruskall-Wallis tests and Dunn's multiple comparison analysis. * determines p<0.05

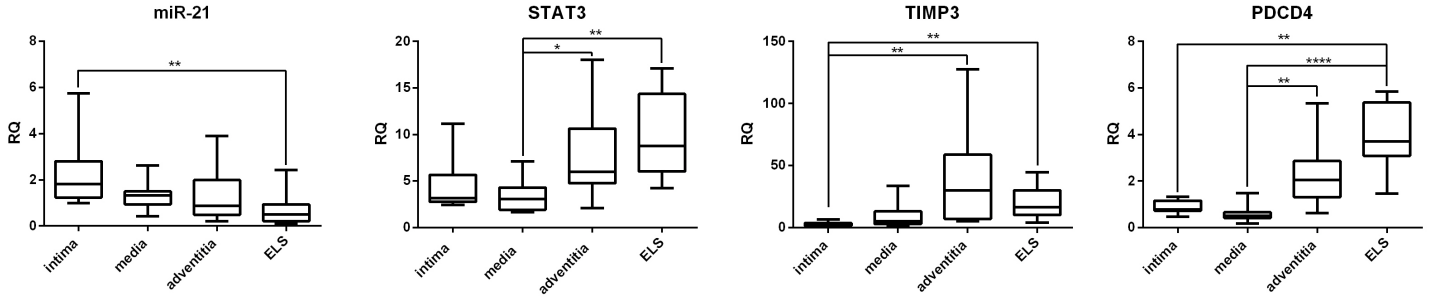

Figure 3. MicroRNA expression levels in cell culture: HUVEC, SMC, fibroblast, PBMC. Cellular expression patterns per miR-21, -146b-5p, -214, -223, and -886-5p. 'Not determined' implicates no amplification or Ct values higher than 35. RQ = relative quantity, HUVEC = human umbilical vein endothelial cells, SMC = smooth muscle cells, PBMC = peripheral blood mononuclear cells

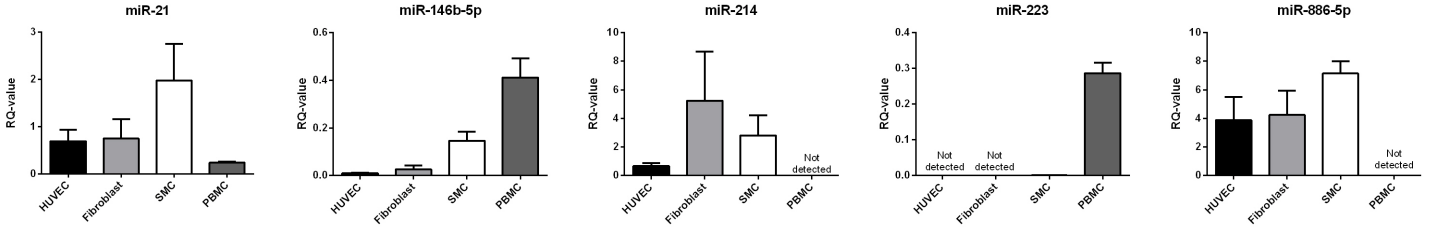

Histology, measurements and immunohistochemistry of AV mouse model

A well-established humanized mouse model was used for in vivo testing of allograft vasculopathy (AV). To verify whether the model was successful and AV developed, histology and morphology was studied. HE and EvG staining showed an increase in intima formation when mice were injected with allogeneic peripheral blood mononuclear cells (PBMCs; **Figure 4A**). However, this varied per mouse pair as in some cases no increase in intima size was detected. EvG stain was used to quantify the increase in intima area and other vessel layers (**Figure 4B**). These measurements indicated that overall there was no change in lumen (p=0.2867) and media (p=0.9447) area, however the intima (p=0.0138) and total vessel area (p=0.0222) increased significantly with PBMC injection confirming intima expansion. The cellular composition of the formed intima was determined with immunohistochemistry (IHC; **Figure 4C**). Part of the intima contained alpha-Smooth Muscle Actin (αSMA) positive cells, suggesting presence of smooth muscle cells or myofibroblasts. Besides, a large proportion of the intima was occupied by CD45 positive leucocytes, with mainly T cells (CD3). Although CD68 IHC showed some aspecific background staining, no macrophages were detected in the grafts.

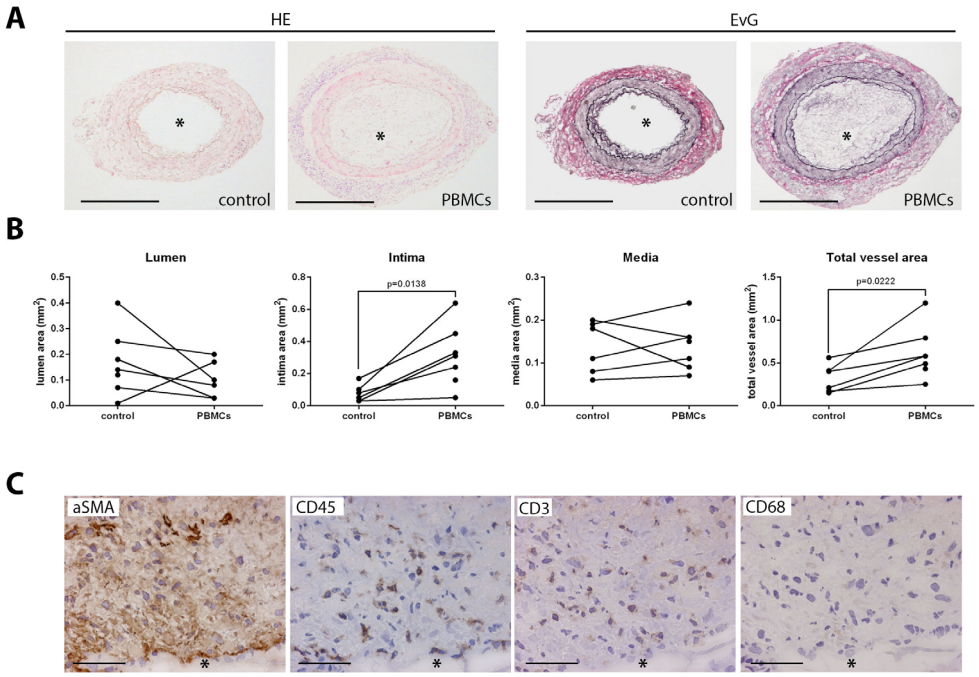

Figure 4. Allograft vasculopathy mouse model; histology, measurements and immunohistochemistry. Histological, morphometric and cellular characterization of the model. **(A)** The Haematoxilin & Eosin (HE) and Elastica von Gieson (EvG) staining showed a clear increase in intima formation when mice were injected with allogeneic peripheral blood mononuclear cells (PBMCs). EvG staining was used for morphometric measurements (scale bar indicates 500μm and asterisk* depicts lumen). **(B)** Absolute measurements of vessel layers and vessel area indicate that overall there was no change in lumen and media area, however the intima and total vessel area increased significantly with PBMC injection. **(C)** Immunohistochemistry showed that the intima was composed of alpha-smooth muscle actin (αSMA) positive cells and T cells ($CD45^+$ and $CD3^+$). No macrophages were detected (CD68). Scale bar indicates 200μm and asterisk* depicts lumen.

Messenger RNA and microRNA expression in AV mouse model

Expression levels of cell specific human mRNAs were determined in whole artery graft segments of mice with and without PBMC reconstitution (**Figure 5A**). No human CD3 expression was found in control mice, whereas CD3 was highly expressed in mice reconstituted with human PBMCs. This indicated that our control mice definitely did not have any human T cells. The mice with PBMCs had detectable levels of CD3 within the graft. Furthermore, relative expression levels of endothelial cell marker PECAM-1 (CD31) showed a non-significant relative decrease in expression level (p=0.0511). Relative expression of smooth muscle cell and fibrosis markers decreased significantly with allograft vasculopathy (AV); TGFβ (p=0.0409), MYH11 (p=0.0121), and Collagen1A1 (p=0.0174).

In a previous study in human CAV, 5 miRs (miR-146b-5p, miR-21, miR-223, miR-214, and miR-886-5p) were selected for their potential role in CAV development *(Huibers et al submitted for publication, Chapter 8,* **Table 1**). To verify whether the humanized mouse model for AV expressed the same microRNAs as found in human CAV, expression levels of these miRs were measured in whole artery segments (**Figure 5B**). Although in human CAV miR-146b-5p, miR-21, miR-223 were upregulated, in this model no significant changes were observed upon PBMC reconstitution (p=0.0907, p=0.4464, p=0.9757 respectively). Interestingly, miR-146b-5p was in 4 out of the 7 pairs upregulated, whereas the other 3 pairs did not change. This suggests two groups; one with and one without an effect on miR-146b-5p expression. In human CAV miR-214 and miR-886-5p were down regulated compared to control. MiR-886-5p did not show significant changes (p=0.5940) although some pair did show a decline with PBMC injection. Expression of miR-214 was significantly reduced in all grafts with AV (p=0.0051).

Vessel layers of the mouse AV model were isolated using laser microdissection and miR expression was measured per area (**Figure 5C**). Although not significant, miR-146b-5p expression was higher after PBMC injection in the intima and media, however this did not change in the adventitia. The upregulated miR-21 in human CAV was in the mouse AV model not significantly upregulated in the media, did not change in the adventitia, and surprisingly showed a down regulation in the intima. MiR-223 (upregulated in human CAV) and miR-886-5p (down regulated in human CAV) did show too much variation in this small number of samples (n=3) to define a trend. Only miR-214 expression was significantly lower in grafts with AV within the media (p=0.0474) and adventitia (p=0.0031), however a non-significant trend in the intima (p=0.1687).

Table 1. Regulation in human CAV and mouse AV. CAV = Cardiac Allograft Vasculopathy, AV = Allograft Vasculopathy, n.s. = non-significant.

	Human CAV		Mouse AV		
microRNA	**Intima (n=15)**	**whole artery (n=7)**	**Intima (n=3)**	**Media (n=3)**	**Adventitia (n=3)**
miR-146b-5p	Up	4/7 up (p=0.091)	Up (n.s.)	Up (n.s.)	no change (n.s.)
miR-21	Up	4/7 up (p=0.446)	Down (n.s.)	Up (n.s.)	no change (n.s.)
miR-223	Up	3/7 up (p=0.796)	no change (n.s.)	no change (n.s.)	no change (n.s.)
miR-214	Down	7/7 down (p=0.005)	no change (n.s.)	Down (p=0.047)	Down (p=0.003)
miR-886-5p	Down	3/7 down (p=0.594)	no change (n.s.)	no change (n.s.)	no change (n.s.)

Discussion

Previously we reported miR expression alterations in the intima of cardiac allograft vasculopathy patients *(Huibers et al submitted for publication, Chapter 8)*. From an objective tissue specific screening of over 750 miRs, eight were selected, and five turned out to be significantly up- (miR-21, -223, and -146b-5p) or down-regulated (miR-886-5p and -214) in CAV. Literature and localization of the tissue-miRs suggested a role in immune regulation or fibrosis [26–28]. Until then, the role of microRNAs was never studied in CAV. If these miRs have a role in CAV development they could be considered potential therapeutic targets.

The pathogenesis of human CAV seems to be two-sided (T cell mediated and fibrosis mediated), which is extensively described in the introduction of this thesis and previously published data *(Chapter 1, [5])*. Our previous miR data confirmed the two-sided process of CAV with the five specific miR-families involved in one (or both) processes. Cell cultures of endothelial cells, smooth muscle cells, fibroblasts and immune cells were used to determine expression patterns of CAV specific miRs. The *in vitro* data indicate that these five miRs are highly cell specific under 'normal' culture conditions. Also these data suggest a separation between immune specific miRs (miR-146b-5p and -223) and myofibroblast specific miRs (miR-21, -214, and -886-5p), confirming our previously described findings *(Huibers et al submitted for publication, Chapter 8)*. Since in CAV arteries cytokines like IFNγ and TGBβ are highly expressed[29,30], it might be interesting to study miR fluctuations in vitro under stimulated conditions in future studies.

The selection of the CAV specific miRs was made solely on intima expression levels. If these miRs would be interesting targets for therapy, it is important to know in what extent these miRs are expressed in the media, adventitia, and ectopic lymphoid clusters (ELS). With these data we could indicate that systemic therapy for a specific miR *in vivo* would only affect the intima, or also other areas. For this reason we used laser microdissection to isolate the specific areas in human CAV arteries and grafts from the AV mouse model.

In human CAV arteries miR-21 and -214 showed high expression levels in the intima suggesting their most prominent role in this area. Whether this role is in fibrosis [28], immunology [31] or angiogenesis [32] is still unknown. Also miR-886-5p was predominantly expressed in the intima, but showed similar expression levels in the media which might indicate a dual role in CAV; T cell and SMC mediated [33]. The expression pattern of miR-146b-5p and miR-223 showed high levels in the adventitia, suggesting an immunological response and possible molecular involvement in allograft vasculopathy [34]. When one of these miRs will be selected for therapy this implicates that not only the intima will be targeted, but also molecular pathways in the adventitia. Overall, the low expression of miR-21, -214, and -886 in ELS compared to intima, suggests their role is more important in CAV development than in ELS formation. Correlation statistics indicated that many miRs were positively correlated with one another. Especially the two immune related miRs, miR-146b-5p and -223, were strongly correlated with each other suggesting a complementary function or expression by the same cells. Interestingly, also miR-21 was correlated to one of the immune mediated miRs (miR-146b-5p or -223), so besides a role in fibrosis [35] suggesting an immunological role in CAV [31].

To test the role of miRs in CAV, mRNA levels of the validated target of that miR were measured. In this manuscript one of the most studied miRs, miR-21 was selected, with three of its validated targets; STAT3 [23], TIMP3, and PDCD4 [36]. This miR is involved in intima

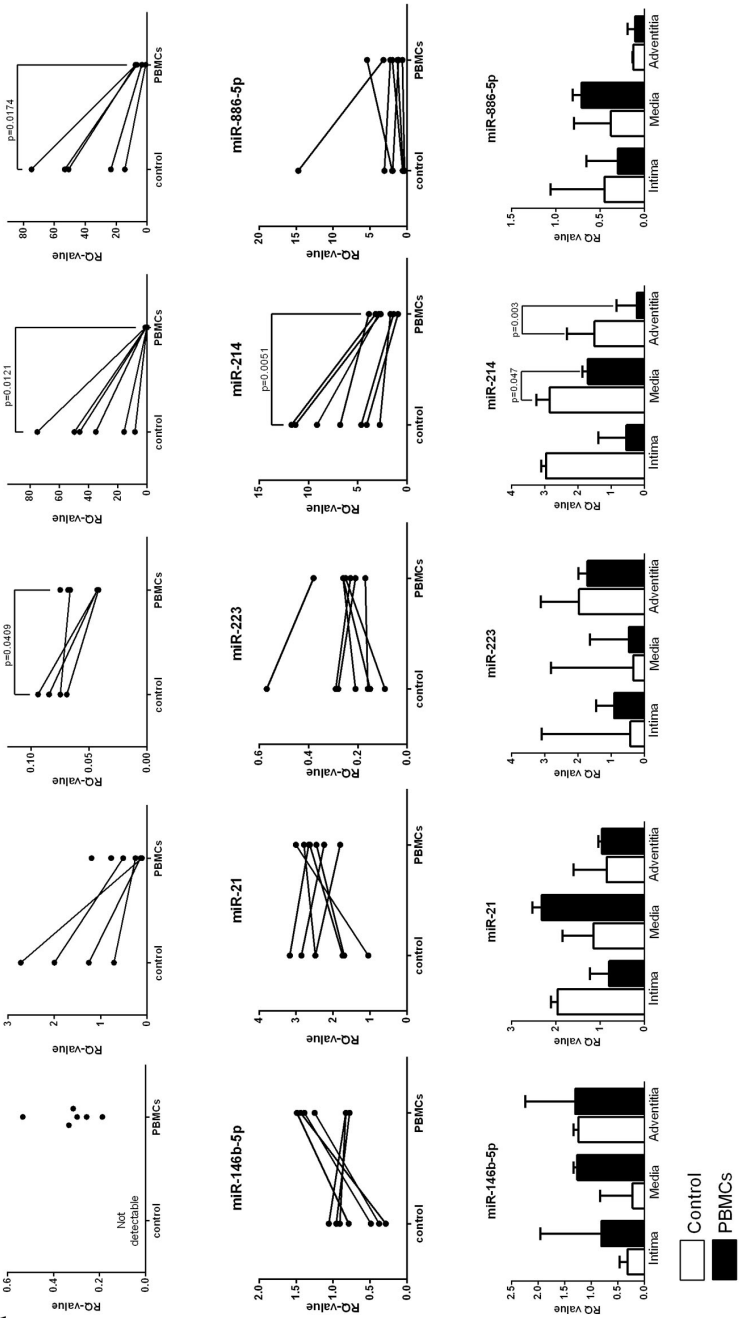

Figure 5. Allograft vasculopathy mouse model: mRNA and microRNA expression levels. (A) mRNA expression levels of whole artery graft segments show no human CD3 expression in control mice, and clear expression in mice reconstituted with PBMCs. Furthermore, relative expression levels of CD31 (n.s.), TGFβ (p=0.0409), MYH11 (p=0.0121), and Collagen1A1 (p=0.0174) decrease after PBMC injection. **(B)** PBMC injection did not significantly change expression of microRNA-146b-5p (miR-146b-5p), miR-21, miR-223, and miR-886-5p of whole artery graft segments. However, miR-214 expression was reduced with PBMC reconstitution (p=0.0051) in all grafts. **(C)** Data per vessel layer show major expression changes in the intima and minor changes in the media and adventitia. Again, only miR-214 showed significantly lower expression between control and PBMC groups within the media (p=0.047) and adventitia (p=0.003). RQ = relative quantity, PBMC = peripheral blood mononuclear cells.

hyperplasia in vein grafts and showed in vitro to affect STAT3, but not TIMP3 and PDCD4 [22]. Our data indicate that in human CAV all three mRNA targets are low in areas where miR-21 expression is high (e.g. intima). These downstream effects suggest a role in fibroblast survival (STAT3; [23]), edothelial-to-mesenchymal transition (TIMP3; [24]), and/or apoptosis (PDCD4; [25]), which could all lead to fibrosis in the end. These data confirmed our hypothesis that miR-21 is not just present in CAV arteries but has a functional role in the process.

Before studying the therapeutic effect of miRs in an *in vivo* mouse model for AV, we need to validate this model to see whether the same expression levels exist as in human CAV. The presented data indicate that the AV mouse model had significant intima hyperplasia. As previously reported, this model has intima expansion, a preserved lumen and outward remodeling (total vessel area increases [37]) as also seen in human CAV [2]. Immunohistochemistry and mRNA levels of CD3 confirmed that T cells are predominantly present in the intima of AV grafts. These data also indicated that control grafts were completely 'clean', meaning no human T cells were carried over during the microsurgical transplantation procedure. The decrease in relative expression levels of PECAM-1 (CD31), TGFβ, MYH11, and Collagen1A1 could be due to normalization with GAPDH (housekeeping gene). If the amount of total cells increases (GAPDH), but the number of mRNA target expressing cells (CD31 / TGFβ / MYH11 / COL1A1) stays the same, the relative values decrease. These changes were previously seen within this model [30].

To investigate whether expression levels were similar between human CAV and the mouse AV grafts, we measured miR expression in whole artery grafts and per vessel layer. In whole artery grafts, miR-214 expression is strongly declined after reconstitution of the mice, which was also observed in human CAV samples. This miR was earlier described to have a protective role in cardiac ischemic injury [38] and inhibits angiogenesis [32]. A recent publication showed that also *in vivo* targeting of this miR showed great effects in bone formation [39]. Although this would be the most optimal target for therapy, it is still difficult to introduce miR mimics that work in the *in vivo* situation. Therefore we focused on the upregulated miRs within human CAV and the AV mouse model. These upregulated miR can easily be targeted by miR-inhibitors which have been shown to be very powerful [17,40,41]. The two potential targets for miR inhibition are miR-146b-5p and miR-21 since both show a trend in upregulation in AV. Within the mouse model, miR-146b-5p seems specifically upregulated in the intima, whereas miR-21 was upregulated in the media of affected arteries. By targeting these two miRs, both processes of AV will be evaluated; T cell (miR-146b-5p, possibly miR-21) and fibrosis (miR-21). This experiment will indicate whether these two miRs are key players in the pathogenesis of CAV and might be potential therapeutic targets.

Acknowledgements

We would like to thank Remco Hoonhout and Suzanne Beerthuijzen for their practical assistance in this study. This work was supported by a travelling scholarship award (2013) from the International Society for Heart and Lung Transplantation to MH.

References

1. Stehlik, J. et al. The Registry of the International Society for Heart and Lung Transplantation: Twenty-eighth Adult Heart Transplant Report--2011. *J. Hear. lung Transplant.* **30**, 1078–94 (2011).
2. Huibers, M. M. H. et al. Distinct phenotypes of cardiac allograft vasculopathy after heart transplantation: A histopathological study. *Atherosclerosis* **236**, 353–359 (2014).
3. Loosdregt, J. van & Oosterhout, M. van. The chemokine and chemokine receptor profile of infiltrating cells in the wall of arteries with cardiac allograft vasculopathy is indicative of a memory T–helper 1. *Circulation* **114**, 1599–1607 (2006).
4. Hagemeijer, M. C. et al. T cells in cardiac allograft vasculopathy are skewed to memory Th-1 cells in the presence of a distinct Th-2 population. *Am J Transpl.* **8**, 1040–1050 (2008).
5. Huibers, M. et al. Intimal fibrosis in human cardiac allograft vasculopathy. *Transpl. Immunol.* **25**, 124–132 (2011).
6. Lorber, M. I. et al. Human allogeneic vascular rejection after arterial transplantation and peripheral lymphoid reconstitution in severe combined immunodeficient mice. *Transplantation* **67**, 897–903 (1999).
7. Tellides, G. et al. Interferon-gamma elicits arteriosclerosis in the absence of leukocytes. *Nature* **403**, 207–211 (2000).
8. Burns, W. R. et al. Recruitment of CXCR3+ and CCR5+ T cells and production of interferon-γ-inducible chemokines in rejecting human arteries. *Am. J. Transplant.* **5**, 1226–1236 (2005).
9. Yi, T. et al. Human allograft arterial injury is ameliorated by sirolimus and cyclosporine and correlates with suppression of interferon-gamma. *Transplantation* **81**, 559–566 (2006).
10. Tellides, G. & Pober, J. S. Interferon-gamma axis in graft arteriosclerosis. *Circ Res* **100**, 622–632 (2007).
11. Tobiasova, Z. et al. Peroxisome proliferator-activated receptor-γ agonists prevent in vivo remodeling of human artery induced by alloreactive T cells. *Circulation* **124**, 196–205 (2011).
12. Lebastchi, A. H. et al. Activation of human vascular cells decreases their expression of transforming growth factor-beta. *Atherosclerosis* **219**, 417–424 (2011).
13. Mas, V. R., Dumur, C. I., Scian, M. J., Gehrau, R. C. & Maluf, D. G. MicroRNAs as biomarkers in solid organ transplantation. *American Journal of Transplantation* **13**, 11–19 (2013).
14. Sukma Dewi, I., Torngren, K., Gidlöf, O., Kornhall, B. & Ohman, J. Altered serum miRNA profiles during acute rejection after heart transplantation: potential for non-invasive allograft surveillance. *J. Hear. lung Transplant.* **32**, 463–6 (2013).
15. Wei, L. et al. Differential expression of microRNAs during allograft rejection. *Am. J. Transplant.* **12**, 1113–1123 (2012).
16. Duong Van Huyen, J.-P. et al. MicroRNAs as non-invasive biomarkers of heart transplant rejection. *Eur. Heart J.* **35**, 3194–202 (2014).
17. Da Costa Martins, P. A. et al. MicroRNA-199b targets the nuclear kinase Dyrk1a in an auto-amplification loop promoting calcineurin/NFAT signalling. *Nat. Cell Biol.* **12**, 1220–1227 (2010).
18. Ali, R. et al. MiR-1 mediated suppression of Sorcin regulates myocardial contractility through modulation of Ca 2+ signaling. *J. Mol. Cell. Cardiol.* **52**, 1027–1037 (2012).
19. Hogenes, M., Huibers, M., Kroone, C. & de Weger, R. Humanized mouse models in transplantation research. Transplantation Reviews 28, 103–110 (2014).
20. Burns, W. R. et al. Recruitment of CXCR3+ and CCR5+ T cells and production of interferon-??-inducible chemokines in rejecting human arteries. *Am. J. Transplant.* **5**, 1226–1236 (2005).
21. Kirkiles-Smith, N. C. et al. Development of a humanized mouse model to study the role of macrophages in allograft injury. *Transplantation* **87**, 189–197 (2009).
22. McDonald, R. A. et al. MiRNA-21 is dysregulated in response to vein grafting in multiple models and genetic ablation in mice attenuates neointima formation. *Eur. Heart J.* **34**, 1636–1643 (2013).
23. Haider, K. H. et al. MicroRNA-21 is a key determinant in IL-11/Stat3 anti-apoptotic signalling pathway in preconditioning of skeletal myoblasts. *Cardiovasc. Res.* **88**, 168–178 (2010).
24. Kumarswamy, R. et al. Transforming growth factor-??-induced endothelial-to-mesenchymal transition is partly mediated by MicroRNA-21. Arterioscler. *Thromb. Vasc. Biol.* **32**, 361–369 (2012).
25. Godwin, J. G. et al. Identification of a microRNA signature of renal ischemia reperfusion injury. *Proc. Natl. Acad. Sci. U. S. A.* **107**, 14339–14344 (2010).
26. Sonkoly, E., Ståhle, M. & Pivarcsi, A. MicroRNAs and immunity: Novel players in the regulation of normal immune function and inflammation. *Seminars in Cancer Biology* **18**, 131–140 (2008).
27. Tsitsiou, E. & Lindsay, M. A. microRNAs and the immune response. *Current Opinion in Pharmacology* **9**, 514–520 (2009).
28. Thum, T. Noncoding RNAs and myocardial fibrosis. *Nat. Rev. Cardiol.* **11**, 655–663 (2014).
29. Pober, J. S., Jane-wit, D., Qin, L. & Tellides, G. Interacting mechanisms in the pathogenesis of cardiac allograft vasculopathy. *Arter. Thromb Vasc Biol* **34**, 1609–1614 (2014).
30. Lebastchi, A. H. et al. TGF-β Expression by Human Vascular Cells Inhibits IFN-γ Production and Arterial Media Injury by Alloreactive Memory T Cells. *Am. J. Transplant* (2011). doi:10.1111/j.1600-6143.2011.03676.x
31. Kroesen, B.-J. et al. Immuno-miRs: Critical regulators of T-cell development, function and ageing. *Immunology* (2014). doi:10.1111/imm.12367

32. Van Mil, A. et al. MicroRNA-214 inhibits angiogenesis by targeting Quaking and reducing angiogenic rowth factor release. *Cardiovascular Research* **93**, 655–665 (2012).
33. Pober, J. S. & Tellides, G. Participation of blood vessel cells in human adaptive immune responses. *Trends in Immunology* **33**, 49–57 (2012).
34. Wehner, J. R. & Baldwin 3rd, W. M. Cardiac allograft vasculopathy: do adipocytes bridge alloimmune and metabolic risk factors? *Curr Opin Organ Transpl.* **15**, 639–644 (2010).
35. Small, E. M. & Olson, E. N. Pervasive roles of microRNAs in cardiovascular biology. *Nature* **469**, 336–342 (2011).
36. Selaru, F. M. et al. MicroRNA-21 is overexpressed in human cholangiocarcinoma and regulates programmed cell death 4 and tissue inhibitor of metalloproteinase 3. *Hepatology* **49**, 1595–1601 (2009).
37. Wang, Y. et al. Alloimmune-mediated vascular remodeling of human coronary artery grafts in immunodeficient mouse recipients is independent of preexisting atherosclerosis. *Transplantation* **83**, 1501–1505 (2007).
38. Aurora, A. B. et al. MicroRNA-214 protects the mouse heart from ischemic injury by controlling Ca 2+ overload and cell death. *J. Clin. Invest.* **122**, 1222–1232 (2012).
39. Wang, X. et al. miR-214 targets ATF4 to inhibit bone formation. *Nat. Med.* **19**, 93–100 (2013).
40. Daniel, J.-M. et al. Inhibition of miR-92a improves re-endothelialization and prevents neointima formation following vascular injury. *Cardiovasc. Res.* **103**, 564–72 (2014).
41. Wahlquist, C. et al. Inhibition of miR-25 improves cardiac contractility in the failing heart. *Nature* **508**, 531–5 (2014).

Supplemental data

Supplemental figure 1. end-to-end anastomotic continuous suture technique.

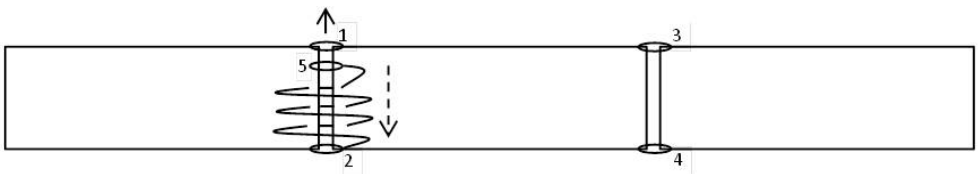

Supplemental figure 2. Anti-miR treatment in a humanized mouse model for AV

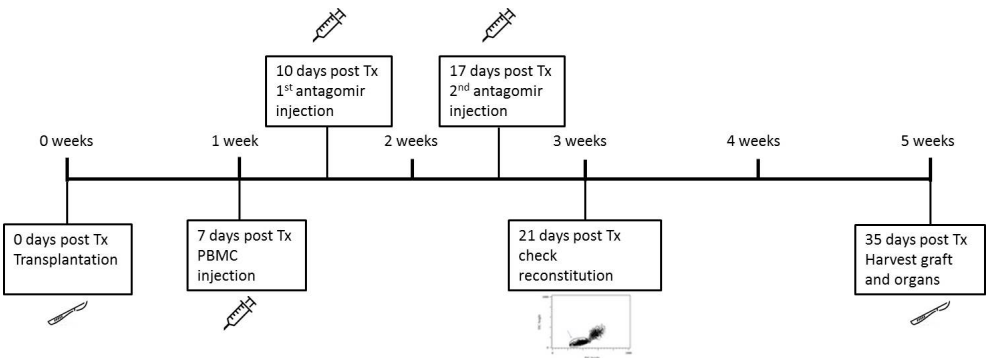

Supplemental table 1. Antibodies used for immunohistochemistry.

Antibody	Target	Staining	Dilution	Manufacturer	Lot number
αSMA	Alpha smooth muscle actin	Cytoplasmic	1:1500	Sigma Aldrich	052K4845
CD3	T cell co receptor	Membrane	1:200	Beckton Dickinson	668
CD45	leukocyte common antigen	Membrane	1:100	Dako	030
CD68	Intracellular glycoproteins	Cytoplasmic/granules	1:1000	Novocastra	6009203

Supplemental table 2. Correlation of microRNA expression values in different vessel layers. Spearman correlation coefficients (r-values). Bold values indicate a significant correlation (** p<0.01, * p<0.05).

		miR-146	miR-214	miR-223	miR-886
miR-21	Intima	0.539	0.527	**0.636***	0.455
	Media	0.091	0.467	0.018	0.527
	Adventitia	**0.879****	0.091	**0.806****	0.164
	ELS	**0.952****	0.310	**0.855***	0.595
miR-146	Intima	-	0.321	**0.636***	0.515
	Media	-	0.248	**0.806****	0.430
	Adventitia	-	0.055	**0.855****	0.164
	ELS	-	0.310	**0.786***	0.500
miR-214	Intima	-	-	**0.806****	**0.709***
	Media	-	-	0.442	**0.770****
	Adventitia	-	-	0.091	0.527
	ELS	-	-	0.524	0.667
miR-223	Intima	-	-	-	0.624
	Media	-	-	-	0.564
	Adventitia	-	-	-	0.382
	ELS	-	-	-	**0.738***

Chapter 10.

GENERAL DISCUSSION

This thesis focused on the pathogenesis of Cardiac Allograft Vasculopathy and elucidated new aspects of this long-term problem after heart transplantation. Besides intima expansion (**Chapter 2** [1]) and fibrosis (**Chapter 3** [2]), which are often referred to as the main features of CAV, this thesis showed that ectopic lymphoid structures (ELS) surrounding CAV arteries should not be underestimated in the pathogenesis of chronic rejection (**Chapter 4 and 5**). New insights in molecular pathways (e.g. microRNA regulation) of other pathologies could be applied on CAV as well (**Chapter 8 and 9**). By understanding the disease mechanism on a morphological, cellular and molecular level, new options for diagnosis, prognosis, and therapy could be considered.

In current clinical practice not much attention is paid to CAV; we know that it exists and happens, but we do not know what to do with it [3]. A main reason for this is that there is no clear possibility to diagnose CAV, no definite follow-up of CAV, and (even more important) no treatment options. Besides that, the mechanism is still not fully understood, it is complicated, and is considered multi-factorial [4,5]. With this in mind, discussions in clinical practice about CAV often bring up many questions [6]; e.g. Where do we start diagnosis for our heart transplant patients? And if diagnosed, what can we do? What treatment options do we have? Fighting CAV in these cases often feels like "having your back against the wall", not knowing where to start. With the research presented in this thesis we tried to open new doors towards understanding CAV and finding clues for novel diagnosis or treatment options.

Diagnosis - imaging

Although CAV has been described since the beginning of transplantation [7] there was no uniform international standard nomenclature for this entity [6]. Diagnosis of CAV was recently standardized by an ISHLT working formulation, which is predominantly based on angiography since this technique is universal in availability for both adult and pediatric patients, clinically accepted, and applicable at any time in the post-transplantation process [6]. This classification is a valuable tool for prognostic stratification of HTx patients (in CAV0, CAV1, CAV2, and CAV3) at 1 year post transplant. Patients with CAV2 and CAV3 are associated with poor prognosis in developing major adverse cardiovascular events (MACE) later after transplant [8]. These developments on angiography classifications helped to determine CAV in a standardized way, but did not take away limitations of the technique [9]. It remains hard to distinguish CAV from classical atherosclerosis since both cause vessel narrowing that is detected by angiography [10]. Well known in atherosclerosis are intra plaque hemorrhage and multi layered thrombosis, which are recently also described in CAV patients [11,12]. Also in these studies, the distinction between atherosclerosis and CAV is not a matter of black and white classification. These two coronary vasculature diseases overlap in risk factors, but are completely different in histology (eccentric and patchy versus concentric and diffuse) and major cause (lifestyle versus transplant).

Although angiography detection for CAV developed, this technique still has some limitations that might be overcome by novel imaging techniques. The question is whether we are ready to switch to these new techniques in clinical practice [13]. Next to the prognostic value of angiography, imaging by intravascular ultrasound (IVUS) showed to have prognostic value [14]. Moreover, IVUS has brought improvements in CAV diagnosis due to its possibility of visualizing the arterial wall [15,16]. In this thesis a histological classification of CAV is presented

that indicate that there are various stages in CAV development. In early stages inflammation is a major component whereas in later stages fibrosis in more prominent. These different stages may require different treatment modalities (**Chapter 2** [1]), requiring a more advanced imaging modality to initiate the right treatment. With a more advanced IVUS technique, Virtual Histology IVUS (VH-IVUS), information can be obtained about vessel wall composition 17,18. The clinical importance of a technique to visualize components of the vessel wall implicates the need for more cellular/molecular imaging technique to classify the pathological process in the patient [19]. Reviews state that understanding CAV lesion types is important in this development [20], which we presented in this thesis (**Chapter 2** [1]) and has been described by others [21].

Newer techniques to visualize coronary arteries post-transplant are currently tested. Coronary computed tomography angiography (CCTA / coronary CTA) shows promising results. It is a reliable noninvasive imaging technique with high sensitivity, specificity, and negative predictive value for the detection of CAV [22,23]. Optical coherence tomography (OCT) is an intravascular imaging technique with high-resolution and allows detailed assessment of the coronary arterial wall with detection of very early morphological changes [24–26]. Besides these techniques, multi parametric cardiovascular magnetic resonance (CMR) shows improvements in diagnosing CAV [27]. Although more accurate techniques are developed for CAV diagnosis, their clinical predictive value in heart transplant patients needs still to be tested.

To understand and follow the process of CAV in cardiac transplant patients, molecular imaging can help out in the future as suggested in the field of oncology [28] and vascular inflammation [29]. If one could inject tracers that target specific components known to be involved in CAV (e.g. T cells, macrophages, IFNγ, etc) the process could be visualized based on that marker [30,31]. With the presence and quantity of that specific marker in the coronary arterial wall personalized treatment for that patient could be applied. If molecular imaging is possible in transplant patients, this technique could be applied for other important graft characteristics in the follow-up period. As presented in this thesis not only the intima is important in CAV development, but also ectopic lymphoid structures (ELS) are involved (**Chapter 4**). When the role of the ELS is established in more detail and we could visualize these structures for their presence and their quantity of B cells or antibodies (**Chapter 5**), these molecular imaging techniques could not only be applied on CAV development after cardiac transplantation, but also to follow up antibody mediated rejection or acute rejection episodes in a patient specific and non-invasive way. Besides, if possible on the transplanted heart, why not on kidney, lung, liver, and other solid organs after transplantation?

Diagnosis - biomarkers

Another approach to follow the process of a transplanted organ is by measurements of biomarkers. Biomarkers serve as a single marker from a non-invasive sample (e.g. blood) which gives enough information regarding the disease process to provide a diagnosis, prognosis, or optimize therapy. Ideally, biomarkers are so sensitive that they could determine an early diagnosis of CAV to apply therapy, before the point of no-return. For CAV biomarkers, most progress was reached on more general inflammatory or injury protein levels from blood samples like C-reactive protein (CRP), Troponin I, von Willebrand factor, BNP, IGF-1, and many others [32–38]. Recently, more broad protein bio-signatures were reported to have the ability

to differentiate between patients with angiographically significant CAV from those without CAV. This signature also provides insight in the underlying immune and non-alloimmune mechanisms of CAV [39].

All presented protein markers provide insight in the pathogenesis, but are not specific enough to apply as biomarker in the clinical setting. Therefore, a more specific CAV marker is necessary to diagnosis and determine the onset of the process. One possibility for such markers are microRNAs, which can be tissue-/cell-specific and are very stable in serum and plasma. They are described as markers for cardiac injury [40] and acute rejection after heart transplantation [41,42]. We are the first to describe altered microRNA expression levels in CAV arteries, that might provide more specific markers for non-invasive, early diagnosis. Unfortunately, the spectrum of miR expression in the intima of CAV arteries, was not directly visualized in the miR spectrum in serum (**Chapter 8**). So, the search for specific miR in serum by more sensitive detection devices that correlate with CAV stage may result in important advances in CAV screening.

With the innovations of more sensitive techniques to measure markers in blood the term 'liquid biopsies' has evolved. This implicates that we do not need invasive biopsies (e.g. endomyocardial biopsies) for disease diagnosis but can diagnose a patient based on liquid samples that mirror the solid disease process, and again the field of oncology is leading in this area [43].

Also in the field of transplantation the possibilities of cell-free DNA in blood samples are explored [44,45]. In cardiac transplantation the first steps are taken to follow graft injury and possible rejection episodes with digital droplet PCR [46–48]. These first studies show promising results which may eventually lead to parallel analysis with endomyocardial biopsies or even replacement of these invasive biopsy procedures [46,49] (**Figure 1**). Further research could elucidate whether cell free DNA could provide information on CAV development as well. In future donor specific markers like detection of X/Y chromosome in mismatched transplants or patient specific single nucleotide polymorphisms (SNPs) could be used [50].

For the best diagnosis and treatment choice of our patients, we should bring together biomarker information and imaging techniques. The earlier and the more detailed we can examine the patient for CAV, the better we can apply personalized treatment options, and the longer graft survival.

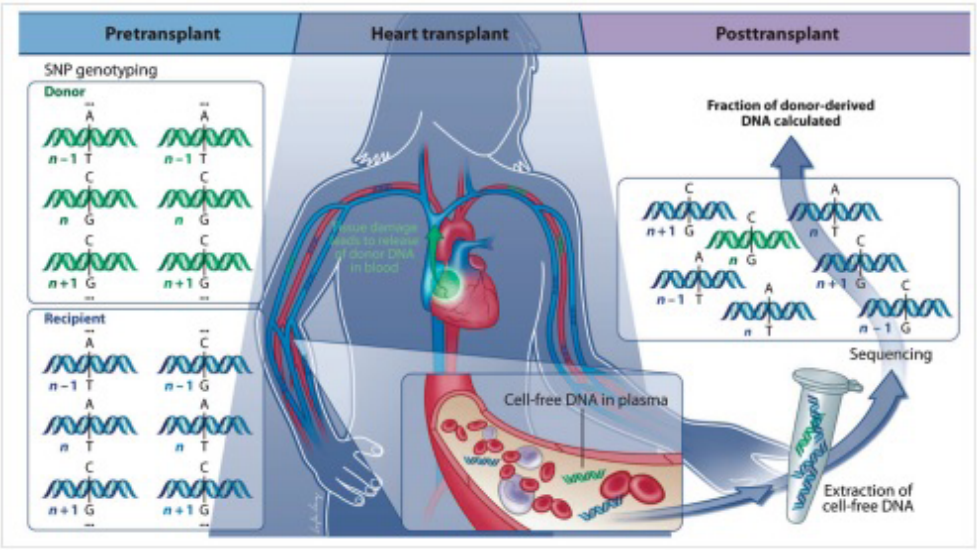

Figure 1. Post-transplant screening using molecular targets in liquid biopsies. Source: De Vlaminck I, Valantine HA, Snyder TM, Strehl C, Cohen G, Luikart H, Neff NF, Okamoto J, Bernstein D, Weisshaar D, Quake SR, Khush KK. Sci Transl Med. 2014 Jun 18;6(241):241ra77. Reproduced with permission.of dr Kiran Kush, December 2014.

Acute cellular rejection, antibody mediated rejection, and Cardiac Allograft Vasculopathy

10

Often we are confused by the different types of rejection and wonder if acute cellular rejection (ACR), antibody mediated rejection (AMR), or cardiac allograft vasculopathy (CAV) is responsible for graft failure. We do know that both, ACR and AMR, are associated with a greater risk of CAV development [51]. As presented at the ISHLT in April 2014, the topic of mixed rejection (AMR and ACR) is not fully understood. Some researchers state that AMR develops after acute cellular rejection (ACR), some state that AMR triggers ACR, and others believe that these two rejection processes can go hand-in-hand. This was nicely demonstrated at the ISHLT scientific meeting 2014 by Dr Kfoury. How antibodies play their role in cardiac allograft vasculopathy is not yet known, but studies on ELS like presented in **chapter 4** and **chapter 5** could contribute in unraveling this phenomenon. Our data indicate that ELS could play an important role in the B cell response (**Chapter 5**).

It is important to understand how antibodies can affect CAV in the search of therapeutic targets. Antibodies can be directed towards donor specific HLA type or non-HLA antigens [52,53]. The effect of non-HLA antibodies suggest a process similar to autoimmunity involved in chronic rejection. Both antibody families could damage the graft via complement binding [54]. Therapies for AMR are still evolving, but studies showed some success with the use of plasmapheresis, intravenous immune globulin (IVIg), immunoadsorption, bortezomib, rituximab, and others [55–57]. However, more research needs to be done to explore how these

therapies work, when they are applied, and what their effects are on CAV. Another important, yet unresolved, issue is how in the transplanted heart locally produced antibodies correlate with antibodies in the blood. These relations are critical for AMR screening of transplanted patients.

Treatment of CAV

When allograft vasculopathy after cardiac transplantation is diagnosed, often this is after the point of 'no return'. In these cases there is no standardized treatment available except for re-transplantation, but this is generally no option due to a lack of donor organs and many patients waiting for a heart transplant [58]. New surgical and therapeutic options are explored to overcome this problem.

The major complication caused by CAV is myocardial infarction due to lumen narrowing of coronary arteries. If specific sites within the vascular tree of the heart are affected, percutaneous coronary interventions (PCA) or coronary artery bypass grafting (CABG) can be applied [59]. Due to the diffuse nature of the disease, affecting all coronary arteries, these surgical interventions are like fighting a running battle. However, since no other treatment options are available, these invasive techniques are experimentally tested [60,61]. Another revascularization technique is the use of bioresorbable vascular scaffolds which attempts to avoid restenosis by transient elution of anti-proliferative drug to inhibit excessive neointimal hyperplasia [62,63]. However, this intervention can only be applied if CAV progression is local, excluding the majority of HTx patients suffering from diffuse allograft vasculopathy. These desperate attempts underline the necessity for new treatment options, applicable in all patients with CAV [64].

Although CAV is often studied in epicardial coronary arteries of the transplanted heart, the microvascular changes are often underestimated. At these sites CAV presents first, the lumen is easily occluded, leading to micro myocardial infarctions, heart failure and the characteristic patchy fibrotic pattern with the heart [65]. Collateral formation due to these occlusions is suggested to play a role in graft survival [66]. The microvasculature is as much affected by CAV, as the larger coronary vessels, but treatment options for microvascular changes are even more difficult. More attention needs to be paid to this feature of chronic rejection.

To target CAV, the pathogenesis of the disease should be understood. If the role of the donor and the recipient cells is known, we could target donor factors (e.g. ischemia reperfusion damage, ex vivo perfusion, etc) or recipient factors (immune suppression, proliferation inhibitors, etc.), which are both involved (**Chapter 6**). The phenotype of CAV should be known before targeting a specific factor within that stage [1,67]. Recently was shown that proliferation inhibitors only slow CAV down when applied early after transplantation, suggesting that in this phase proliferation can be targeted [68].

To understand CAV from multiple perspectives, a proper mouse model is necessary for pre-clinical research. The available humanized mouse models used in transplantation research are presented in **Chapter 7** [69]. However, these models are not optimal yet since they still do not fully mimic the human system. The most optimal model is the model described in **Chapter 9**, which is mainly based on the influx of memory T cells [70–72]. However, as stated in **Chapter 3** [2], the role of macrophages should not be underestimated. We think that

macrophages can give the last boost to the process of allograft vasculopathy to eventually cause a fibrotic lesion. The lack of macrophages in the current humanized mouse models hampers the understanding of this final phase [73]. Next to macrophages, also antibodies are involved in CAV progression as we presented in **Chapter 4** and **5**. Small animal models showed that although antibodies contribute to allograft vasculopathy, lesions still develop in the absence of a humoral response [74-77]. The lack of a biological human B cell response in these models limits our understanding of the humoral response in allograft vasculopathy. New, "next generation" humanized mouse models with improvements on macrophage and B cells are currently developed [78]. Approaches to genetically modify mice in a way that improves human cell engraftment and allows expression of human-specific growth factors and cytokines should provide opportunities, but it will probably take several years before fully implemented in the field of transplantation.

Within the experimental field many approaches are tried to find new targets for therapy in allograft vasculopathy. In the experimental setting influencing factors like CTGF [79], NKG2D [80], OX40L [81], Tim-1-Fc [82], $CD14^+$ monocytes [83], and regulatory T cells [84] have all been described as 'promising targets'. Many researchers go from an experimental approach to confirmation in the transplant population. Whereas others, ourselves included, start the other way around; from the human perspective (**Chapter 8**), where after confirmation of these principles in experimental models (**Chapter 9**).

Proliferation inhibitors (everolimus and sirolimus) were shown only affective in the early phases of CAV [68,85]. This indicates that mTOR inhibitors cannot be generally applied, but can only be used in patients with CAV lesions containing proliferating lymphocytes or SMCs. Patients with end-stage, fibrotic lesions will probably not react on these anti-proliferative therapies. In these patients other strategies, associated with fibrosis (e.g. miR-21), should be used. Information about the composition of the arterial wall, as described in **Chapter 2**, is crucial [1].

Within our quest for molecular targets to tune the process of CAV, we choose small non-coding RNAs (**Chapter 8** and **9**). These small molecules (microRNAs) are presumably disease specific, stable in *in vivo* application and cause less side effects due to subtle regulation of the process. In all pathways of the CAV process (immunology, proliferation, or fibrosis) miRs are involved, we 'just' need to pick the right miR for the right process.

The way of administration of the specific microRNA can be by intra venous injection at the time of CAV onset or administration to the donor heart prior to transplantation. The latter option could be used as prophylaxis for CAV by 'resetting' the donor organ. The donor organ could be flushed with donor-specific medication to prevent vascular injury after transplantation. This theory is already applied in experimental models for lung transplantation using ex vivo perfusion systems [86,87]. As presented in **Chapter 8** and **9**, miR-214 was significantly lower in arteries with allograft vasculopathy, suggesting a protective role for this microRNA. Flushing the heart with this microRNA (mimic) prior to transplantation, could potentially protect the heart from vascular injury and eventually CAV development. The same accounts for the two miRs chosen without our experimental setting (**Chapter 9**); miR-21 and miR-146b-5p. When *ex vivo* heart perfusion would be applicable in future clinical practice, we could apply factors necessary for that specific donor organ to prolong graft survival. These factors can target pathways involved in endothelial damage, cell death, ischemia-reperfusion injury, and many other processes related to CAV. For each donor organ we could apply 'personalized medicine' with the specific factor (e.g. microRNA) to restore the damaged organ and get better long-

term outcomes after cardiac transplantation. If a donor-recipient organ combination would suggest a fierce immune response, lowering miR-146b-5p expression prior to transplantation could prevent this. If the risk of a more fibrotic process is predicted, anti-miR treatment for miR-21 could be suggested.

As miRs are regulator of protein transcription, regulation of "immune regulators" might be a good approach for targeted therapy as well [88]. Recently was shown that instead of targeting cytokines or T cells directly, the regulation of cytokine signals could be an interesting approach. SOCS1 (suppressor of cytokine signaling 1) showed to play an important role in AV [89]. Since no therapeutics towards SOCS1 are developed, regulation of this target could be done by miR inhibition (e.g. miR-155 and -122). Regulation of "regulators" (miRs, SOCS1, etc) in general might be an appropriate approach to avoid side effects and tune the process of CAV.

The good side

Although this thesis focused on heart transplantation with chronic complications hampering long-term survival, we need to remember that this treatment saves many lives. Cases are described with over 20 year survival after cardiac transplantation[90] suggesting there are possibilities for many more patients in the future. Although not found yet, the 'holy grail' for long-term graft survival is somewhere out there.

References

1. Huibers, M. M. H. et al. Distinct phenotypes of cardiac allograft vasculopathy after heart transplantation: A histopathological study. *Atherosclerosis* **236**, 353–359 (2014).
2. Huibers, M. et al. Intimal fibrosis in human cardiac allograft vasculopathy. *Transpl. Immunol.* **25**, 124–132 (2011).
3. Arora, S. & Gullestad, L. The challenge of allograft vasculopathy in cardiac transplantation. *Curr. Opin. Organ Transplant.* **19**, 508–14 (2014).
4. Pober, J. S., Jane-wit, D., Qin, L. & Tellides, G. Interacting mechanisms in the pathogenesis of cardiac allograft vasculopathy. *Arter. Thromb Vasc Biol* **34**, 1609–1614 (2014).
5. Costello, J. P., Mohanakumar, T. & Nath, D. S. Mechanisms of chronic cardiac allograft rejection. *Tex Hear. Inst J* **40**, 395–399 (2013).
6. Mehra, M. R. et al. International Society for Heart and Lung Transplantation working formulation of a standardized nomenclature for cardiac allograft vasculopathy-2010. *J. Hear. lung Transplant.* **29**, 717–27 (2010).
7. Billingham, M. E. Cardiac transplant atherosclerosis. *Transplant. Proc.* **19**, 19–25 (1987).
8. Prada-Delgado, O., Estévez-Loureiro, R., Paniagua-Martín, M. J., López-Sainz, A. & Crespo-Leiro, M. G. Prevalence and prognostic value of cardiac allograft vasculopathy 1 year after heart transplantation according to the ISHLT recommended nomenclature. *J. Hear. lung Transplant.* **31**, 332–3 (2012).
9. Cai, Q., Rangasetty, U. C., Barbagelata, A., Fujise, K. & Koerner, M. M. Cardiac allograft vasculopathy: advances in diagnosis. *Cardiol. Rev.* **19**, 30–5 (2011).
10. Angelini, A. et al. Coronary cardiac allograft vasculopathy versus native atherosclerosis: difficulties in classification. *Virchows Arch* **464**, 627–635 (2014).
11. Castellani, C. et al. Intraplaque hemorrhage in cardiac allograft vasculopathy. *Am. J. Transplant.* **14**, 184–192 (2014).
12. Matsuo, Y. et al. Repeated episodes of thrombosis as a potential mechanism of plaque progression in cardiac allograft vasculopathy. *Eur. Heart J.* **34**, 2905–2915 (2013).
13. Kobashigawa, J. Coronary computed tomography angiography: is it time to replace the conventional coronary angiogram in heart transplant patients? *J. Am. Coll. Cardiol.* **63**, 2005–6 (2014).
14. Kobashigawa, J. A. et al. Multicenter intravascular ultrasound validation study among heart transplant recipients: Outcomes after five years. *J. Am. Coll. Cardiol.* **45**, 1532–1537 (2005).
15. Torres, H. J. et al. Prevalence of cardiac allograft vasculopathy assessed with coronary angiography versus coronary vascular ultrasound and virtual histology. *Transplant. Proc.* **43**, 2318–2321 (2011).
16. Logani, S., Saltzman, H. E., Kurnik, P., Eisen, H. J. & Ledley, G. S. Clinical utility of intravascular ultrasound in the assessment of coronary allograft vasculopathy: A review. *J. Interv. Cardiol.* **24**, 9–14 (2011).
17. Hernandez, J. M. de la T. et al. Virtual histology intravascular ultrasound assessment of cardiac allograft vasculopathy from 1 to 20 years after heart transplantation. *J. Heart Lung Transplant.* **28**, 156–162 (2009).
18. König, A. et al. Assessment and Characterization of Time-related Differences in Plaque Composition by Intravascular Ultrasound-derived Radiofrequency Analysis in Heart Transplant Recipients. *J. Hear. Lung Transplant.* **27**, 302–309 (2008).
19. Tomai, F. et al. Coronary plaque composition assessed by intravascular ultrasound virtual histology: Association with long-term clinical outcomes after heart transplantation in young adult recipients. *Catheter. Cardiovasc. Interv.* **83**, 70–77 (2014).
20. Pollack, A., Nazif, T., Mancini, D. & Weisz, G. Detection and imaging of cardiac allograft vasculopathy. *JACC Cardiovasc. Imaging* **6**, 613–623 (2013).
21. Devitt, J. J. et al. Impact of donor benign intimal thickening on cardiac allograft vasculopathy. *J. Hear. lung Transplant.* **32**, 454–60 (2013).
22. Mittal, T. K., Panicker, M. G., Mitchell, A. G. & Banner, N. R. Cardiac allograft vasculopathy after heart transplantation: electrocardiographically gated cardiac CT angiography for assessment. *Radiology* **268**, 374–81 (2013).
23. Wever-Pinzon, O. et al. Coronary computed tomography angiography for the detection of cardiac allograft vasculopathy: A meta-analysis of prospective trials. *J. Am. Coll. Cardiol.* **63**, 2005–2006 (2014).
24. Khandhar, S. J. et al. Optical coherence tomography for characterization of cardiac allograft vasculopathy after heart transplantation (OCTCAV study). *J. Hear. Lung Transplant.* **32**, 596–602 (2013).
25. Cassar, A. et al. Coronary atherosclerosis with vulnerable plaque and complicated lesions in transplant recipients: New insight into cardiac allograft vasculopathy by optical coherence tomography. *Eur. Heart J.* **34**, 2610–2617 (2013).
26. Imamura, T. et al. Donor-Transmitted Coronary Atherosclerosis by Optical Coherence Tomography Imaging in a Heart Transplantation Recipient Double Layered Intimal Thickness. *Int. Heart J.* **55**, 178–180 (2014).
27. Miller, C. A. et al. Multiparametric cardiovascular magnetic resonance assessment of cardiac allograft vasculopathy. *J. Am. Coll. Cardiol.* **63**, 799–808 (2014).
28. Massoud, T. F. & Gambhir, S. S. Molecular imaging in living subjects: seeing fundamental biological processes in a new light. *Genes Dev.* **17**, 545–580 (2003).
29. Ammirati, E. et al. Non-invasive imaging of vascular inflammation. *Front. Immunol.* **5**, 399 (2014).
30. Weissleder, R., Nahrendorf, M. & Pittet, M. J. Imaging macrophages with nanoparticles. *Nat. Mater.* **13**, 125–38 (2014).

31. Chakravarty, R., Goel, S. & Cai, W. Nanobody: The "magic bullet" for molecular imaging? *Theranostics* **4**, 386–398 (2014).
32. Eisenberg, M. S. et al. Elevated levels of plasma C-reactive protein are associated with decreased graft survival in cardiac transplant recipients. *Circulation* **102**, 2100–2104 (2000).
33. Labarrere, C. A. et al. C-reactive protein, arterial endothelial activation, and development of transplant coronary artery disease: A prospective study. *Lancet* **360**, 1462–1467 (2002).
34. Labarrere, C. A. & Jaeger, B. R. Biomarkers of heart transplant rejection: the good, the bad, and the ugly! *Transl Res* **159**, 238–251 (2012).
35. Martínez-Dolz, L. et al. Follow-up study on the utility of von Willebrand factor levels in the diagnosis of cardiac allograft vasculopathy. *J. Hear. lung Transplant.* **27**, 760–766 (2008).
36. Mehra, M. R., Uber, P. A., Ventura, H. O., Scott, R. L. & Park, M. H. The impact of mode of donor brain death on cardiac allograft vasculopathy: An intravascular ultrasound study. *J. Am. Coll. Cardiol.* **43**, 806–810 (2004).
37. Aharinejad, S. et al. Low serum IGF-1 is a risk factor for cardiac allograft vasculopathy in cardiac transplant recipients. *Transplantation* **93**, 309–13 (2012).
38. Seki, A. & Fishbein, M. C. Predicting the development of cardiac allograft vasculopathy. *Cardiovasc. Pathol.* **23**, 253–60 (2014).
39. Lin, D. et al. Plasma protein biosignatures for detection of cardiac allograft vasculopathy. *J. Hear. lung Transplant.* **32**, 723–33 (2013).
40. Wang, E. et al. Circulating miRNAs reflect early myocardial injury and recovery after heart transplantation. *J. Cardiothorac. Surg.* **8**, 165 (2013).
41. Sukma Dewi, I., Torngren, K., Gidlöf, O., Kornhall, B. & Ohman, J. Altered serum miRNA profiles during acute rejection after heart transplantation: potential for non-invasive allograft surveillance. *J. Hear. lung Transplant.* **32**, 463–6 (2013).
42. Duong Van Huyen, J.-P. et al. MicroRNAs as non-invasive biomarkers of heart transplant rejection. *Eur. Heart J.* **35**, 3194–202 (2014).
43. Diaz, L. A. & Bardelli, A. Liquid biopsies: Genotyping circulating tumor DNA. *J. Clin. Oncol.* **32**, 579–586 (2014).
44. Oellerich, M. et al. Use of graft-derived cell-free DNA as an organ integrity biomarker to reexamine effective tacrolimus trough concentrations after liver transplantation. *Ther. Drug Monit.* **36**, 136–40 (2014).
45. Macher, H. C. et al. Monitoring of Transplanted Liver Health by Quantification of Organ-Specific Genomic Marker in Circulating DNA from Receptor. *PLoS One* **9**, e113987 (2014).
46. De Vlaminck, I. et al. Circulating cell-free DNA enables noninvasive diagnosis of heart transplant rejection. *Sci. Transl. Med.* **6**, 241ra77 (2014).
47. Hidestrand, M. et al. Highly sensitive noninvasive cardiac transplant rejection monitoring using targeted quantification of donor-specific cell-free deoxyribonucleic acid. *J. Am. Coll. Cardiol.* **63**, 1224–6 (2014).
48. Beck, J. et al. Digital droplet PCR for rapid quantification of donor DNA in the circulation of transplant recipients as a potential universal biomarker of graft injury. *Clin. Chem.* **59**, 1732–1741 (2013).
49. Snyder, T. M., Khush, K. K., Valantine, H. A. & Quake, S. R. Universal noninvasive detection of solid organ transplant rejection. *Proc. Natl. Acad. Sci. U. S. A.* **108**, 6229–6234 (2011).
50. Li, L. et al. Identification of common blood gene signatures for the diagnosis of renal and cardiac acute allograft rejection. *PLoS One* **8**, (2013).
51. Frank, R. et al. Circulating donor-specific anti-human leukocyte antigen antibodies and complement c4d deposition are associated with the development of cardiac allograft vasculopathy. *Am. J. Clin. Pathol.* **142**, 809–15 (2014).
52. Reinsmoen, N. L. et al. Increased negative impact of donor HLA-specific together with non-HLA-specific antibodies on graft outcome. *Transplantation* **97**, 595–601 (2014).
53. Dragun, D., Philippe, A. & Catar, R. Role of non-HLA antibodies in organ transplantation. *Curr. Opin. Organ Transplant.* **17**, 440–5 (2012).
54. Jane-Wit, D. et al. Alloantibody and complement promote T cell-mediated cardiac allograft vasculopathy through noncanonical nuclear factor-kappaB signaling in endothelial cells. *Circulation* **128**, 2504–2516 (2013).
55. Kittleson, M. M. & Kobashigawa, J. A. Antibody-mediated rejection. *Curr Opin Organ Transpl.* **17**, 551–557 (2012).
56. Fishbein, M. C. & Kobashigawa, J. Biopsy-negative cardiac transplant rejection: etiology, diagnosis, and therapy. *Curr. Opin. Cardiol.* **19**, 166–169 (2004).
57. Sadaka, B., Alloway, R. R. & Woodle, E. S. Management of antibody-mediated rejection in transplantation. *Surg. Clin. North Am.* **93**, 1451–1466 (2013).
58. Saito, T., Hiemann, N., Krabatsch, T., Potapov, E. & Hetzer, R. Cardiac allograft failure: retransplant or long-term ventricular assist device? *J. Thorac. Cardiovasc. Surg.* **147**, e29–30 (2014).
59. Prada-Delgado, O. et al. Percutaneous coronary interventions and bypass surgery in patients with cardiac allograft vasculopathy: A single-center experience. *Transplant. Proc.* **44**, 2657–2659 (2012).
60. Agarwal, S. et al. Long-term mortality after cardiac allograft vasculopathy: implications of percutaneous intervention. *JACC. Heart Fail.* **2**, 281–8 (2014).
61. Tadwalkar, R. & Lee, M. Unprotected left main coronary artery percutaneous coronary intervention in a pediatric patient with cardiac allograft vasculopathy. *J. Invasive Cardiol.* **26**, E156–60 (2014).
62. Ribichini, F., Pighi, M., Faggian, G. & Vassanelli, C. Bioresorbable vascular scaffolds in cardiac allograft vasculopathy: a new therapeutic option. *Am. J. Med.* **126**, e11–4 (2013).

63. Serruys, P. W. et al. A bioabsorbable everolimus-eluting coronary stent system (ABSORB): 2-year outcomes and results from multiple imaging methods. *Lancet* **373**, 897–910 (2009).
64. Benatti, R. D. & Taylor, D. O. Evolving concepts and treatment strategies for cardiac allograft vasculopathy. *Curr. Treat. Options Cardiovasc. Med.* **16**, 278 (2014).
65. Tona, F. et al. Recent developments on coronary microvasculopathy after heart transplantation: a new target in the therapy of cardiac allograft vasculopathy. *Curr Vasc Pharmacol* **10**, 206–215 (2012).
66. Lavine, K. J. et al. Coronary collaterals predict improved survival and allograft function in patients with coronary allograft vasculopathy. *Circ. Hear. Fail.* **6**, 773–784 (2013).
67. Lu, W. H. et al. Diverse morphologic manifestations of cardiac allograft vasculopathy: A pathologic study of 64 allograft hearts. *J. Hear. Lung Transplant.* **30**, 1044–1050 (2011).
68. Masetti, M. et al. Differential effect of everolimus on progression of early and late cardiac allograft vasculopathy in current clinical practice. *Am. J. Transplant.* **13**, 1217–26 (2013).
69. Hogenes, M., Huibers, M., Kroone, C. & de Weger, R. Humanized mouse models in transplantation research. *Transplant. Rev.* **28**, 103–110 (2014).
70. Lorber, M. I. et al. Human allogeneic vascular rejection after arterial transplantation and peripheral lymphoid reconstitution in severe combined immunodeficient mice. *Transplantation* **67**, 897–903 (1999).
71. Burns, W. R. et al. Recruitment of CXCR3+ and CCR5+ T cells and production of interferon-γ-inducible chemokines in rejecting human arteries. *Am. J. Transplant.* **5**, 1226–1236 (2005).
72. Yi, T. et al. Human allograft arterial injury is ameliorated by sirolimus and cyclosporine and correlates with suppression of interferon-gamma. *Transplantation* **81**, 559–566 (2006).
73. Kirkiles-Smith, N. C. et al. Development of a humanized mouse model to study the role of macrophages in allograft injury. *Transplantation* **87**, 189–197 (2009).
74. Chow, L. H., Huh, S., Jiang, J., Zhong, R. & Pickering, J. G. Intimal thickening develops without humoral immunity in a mouse aortic allograft model of chronic vascular rejection. *Circulation* **94**, 3079–3082 (1996).
75. Gareau, A., Hirsch, G., Lee, T. & Nashan, B. Contribution of B cells and antibody to cardiac allograft vasculopathy. *Transplantation* **88**, 470–477 (2009).
76. Russell, P. S., Chase, C. M. & Colvin, R. B. Alloantibody- and T cell-mediated immunity in the pathogenesis of transplant arteriosclerosis: lack of progression to sclerotic lesions in B cell-deficient mice. *Transplantation* **64**, 1531–1536 (1997).
77. Zeng, Q. et al. B cells mediate chronic allograft rejection independently of antibody production. *J Clin Invest* **124**, 1052–1056 (2014).
78. Brehm, M. A., Wiles, M. V., Greiner, D. L. & Shultz, L. D. Generation of improved humanized mouse models for human infectious diseases. *Journal of Immunological Methods* (2014). doi:10.1016/j.jim.2014.02.011
79. Pantou, M. P., Manginas, A., Alivizatos, P. A. & Degiannis, D. Connective tissue growth factor (CTGF/CCN2): A protagonist in cardiac allograft vasculopathy development? *J. Hear. Lung Transplant.* **31**, 881–887 (2012).
80. Chen, H. et al. NKG2D blockade attenuated cardiac allograft vasculopathy in a mouse model of cardiac transplantation. *Clin. Exp. Immunol.* **173**, 544–552 (2013).
81. Wang, H. et al. Memory T Cells Mediate Cardiac Allograft Vasculopathy and are Inactivated by Anti-OX40L Monoclonal Antibody. *Cardiovasc Drugs Ther* **28**, 115–122 (2014).
82. Shi, X. et al. Tim-1-Fc suppresses chronic cardiac allograft rejection and vasculopathy by reducing IL-17 production. *Int J Clin Exp Pathol* **7**, 509–520 (2014).
83. Salama, M. et al. Association of CD14+ monocyte-derived progenitor cells with cardiac allograft vasculopathy. *J. Thorac. Cardiovasc. Surg.* **142**, 1246–53 (2011).
84. Zhu, H. et al. T cell receptor deficiency attenuated cardiac allograft vasculopathy and promoted regulatory T cell expansion. *Scand. J. Immunol.* **78**, 44–49 (2013).
85. Matsuo, Y. et al. Attenuation of cardiac allograft vasculopathy by sirolimus: Relationship to time interval after heart transplantation. *J. Heart Lung Transplant.* **32**, 784–91 (2013).
86. Cypel, M. & Keshavjee, S. Extending the Donor Pool: Rehabilitation of Poor Organs. *Thorac. Surg. Clin.* **25**, 27–31 (2015).
87. Machuca, T. N. et al. Protein Expression Profiling Predicts Graft Performance in Clinical Ex Vivo Lung Perfusion. *Ann. Surg.* **00**, 1–7 (2014).
88. De Weger, R. a. Immune regulators regulated to prevent transplant reactions. *J. Am. Coll. Cardiol.* **63**, 30–2 (2014).
89. Qin, L. et al. SOCS1 prevents graft arteriosclerosis by preserving endothelial cell function. *J. Am. Coll. Cardiol.* **63**, 21–29 (2014).
90. Rodriguez Cetina Biefer, H. et al. Surviving 20 years after heart transplantation: A success story. *Ann. Thorac. Surg.* **97**, 499–505 (2014).

Chapter 11.

SUMMARY / SAMENVATTING

Summary in English

Human Cardiac Allograft Vasculopathy (CAV) is one of the major complications for patients after heart transplantation. It is characterized by a concentric luminal narrowing due to (neo) intimal expansion in the coronary arteries of donor hearts after heart transplantation. The main purpose of this thesis was to study the pathogenesis of Cardiac Allograft Vasculopathy on a morphological, cellular, and molecular level and determine the role of ectopic lymphoid structures surrounding CAV arteries. Ultimately, we aimed to identify a molecular target against the inducing allograft response and/or the fibrosis, and test the ability of this therapy in a well-established humanized mouse model for CAV.

Chapter 1 is a general introduction which describes the role of heart transplantation in heart failure, and the need for more knowledge regarding chronic rejection with CAV in particular. The immunological and fibrotic processes involved in the development of CAV are summarized. The inflammatory response results in dysfunction of the endothelium and migration and proliferation of smooth muscle cells (SMCs). This chapter ends with the aims of this thesis; to study (1) the pathogenesis of Cardiac Allograft Vasculopathy on a morphological, cellular, and molecular level, (2) to investigate the role of ectopic lymphoid structures surrounding CAV arteries, and (3) to identify a molecular target against the inducing allograft response and/or the fibrosis, and test the ability of this therapy in a well-established humanized mouse model for CAV.

Chapter 2 presents our novel formulated histological phenotypes for CAV in relation with clinical patient characteristics. We determined four histological CAV phenotypes (H-CAV 0-3) ranging from benign intima thickening only (H-CAV0), mononuclear inflammatory infiltrate in loose connective tissue (H-CAV1), a second layer of smooth muscle cells in different orientation (H-CAV2), to complete concentric fibrosis (H-CAV3). These stages are related to time after transplantation, age at transplantation, the amount of atherosclerotic disease and the occurrence of infection. In addition, morphometric analysis revealed that higher H-CAV types have a relatively larger intimal area, accompanied by a thinner media and unaltered luminal area. Our results suggest that early CAV consists of high inflammatory lesions, whereas longer after transplantation a more fibrotic phenotype of CAV can be observed.

Chapter 3 studied the process of fibrosis within the vessel wall in more detail analyzing the factors and cells involved. The strongest mRNA expression of (predominantly pro-) fibrotic factors was found in the neo-intima. Especially, connective tissue growth factor (CTGF) expression was higher in the CAV vessels than in the controls. Interferon gamma (IFNγ) expression was only seen in CAV vessels. Infiltrated lymphocytes simultaneously expressed transforming growth factor beta (TGFβ) and IFNγ. Anti-fibrotic factors were only expressed in CD3-/CD68- stromal cells. Macrophages present in the CAV and control vessels showed to be of the M2 type and did not produce these factors. In conclusion, T cells producing both IFNγ and TGFβ, may play an important role in the fibrotic process in CAV vessels by upregulation of connective tissue growth factor production.

In **Chapter 4** ectopic lymphoid structures (ELS) are characterized along epicardial coronary arteries with CAV. The cellular composition of the ELS differs from the cellular infiltrate in CAV intimal lesions with many B cells present. The occurrence of memory B lymphocytes and IgM- and IgG-producing plasma cells suggests that ELS are related to local antibody production potentially contributing to antibody-mediated CAV. The extent of ELS in

transplanted hearts is related to time after transplantation and H-CAV stage, suggesting they are involved in lesion development. Besides, they show features of underdeveloped TLOs; classical TLOs may not develop due to the given immunosuppression.

Chapter 5 further determined the function of the ELS and their role in the humoral immune response. Cellular interactions and antigenic targets of the antibodies are investigated. The detected cytokine profile suggests active recruitment and proliferation of T- and B- lymphocytes within ELS. The absence of certain interleukins could be explained by immune suppression of these transplanted patients. Patients with ELS exhibit actively antibody (IgG and IgM) producing plasma cells with no monoclonal expansion. The antibody levels are high in cardiac transplant patients with large ELS. These locally produced antibodies are in some cases directed against the donor HLA-II type (19% of patients with ELS) or non-HLA antigens (anti-angiotensin-II type-1 receptor; 52% of ELS patients). Local antibody production may mediate rejection which has major consequences for the graft.

Chapter 6 gives an overview describing the role of donor and recipient cells in CAV. Many researchers believe in an allogeneic immune response of the recipient, whereas others show contradictory results in which donor-derived cells induce an immune response. Besides, intimal fibrosis can be induced by recipient-derived circulating cells or donor-derived cells. Dual outcomes were found regarding the contribution of donor and recipient cells in the immune response and fibrotic process. Future research should focus more on the potential synergistic interaction of donor and recipient cells leading to CAV.

Chapter 7 presented humanized mouse models used in transplantation research. The design of these models is still improving. The decision regarding 'the best model' will differ for one to another and depends on the hypothesis being tested. This chapter provides a guide to the most common humanized mouse models, with regards to different mouse strains, transplantation material, transplantation techniques, pre- and post-conditioning and references to advantages and disadvantages. Experiences in studies on Graft versus Host Disease and allograft rejection is provided.

Chapter 8 aimed to find microRNAs (miRs) as biomarker or therapeutic target for CAV. The role of miRs was never described in CAV. Presence of miRs in CAV-intima and plasma after heart transplantation showed that alterations in the intima are not reflected in plasma. Validation of selected miRs from the intima showed five as significantly up- (miR-21, -223, and -146b-5p) or down-regulated (miR-886-5p and -214). Locating these miRs by *in situ* hybridization confirmed that these were found in either (myo)fibroblast-like or immune cells. If these miRs have a role in CAV development they could be considered as potential therapeutic targets.

Chapter 9 further analyzed the validated miRs (miR-21, -146b-5p, -214, -223, -886-5p) using a well-established humanized mouse model for allograft vasculopathy. Expression level of the selected miRs was determined in other arterial layers within CAV patients. Interestingly, downstream mRNA targets (STAT3, TIMP3, PDCD4) for miR-21 were low in areas where miR-21 expression was high. Although not significant, miR-146b-5p showed a upregulating trend in AV grafts compared to controls. The allograft vasculopathy huSCID/bg model shows similarities with human CAV regarding miR expression levels, making this an appropriate model to study AV. The molecular process of CAV is two sided, with miR-146b-5p as immune and miR-21 as fibrosis modulator with downstream mRNA effects. Targeting these two processes in vivo could offer a new therapeutic approach for CAV.

Chapter 10 contains a general discussion with future perspectives in CAV research. Besides intima expansion and fibrosis, this thesis showed that ectopic lymphoid structures (ELS) surrounding CAV arteries should not be underestimated in the pathogenesis of chronic rejection. New insights in molecular pathways (e.g. microRNA regulation) of other pathologies could be applied on CAV. By understanding the disease mechanism on a morphological, cellular and molecular level, new options for diagnosis, prognosis, and therapy could be considered.

Nederlandse samenvatting

Coronair lijden na harttransplantatie, Cardiac Allograft Vasculopathy (CAV) genaamd, is een van de belangrijkste complicaties na hart transplantatie. Momenteel is er geen behandeling voor transplantatie patiënten die CAV ontwikkelen. Re-transplantatie zou de enige mogelijkheid zijn om deze patiënten te genezen, echter het beperkte aanbod van donor organen maakt dit in de dagelijkse praktijk niet haalbaar. Daarom is het van belang om in een vroege fase na transplantatie deze aandoening gunstig proberen te beïnvloeden.

Hoofdstuk 1 is een algemene introductie die de rol van harttransplantatie bij hartfalen beschrijft waarbij wordt aangegeven dat er meer kennis nodig is van chronische afstoting en CAV in het bijzonder. Het immunologische en fibrose (verbindweefseling) proces bij CAV wordt hier beschreven. De ontstekingsreactie zorgt voor disfunctie van het endotheel met migratie en deling van gladde spiercellen. Dit hoofdstuk eindigt met het benoemen van de doelen van deze dissertatie; het bestuderen van (1) de pathogenese van CAV op een morfologisch, cellulair, en moleculair niveau, (2) de rol van ectopische lymfoïde structuren rondom CAV vaten, en (3) het vinden van een moleculair aangrijpingspunt voor therapie bij CAV.

Hoofdstuk 2 introduceert de nieuw geformuleerde histologische fenotypes van CAV in relatie tot klinische patiënten gegevens. We presenteren hier vier histologische CAV fenotypes (H-CAV 0-3) variërend van normale intima verdikking ("Benign Intima Thickening"; H-CAV0), neo-intima met een mononucleair ontstekingsinfiltraat in losmazig bindweefsel (H-CAV1), een extra laag met gladde spiercellen in tegengestelde oriëntatie (H-CAV2), tot volledige concentrische fibrose (H-CAV3). Deze stadia zijn gerelateerd aan tijd na transplantatie, atherosclerose (aderverkalking), en infecties. Daarnaast liet de morfometrische analyse van de CAV vaten zien dat een hoger H-CAV stadium gerelateerd is aan een dikkere intima laag, dunnere media laag, en een onveranderd lumen oppervlak. Deze bevindingen suggereren dat vroege CAV gepaard gaat met heftige inflammatoire laesies, terwijl CAV langer na transplantatie een meer fibrotisch fenotype heeft.

Hoofdstuk 3 bestudeert de verbindweefseling (fibrose) van de vaatwand in meer detail, waarbij betrokken factoren en cellen in kaart worden gebracht. Sterke gen expressie (mRNA) van (vooral pro-) fibrotische factoren werd gevonden in de neo-intima. Met name CTGF (connective tissue growth factor) was verhoogd in CAV vaten t.o.v. controles. Expressie van interferon gamma (IFNγ) werd allen gevonden in CAV vaten, waarbij de lymfocyten in de intima zowel IFNγ als TGFβ (transforming growth factor beta) tot expressie brengen. Anti-fibrotische factoren werden alleen tot expressie gebracht door stromale cellen (CD3-/CD68-). Macrofagen in de CAV en controle vaten waren vooral van het M2 type en produceerde deze factoren niet. Concluderend, T cellen produceren vooral IFNγ and TGFβ en zijn betrokken bij het fibrose proces door het verhogen van CTGF expressie.

In **Hoofdstuk 4** zijn de 'Ectopic lymphoid structures' (ELS) die langs de epicardiale coronair vaten liggen gekarakteriseerd. De compositie van cellen in de ELS is erg verschillend ten opzichte van de intima, waarbij in de ELS opmerkelijk veel B cellen aanwezig zijn. De aanwezigheid van geheugen B cellen (memory B cells) en IgM en IgG positieve plasma cellen suggereert dat er lokale productie is van antilichamen die kunnen bijdragen bij antilichaam gemedieerde CAV. De grootte van de ELS is gerelateerd aan tijd na transplantatie en H-CAV stadium, wat suggereert dat ELS betrokken zijn bij vasculopathie. De ELS tonen kenmerken van tertiair lymfoïde organen (TLOs); door de immuun suppressie kunnen deze waarschijnlijk

niet tot volgroeide TLOs ontwikkelen.

Hoofdstuk 5 gaat dieper in op de functie van de ELS en hun rol bij de humorale immuun respons. De interactie tussen cellen in ELS en de antigenen waar de antilichamen tegen gericht zijn worden hier verder onderzocht. Het cytokine profiel suggereert actieve aantrekking en deling van T en B cellen in de ELS. Afwezigheid van bepaalde interleukines kan verklaard worden door de continue immuun suppressie bij deze transplantatie patiënten. De ELS bevatten actieve plasma cellen die antilichamen (IgG en IgM) produceren zonder monoklonale expansie. Het epicard van hart transplantatie patiënten met grote ELS bevat veel antilichamen. Deze lokaal geproduceerde antilichamen zijn soms gericht tegen donor HLA-II (19% van de patiënten met ELS) of tegen non-HLA antigenen (anti-angiotensine-II type-1 receptor; 52% van de ELS patiënten). Lokaal geproduceerde antilichamen kunnen bijdragen aan afstoting met nadelige consequenties voor het donor hart.

Hoofdstuk 6 geeft een overzicht van de rol van donor en recipiënt cellen in CAV. Velen geloven in een allogene immune response van de donor gericht tegen de recipiënt, terwijl anderen tegenstrijdige resultaten laten zien waarin juist donor cellen het immuun systeem activeren. Intima fibrose kan geïnduceerd worden door circulerende cellen van de recipiënt of aanwezige donor cellen. Tweeledige resultaten zijn gevonden waarbij zowel donor als recipiënt cellen bij de immuun response en fibrose betrokken zijn. Toekomstig onderzoek zal meer moeten focussen op synergetische interactie tussen donor en recipiënt cellen bij CAV.

Hoofdstuk 7 presenteert gehumaniseerde muismodellen die gebruikt worden in transplantatie onderzoek. Het optimaliseren van deze modellen is nog steeds in volle gang. Welk model 'het beste' is, is sterk afhankelijk van de hypothese die getoetst dient te worden. Dit hoofdstuk leidt de lezer langs de meest gebruikte gehumaniseerde muismodellen, met betrekking tot muis ras, transplantatie materiaal, transplantatie technieken, voor en na behandeling, en voor en nadelen van al deze methoden. Gebruikte modellen bij studies naar 'graft versus host disease' en orgaan afstoting worden uiteindelijk in een overzicht gegeven.

Het doel van **Hoofdstuk 8** was om microRNAs (miRs) als biomarker of therapeutisch target te vinden bij CAV. De detectie van miRs in de CAV intima en plasma na transplantatie lieten veranderingen zien die niet met elkaar overeenkwamen. Validatie van de geselecteerde miRs uit de intima toonde vijf miRs met significant verhoogde (miR-21, -223, and -146b-5p) of verlaagde expressie (miR-886-5p and -214). Locatie van deze vijf miRs werd bevestigd met in situ hybridisatie waarbij ze of aanwezig waren in myofibroblast-achtige cellen of in immuun cellen. Wanneer deze miRs een rol spelen bij CAV zouden ze mogelijk als therapeutisch target kunnen dienen.

In **Hoofdstuk 9** worden de gevalideerde miRs verder bestudeerd in een gehumaniseerd muis model voor allograft vasculopathie (AV). Expressie niveaus van de miRs werden gemeten in alle lagen van de CAV vaten afkomstig van transplantatie patiënten. Opmerkelijk was dat targets van miR-21 (STAT3, TIMP3, PDCD4) laag waren wanneer miR-21 expressie hoog was. MiR-146b-5p liet een trend in verhoogde expressie zien in AV vaten vergeleken met de controles. Het allograft vasculopathie huSCID/bg model laat overeenkomsten zien met humane CAV wat betreft miR expressie, waardoor dit een geschikt model is voor deze studie. Het moleculaire proces van CAV is tweezijdig met miR-146b-5p als immuun en miR-21 als fibrose modulator met downstream effecten. Het aangrijpen van deze twee processen in vivo zou een nieuwe therapeutische benadering zijn voor CAV.

Hoofdstuk 10 bevat een algemene discussie met toekomst perspectieven binnen CAV onderzoek. Naast intima verdikking en fibrose, laat deze dissertatie zien dat ook extravasculaire lymphoïde structuren (ELS) rondom CAV arteriën niet onderschat moeten worden in de pathogenese van chronische afstoting. Nieuwe inzichten in moleculaire reacties (bijvoorbeeld microRNA regulatie) kunnen worden toegepast op CAV. Door het ziekte beeld te begrijpen op een morfologisch, cellulair en moleculair niveau kunnen nieuwe opties voor diagnose, prognose en therapie ontwikkeld worden.

Chapter 12.

DANKWOORD / ACKNOWLEDGEMENTS

Dankwoord / Acknowledgements

In dit laatste stuk van mijn boekje wil ik graag stilstaan bij alle mensen die mij geholpen hebben om tot dit mooie resultaat te komen.

Allereerst, Paul van Diest, bedankt dat ik op deze prachtige afdeling mijn promotie onderzoek mocht doen waarbij jij mij in de gaten hield als promotor en afdelingshoofd.

Daarnaast wil ik mijn co-promotoren, Nicolaas en Roel, bedanken voor de intensieve begeleiding van de afgelopen 4 jaar. Nicolaas, dank voor jouw altijd kritische blik vanuit de kliniek die ons onderzoek o zo veel meer waard maakt. Je hielp mij bij het selecteren van patiënten, het zoeken naar klinische gegevens en het formuleren van mooie zinnen in de publicaties die volgden.

Roel, hoe kan ik jou bedanken in een paar zinnen? Vanaf het moment dat ik binnen kwam heb jij mij alle mogelijkheden geboden die ik aan kon. Van muizen, Ok-setjes, reagentia, hulp van analisten, congressen, Yale-avonturen en publicaties, tot onderwijs ervaring, mensen kennis, grant aanvragen, en financiën, tot nu een prachtige opleidingsplek in de wereld van de Klinisch Moleculair Bioloog in de Pathologie. Ongelofelijk hoe goed jij bent als leidinggevende, mentor, en docent. Dank voor alle kennis die ik nu al van je heb gekregen en ik in de toekomst nog ga krijgen.

Ondanks op de achtergrond, ook veel dank voor mijn mentoren, Joost Sluijter als 'die-hard' onderzoeker en Hans Kirkels als 'goede' cardioloog. Fijn om te weten dat ik bij jullie beide terecht kon. Het onderzoek zou nergens zijn zonder de goede samenwerking met de cardiologie; Corine Klöpping, Hanneke, Nanneke, Albert, Nelienke en Annemarie, dank dat jullie ons altijd weten te bereiken en wij bij jullie terecht kunnen.

Ook veel dank aan de afdeling cardio thoracale chirurgie met in het bijzonder Jaap Lahpor en Marc Buijsrogge. Dank voor jullie enthousiasme voor ons technisch lastige muis-model. Met al die vaatjes heb ik een heleboel operaties uit kunnen voeren die jammer genoeg niet meteen in succes resulteerden. Echter door continue steun van Jaap heeft dit geleid tot een voortdurende samenwerking met de 'Tellides-group', een flinke leercurve, en een laatste hoofdstuk in dit boekje.

Dank ook aan de hulp vanuit het GDL voor het continue opvangen van mijn teleurgestelde indrukken; Anja, Sabine, Helma, Jan en Hans Vosmeer. Fijn dat ik ook niet alleen hoefde te ploeteren in 'de micro', Hanna Talacua en Nynke Oosterhuis dank voor jullie hulp. In het bijzonder wil ik stilstaan bij een collega die mij door di(c)k en dun steunde; Dick. 'Kip ik heb je', molens uit Gouda, 'het zijn geen bakstenen', en wij maar opereren tot in de late uurtjes. Je leerde mij alles wat nodig was om de reis naar dit model te laten slagen. Maar ook was je een kei in immuno's, in situ's en kweken, dank voor jouw geduld en eeuwige steun!

In April 2013 I visited the research group of George Tellides. George, thank you for accepting me as one of your lab members, taking me to several OR's in New England, the interesting conservations on route, and the wonderful BBQ with your family. Lingfeng, you are 'the master of microsurgery', I never met a person with skills that special. Jack, thank you for being my friend, Walmart groceries, running in the weekend, and conversations in English. Jing, thanks for teaching me FACS, you were a wonderful colleague. In those months in New Haven I met

some wonderful friends; Ashley, Alison, Laura, Wouter and Martine, thanks for the wonderful dinners, weekends and spare time we spent together.

During this PhD-journey I also met some great researchers from Canada. Tim, thank you for diner in Montreal with your post-docs, the shared interest for BIT and ELS, and for eventually being part of my committee. We published one of the chapters in this thesis together with you and Alison. Alison, it was wonderful to have you in Utrecht for a month. We worked hard and had fun cooking 'boerenkool' and 'hutspot' at Roel's place.

Dit boekje had natuurlijk nooit zo mooi kunnen worden zonder hulp van een geweldig HTx-team. Sjoukje, roomie, dank voor jouw mooie persoonlijkheid en voorbeeld in het promotie traject. Joyce, fijn om altijd jouw structuur en helderheid te mogen ervaren, ook vanuit San Diego op skype tijdens het 'keukentje spelen'. Erica, doeltreffend en recht door zee, dank voor de zetjes die jij mij gaf in het maken van beslissingen. Aryan, dank voor jou kritische blik als patholoog, op de CAV vaten en mijn artikelen. En Petra, jij weet wat je wilt, bij de HTx en als hoofdanalist, dank voor ook jouw steun.

Daarnaast wil ik alle MIP analisten bedanken voor alle vragen, hulp en gezelligheid; Sabrina, Remco, Joyce R, Erwin, Ana, Michiel, Erika, Eric, Maryleen, Carmen, Domenico, Dorine, Daphne, Eline, Kevin, Marije, Shivanand, Petra H, Tessa, en Roel B. Marja, dank voor het altijd klaarstaan en om 7u 's ochtends aanwezig zijn voordat ik geopereerd werd aan mijn pols. Ton, FISH koning, met of zonder FISH-diploma, dank voor jouw hulp in ons microRNA avontuur. Ook dank aan alle studenten die samen met mij onderzoek hebben gedaan; Heleen, Bastiaan, Hannah, Rianne, Remco, Suzanne, Dongqing, Chantal, Femke, Manon, Patricia, Ronald, en Wouter. Alle andere studenten, Fay, Dianne, Ankie, Maartje, dank voor jullie gezelligheid bij etentjes en wadlopen.

Ook wil ik het HLA lab bedanken voor alle snelle hulp; Elena, Daniel, en Loes. Henny Otten, super dat je ons hielp in de wondere wereld van de Luminex. Collega's van het PRL; Annette, Jeroen, Stefanie, Robbert, Lucas, Stefan, Cathy, Petra vd G, Willemijne, Ellen, Paulien, en Jolien, dank voor de gezellige borrels en input bij AIO/PD meetings. Wendy, op naar een prachtige tijd als eerste "KMBPers io". Lieve (school-)vrienden, Erik, en Steef, Rick en Peter, fijn dat we samen zulke leuke momenten meemaakten in de afgelopen jaren. Ondanks jullie zo verschillende achtergrond, met bv's, belastingen en vele afkortingen waar ik niks van snap, hebben we zo veel gelachen.

Zo veel weekenden in het mooie Haps doorgebracht, Ineke, Peter, Ward, Manon en Muriel, fijn dat ik altijd bij jullie terecht kan.

Lieve paranimfen, Alja en Petra, dank voor jullie steun en hulp bij de organisatie van deze mooie dag op 13 April 2015. Jullie zijn een bijzonder stel, Alja stress voor vragen vanuit de commissie, Petra met meer ervaring en rust.

Alja; dondersteen, drukte maker, stress, slimmerd, privé fysio, sloper, no worries! Teije; boevenpoef, installateur, wings, psycholoog, trots op jou! Paps; en jij maar denken dat ik muizen chirurg ben... kaft, trots (ook bij deze happening?), constructeur, ontwerpen, maar vooral de beste timmerman ooit. Mams; steun, dagelijks bellen, zorgzaam, ook als ik mijn arm breek, super bouwvakker, en schilder. Dank voor jullie onvoorwaardelijke steun!

Niels, eerst vertrok ik naar Enschede, toen naar Utrecht, naar New Haven, en uiteindelijk naar Bunnik. Altijd ging jij met me mee en steunde mij van begin tot eind in het nastreven van mijn dromen, ook als dat tot de late uurtjes werken betekende. Je bent mijn metselaar, ijdeltuit, en vriendje. Dank voor alles.

Review committee

Prof.dr. C.C. Baan
Inwendige Geneeskunde-Transplantatie & Nefrologie, Laboratorium
Erasmus Medical Center
Rotterdam, the Netherlands
c.c.baan@erasmusmc.nl

Prof. dr R. Goldschmeding
Pathology
University Medical Center Utrecht
Utrecht, the Netherlands
r.goldschmending@umcutrecht.nl

Prof. dr. J.R. Lahpor
Cardiothoracic Surgery
University Medical Center Utrecht
Utrecht, the Netherlands
j.r.lahpor@umcutrecht.nl

Prof.dr. T.D.G. Lee
Transplant research
Dalhousie University
Halifax, Canada
tim.lee@dal.ca

Prof.dr. G. Tellides
Cardiac Surgery
Yale School of Medicine
New Haven, USA
george.tellides@yale.edu

List of publications

Balemans MC, Huibers MM, Eikelenboom NW, Kuipers AJ, van Summeren RC, Pijpers MM, Tachibana M, Shinkai Y, van Bokhoven H, Van der Zee CE. Reduced exploration, increased anxiety, and altered social behavior: Autistic-like features of euchromatin histone methyltransferase 1 heterozygous knockout mice.
Behavioral Brain Research. 208(1):47-55 (2010)

Huibers M, De Jonge N, Van Kuik J, Koning ES, Van Wichen D, Dullens H, Schipper M, De Weger R. Intimal fibrosis in human cardiac allograft vasculopathy.
Transplant Immunology. 25(2-3):124-132 (2011)

Balemans MC, Ansar M, Oudakker AR, van Caam AP, Bakker B, Vitters EL, van der Kraan PM, de Bruijn DR, Janssen SM, Kuipers AJ, Huibers MM, Maliepaard EM, Walboomers XF, Benevento M, Nadif Kasri N, Kleefstra T, Zhou H, Van der Zee CE, van Bokhoven H. Reduced Euchromatin histone methyltransferase 1 causes developmental delay, hypotonia, and cranial abnormalities associated with increased bone gene expression in Kleefstra syndrome mice.
Developmental Biology. 386(2):395-407 (2014)

Hogenes MCH*, Huibers MMH*, Kroone C, de Weger RA. Humanized mouse models in transplantation research.
Transplantation Reviews. 28(3):103-110 (2014).

Huibers MM, Vink A, Kaldeway J, Huisman A, Timmermans K, Leenders M, Schipper ME, Lahpor JR, Kirkels HJ, Klöpping C, de Jonge N, de Weger RA. Distinct phenotypes of cardiac allograft vasculopathy after heart transplantation: A histopathological study.
Atherosclerosis. 236(2):353-359 (2014)

Huibers MMH, Gareau AJ, Vink A, Kruit R, Feringa H, Beerthuijzen JMT, Siera-de Koning E, Peeters T, de Jonge N, de Weger RA, Lee TDG. The composition of Ectopic Lymphoid Structures suggests involvement of a local immune response in Cardiac Allograft Vasculopathy.
ournal of Heart and Lung Transplantation. doi: 10.1016/j.healun.2014.11.022 (2014). [Epub ahead of print]

12

van den Hoogen P*, Huibers MMH*, Sluijter JPG, de Weger RA. Cardiac Allograft Vasculopathy: a donor or recipient induced pathology?
Journal of Cardiovascular Translational Research [Epub ahead of print] (2015)

* Authors contributed equally to the work

Manuscripts in preparation

Jansen MAA, Otten HG, de Weger RA, Huibers MMH. Immunological and fibrotic mechanisms in Cardiac Allograft Vasculopathy
Transplantation. Resubmitted with revisions (Jan 2015)

Huibers MMH, Vroman H, van Holthe tot Echten B, van Kuik J, Siera-De Koning E, Peeters ALM, Vink A, Lahpor JR, de Jonge N, de Weger RA. Alterations in human coronary artery microRNA profile during Cardiac Allograft Vasculopathy are not reflected by circulating microRNAs.
Submitted

Huibers MMH, Beerthuijzen JMT, Gareau AJ, Siera-de Koning E, van Kuik J, Kamburova EG, de Jonge N, Lee TDG, Otten HG, de Weger RA. Antigenic targets of local antibodies produced in Ectopic Lymphoid Structures in Cardiac Allografts.
Manuscript in preparation

Huibers MMH, de Weger RA, Sluijter JPG, de Jonge N, van Kuik J, Siera-de Koning E, Lahpor JR, Qin L, Tellides G. Functional role of selected microRNAs in Cardiac Allograft Vasculopathy
Manuscript in preparation

Abstracts presented at conferences

2009 VSNU, Zeeland, research in education. September 2009
Poster: Bachelor internship. Brain development and behavioral analysis of EHMT1$^{+/-}$ mice; a new model for mental retardation. M.M.H.Huibers, under supervision of M.C.M.Balemans and I. van der Zee.

2011 Cardiovascular conference, Noordwijkerhout, the Netherlands. March 2011
Poster 1: Cardiac allograft vasculopathy: a quantitative analysis of changes in coronary artery wall architecture after heart transplantation. M.M.H. Huibers, J. Kaldeway, A. Huisman, H.F.J. Dullens, M.E.I. Schipper, N. de Jonge, and R.A. de Weger.
Poster 2: Circulating microRNAs in patients with cardiac allograft vasculopathy after heart transplantation. H. Vroman, M.M.H. Huibers, J. van Kuik, N. de Jonge, and R.A. de Weger.

2011 Bootcongres, Dutch Transplant Society, Amsterdam, the Netherlands. March 2011
Presentation: Cardiac allograft vasculopathy: a quantitative analysis of changes in coronary artery wall architecture after heart transplantation. M.M.H. Huibers, J. Kaldeway, A. Huisman, H.F.J. Dullens, M.E.I. Schipper, N. de Jonge, and R.A. de Weger.
Poster: Circulating microRNAs in patients with cardiac allograft vasculopathy after heart transplantation. H. Vroman, M.M.H. Huibers, J. van Kuik, N. de Jonge, and R.A. de Weger.

2012 Bootcongres, Dutch Transplant Society, Maastricht, the Netherlands. March 2012
Presentation: Changes of plasma microRNAs in heart transplantation patients do not reflect microRNA changes in the CAV vessel wall. M.M.H. Huibers, H. Vroman, J. van Kuik, E. Siera-De Koning, N. de Jonge, and R.A. de Weger.

2013 Pathology Winter meeting, Utrecht, the Netherlands. January 2013
Poster 1: The Composition of Macrophages in Extravascular Infiltration after Heart T ransplantation. M Huibers, H Feringa, R Kruit, A Vink, T Peeters, N de Jonge, and R de Weger. Journal of Pathology - Abstract Publication.
Poster 2: Cardiac Allograft Vasculopathy: a Quantitative Analysis of Changes in Coronary Artery Wall Architecture after Heart Transplantation. M.M.H. Huibers, J. Kaldeway, A. Huisman, H.F.J. Dullens, M.E.I. Schipper, N. de Jonge, R.A. de Weger. Journal of Pathology - Abstract Publication.

2013 International Society of Heart and Lung Transplantation, Montreal, Canada. April 2013
Poster 1: Long-term survival after heart transplantation depends on proper outward remodeling of epicardial arteries with Cardiac Allograft Vasculopathy. M.M.H. Huibers, J. Kaldeway, A. Huisman, K. Timmermans, M. Leenders, M.E.I. Schipper, A. Vink, J.R. Lahpor, J.H. Kirkels, C. Klöpping, N. de Jonge, R.A. de Weger.
Poster 2: Changes of plasma microRNAs in heart transplantation patients do not reflect microRNA changes in the Cardiac Allograft Vasculopathy vessel wall. M.M.H. Huibers, H. Vroman, J. van Kuik, E. Siera-De Koning, N. de Jonge, and R.A. de Weger.

2013 European Society of Cardiology, Amsterdam, the Netherlands. September 2013
Poster: Long-term survival after heart transplantation depends on proper outward remodeling of epicardial arteries with Cardiac Allograft Vasculopathy. M.M.H. Huibers, J. Kaldeway, A. Huisman, K. Timmermans, M. Leenders, M.E.I. Schipper, A. Vink, J.R. Lahpor, J.H. Kirkels, C. Klöpping, N. de Jonge, R.A. de Weger.

2014 European Society for Heart and Lung Transplantation. Wengen, Switzerland. January 2014. Young investigators travel award.
Presentation: Cardiac Allograft Vasculopathy, Unravelling the role of microRNAs. M.M.H. Huibers, R.B. van Holthe tot Echten, T. Peeters, N. de Jonge, G. Tellides, R.A. de Weger.

2014 International Society of Heart and Lung Transplantation, San Diego, USA. April 2014
Poster 1: Localization of microRNAs in Cardiac Allograft Vasculopathy with In Situ Hybridization; a Role in Immune Regulation and/or Fibrosis? M.M.H. Huibers, R.B. van Holthe tot Echten, T. Peeters, N. de Jonge, G. Tellides, R.A. de Weger.
Poster 2: Characterization of lymphoid clusters in the transplanted heart; an effort to form tertiary lymphoid organs? M.M.H. Huibers, A. Gareau, T.D.G. Lee, R. Kruit, H. Feringa, E. Siera-de Koning, N. de Jonge, and R.A. de Weger.

2014 European Society of Clinical Investigation, Utrecht, NL, 30th April until 2nd May
Poster 1: Localization of microRNAs in Cardiac Allograft Vasculopathy with In Situ Hybridization; a Role in Immune Regulation and/or Fibrosis? M.M.H. Huibers, R.B. van Holthe tot Echten, T. Peeters, N. de Jonge, G. Tellides, R.A. de Weger.
Poster 2: Characterization of lymphoid clusters in the transplanted heart; an effort to form tertiary lymphoid organs? M.M.H. Huibers, A. Gareau, T.D.G. Lee, R. Kruit, H. Feringa, E. Siera-de Koning, N. de Jonge, and R.A. de Weger.

Grants and awards

2008 Dr. J. Bex Price (€50) for best bachelor internship of Biomedical Sciences Nijmegen, the Netherlands.

2011 Best Poster presentation (MiVaB; €250) Cardiovascular Conference, Noordwijkerhout, the Netherlands

2013 Travel Scholarship Award (6,000$), International Society of Heart and Lung Transplantation, Applicant: Manon Huibers (under supervision of Roel de Weger, UMC Utrecht, Utrecht, the Netherlands). Hosting institution: George Tellides (Yale University, New Haven, USA)

2014 Young investigators travel award (invited speaker: hotel, travel and conference costs included). European Society for Heart and Lung Transplantation, Wengen, Switzerland

2014 Travel Scholarship Award (4,000$ for 1 month) International Society of Heart and Lung Transplantation, Applicant: Alison Gareau (under supervision of Timothy Lee, Dalhousie University, Halifax, Canada). Hosting institution: Manon Huibers (under supervision of Roel de Weger, Utrecht, the Netherlands)

2014 OHSE Grant (40,000$ for one year, until June 2015), Department of Surgery, Yale University, New Haven, USA. Applicant: George Tellides (Yale University, New Haven, USA) and Manon Huibers (under supervision of Roel de Weger, UMC Utrecht, Utrecht, the Netherlands).

Curriculum Vitae

Manon Huibers finished her bilingual secondary education at the Kandinsky College in Nijmegen in 2005. She studied Biomedical Sciences at the Radboud University Nijmegen where she got her Bachelors of Science in Human Pathobiology in 2008. She finished her Bachelors with an internship on the EHMT1 gene at the Nijmegen Center for Molecular Life Sciences at the department of Cell Biology (dr Ineke van der Zee) in collaboration with the department of Human Genetics (dr. Monique Balemans and prof. Hans van Bokhoven). She finished her Masters of Science in 2010 with a double Major in Human Pathobiology and Human Movement Sciences. Within this period she did an internship on Hepatitis C virus resistance at the Florida State University (dr Hengli Tang and dr Feng Yang) and at the Roessingh Research and Development on ankle foot orthosis and gait (dr Jaap Buurke and Corien Nikamp). In 2010 she started her PhD under supervision of dr Roel de Weger (Molecular and Immuno Pathology) and dr Nicolaas de Jonge (Cardiology) at the department of Pathology in the University Medical Center Utrecht. Her PhD research focusses on molecular and immunological mechanisms of allograft vasculopathy after heart transplantation described in this thesis. In her research she collaborates with George Tellides (Yale University USA) and Timothy Lee (Dalhousie University CAN). She visited the lab of George Tellides in 2013 as a research fellow. In the summer of 2014 she received her university teaching qualification (Basis Kwalificatie Onderwijs). In April 2015 she will defend her PhD thesis in Utrecht, where she will continue as trainee for Clinical Molecular Biologist in Pathology.